UMTRI 92-2

EFFECTS OF HEAVY VEHICLE CHARACTERISTICS ON PAVEMENT RESPONSE AND PERFORMANCE

FINAL REPORT
Project 1-25(1)

Prepared for

National Cooperative Highway Research Program
Transportation Research Board
National Research Council

Thomas D. Gillespie
Steven M. Karamihas
David Cebon
Michael W. Sayers
Mohammad Asghar Nasim
Will Hansen
Nadeem Ehsan

August 1992

UMTRI The University of Michigan
Transportation Research Institute

Acknowledgement

This work was sponsored by the American Association of State Highway and Transportation Officials, in cooperation with the Federal Highway Administration, and was conducted in the National Cooperative Highway Research Program which is administered by the Transportation Research Board of the National Research Council.

1. Report No. UMTRI 92-2	2. Government Accession No.	3. Recipient's Catalog No.

4. Title and Subtitle	5. Report Date
EFFECTS OF HEAVY VEHICLE CHARACTERISTICS ON PAVEMENT RESPONSE AND PERFORMANCE	August 1992
	6. Performing Organization Code

7. Author(s) T. D. Gillespie, S. M.Karamihas, D. Cebon, et al.	8. Performing Organization Report No.

9. Performing Organization Name and Address	10. Work Unit No. (TRAIS)
The University of Michigan Transportation Research Institute 2901 Baxter Road Ann Arbor, Michigan 48109	11. Contract or Grant No.
	13. Type of Report and Period Covered

12. Sponsoring Agency Name and Address	13. Type of Report and Period Covered Final Report Sept. 1988 - Dec. 1991
National Research Council, Transportation Research Board 2101 Constitution Avenue Washington, D.C. 20418	14. Sponsoring Agency Code

15. Supplementary Notes

This research was conducted in collaboration with Cambridge University via participation and contributions of Dr. David Cebon

16. Abstract

The high wheel loads of heavy trucks are a major source of pavement damage by causing fatigue, which leads to cracking, and by permanent deformation, which produces rutting. Among heavy trucks, all do not cause equal damage because of differences in wheel loads, number and location of axles, types of suspensions and tires, and other factors. Further, the damage is specific to pavement properties, operating conditions, and environmental factors.

The mechanics of truck-pavement interaction were studied to identify relationships between truck properties and damage (fatigue and rutting). Computer models of trucks were used to generate wheel load histories characteristic of the different trucks and operating conditions. Influence functions, obtained from rigid and flexible pavement structural models, were used to predict responses along the pavement resulting from the truck motions. The pavement responses were evaluated to estimate overall pavement damage caused by each truck.

The study assessed the significance of truck, tire, pavement, and environmental factors as determinants of pavement damage. Maximum axle load and pavement thickness have the primary influences on fatigue damage. Truck properties, such as number and location of axles, suspension type, and tire type, are important but less significant. High temperatures in flexible pavements and temperature gradients in rigid pavements adversely affect the damage caused by truck wheel loads with a fairly strong interaction. The report discusses and quantifies the influence of these variables.

17. Key Words Truck dynamics, suspensions, tires, pavement damage, fatigue, rutting	18. Distribution Statement Unlimited		
19. Security Classif. (of this report) Unclassified	20. Security Classif. (of this page) Unclassified	21. No. of Pages 255	22. Price

TABLE OF CONTENTS

LIST OF FIGURES

LIST OF TABLES

ACKNOWLEDGEMENTS

SUMMARY

The wheel loads of heavy trucks contribute to various forms of pavement distress. Of the various types, fatigue (which leads to cracking) and permanent deformation (rutting) are of great importance and are the primary focus in this study. Among heavy trucks, all do not cause equal damage because of differences in wheel loads, number and location of axles, types of suspensions and tires, and other factors. Further, the damage is specific to the properties of the pavement, operating conditions, and environmental factors.

The mechanics of truck pavement interaction were studied to identify relationships between truck properties and damage (fatigue and rutting). Computer models of trucks were used to generate representative wheel load histories characteristic of the different trucks and operating conditions. Rigid and flexible pavement structural models were used to obtain pavement "influence functions" which characterize the pavement response to tire loads at any location on the roadway. The pavement responses arising from the combined loads from all wheels of a truck were then evaluated to estimate overall pavement damage caused by each truck.

The study assessed the significance of truck, tire, pavement, and environmental factors as determinants of pavement damage. While most of the findings reinforce the existing understanding of pavement damage from heavy truck loads the treatment in this study provides a systematic overview of the interactions, as well as new insights on the mechanics involved. It is of most interest to examine the findings from the perspective of the truck characteristics that affect pavement damage, and the pavement and environmental factors that influence sensitivity to truck wheel loads.

TRUCK CHARACTERISTICS AFFECTING PAVEMENT DAMAGE

Fatigue damage to rigid and flexible pavements is most directly determined by maximum axle loads and pavement thickness. Fatigue damage varies over a range of 20:1 with typical variations in axle loads and over the same range with typical variations in pavement thickness. Other vehicle properties have a smaller, but still significant, influence on fatigue. The relationships between damage and certain truck properties of interest are discussed below:

- Axle loads—Fatigue damage is dominated by the most heavily loaded axles because of the power-law relationship of load and fatigue. The first-order determinant of overall fatigue damage for a vehicle combination is the sum of the ESALs (Equivalent Single Axle Loads) for each axle. Typical truck axle loads vary from 10,000 to 22,000 lb (10 to 22 kips). Assuming a 4th power damage relationship, a 22-kip axle is 23 times as damaging as a 10-kip axle. Although the relative fatigue damage varies with the exponent assumed in the power law, the importance of axle load dominates for all reasonable values of the exponent.

- Tandem suspensions—Theoretically, tandem axles have the potential to be no more damaging to roads than single axles with equivalent load per axle (i.e., a 36-kip tandem can be no more damaging than two 18-kip singles). In practice, certain deficiencies in the performance of tandem suspensions preclude these benefits:

  — Inequalities in static load sharing cause disproportionate fatigue from the heavily loaded axle. Load sharing coefficients (load on the heaviest axle normalized by the average of both axles) have been observed to vary from 1.02 to 1.21. A 34-kip tandem with a load sharing coefficient of 1.15 produces damage equivalent to two 18-kip axles (ESALs).

  — Most tandem suspensions produce dynamic loads comparable to their single axle equivalents. The walking-beam tandem suspension is an exception in that it produces unusually high dynamic loads. On rough and moderately-rough roads, walking-beam suspensions (without shock absorbers) are typically 50% more damaging than other suspension types.

- Axle spacing—Aside from the suspension effects discussed above, locating axles at a close spacing does not contribute to pavement damage. Damage on flexible pavements is largely insensitive to axle spacing down to the limits dictated by current tire diameters. Rigid pavements actually benefit from stress interactions between axles and produce less fatigue with closely-spaced axles. Thus, axle spacing is not an important truck characteristic affecting pavement damage.

- Tire inflation pressure—Elevated tire inflation pressure greatly increases the fatigue damage of flexible pavements. Over-inflation of conventional tires (e.g., 11R22.5) by 25 psi nearly doubles flexible pavement fatigue. Similarly, over-inflation of wide-base single tires is especially critical, increasing fatigue by a factor of four. Tire pressure has a moderate influence on rigid pavement fatigue.

- Tire configuration—Of the various tire configurations used on trucks, the most significant to damage is the heavily loaded conventional tire on steer axles. Single tires, typically loaded to 12 kips, cause the steer axle to be more damaging in fatigue and rutting to flexible pavement than a 20-kip axle (the current legal limit) with dual tires. Steer axle loads should be reduced to 11 kips or less to eliminate this disparity. Wide-base singles at their rated load capacity cause more fatigue and rutting damage than conventional dual tires on a 20-kip axle. Load on wide-base singles would have to be limited to approximately 90% of their rated capacity to eliminate this disparity.

Of the truck properties discussed above, axle loads have the greatest influence on fatigue damage of flexible pavements. However, flexible pavements may also be damaged by rutting. The permanent deformation of the asphalt concrete layer caused by a vehicle is directly dependent on its gross vehicle weight. To the extent that frieght must be carried by trucks, rutting cannot be alleviated by regulating truck gross weight, because lower weight limits will only put more trucks on the road to meet commercial hauling needs. Among the vehicle factors, tire type and inflation pressure have small influences on rutting.

PAVEMENT AND ENVIRONMENTAL FACTORS

Over the range of pavement designs typical of primary and secondary roads, fatigue damage varies by a factor of 20. The primary pavement and environmental factors affecting damage are:

- Roughness in the road surface excites truck dynamic axle loads which increases fatigue damage. Rough pavements (2.5 PSI) experience damage at a rate that is approximately 50% greater than that of smooth roads (above 4 PSI) for most typical truck suspensions. With a walking-beam tandem suspension, however, rough roads may experience damage as much as 3 times greater than that of smooth roads. Roughness does not systematically affect rutting damage of flexible pavements.

- Elevated temperatures increases permanent deformation of the pavement layers in flexible pavements. Over the temperature range from 77° to 120°F, the rutting damage from this mechanism increases by a factor of 16.

- The temperature gradient in a rigid pavement slab is most important to fatigue damage, because of the thermal stress created. With a gradient of one degree Fahrenheit per inch in the slab, the fatigue damage from most trucks increases by a factor of 10 over that of a zero-gradient condition.

In the process of conducting this study, shortcomings and deficiencies in the knowledge affecting our ability to predict truck-road interactions have been identified. The pavement models for flexible pavements need general improvement, along with the methods for predicting damage. Rigid pavement models need more development for analysis of damage accrual at cracks and joints, and methodology for studying damage needs to be modified to investigate damage under stress conditions that include tensile and compressive loading. Broad shortcomings in the knowledge of trucks are apparent. More empirical information on the dynamic properties of trucks and truck suspensions is needed, along with more information on truck tire properties.

INTRODUCTION AND RESEARCH APPROACH

PROBLEM STATEMENT

Highway networks serve society as routes for personal transport and movement of goods. Repeated loadings imposed by the wheels of vehicles using the road deteriorate the pavement structure. The service offered by a pavement is consumed by road users through damage to the structure. As a result, pavements must be periodically replenished by maintenance, resurfacing, and eventual reconstruction.

Trucks[1] are a major consumer of the pavement structure because they apply the highest loads to the road surface. Among heavy trucks, all do not cause equal damage because of variations in wheel load (static and dynamic), number and location of axles, types of suspensions, number of wheels, tire type and inflation pressure, and other factors. Regulation of the trucks permitted to use the highway and apportionment of costs to vehicles in accordance with road wear should be based upon a thorough understanding of the way in which trucks interact with and damage pavements.

The same knowledge greatly benefits the highway engineer. Pavement design involves a compromise between the high initial cost of thicker high-strength structures and the high maintenance cost of thinner low-strength alternatives. Optimization of design and maintenance practices is dependent upon careful consideration of the heavy vehicles that use the roadway.

Heavy trucks are increasing in the diversity of their design and use. New configurations, new suspensions, new tire types, and higher inflation pressures are changing the loads imposed on the pavement surface. Although relevant truck properties (weights, axle loads, dimensions, etc.) are regulated, it has been recognized in recent years that there is a lack of detailed or conclusive information on characteristics of heavy vehicles relevant to pavement longevity. Similarly, many variables of the pavement affect the behavior of the truck and the response of the roadway structure. These include such properties as surface roughness, construction material, structural design, environmental factors, geometry and traffic mix. These, in combination with the diversity in heavy-vehicle characteristics, require a reassessment of input parameters to pavement design and analysis practice. A need exists for procedures and techniques for optimizing pavement and heavy vehicle designs to provide efficient operation of rural and urban roadways.

This knowledge is essential to better management of the highway transportation network. A more detailed understanding of the interaction of trucks with the pavement

---

[1] The term "truck" is used here to represent any vehicle whose primary mission is to transport cargo on highways. Thus, trucks encompass the single-unit vehicles known as straight trucks (also buses), and multi-unit (articulated) vehicles covering the various combinations of tractor-semitrailers, doubles and triples.

structure will facilitate more rational regulation of truck traffic, particularly with respect to acceptance of new designs and innovations in vehicle configurations. Such knowledge will also allow highway engineers to make more informed design decisions regarding initial and long-term costs under the diversity of traffic, materials, and environmental variables specific to a project. Finally, it may be anticipated over the long-term that as the knowledge of pavement damage mechanisms reaches maturity, the appropriation of costs to road users will be in proportion to consumption of a road's service utility.

The purpose of this report is to present findings from a research project in which computer analysis methods were used to determine the significance and influence of major vehicle and pavement variables influencing road damage.

RESEARCH OBJECTIVE

The objective of this research was to analyze the interaction between heavy vehicles and pavements in order to assess the cumulative damage to the pavement structure as a result of trucks using the road. In broad terms, the desire was to relate the characteristics and properties of trucks to damage, to identify which truck properties are most critical, and to provide insights into the mechanics of damage to aid in pavement management.

Heavy vehicle characteristics of interest include gross vehicle weight, axle loads, axle configuration (spacing and location), suspension properties (singles and tandems, load sharing, and dynamic response), tire types (bias ply, radial, low profile, and wide-base single), tire pressures, tire contact area, tire configuration (single and dual), and operating conditions (speeds and acceleration or deceleration). Pavement factors of interest include design (flexible and rigid), surface condition (smooth, rough, and jointed), and geometrics.

RESEARCH APPROACH

The investigation of the interactions between heavy vehicles and pavements in the past has largely centered on rather simple analyses of pavement loading responses (stresses, strains, deflections), or empirical studies, such as the AASHTO Road Test (1), or specific research projects (2). (See Appendix A for a review of past work in this area.) The phenomena associated with truck loads on a highway are a complex pattern of responses in the pavement which travels through the pavement structure synchronously with the truck, as shown in Figure 1. The project relied on analytical methods to replicate as faithfully as possible the mechanics of these interactions as a foundation for evaluating damage to the pavement. Existing mechanistic models of trucks and pavement structures were integrated into a cohesive vehicle/roadway simulation system which allowed systematic study of the interactions between these two elements. The analytical approach, illustrated in Figure 2, uses vehicle response models and pavement models independently. This approach is possible by virtue of the fact that the pavement is much stiffer than a truck. Consequently, the responses of the vehicle and the pavement are uncoupled.
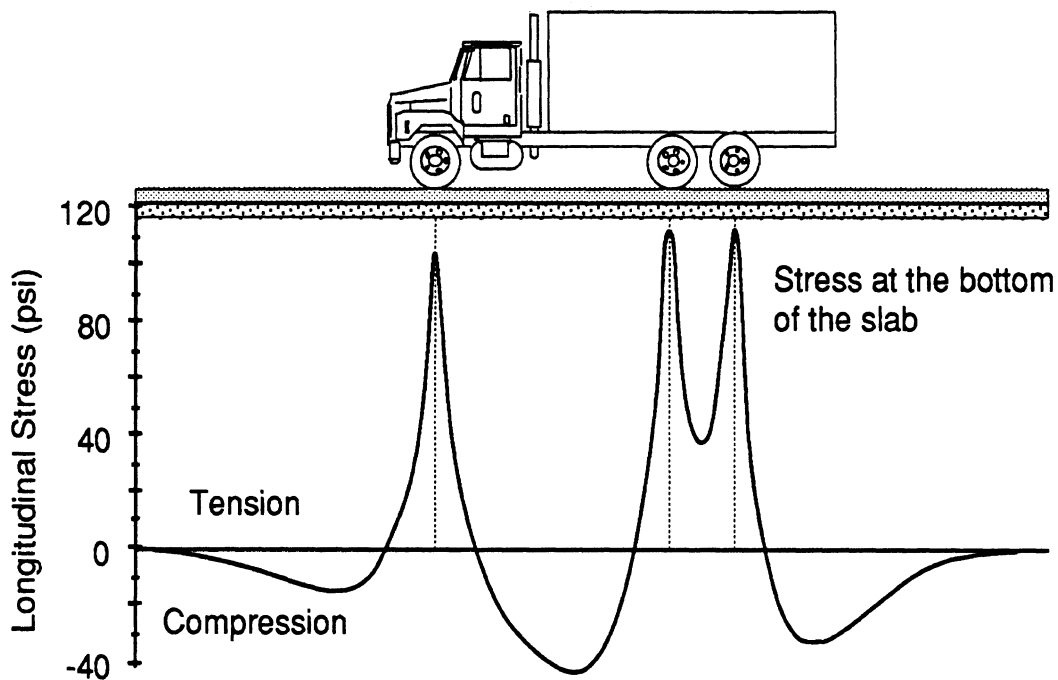
Figure 1. Stress imposed in a concrete pavement structure by a 3-axle truck.

Road surfaces (or pavements) may be classified as flexible, composite or rigid. A flexible pavement consists of one or more layers of flexible (asphalt) material supported by a granular subbase. Composite pavements consist of a flexible surface layer supported by a rigid Portland Cement Concrete (PCC) slab, and rigid pavements consist of a layer of PCC over a subbase or subgrade. Rigid pavements can further be classified according to their jointing and use of temperature steel. Each of these road types has a number of characteristic failure mechanisms, and each failure mechanism is affected by many factors. In this research, pavement "damage" was limited to three categories that are closely linked to the history of applied vehicle loads: (1) fatigue damage of rigid pavements, (2) fatigue damage of flexible pavements, and (3) permanent deformation (rutting) of flexible pavements.

Structural models of pavements were used to compute "influence functions" characterizing the responses (stresses, strains and deflections) at a point of interest in the pavement to loads, or combinations of loads, distributed at other points on the surface. The influence functions for each pavement were used to calculate responses for tire load inputs from every vehicle at every operational condition (speed, roughness, etc.). ILLI-SLAB, a finite element model described in Appendix B, was used for representation of rigid pavements. VESYS-DYN, a multi-layer elastic model described in Appendix C, was used for flexible pavements. Because damage caused by a truck is specific to the pavement structure, matrices covering full ranges of rigid and flexible pavement designs were prepared. (The matrices are presented in Appendices B and C.)
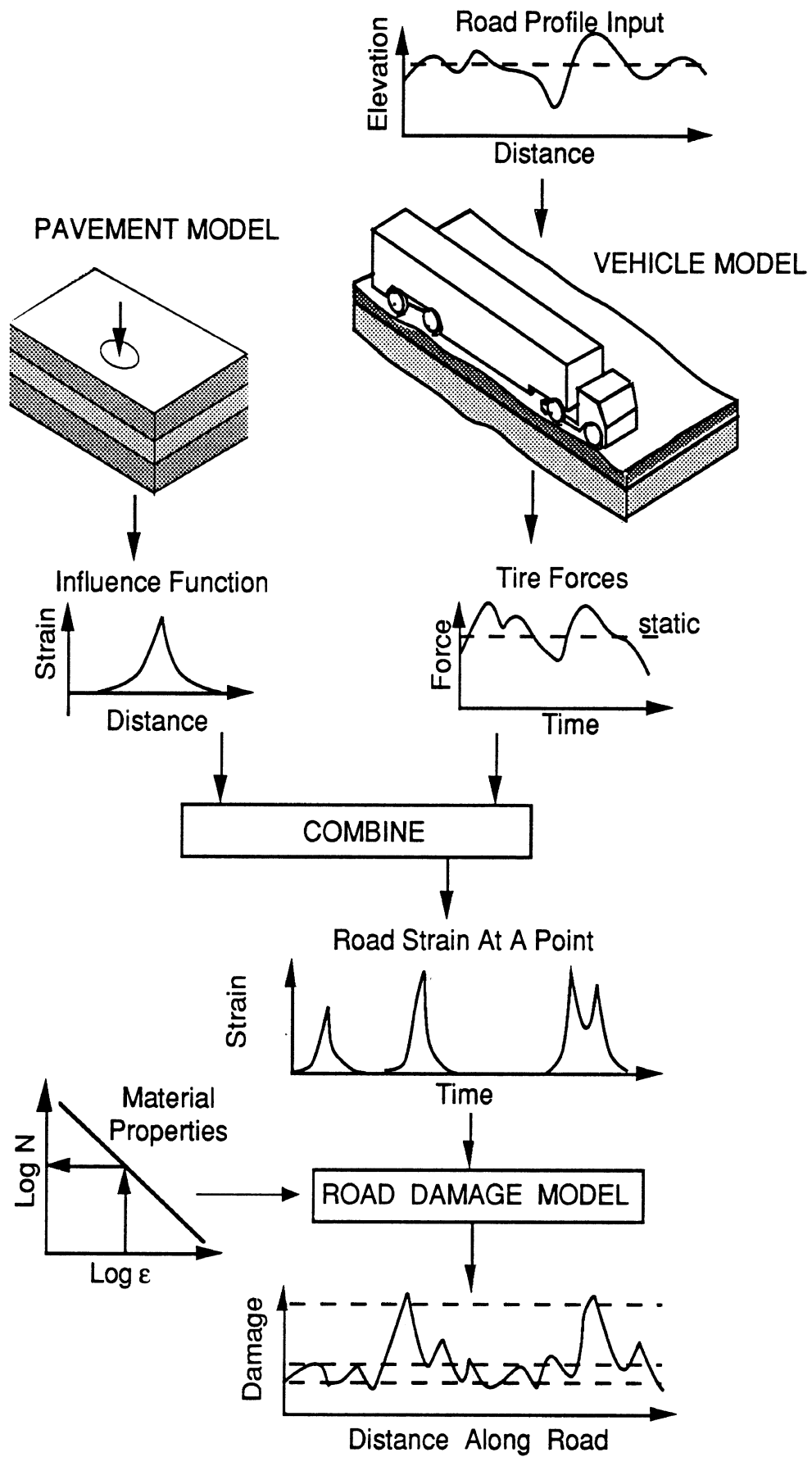
Figure 2. Analytical approach to pavement damage evaluation.

The permanent deformation resulting in rutting was modeled similarly by ascribing linear viscoelastic properties to the pavement materials, such that the deformation under load did not recover. The linear assumption is not strictly valid for all pavement materials or conditions. Nevertheless, the method is very useful for comparing the road damaging potential of different vehicles and evaluating the important trends. This process directly duplicates plastic flow rutting (see Appendix C). The compaction process that also contributes to rutting behaves similarly although the apparent viscosity increases as consolidation occurs. Inasmuch as the objective here was to model the relative effects of different truck configurations, no attempt was made to predict deformation arising from compaction separately. Thus, the predictions of rutting contained here specifically replicate plastic flow rutting and the relative effects would be comparable for compaction in the base, subbase and subgrade layers.

The vehicle dynamics model is described in Appendix D. Inputs to the vehicle model were vehicle parameters, speed, and roughness profiles synthesized to match the spectral content representative of the particular type of road under study as a source of dynamic excitation to the trucks. Details of the roughness models are presented in Appendix E. In attempting to characterize the mechanisms and magnitudes of pavement damage caused by trucks, it must be recognized that no two trucks are alike any more than any two pavements are alike. Rather, the truck population consists of a spectrum of vehicles varying in all the primary variables: weight, number of axles, length, etc. As a basis for developing generalized rules regarding pavement damage, a base matrix of 15 representative trucks was formulated to cover the primary arrangements of axles and trailers. When variations in suspensions, tires, and loading are added, the matrix of trucks expands to 29 vehicles. The matrix of trucks is shown in Table 1. In each case, the vehicle is assumed to be at the greatest permissible weight, which is the most damaging condition. (See Appendix D for details of the vehicle simulation methods and the truck matrix.) Because the vehicle and pavement models are uncoupled, the wheel load histories from one vehicle simulation run can be applied to every pavement for which the roughness profile is appropriate.
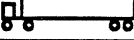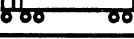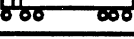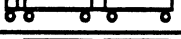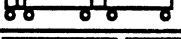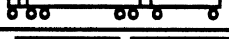
The pavement response "influence functions" from the pavement models were combined with the wheel load histories from the vehicle models, to determine the response at a point in the pavement as a multi-axle vehicle passes by. Details of the methodology for combining pavement and vehicle responses are provided in Appendix F. Finally, the total pavement response was evaluated in a damage model, with parameters chosen appropriate for the type of pavement, to quantify the influence of the vehicle on the pavement life. Appendix F also describes details of this stage of the analysis.

The results from these analyses were used to associate a relative damage level with each truck and truck variable. The damage is expressed relative to that of an 18-kip axle, or when appropriate, the fraction of pavement life consumed by the truck.

In order to build confidence in the models, limited field experiments were conducted in the project for validation purposes. A truck, instrumented for measurement of wheel loads, was driven over a rigid pavement section in which gauges recorded the strains at the bottom of the slab. The rigid pavement model was used to calculate the strains in those same locations using the comparisons of the measured and predicted strain histories as a basis for

validation (see Appendix B and reference (*3*)). The same vehicle was used for validating the vehicle dynamics model by running the truck on roads with measured profiles so that measured and computed responses could be compared. In some cases, experimental data acquired from hydraulic road simulators were used to "calibrate" the dynamic properties of truck suspension systems in the simulation models.

Table 1. Truck Matrix Sizes and Weights.

Truck Num.	Truck Configuration	Configuration Name	GCVW (kips)	Axle Loads (kips)	Wheelbases* (feet)
1-2		2 Axle Straight Truck	32	12/20	15
3-4		3 Axle Straight Truck	46	12/34	18
5-8		3 Axle Refuse Hauler	64	20/44	17.5
9-12		4 Axle Concrete Mixer	68	18/38/12	20/12
13		3 Axle Tractor-Semitrailer	52	12/20/20	10/36
14-15		4 Axle Tractor-Semitrailer	66	12/20/34	12/36
16-20		5 Axle Tractor-Semitrailer	80	12/34/34	12/36
21		5 Axle Tractor-Semitrailer	80	14/33/33	10/36
22		5 Axle Tanker	80	12/34/34	12/36
23-24		6 Axle Tanker	85	12/34/39	12/38
25		5 Axle Doubles	80	10/18/17/18/17	10/22/22
26		5 Axle Doubles	80	10/20/15/20/15	10/22/22
27		7 Axle Doubles	120	12/34/34/20/20	12/38/22
28		9 Axle Doubles	140	12/32/32/32/32	12/38/38
29		Turner Doubles	114	10/26/26/26/26	12/22/22

* Wheelbases to tandem centers. Tandem spreads set at 52 inches.

FINDINGS

The economics of pavement design involves a compromise between the higher initial cost of high-strength, thicker structural pavement sections as compared with the higher maintenance cost of low-strength, thinner alternatives. Optimizing the compatibility of heavy vehicles to suit the road system is a very complex problem, but must start with a mechanistic understanding of the ways in which trucks interact with the road to cause deterioration of the structure. With that foundation it is possible to regulate the trucks that are allowed on the road more rationally, as well as to design roads that are more resistant to damage.

Truck/road interactions were simulated in this project for the purpose of determining the relative magnitude of road damage associated with specific truck characteristics. This chapter begins with a summary of the significant truck and road factors that were found to influence the rate of damage. The summary attempts to put into a simple picture the relative significance of controllable factors that determine the life of a road. Subsequent sections discuss the major factors in more detail, providing quantitative results and explanations of why the factors influence pavement damage as they do.

The findings to be presented result from an analytical treatment of the mechanics of truck-pavement interaction. The treatment is based on the best available models for vehicles and pavement structures. The current understanding of road damage still has deficiencies in many areas; thus, the response and damage models are only as good as the current state-of-the-art in civil engineering.

In most cases the explanations of the mechanics behind the results are reasonable and straightforward, giving confidence that the analytical predictions are reasonable. However, some caution is warranted in applying the findings, because not all of the assumptions and simplifications underlying the analyses have been validated experimentally. The findings regarding differences in performance of truck suspensions are based on parametric data from a very limited sample. Although the differences observed are believed to be representative of generic differences between suspensions, they may not be accurate when applied to specific vehicles that fall outside the domain of designs considered in the study. For example, the walking-beam tandem suspension was found to cause more damage than other suspension designs as a result of a poorly-damped "tandem-hop" vibration mode. However, a truck with a walking-beam suspension that incorporated shock absorbers would not exhibit the same damaging behavior.

SUMMARY OF SIGNIFICANT FACTORS

The relative damage to a pavement caused by heavy trucks is dependent on vehicle, tire, and pavement factors. In order to understand the relative damage potential of a truck, the vehicle and tire characteristics that are relevant to pavement damage must be understood along with the design variables that effect a pavement's resistance to damage induced by truck wheel loads.

The influence of many factors is revealed in the analysis of truck-pavement interactions under static load conditions. In those cases static loads are used so that trends are readily discerned without the random scatter that arises when dynamic effects are included. Consideration of the dynamic behavior of trucks is only necessary in analysis of the vehicle factors of speed and suspension properties, and in analysis of the pavement factor of roughness.

Figures 3, 4, and 5 summarize the findings regarding fatigue damage of rigid and flexible pavements, and rutting of flexible pavements, where rutting refers only to plastic flow rutting, and does not include compaction of the pavement layers. The respective figures estimate the range over which damage will vary when individual vehicle, tire, and pavement factors vary over their typical range. The reference in the calculations for each variable of interest is a nominal value that is either common in practice, or in the case of variables that affect truck dynamics, the damage caused by "static" loads. Table 2 gives the nominal value and range of values for each of the variables in the figures. A ratio value of 1 means the damage is equivalent to the reference, and a ratio of 2 means the damage is twice as severe. Each factor is varied over the range found in the full matrices of vehicles, tires, pavement designs, roughness levels, and speeds listed in Appendices B, C, D, and E. The following paragraphs present specific findings with regard to damage arising from the individual vehicle, tire, and pavement factors addressed in this study.

Static axle load applied to the pavement is the single vehicle factor that has the greatest effect on fatigue damage. Fatigue of both rigid and flexible pavements varies by a factor of more than 20:1 over the range of axle loads from 10 to 22 kips. This is because the fatigue damage is exponentially related to static load on an individual axle. The same range of static loads causes rutting to vary by a factor of 2.2:1, because rutting is linearly related to axle load.

Vehicle gross weight has a direct influence on rutting, because rutting is linearly related to weight. The range shown corresponds to the variation for vehicles ranging in weight from 32-kips to 140-kips. Fatigue of both rigid and flexible pavements varies significantly over the range of gross weights of the vehicles included in this study. However, fatigue is not systematically related to gross weight but varies in accordance with the maximum axle loads on each vehicle combination. Heavier trucks are not necessarily more damaging.

Axle spacing has a moderate effect on rigid pavement fatigue, particularly the spacing of the axles within axle groups. For tandem axles, the optimal spacing falls between 6.75 ft (for thin rigid pavements) and 9 ft (for thick rigid pavements). On thin rigid pavements the fatigue damage caused by a closely-spaced (4.25 ft) tandem axle can be reduced by 25% if the tandem spread is increased to 6 ft. Axle spacing has little effect on flexible pavement fatigue for the range of pavement thicknesses considered. Surface rutting is also unaffected by axle spacing.

Damage Ratio Based on Nominal Value

0.1   0.2   0.5   1   2   5   10

Vehicle Factors	
Axle loads	
Gross weight	
Axle spacing	
Tandem static load sharing	
Speed	
Single axle susp. type	
Tandem dynamics	
Tire Factors	
Inflation pressure	
Dual vs. wide-base single	
Wheel path location	
Pavement Factors	
Roughness	
Slab thickness	
Base layer thickness	
Subgrade strength	
Slab length	
Joint load transfer	
Temperature gradient	

Figure 3. Factors influencing rigid pavement fatigue damage.

Damage Ratio Based on Nominal Value

0.1   0.2   0.5   1   2   5   10

Vehicle Factors	
Axle loads	
Gross weight	
Axle spacing	
Tandem static load sharing	
Speed	
Single axle susp. type	
Tandem dynamics	
Tire Factors	
Inflation pressure	
Dual vs. wide-base single	
Pavement Factors	
Roughness	
Surface temperature	
Wear course thickness	
Base layer thickness	
Subgrade strength	
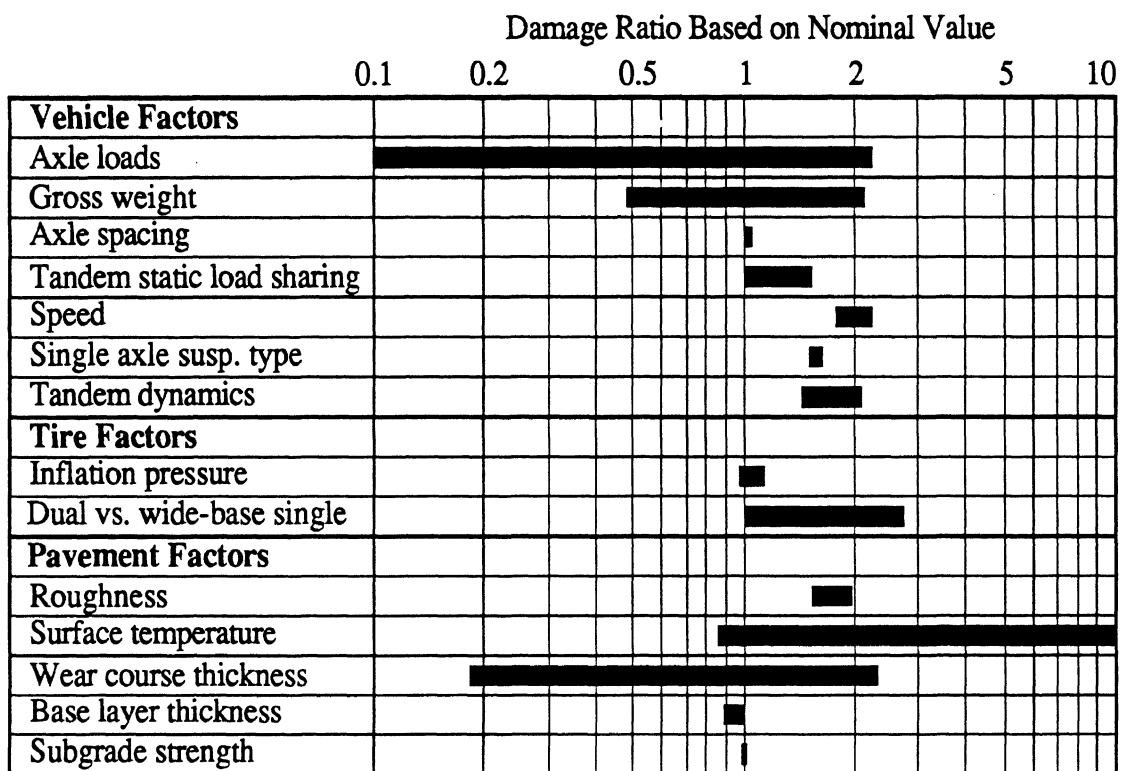
Figure 4. Factors influencing flexible pavement fatigue damage.

9

Damage Ratio Based on Nominal Value

	0.1	0.2	0.5	1	2	5	10	20
Vehicle Factors								
Axle loads								
Gross weight								
Axle spacing								
Tandem static load sharing								
Speed								
Single axle susp. type								
Tandem dynamics								
Tire Factors								
Inflation pressure								
Dual vs. wide-base single								
Pavement Factors								
Roughness								
Surface temperature								
Wear course thickness								
Base layer thickness								
Subgrade strength								
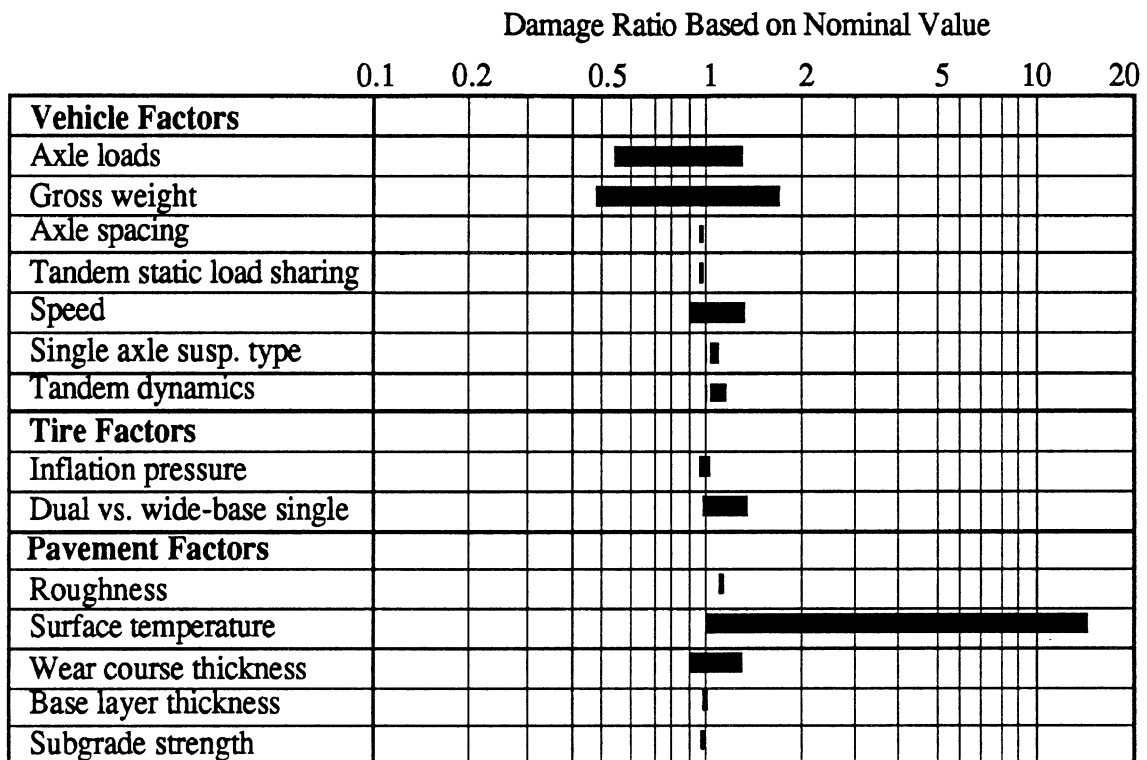
Figure 5. Factors influencing plastic flow rutting of flexible pavement.

Static load sharing within a multiple axle group influences fatigue of rigid and flexible pavements moderately as a result of the higher load on one axle when sharing is not equal. Increasing the load on one axle of a tandem set disproportionately increases the fatigue from that axle because of the exponential relationship between load and fatigue. The reduced load on the other axle reduces its contribution to fatigue, but not enough to offset the increase from the heavy axle. If the individual loads of a multiple axle group are held to within 5% of the mean load for the group, very little additional fatigue will result. If the load disparity gets as high as 25%, fatigue damage increases as much as 60%. Static load sharing has no influence on rutting by virtue of the linear relationship between rutting and axle load.

The significance of loads and load-distribution factors discussed above is not directly linked to the dynamic behavior of trucks. Thus, they have been evaluated under static load conditions. The dynamic component of axle loads can elevate the damage experienced by a pavement above that induced by static axle loads. Mean fatigue damage along a pavement may be as much as 30% higher, and in the most severely loaded pavement locations fatigue damage may be up to 300% higher. The dynamic effects are directly evident in the damage influences of speed, roughness and suspension type.

Table 2. Nominal value and range of values for each of the vehicle, tire, and pavement variables included in Figures 3, 4, and 5.

	Range of Values	Nominal Value
Truck Factors		
Axle loads	10-22 kips	18 kips
Gross vehicle weight	32-140 kips	80 kips
Axle spacing	48-96"	51"
Tandem static load sharing	LSC=1-1.25	perfect load sharing
Speed	45-65 mph	55 mph, tire loads held at static values
Single axle suspension type	air spring, taper leaf, flat leaf	static loads
Tandem axle suspension type	air spring, 4-spring, walking beam	static loads
Wheel path location	lane edge to lane center	lane center
Tire Factors		
Inflation pressure	75-120 psi	85 psi
Dual versus wide-base single	dual and wide-base single	dual tires
Rigid Pavement Factors		
Roughness	80-240 in/mi (4.25-2.5 PSI)	tire loads held at static values
Slab thickness	7-10 inches	10 inches
Base layer thickness	0-8 in. granular	8 inches, granular
Subgrade strength	50-300 pci	200 pci
Slab length	12-60 feet	CRCP
Joint load transfer	aggregate interlock vs. dowel bars	CRCP
Temperature gradient	1°F/in	0°F/in
Flexible Pavement Factors		
Roughness	80-240 in/mi (4.25 - 2.5 PSI)	Static Loads
Surface temperature	77-120°F	77°F
Wear course thickness	2-6.5 inches	5 inches
Base layer thickness	4-11 inches	8 inches
Subgrade strength	1-20 ksi	2.5 ksi

Vehicle _speed_ influences rigid pavement fatigue by increasing peak dynamic wheel loads. Compared to the static case (which is equivalent to zero speed) the fatigue damage at normal road speeds is 50% to 100% greater on a moderately rough road (160 in/mi IRI). Yet, over the normal speed range of 45 to 65 mph, the fatigue damage to a rigid pavement from a typical tandem suspension may vary only 20%. Vehicle speed also affects the primary response of flexible pavements through the duration of loading. The increase in

dynamic loads with speed is compensated for by the shorter duration of an applied axle load at increased speed. Thus, flexible pavement fatigue remains fairly constant with speed in most cases. Rutting is diminished by the decreased loading time at high speed. Thus, it decreases with speed and there is little additional increase in the average rut depth along a road arising from dynamic truck behavior. At most, the localized deformations at points of high dynamic load may contribute to the development of surface roughness.

Single axle suspension type (air- and leaf-spring) has only a moderate effect on rigid or flexible pavement fatigue. Although the suspension plays a primary role in dynamic behavior and the increased fatigue damage that results, the range of variation in stiffness properties believed typical of single-axle suspensions is small enough that the suspension type has only second-order influence on fatigue. Tandem dynamics have a much greater influence on fatigue of rigid and flexible pavements. Fatigue damage of rigid and flexible pavements may vary by 25% to 50% between the best (air-spring) and worst (walking-beam) suspensions. Suspension type has little influence on flexible pavement rutting.

Maneuvering of trucks can also lead to increased pavement fatigue by temporarily shifting load among axles. During acceleration the load shift onto rear axles is small enough that the influence on pavement fatigue is generally insignificant. Load transfer onto front axles during braking is unlikely to affect rigid pavement fatigue, but on flexible pavements localized fatigue damage could increase by as much as 100% to 1000% depending on the severity of braking. Rutting is not directly affected by the transfer of load between axles during braking because it is linearly related to gross vehicle weight, and the weight remains constant during braking, despite a redistribution among axles. It should be noted, however, that the reduction in speed strongly increases rutting, such that rutting will increase in locations where trucks routinely slow or stop. Cornering increases pavement fatigue and rutting by shifting the load to one side of a vehicle. Wheel loads on one side of the truck might typically increase by 20%, causing a 100% increase in fatigue and a 20% increase in rutting.

Lateral variation in wheel path location of trucks may increase damage in some cases and decrease it in others. To the extent that wheel path location varies, damage is spread over a broader area and accumulation of damage to the point of failure will take longer. In the case of rigid pavements the potential for an axle to cause fatigue damage increases significantly (a factor of 9) if it tracks near the edge of the lane as opposed to the center of the lane.

Variations in contact patch size are responsible for the wide variation in the pavement damaging potential of single, dual, and wide-base tires. Flexible pavement fatigue is highly sensitive to variations in size of the tire contact patch. Single tires are so damaging relative to duals that an axle loaded to 12 kips with single tires (typical of a steer axle) will often cause more flexible pavement fatigue than an axle with dual tires loaded to 20 kips. Rigid pavement fatigue is not as sensitive to tire contact conditions. Thus, axles with single tires are no more damaging than those with duals when operated within the rated loads of the tires. Rutting is dependent on load and contact area. For a given load, rut *depth* is higher when it is carried on single tires, although the rut *volume* differs little between single and dual tires.

Variations in tire inflation pressure affect pavement damage by changing contact patch size and tire vertical stiffness. The decrease in contact area at high inflation pressures has a moderate impact on rigid pavement fatigue. On the other hand, flexible pavement fatigue is strongly affected by these changes and can increase by more than 50% with a 10 psi increase in pressure. Rutting increases only slightly with inflation pressure. Changes in tire vertical stiffness with inflation pressure have little impact on damage.

Tire ply type (radial vs. bias) has minimal direct impact on fatigue of rigid and flexible pavements. Different camber and cornering properties of radial and bias-ply tires may affect wheel tracking behavior. Trucks with radial-ply tires will tend to track more precisely, and the low camber stiffness makes it easier for tires to track in existing pavement ruts. Trucks with bias-ply tires will tend to climb out of ruts. This will lead to accelerated damage from trucks with radial-ply tires, because once a rut is formed, fatigue and rutting damage is concentrated in a narrow wheeltrack.

Roughness excites dynamic behavior of trucks increasing damage. The nominal value is the theoretical case of 0 in/mi on the International Roughness Index (IRI) scale, which corresponds to a Pavement Serviceability Index (PSI) of 5, but because no road is perfectly smooth, the range of roughness does not extended to zero. Over most roads roughness varies from 80 to 240 in/mi IRI. A smooth road at 80 in/mi IRI is approximately 4.25 PSI, and a rough road at 240 in/mi is approximately 2.5 PSI. The presence of roughness on even the smoothest roads increases fatigue by approximately 50% above that of the static axle loads. On the roughest roads fatigue damage may increase by 200% to 400% depending on the type of road and truck properties.

Pavement temperature has a very strong influence on flexible pavement fatigue and rutting, although it is the temperature gradient that is most significant to rigid pavements. Temperature gradients in rigid pavements add curling stresses in the slab which can add to the stress caused by a passing truck. With reasonably modest temperature gradients, the damage from a truck may typically increase by a factor of ten. Temperature strongly affects the properties of flexible pavements, particularly affecting rutting. Rutting from this mechanism may increase by a factor of 16 or more with a surface temperature change from 77° to 120°F.

Finally, the pavement layer thicknesses and subgrade strengths have a very strong influence on fatigue and rutting. Overall, typical variation in the thickness of a pavement may affect its damage sensitivity by a factor of 20. Pavement layer thickness is the only factor comparable to axle load in the magnitude of its influence on damage.

The figures illustrate the general sensitivity of road damage to each factor, but do not imply a functional relationship between a factor and damage; neither do they take into account interactions among factors. The relative damage values given for each variable may change if the nominal level of another variable is altered. For instance, relative to dual tires, a wide-base single tire is less damaging on thick pavements than on thin pavements. Thus, changing the nominal value of pavement thickness used in the calculations for the figures will change the range of damage. This is termed an interaction between variables.

Tables 3, 4, and 5 show the interactions found in this study for rigid pavement fatigue, flexible pavement fatigue, and plastic flow rutting, respectively. These interactions identify what combinations of variables must be considered when attempting to optimize truck-pavement compatibility.

Table 3. Rigid Pavement Fatigue Interactions.

	Axle loads	Gross weight	Axle spacing	Static load sharing	Speed	Single axle susp. type	Tandem dynamics	Maneuvering	Inflation pressure	Single, dual, wide-base	Ply type	Wheel path location	Roughness	Temperature gradient	Slab thickness	Base layer thickness	Subgrade strength	Slab length	Joint load transfer
Vehicle/Tire Factors																			
Axle loads	●							○	○	●	○			○					
Gross weight		●						○						○					
Axle spacing			●	●					○	○		○			○	○		○	○
Static load sharing			●	●											○	○			
Speed					●	○	●	○					●					○	○
Single axle susp. type					○	●		○		○			○					○	○
Tandem dynamics					●		●	○	○	○			●					○	○
Maneuvering	○	○			○	○	○	●											
Inflation pressure	○		○				○		●	●	●				○				
Single, dual, wide-base	●		○			○	○		●	●	○	○			○	○			
Ply type	○								●	○	●								
Wheel path location			○							○		●		○				○	○
Pavement Factors																			
Roughness					●	○	●						●	○				○	●
Temperature gradient	○	○										○	○	●	○	○		●	○
Slab thickness			○	○					○	○				○	●	●			○
Base layer thickness			○	○						○				○	●	●			○
Subgrade strength																	●		
Slab length			○		○	○	○					○	○	●				●	●
Joint load transfer			○		○	○	○					○	●	○	○	○		●	●

● = Strong interaction   ○ = Weak interaction   (blank) = No interaction

14

Table 4. Flexible Pavement Fatigue Interactions.

	Vehicle/Tire Factors	Axle loads	Gross weight	Axle spacing	Static load sharing	Speed	Single axle susp. type	Tandem dynamics	Maneuvering	Inflation pressure	Single, dual, wide-base	Ply type	Pavement Factors	Roughness	Surface temperature	Wear course thickness	Base layer thickness	Subgrade strength
Vehicle/Tire Factors																		
Axle loads		●							○	●	●	○						
Gross weight			●						○							○		
Axle spacing				●	○						○				●	●		
Static load sharing				○	●						○				●	●	○	○
Speed						●	○	●	○					●				
Single axle susp. type						○	●		○		○			○				
Tandem dynamics						●		●	○	○	○			●				
Maneuvering		○	○			○	○	○	●									
Inflation pressure		●						○		●	●	●			○	●		○
Single, dual, wide-base		●		○	○		○	○		●	●	○			●	●	○	○
Ply type		○								●	○	●			○	○		
Pavement Factors																		
Roughness						●	○	●						●				
Surface temperature				●	●					○	●	○			●	●	○	
Wear course thickness			○	●	●					●	●	○			●	●	●	
Base layer thickness					○						○				○	●	●	○
Subgrade strength					○					○	○						○	●

● = Strong interaction   ○ = Weak interaction   (blank) = No interaction

15

Table 5. Rutting Interactions.

	Axle loads	Gross weight	Axle spacing	Static load sharing	Speed	Single axle susp. type	Tandem dynamics	Maneuvering	Inflation pressure	Single, dual, wide-base	Ply type	Roughness	Surface temperature	Wear course thickness	Base layer thickness	Subgrade strength
Vehicle/Tire Factors																
Axle loads	●								○	○						
Gross weight		●							○					○		
Axle spacing			●													
Static load sharing				●												
Speed					●		○	○				●				
Single axle susp. type						●		○				○				
Tandem dynamics					○		●	○		○		●				
Maneuvering	○					○	○	●								
Inflation pressure	○								●	●	○		○	○		
Single, dual, wide-base	○						○		●	●	○		●	●	○	
Ply type									○	○	●		○	○		
Pavement Factors																
Roughness					●	○	●					●				
Surface temperature									○	●	○		●	●		
Wear course thickness		○							○	●	○		●	●	○	
Base layer thickness										○				○	●	
Subgrade strength																●

● = Strong interaction   ○ = Weak interaction   (blank) = No interaction

16

VEHICLE FACTORS

In order to describe influences of vehicle factors on pavement damage, the concept of a reference vehicle axle is used. The reference is the single axle, with dual tires, loaded to 18,000 lb (18 kips) traditionally used by the highway community. The damage caused by this reference is called an equivalent single axle loading (ESAL). In the descriptions that follow, damage caused by one pass of a vehicle or axle group over a pavement is described by the number of ESALs necessary to consume the same amount of pavement life. Note that damage expressed in ESALs is *relative*. By definition, it removes the effect of pavement design, age, and condition variables. For example, one ESAL on a strong pavement corresponds to a much lower proportion of its fatigue life than one ESAL on a weak pavement.

The ESAL is not the only reference that could be used to normalize pavement damage due to a vehicle or axle group. For example, given that the mission of heavy trucks is generally to haul cargo, a more appropriate measure might be to normalize damage per ton of cargo transported. Or, given a basic vehicle configuration, damage could be normalized to a reference vehicle. However, given that the ESAL is one of the simplest ways to normalize damage due to a vehicle pass, and that it is a familiar and accepted standard, the ESAL is used in this report wherever practical to indicate relative damage due to one pass of a heavy truck.

Axle Loads

When a loaded axle moves along a pavement it deflects the pavement downward creating a deflection basin as illustrated in Figure 6. The deflection creates short-duration stresses and strains which fatigue the pavement structure, and, in the case of linear plastic material, add incrementally to permanent deformation (rutting). In general, the pavement structure is linear in the way it responds to the loading applied by a passing axle. Thus, for the models used in this study, damage is directly related to load. Rutting damage is proportional to axle load, and fatigue damage is roughly proportional to load raised to the fourth power (see Appendix B and C).
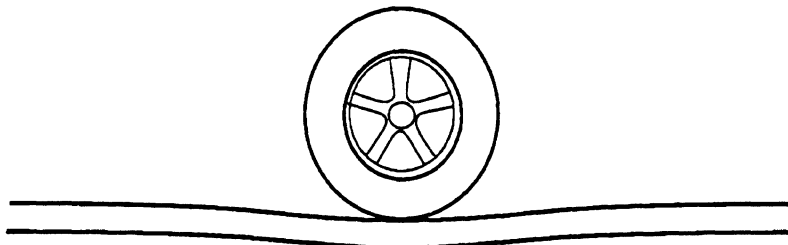
Figure 6. Deflection basin under a loaded wheel.

The damage from axle load is evaluated at the static loading of the axles. Dynamic loads on an axle contribute to damage but are dependent on speed, suspension properties, and tire properties, all of which are independent of the static axle load. Therefore, the damage associated with the "static load footprint" of the vehicle is evaluated here. The influence of speed, suspension, and tire factors are treated under separate sections of the report.

Rigid Pavement Fatigue

Damage to the pavement is dominated by fatigue arising from the peak cycles of longitudinal stress at the bottom of the slab, under the center of the path travelled by the tires on each side of the vehicle. Figure 7 shows one such stress cycle generated at the bottom of a 10-in thick slab by an isolated 18-kip axle moved slowly over the point. The shape of the deflection basin dictates that the stress is compressive in direction during the approach or departure from the location of interest. The compressive stresses are relatively low in magnitude and are not particularly damaging because of the high strength of Portland Cement Concrete in compression. Rather, the primary damage occurs when the wheel is directly over the location of interest because the tensile stress is much higher than the compressive stress, and concrete is very weak in tension. The stress cycle in Figure 7 is representative of a continuous reinforced concrete pavement, or the mid-slab of a jointed pavement. Near joints the stress cycle is not symmetrical, although the peak tensile stress still occurs when the wheel is directly over the point of interest. More detail on stress variations along the slab are provided in the Rigid Pavement section of this chapter.
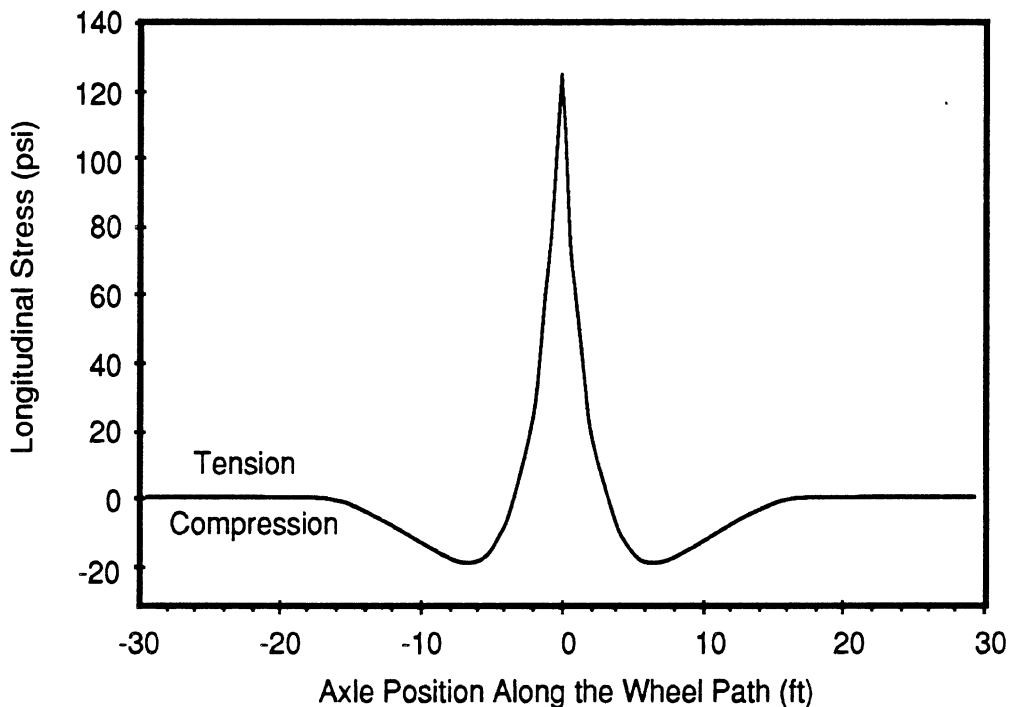
Figure 7. Stress at the bottom of a rigid pavement slab imposed by a passing axle.

With single axles that are well separated from other axles, the stress cycle closely follows that shown in Figure 7, with some distortion due to variations in load arising from truck dynamics. The peak stress under a single axle is proportional to its load, and the damage is proportional to load raised to the fourth power (see Appendix B). Thus, fatigue of rigid pavement is highly dependent on axle load. A single axle loaded to 20 kips is 16 times as damaging as a single axle loaded to 10 kips.

At a fixed tire inflation pressure variations in axle load also cause changes in tire contact area. However, tires that carry higher loads need to be inflated to higher pressures (4). Overall, the specified tire pressures increase with load rating such that the contact area is effectively constant. Therefore, contact area is held constant in these calculations.

Figure 8 shows how relative fatigue on a 10-in thick pavement varies with load for single, tandem, and tridem axle groups. Axles of multiple axle groups are spaced 4.25 ft apart in these calculations and have the same static load (perfect load sharing). Note that, by definition, the ESAL for a single axle loaded to 18-kip load is unity. With multiple axles in close proximity, the stress cycles are modified by beneficial interactions between the loading points as described later in the section Axle Spacing, with the result that axles on a tandem suspension are less damaging than the same two axles, similarly loaded, but spread far apart. As seen in Figure 8, a tandem set loaded to carry 36 kips (18 kips on each axle) does not correspond to two ESALs, but instead accounts for only 1.4 ESALs. This is not in agreement with the AASHTO Design Guide for Pavement Structures (5) which states that the load equivalency factors for a tandem axle loaded to 36 kips range from 2.41-2.53
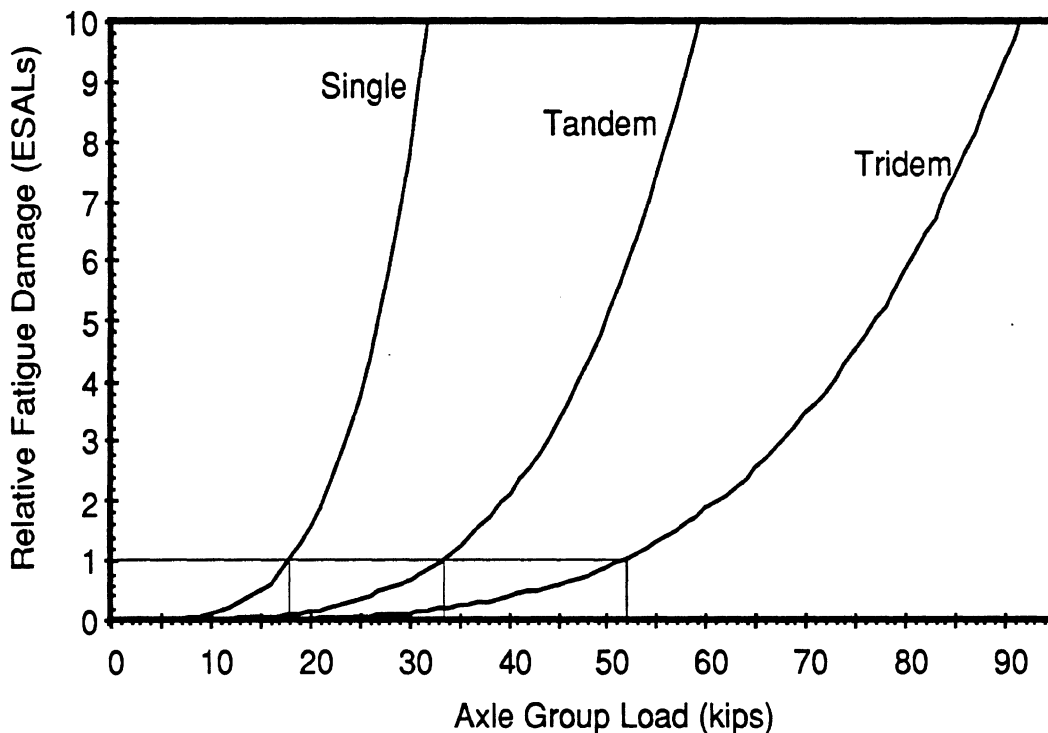
Figure 8. Relative fatigue of rigid pavement vs. axle load.

for rigid pavement. The discrepancy is partially explained in the Axle Spacing section of this chapter, but is mostly attributed to the fact that the AASHTO equivalency factors are based on empirical methodology that emphasizes terminal serviceability, and includes environmental factors and other variables. The methodology in this research is one in which damage is related only to stresses in the pavement structure.

A tandem axle loaded to 33 kips and a tridem loaded to 52 kips are both below 1 ESAL. This result will change when axle spacing or pavement thickness is varied, but it demonstrates that spreading the load over several axles and keeping individual axle loads low will significantly reduce rigid pavement fatigue.

Overall, the power of the fatigue law has a profound influence on the significance of axle loads. In the case of the fourth-power law, doubling the axle load increases fatigue by a factor of 16. However, if a power of 3.29 is used in the damage law as has been suggested by others (6), doubling the axle load increases fatigue by a factor of only 9.8. In the assessment of load-induced damage, one must recognize that the current knowledge about fatigue of rigid pavements is too limited to allow precise predictions on an absolute scale.

Flexible Pavement Fatigue

Fatigue damage to flexible pavement is predominantly caused by cyclic longitudinal strain at the bottom of the wear course. Strain cycles created by a loaded wheel on a flexible pavement are very similar to those experienced on rigid pavements, but their area of influence is much smaller. Figure 9 shows a typical strain cycle on the bottom of a 5-in wear course as a single isolated axle goes by. Note that at a distance of 4 ft from the point of loading, there is only a small influence on the longitudinal strain. Thus, the beneficial effects of closely-spaced axles are not nearly as significant as is the case for rigid pavements. Figure 10 shows how relative fatigue on a 5-in thick surface layer varies with load for single, tandem, and tridem axle groups. Axles of multiple axle groups are 4.25 ft apart in these calculations and have perfect static load sharing.

The strain cycle level imposed by a single axle is proportional to its load, and the fatigue damage is proportional to load raised to the fourth power (see Appendix C). Thus, fatigue of a flexible pavement is highly dependent on axle load. A single axle loaded to 20 kips is 16 times as damaging as a single axle loaded to 10 kips. Because the pavement structure does not transmit significant strains as far as the distance between axles for the range of pavement strengths studied, two axles in a tandem suspension have the same effect as two independent axles. Consequently, the figure shows that a 36-kip tandem is simply equivalent to 2 ESALs. This is not in agreement with the AASHTO Design Guide of Pavement Structures (5) which states that the load equivalency factor for a tandem axle loaded to 36 kips is 1.38 for flexible pavement. The discrepancy is attributed to the fact that the AASHTO equivalency factors are based on empirical methodology, that includes environmental factors and other variables. The methodology in this research is one in which fatigue damage is related only to strains in the pavement structure.
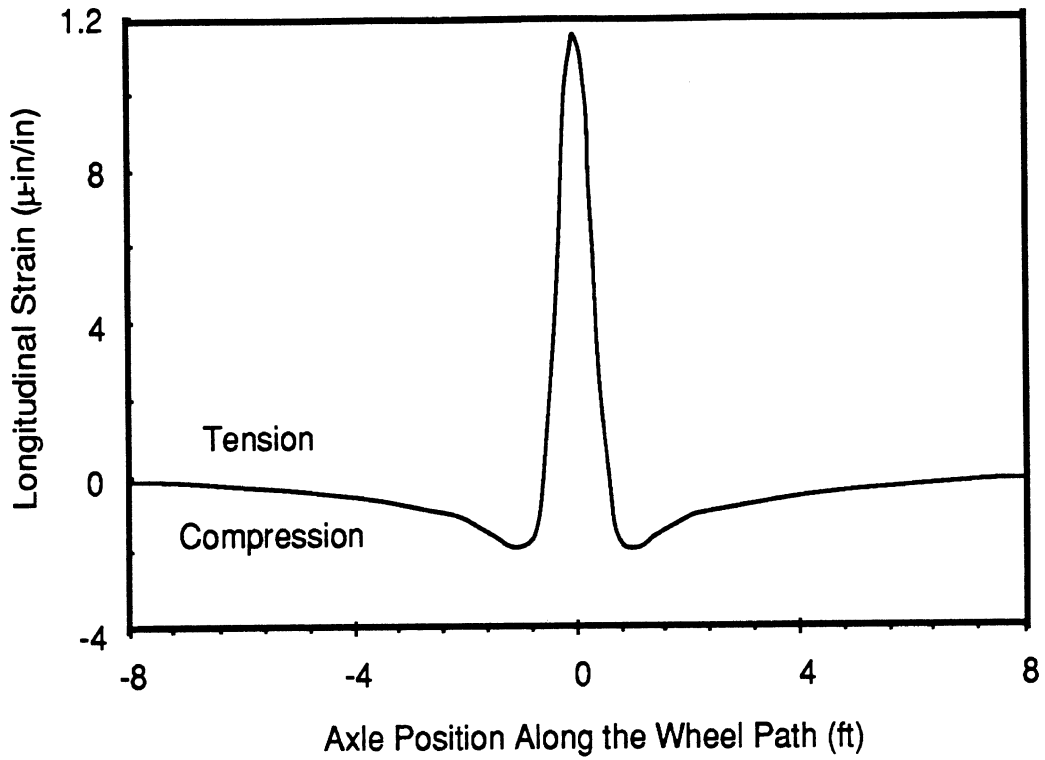
Figure 9. Strain under the wear course of a flexible pavement imposed by a passing axle.
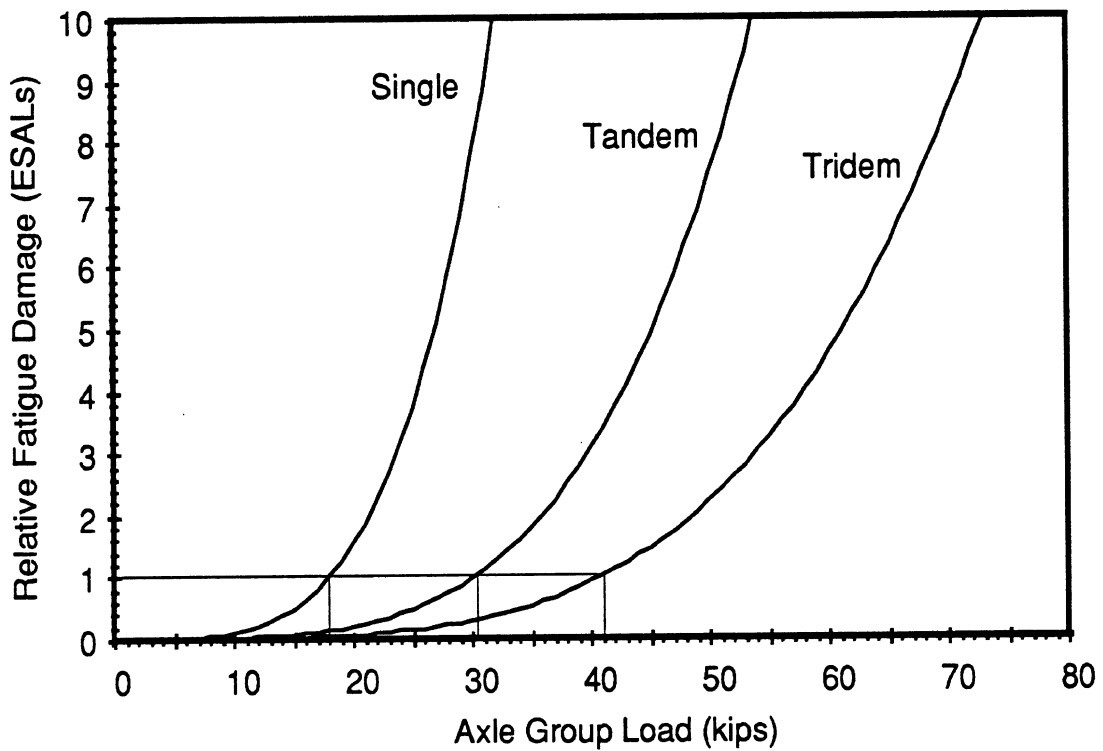
Figure 10. Relative fatigue of flexible pavement vs. axle load.

A tandem axle loaded to 30 kips and a tridem loaded to 41 kips are both below 1 ESAL. This demonstrates that spreading the load over several axles and keeping individual axle loads low will significantly reduce flexible pavement fatigue.

Overall, the power of the fatigue law has a profound influence on the significance of axle loads. In the case of the 4th power law, doubling the axle load increases fatigue by a factor of 16. Fatigue law exponents suggested for flexible pavements have a range of 2-6 (7). Doubling the axle load under a power of 3.5 increases fatigue by a factor of only 11.3. In the assessment of axle load damage, one must recognize that the current knowledge about fatigue of flexible pavements is too limited to allow precise predictions on an absolute scale.

Rutting

The rut depth caused by a passing axle is assumed to arise from linear plastic deformation of the pavement layers (see Appendix C). It is calculated by integrating under the influence function scaled proportionally by the axle load (and inversely by the speed). Thus, the incremental increase in rut depth from a single axle predicted by this method is simply proportional to axle load.

Gross Weight

In the public eye, there is the perception that large trucks damage the road system by virtue of their weight. However, analyses of the damage mechanisms show that gross weight is not directly linked with fatigue damage of either rigid or flexible pavements. That is, it is not the total weight of the truck that "breaks-up" the road, but rather it is high axle loads. High gross weights can be tolerated by the road system if distributed uniformly among a sufficient number of axles. In the case of rutting, damage per vehicle pass increases with gross weight. However, heavier vehicles are more favorable because a larger fraction of gross vehicle weight is cargo, and less rutting damage is incurred for each pound of cargo transported.

Rigid Pavement Fatigue

Given the existing variations in individual axle loads, gross vehicle weight is not systematically related to fatigue of rigid pavements except to the extent that an increase in gross weight might be linked to higher individual axle loads or more axles of a given maximum load.

Figure 11 shows how different truck types compare in causing fatigue damage to a thin pavement (slab thickness of 7 inches on an 8-inch granular subbase), and a thick pavement (slab thickness of 12 inches on an 8-inch granular subbase). The fatigue damage from one pass of each vehicle with the axles at their static loads is plotted in terms of ESALs. The figure demonstrates that a vehicle with a very high gross weight may fatigue the pavement much less than a lighter vehicle if its load is distributed over multiple axles so that the individual axle loads are low. In an extreme example, the top vehicle, a 3-axle refuse hauler loaded to 64-kips, causes nearly 3.5 times as much fatigue as a 114-kip, 9-axle Turner vehicle (near the bottom of the figure). The axles of the Turner vehicle are all loaded to 13

kips or less, whereas the refuse hauler has two axles loaded to 22 kips and one loaded to 20 kips. (See Appendix D for details on the truck axle loads.)
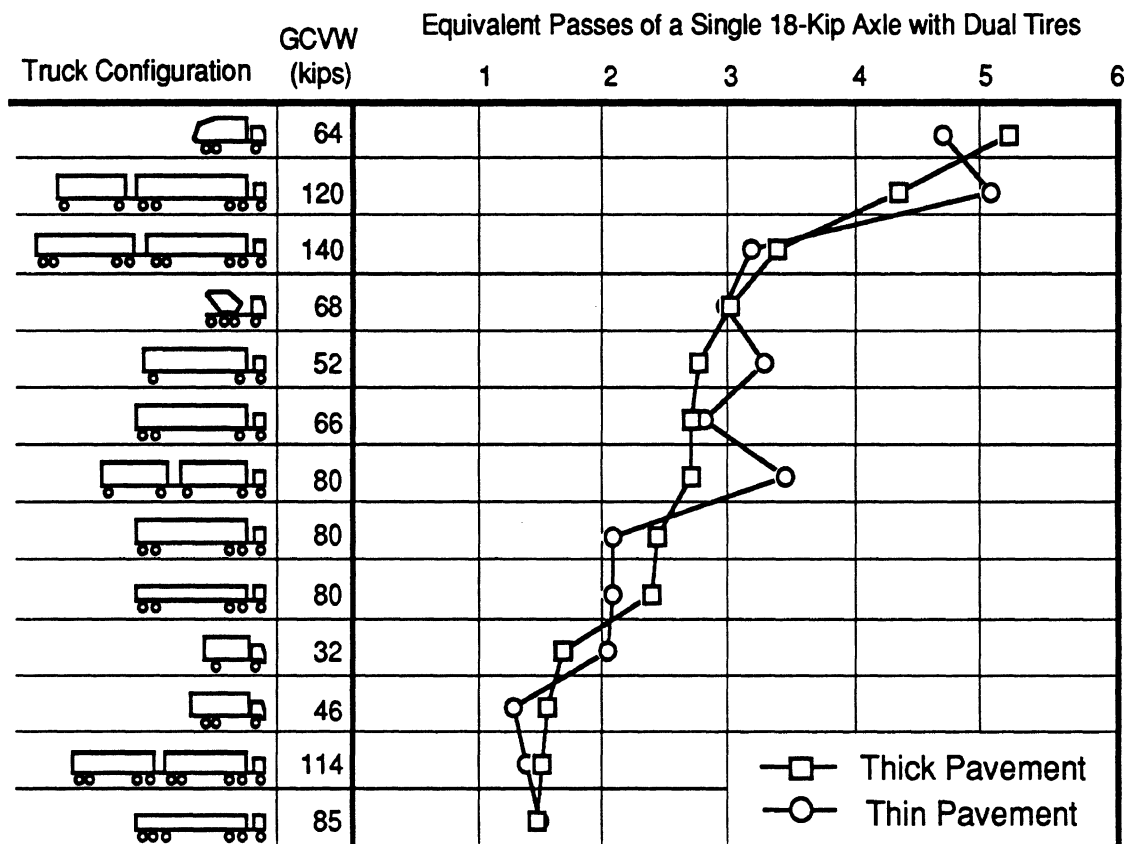
Figure 11. Relative rigid pavement fatigue over a range of trucks and pavement thicknesses.

Cases do exist in which many axles at low load are more damaging than a few axles at higher load. The number of axles at low load required to cause more fatigue damage than a few axles at higher load depends on the power of the fatigue law applied to the pavement. As the power of the fatigue law increases, the damage caused by lightly-loaded axles becomes less significant compared to heavier axles. Thus, fatigue laws with higher exponents increase the importance of individual axle loads and diminish the relevance of gross vehicle weight.

Note that relative damage shown in Figure 11 is nearly equivalent for thin and thick pavements, even though the absolute damage levels are much greater for the thin pavement. In part, this is because relative damage levels shown for the thin pavement are normalized by a single 18-kip axle traversing the thin pavement, and relative damage levels for the thick pavement are normalized by the 18-kip reference traversing the thick pavement. It should also be noted that the pavements were both continuous reinforced concrete. Damage evaluation on jointed pavement is more complex because variations in load transfer properties at the joints complicate the interaction between adjacent truck axles. This issue is addressed in the Rigid Pavement section.

Flexible Pavement Fatigue

As was the case for rigid pavement fatigue, gross vehicle weight is not systematically related to fatigue of flexible pavements except to the extent that an increase in gross weight might be linked to higher individual axle loads or more axles of a given maximum load. Figure 12 shows how different truck types compare in causing fatigue damage to flexible pavements of various wear course thicknesses.
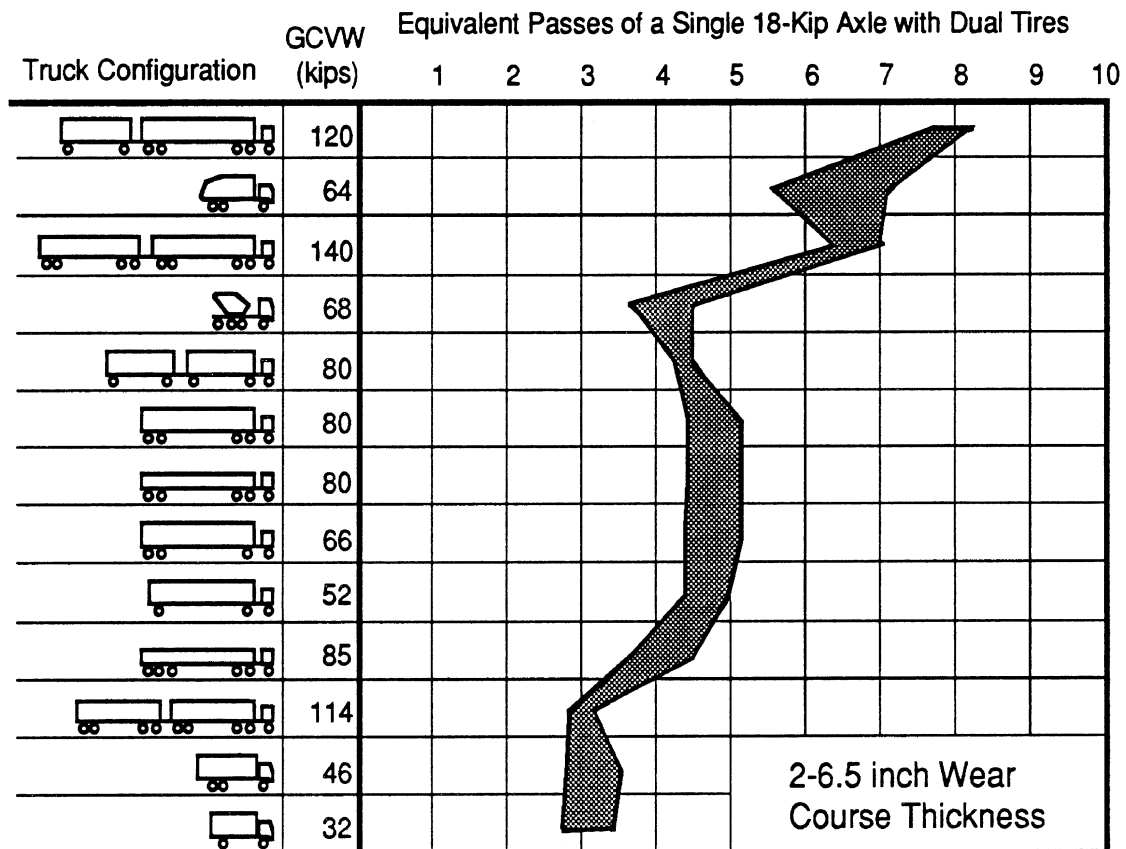
Figure 12. Relative flexible pavement fatigue over a range of trucks and pavement wear course thicknesses.

The fatigue damage from one pass of each vehicle with the axle loads at their static values is plotted in terms of ESALs. Note that the relative damage is greater on thin pavements, and ranking of the trucks relative to their damage can change for the different pavement designs. This is because the damaging potential of conventional single and wide-base single tires relative to dual tires changes with pavement thickness. As a result, fatigue damage from the steer axle (with single tires) increases as pavement thickness decreases. The contribution of the steer axle is significant, even at a load of 12 kips. For example, the 12-kip steer axle of the 5-axle tractor-semitrailer is responsible for 36% of the damage caused by the whole vehicle to the pavement with a 2-inch thick wear course. Thus, when the damage caused by the steer axle diminishes, so does that caused by the whole vehicle. An example of the influence of the steer axle on relative damage is seen with the Turner vehicle (3rd from the bottom). It has steer axle loaded to only 10 kips. The damage relative

to an 18-kip axle with dual tires caused by the Turner vehicle changes much less with wear course thickness than the other vehicles with 12-kip steer axles shown in the figure.

Figure 12 shows that a vehicle with a very high gross weight may fatigue the pavement much less than a lighter vehicle if its load is distributed over several axles so that the individual axle loads are low. In an extreme example, a 64-kip, 3-axle refuse hauler causes over twice as much fatigue as a 114-kip, 9-axle Turner vehicle to a pavement with a 3-in thick wear course. The axles of the Turner vehicle are all loaded to 13 kips or less, whereas the refuse hauler has two axles loaded to 22 kips and one loaded to 20 kips.

As was found for rigid pavements, cases do exist in which several axles at low load are more damaging than a few axles at higher load. Also, the nature of the damage law is critical in determining trade-offs between damage from a few axles at high loads or many at reduced loads. Fatigue laws that are based on higher exponents increase the importance of individual axle loads and diminish the relevance of gross vehicle weight.

Rutting

Gross weight is the main determinant of rutting per vehicle pass. The results of the study, summarized in Figure 13, show that the total vehicle weight governs the rutting damage. This is because a linear integration method (see Appendix C) is used to determine rut depth. As the permanent vertical deformation under one axle is not affected by other nearby axles, the rut depth caused by a truck is simply the sum of the rutting caused by each of its axles. Although gross weight is the first-order determinant of rutting, exact proportionality is not obtained because of differences in rutting among the mix of tires used on the vehicles.

Figure 13 shows the rut depth caused by the trucks in the matrix (Appendix D) with their axle loads held to their static values as if they were running over a perfectly smooth road. The thick line represents the range of relative damage induced by each truck over a range of wear course thicknesses from 2 to 6.5 in.

The analysis indicates that the gross weight of a truck is a dominant factor affecting rutting when it is assumed that rutting arises from viscoelastic behavior that leads to plastic deformation. However, it is inappropriate to conclude that rutting can be reduced by limiting the gross weight of trucks. Inasmuch as cargo must be transported by highways, reducing truck loads would require more trucks to carry the same tonnage. In the process the tare weight of the additional transport vehicles would increase the road's exposure to rutting mechanisms. The fact that payload is a higher percentage of truck weight with larger truck combinations favors larger vehicles as means to reduce rutting.

Axle Spacing

The influence of axle spacing on pavement wear depends on the degree to which the response under one axle is affected by the response induced by a nearby axle. Rigid pavements distribute loads over distances that are on the same order as common axle spacings. Therefore, axle spacing is a factor in determining rigid pavement fatigue. On the other hand, stresses are more localized in the wear course of flexible pavements, with the effect that axle spacing has little effect on their damage.

Truck Configuration	GCVW (kips)	Equivalent Passes of a Single 18-Kip Axle with Dual Tires
	140	
	120	
	114	
	85	
	80	
	80	
	80	
	68	
	66	
	64	
	52	
	46	
	32	

2-6.5 inch Wear Course Thickness
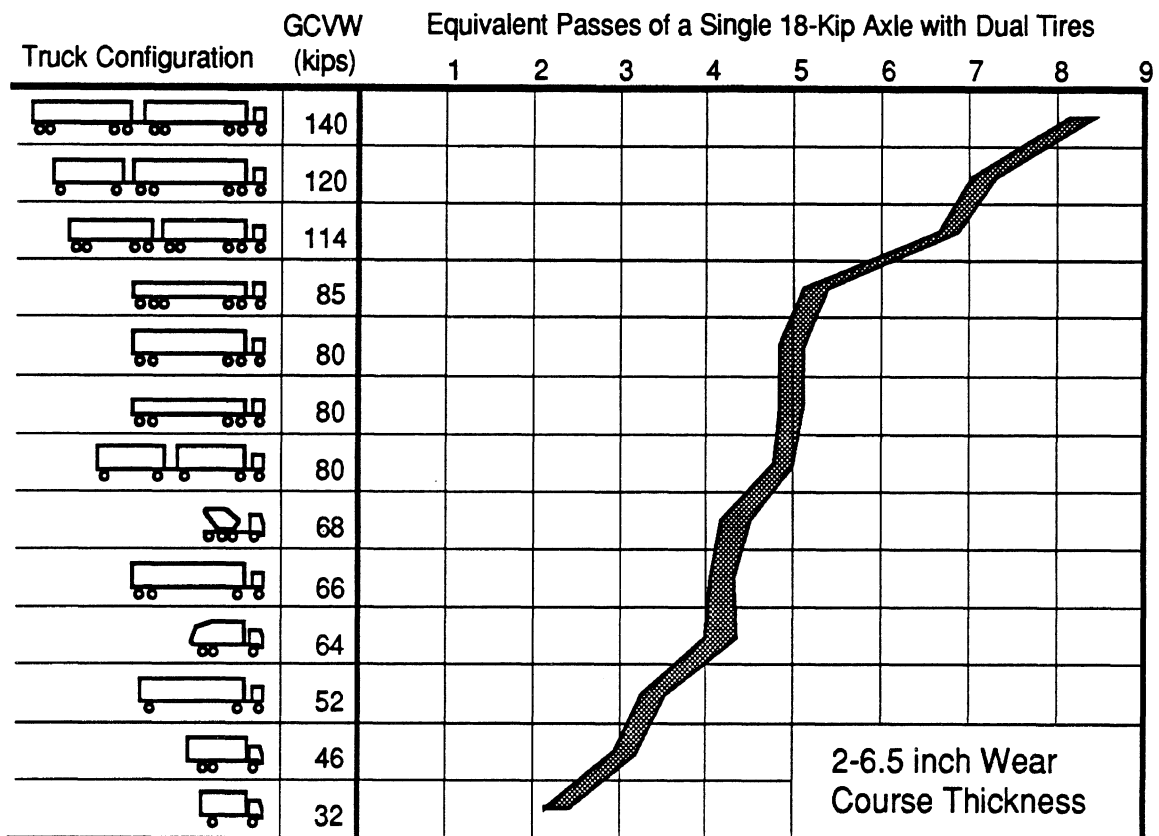
Figure 13. Rut depth production expressed as ESAL exposure per pass deriving over a range of trucks and pavement wear course thickness.

Rigid Pavement Fatigue

Figure 14 illustrates the longitudinal stress pattern under the slab of a rigid pavement caused by a 3-axle truck with a 12-kip front axle load and a 34-kip tandem. The largest tensile stresses are directly under the tandem axles, however, the peak stresses are not proportional to axle load. The 17-kip load on each rear axle causes peak stress levels only slightly larger than that of the 12-kip front axle. The reason is that the some of the tensile stress under one tandem axle is reduced by compressive stress induced in that region of the pavement by the other axle.

The interaction between closely-spaced axles can be explained by the shape of the influence function. Figure 15 shows the longitudinal stress influence function for wheel load on a typical rigid pavement (10-inch slab on a 8-inch granular subbase). If the spacing between two axles is between 3.25 and 15 ft, the peak tensile stress under one axle benefits from compressive stress due to the other axle. On the other hand, if an axle is located in the tensile range of the influence function, which is between 0 and 3.25 ft, the interaction between axles increases the peak tensile stress under each axle. Fortunately, the tensile range of the influence functions for rigid pavements is nearly always under 4 ft. Given current sizes of truck tires, it is not possible to locate axles closer than 4 ft, so the tandem axles benefit from the compressive region of the influence function. The optimal axle spacing for this pavement design is 6.75 ft. At this spacing the influence function has a
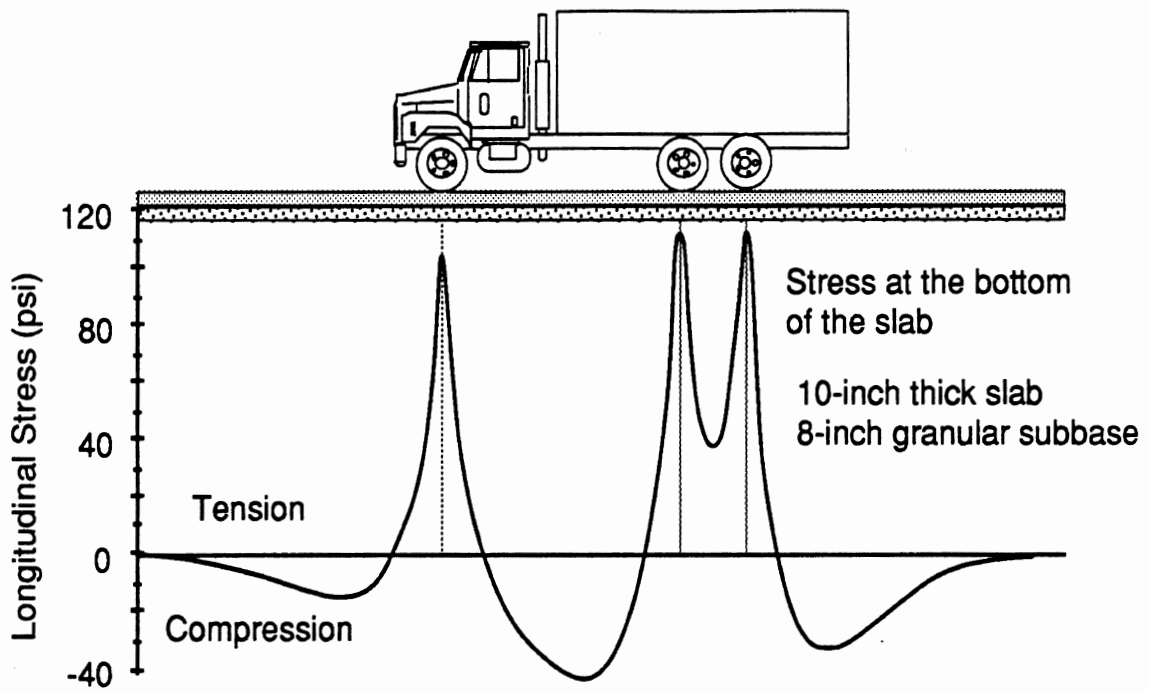
Figure 14. Stress imposed under a rigid pavement slab by a 3-axle truck.
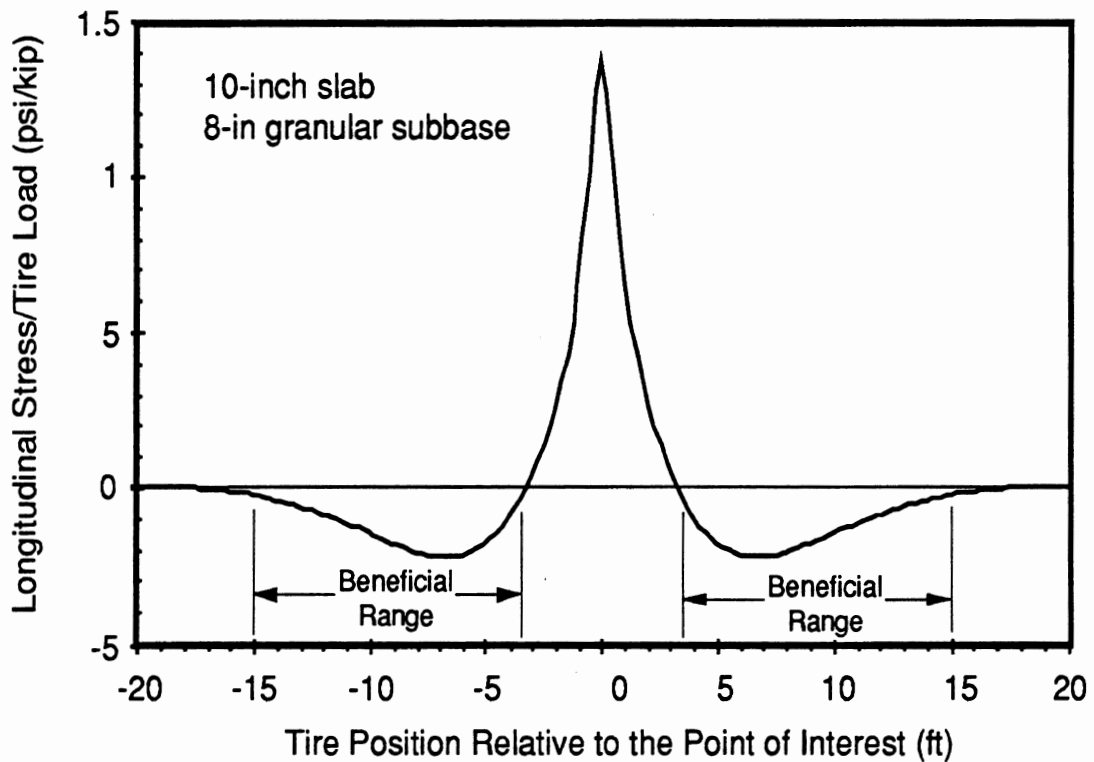
Figure 15. Influence function for a 10-in thick rigid pavement.

27

compressive value that is 16% of the peak tensile value directly under the tire. This means that if equally-loaded axles are spaced at 6.75 ft on this pavement, the peak tensile stress under each of them will be reduced to 84% of the peak tensile value that would prevail if they were acting individually. Consequently, the damage caused by a 36-kip tandem would be equivalent to 1.02 passes of a single 18-kip axle. That is, 36 kip can be carried on two axles with no more damage than 18 kip on one. On this pavement, the common tandem spacing of 4.25 ft produces the benefit of a 9% reduction in peak tensile stress under each axle. This corresponds to a 30% reduction in the total damage caused by the two axles. Hence a 36-kip tandem with a 4.25-ft spacing generates only 1.40 ESALs.

Pavement thickness is a factor that determines, in part, the optimal axle spacing, range of beneficial spacings, and the degree to which the spacings are beneficial. Figure 16 shows how relative fatigue damage caused by a tandem axle varies with axle spacing on a thick pavement and a thin pavement. The thin pavement has a slab thickness of 7 inches and an 8-inch granular subbase. The thick pavement has a slab thickness of 12 inches and an 8-inch granular subbase. The optimal spacing for the thick pavement is 8 feet, in comparison to an optimal spacing of 5 feet for the thin pavement. The optimal spacing is larger on thick pavements because they distribute loads over a wider span than thin pavements, so the influence function is wider. In the figure, a beneficial spacing is one for which the relative fatigue damage is less than 2 ESALs (the equivalent of the two axles acting individually). It is evident that the close spacing used on most tandem axles (4.0 to 4.25 ft) is not optimal for rigid pavements. On thin pavements where damage is most critical, tandems with a 5-ft spacing could reduce damage by about 10% from current levels. On thicker pavements, greater benefits can be gained.
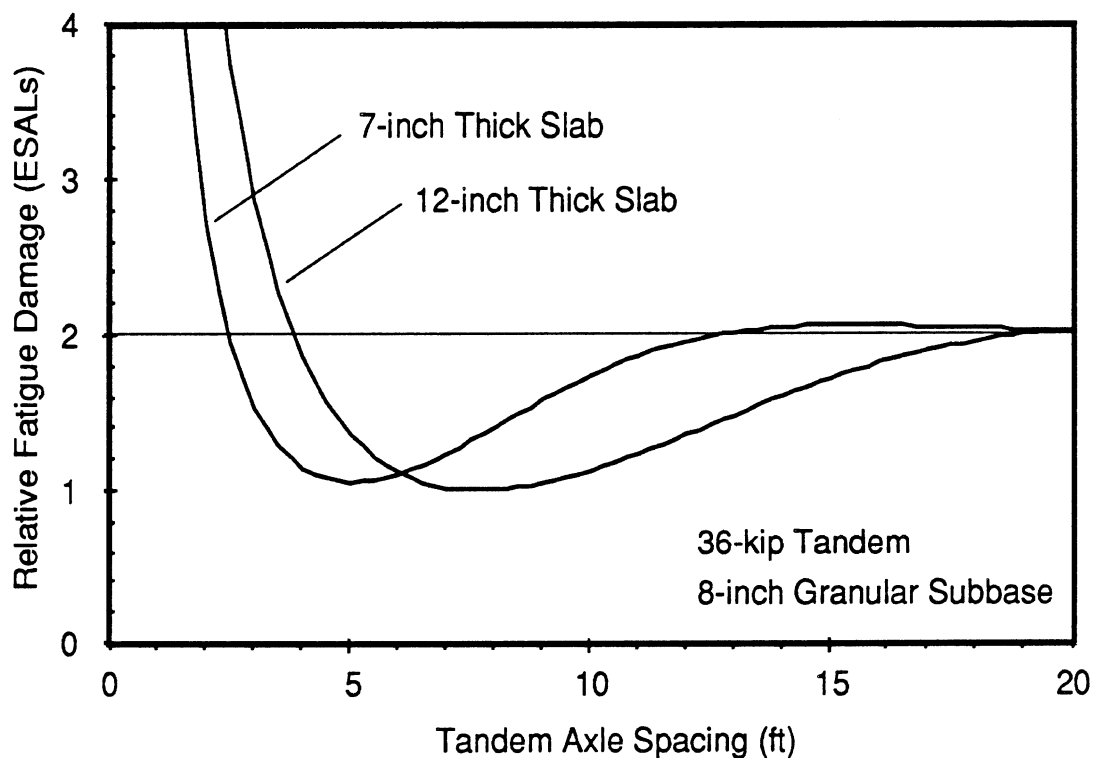
Figure 16. Influence of tandem axle spacing on rigid pavement fatigue.

Figure 17 shows how tridem axle spacing affects pavement fatigue. In the figure, the spacing on a tridem is defined as the distance between two adjacent axles. ESALs of less than 3 indicate beneficial spacings at which the three axles are less damaging than three individual axles at the same load. Note that a 54-kip tridem with a spacing in the 4-ft range are no more damaging than a single 18-kip axle on a thin pavement.
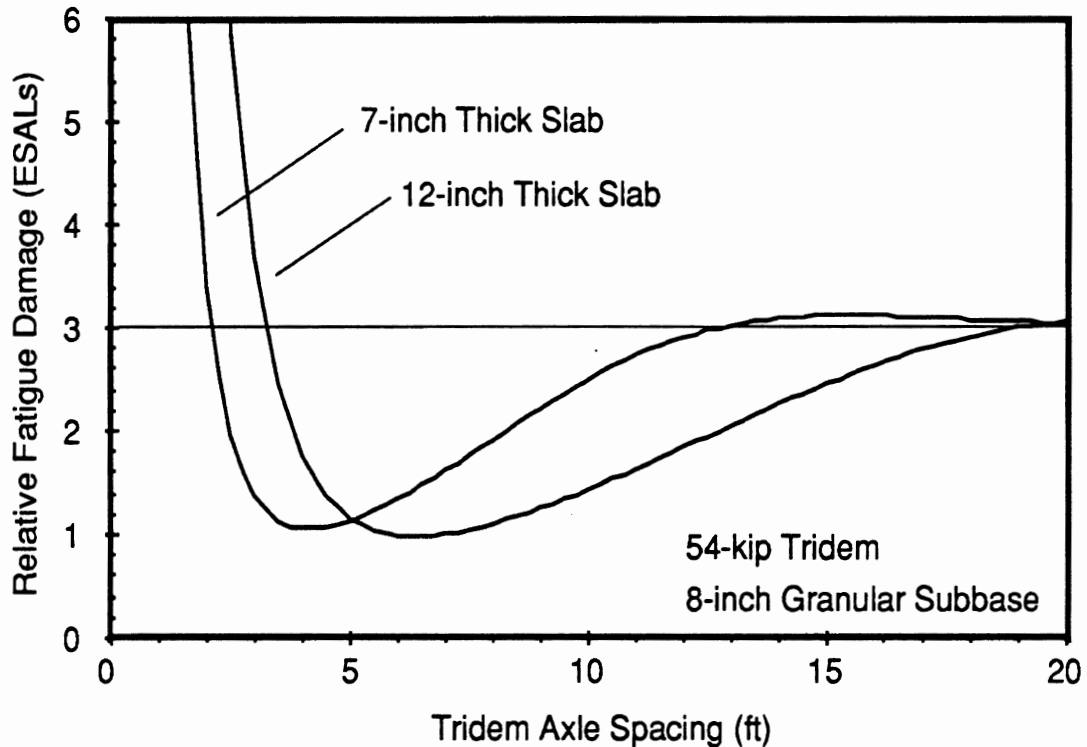
Figure 17. Influence of tridem axle spacing on rigid pavement fatigue.

In summary, tandem spacings of 3.5 to 15 ft on 34-kip tandem axles are less damaging to thin rigid pavements than a 20-kip single axle (the maximum axle load permitted by road use laws). On thick pavements, spacings of 5 to 20 ft on 34-kip tandem axles are less damaging than a single 20-kip axle.

Flexible Pavement Fatigue

Flexible pavement fatigue is hardly affected by axle spacing for the range of wear course thicknesses considered because the pavement structure does not distribute stress far enough in the top layer for the responses of different axles to interact significantly. Figure 18 shows the relative fatigue damage from a 34-kip tandem axle when axle spacing is varied. There is essentially no influence on damage with a 3-inch wear course at a 4-foot spacing, the minimum practical axle spacing. Even in the most extreme cases investigated, it was found that flexible pavement fatigue was changed by only 4% due to the effect of axle spacing. Thus, it is reasonable to ignore axle spacing and simply assess fatigue damage on flexible pavements on the basis of individual axles.

29
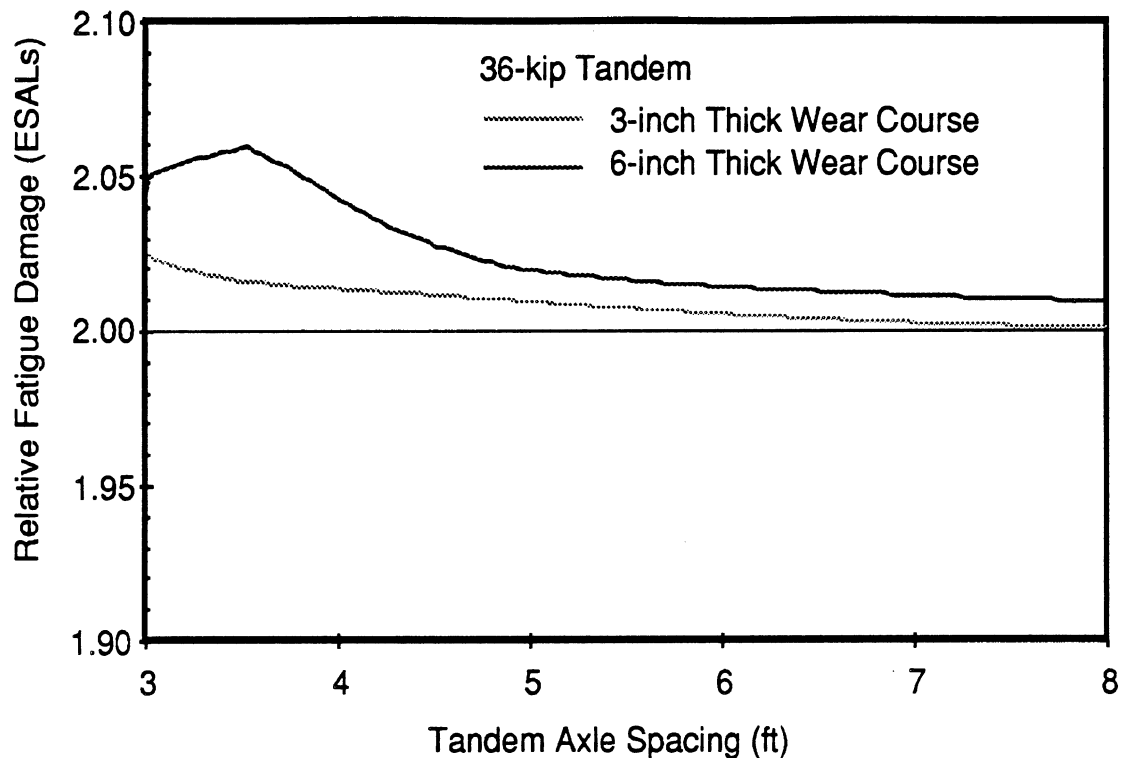
Figure 18. Influence of tandem axle spacing on relative flexible pavement fatigue.

Rutting

Axle spacing does not affect surface rutting because the range of influence of a tire on surface rutting is less than 20 inches, which is much smaller than any practical axle spacing.

Static Load Sharing

Most tandem and tridem truck suspensions are designed to equalize the static loads carried by the axles in a group. In practice, the effectiveness of load equalization on moving vehicles varies significantly among suspensions.

Sweatman (*8*) characterized load sharing performance by a "Load Sharing Coefficient" (LSC), defined as:

$$\text{LSC} = \frac{\text{Mean measured wheel load}}{\text{(Total group static load/Number of wheels in group)}}. \tag{2-1}$$

The LSC is unity for perfect load sharing. Poor static load sharing leads to an elevated load on one axle of a tandem and a diminished load on the other. Experimental tests indicate that the load sharing is not perfect during normal on-road operation. The imperfection arises from friction in the equalization linkages, inter-axle load transfer associated with braking or drive torques, etc. Typically the LSC (calculated for the heaviest axle) varies on-road in the range of 1.02 - 1.21 for tandem suspensions, i.e. 2% - 21% equalization error respectively. In this section, a range of 1 to 1.25 is used for LSC.

30

Rigid Pavement Fatigue

Rigid pavement fatigue increases with poor load equalization on tandem axles. The degree to which this occurs depends modestly on the tandem spread.

Poor load sharing increases rigid pavement damage because fatigue rises exponentially with axle load. Therefore, increasing the load on one axle of a tandem set causes a large increase in fatigue from that axle. The reduced load on the other axle reduces its contribution to fatigue, but not enough to offset the increase from the heavy axle.

Figure 19 shows how fatigue varies with LSC for a 34-kip tandem operating on a 10-inch rigid pavement with an 8-inch granular subbase. For LSC values under 1.05 (i.e., the load on the heavier axle of a tandem is no more than 5% above its share), rigid pavement fatigue remains relatively unchanged. For instance, a tandem axle at a spacing of 4.25 ft with an LSC of 1.05 causes about 2% more pavement damage than an equivalent tandem with perfect load sharing. Increasing the LSC of the same tandem set to 1.25 increases fatigue life consumption by 54%. The figure includes axles with tandem spreads of 4.25, 5, and 6 ft to illustrate the interaction of axle spacing and load sharing in determination of rigid pavement fatigue. Fatigue life consumption at perfect load sharing varies with axle spacing because the peak stress under one axle benefits from the compressive influence of the companion axle, as was described earlier in the "Axle Spacing" section.
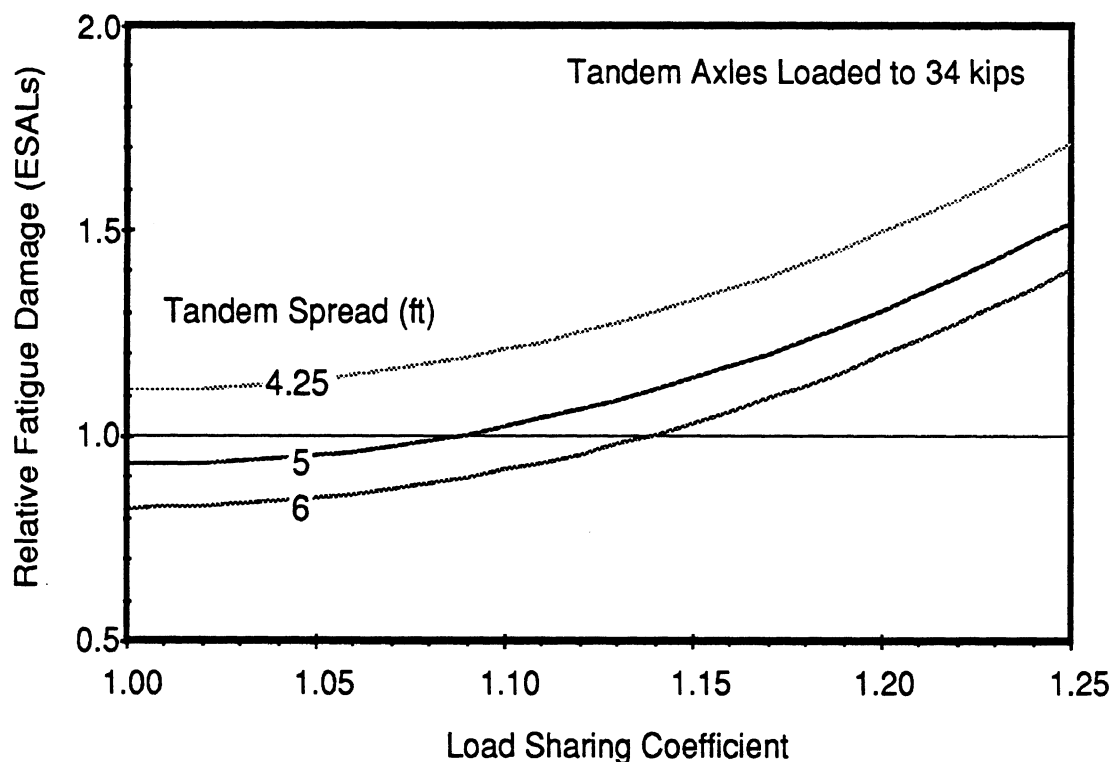
Figure 19. Influence of load sharing coefficient and tandem spread on rigid pavement fatigue.

If tandem LSCs are held at a reasonable level (less than 1.05) very little additional fatigue will result. When the LSC is allowed to exceed levels above 1.10, fatigue begins to increase rapidly. Thus, perfect static load sharing is not necessary, but a target level, such as LSC = 1.05, would eliminate any significant road wear from this mechanism.

Flexible Pavement Fatigue

Flexible pavement fatigue damage increases with poor load equalization on tandem axles. The effect is independent of axle spacing, but interacts somewhat with layer thickness.

Poor load sharing increases flexible pavement damage due to the exponential relationship between load and fatigue. Therefore, increasing the load on one axle of a tandem set causes a large increase in fatigue from that axle. The reduced load on the other axle reduces its contribution to fatigue, but not enough to offset the increase from the heavy axle.

Figure 20 shows how fatigue varies with LSC for a 34-kip tandem operating on flexible pavements of various wear course thicknesses. Damage rises more rapidly with LSC on the pavements with thinner surface layers (weaker pavements). For LSCs under 1.05, flexible pavement fatigue remains relatively unchanged. For instance, a tandem axle with a LSC of 1.05 causes about 6% more pavement fatigue than an equivalent tandem axle with perfect load sharing. Increasing the LSC of the same tandem set to 1.25 raises damage by 45% to 50%.
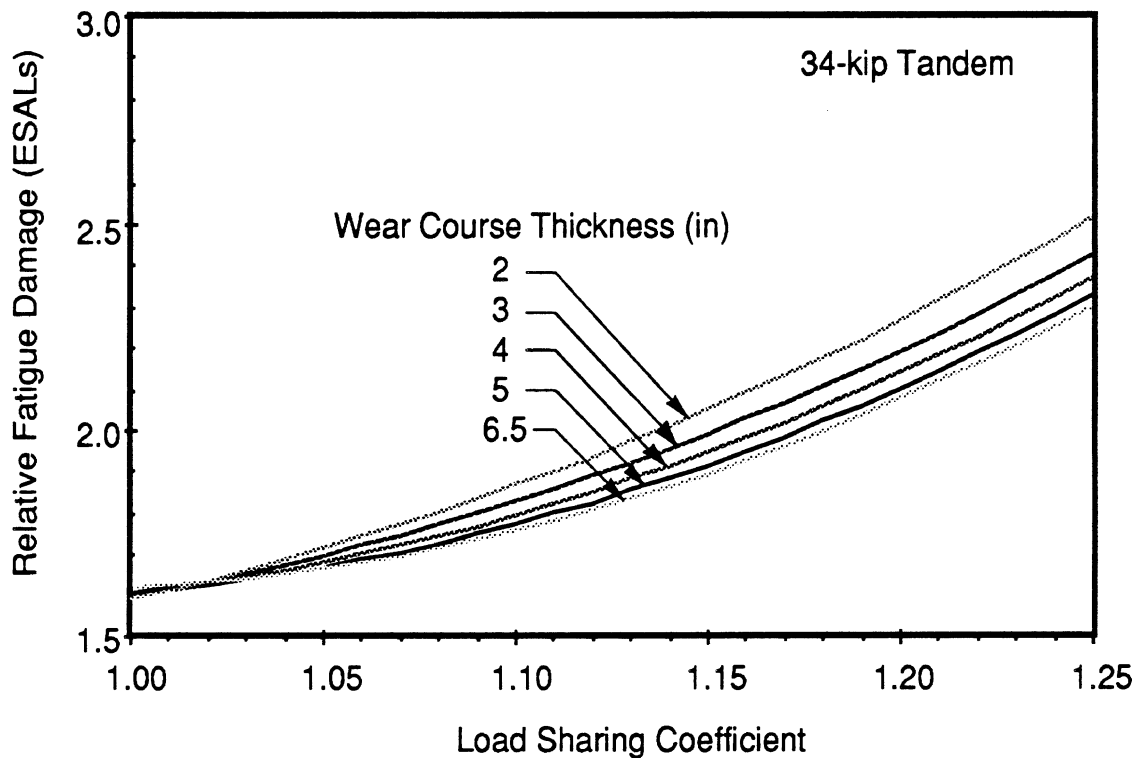
Figure 20. Influence of load sharing coefficient and wear course thickness on flexible pavement fatigue.

If tandem LSCs are held to less than 1.05, very little additional fatigue will result. When the LSC is allowed to exceed levels above 1.10 fatigue begins to increase rapidly. Thus, perfect static load sharing is not necessary, but a target level, such as LSC = 1.05, would eliminate any significant road wear from this mechanism.

Rutting

Rutting is modeled in this work as linear, plastic deformation of the pavement layers. With that model static load sharing among multiple axles has no effect on rut depth. Rutting is proportional to the total load on the axles, regardless of how it is distributed.

Speed

Speed is one of the most important factors influencing pavement damage arising from dynamics of a vehicle. The presence of the dynamic component of wheel loads elevates the mean value of fatigue damage along the pavement and is capable of elevating fatigue at the most severely loaded locations by a factor of more than 2 in some cases.

The influence of speed on dynamic wheel loads is well understood, but complex. When considering the dynamic response of a vehicle to road irregularities, the factors of speed and road roughness are inseparable. The speed determines how the roughness of the profile is "seen" by the moving vehicle. Further, axle spacing plays a role in this interaction. The dynamic inputs due to roughness, speed, and axle spacing cause vehicle vibrations and dynamic variations in wheel loads about the static value. Because the fatigue laws are highly nonlinear, occurrences of high dynamic loads in some locations are not fully compensated by occurrences of low loads in others, with the overall effect that pavement fatigue is accentuated. The degree to which dynamic loads increase pavement damage increases with the power of the fatigue law. If dynamic loads are spatially repeatable among trucks, the most severely loaded locations will wear much more quickly than they would if the dynamic loads are randomly distributed as a result of dynamic variations among trucks.

Speed alone has a second effect unique to damage of flexible pavements. Higher speeds reduce the time duration of wheel load on a given pavement location. The reduced exposure time can reduce fatigue and rutting of the viscoelastic material in flexible pavements.

Figure 21 shows a probability distribution of the instantaneous axle load carried by a typical truck axle in one of the simulated runs from the study. The distribution has a mean value, $\bar{F}$, which equals the static axle load. The distribution also has a standard deviation, σ. Normalizing the standard deviation by the static load defines a dimensionless variable called the Dynamic Load Coefficient (DLC) (*8*):

$$DLC = \frac{\sigma}{\bar{F}} \qquad (2\text{-}2)$$

DLC is a simple measure of the magnitude of the dynamic variation of axle load for a specific combination of road roughness and speed. As a point of reference, all axles of a truck moving over a perfectly smooth road would theoretically have DLC values close to zero. Maximum values of DLC have been observed in the range of 0.30-0.35 (*8,9*).
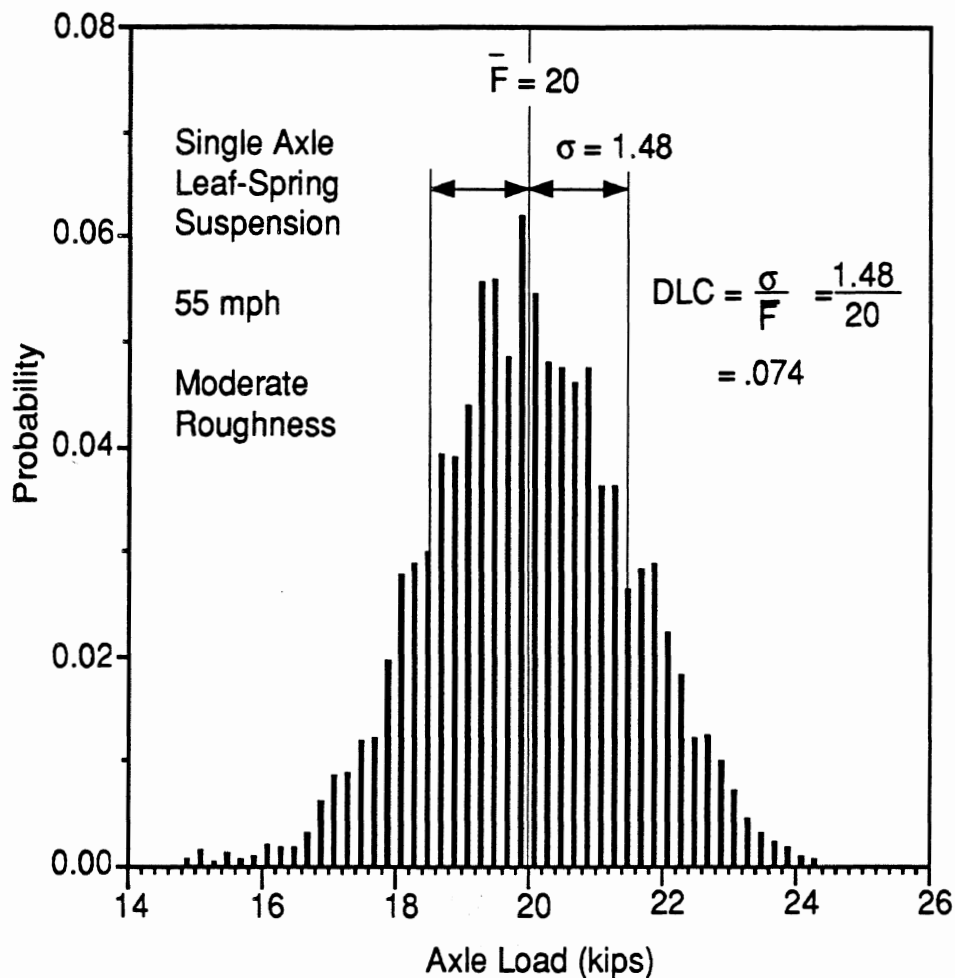
Figure 21. Probability distribution of dynamic load on an axle.

Simple Interaction Between Speed and Roughness

Speed and road roughness are inseparable in defining the dynamic input to a vehicle. Speed influences the input to the vehicle in two ways. First, variations in pavement elevation along the length of a travelled wheel path are "seen" by the vehicle as changes in elevation with time, with the relationship between longitudinal position and time defined by the vehicle speed. That is, the elevation Z, seen as a function of time, depends on profile and speed according to the relation:

$$Z(x) = Z(V, t) \qquad (2-3)$$

where $Z(x)$ is the profile as a function of longitudinal position, x, V is vehicle speed, and t is time. The influence of speed here is determined by the nature of the road roughness. For a road whose profile has statistics that exactly match an idealized model of the average road, it is possible to derive a relationship between speed and dynamic response. For many roads, the relationship is approximately that DLC and other response variables are proportional to the square root of speed (*9-12*). In general, however, the relationship depends on the spectral distribution of roughness over different wavelengths. For example,

Figure 22 shows how the DLC increases with speed for a typical 4-spring flat-leaf tandem suspension running over three different roads with International Roughness Index (IRI) levels of 80, 160, and 240 in/mi. The three roads used for the figure have broadly distributed roughness properties distributed over the full spectrum of wavelengths, with no peculiar roughness characteristics. Thus, the curves showing sensitivity to speed for these roads are well behaved.
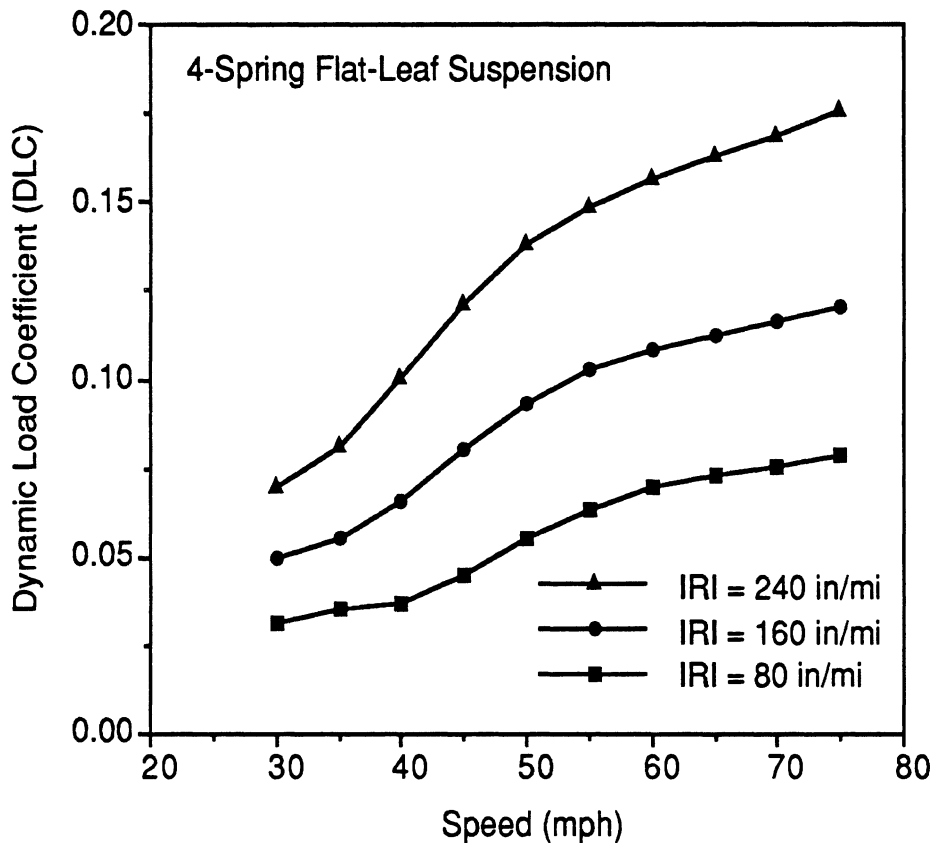
Figure 22. The general influence of speed on DLC.

Wheelbase Filtering

Axle spacing is also a factor in determining how speed interacts with profile roughness. The inputs to the various axles of a vehicle are not independent. When all tires on one side of the vehicle follow the same wheel path, the variations in elevation seen by one axle are simply delays of the variations seen under the preceding axle. The amount of the delay is the axle spacing divided by the vehicle speed. For example, if two axles are separated by 12 ft, and the vehicle is traveling at 72 ft/sec, the elevation under the second axle is exactly the same as the elevation that was under the front axle 12/72 (.1667) sec earlier. The delay due to axle spacing acts to "filter" the profile as a function of wavelength, as illustrated in Figure 23. For a sinusoidal input whose wavelength equals the axle spacing, both wheels are forced up and down together. For this wavelength, any vibration mode of the vehicle in which the axles move vertically "in phase" receives a full input. On the other hand, vibration modes in which the axles move vertically "out of phase" receives absolutely no input for the same wavelength. A completely opposite effect exists for wavelengths that are

twice the axle spacing. In this case, the vehicle receives zero input for modes in which the axles move "in phase," because the trailing axle receives an input that is exactly opposite of that of the leading axle. However, vehicle vibration modes in which the axles move "out of phase" receive maximum inputs.

spacing = wavelength
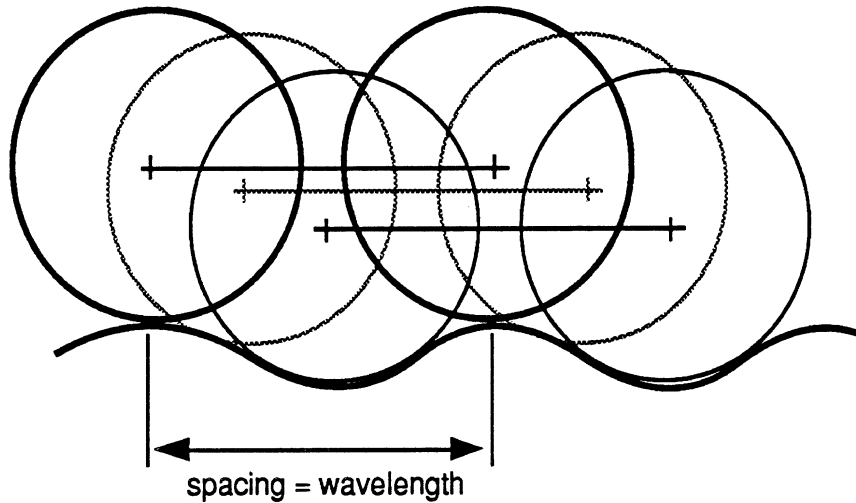
a. Full bounce response, no pitch

spacing = 1/2 wavelength
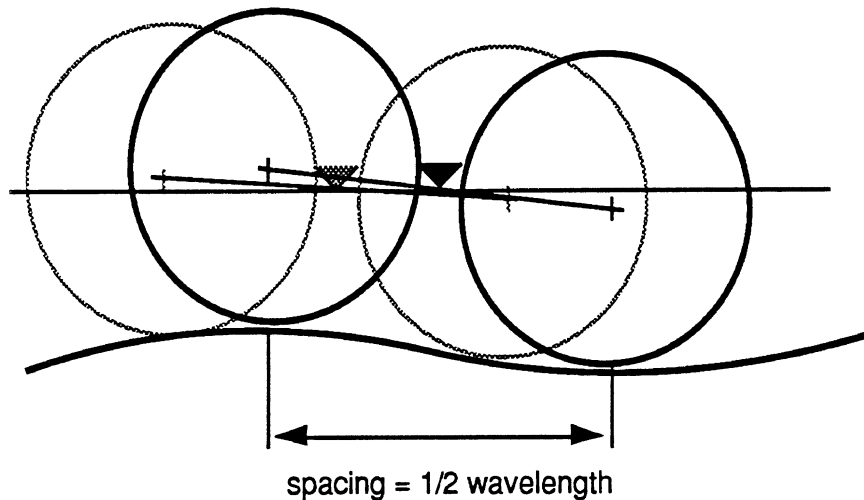
b. Full pitch response, no bounce

Figure 23. Wheelbase filtering.

The geometric influence of wheelbase filtering interacts with speed to influence the dynamic excitation to the vehicle. For axle spacing L and speed V, the vehicle receives a maximum "bounce" (in-phase) excitation at the frequency V/L, where L and V are expressed in appropriate units (length, length/time). At the same time, it is receiving maximum "pitch" (out-of-phase) excitation at the frequency V/(2L). For example, a vehicle with axle spacing of 12 ft traveling at 72 ft/sec receives a maximum bounce input at 6

cycle/sec and a maximum pitch input at 3 cycle/sec. When the vehicle travels at a speed where the wavelength associated with bounce is "seen" at a resonance frequency for a bounce mode of vibration, an amplified response can result. The same effect exists for pitch.

Figure 24 shows an example of a truck "tuning" to a road at a particular speed. In the figure, DLC is given as a function of speed for the drive and trailer axles of a 3-axle tractor-semitrailer traveling over a road of random roughness. Whereas the DLC is expected to rise continuously with speed due to the basic mechanics of road interaction with the vehicle, the DLCs of both axles exhibit a peak at 50 mph, particularly noticeable on the trailer axle. This indicates a resonant behavior of the trailer.
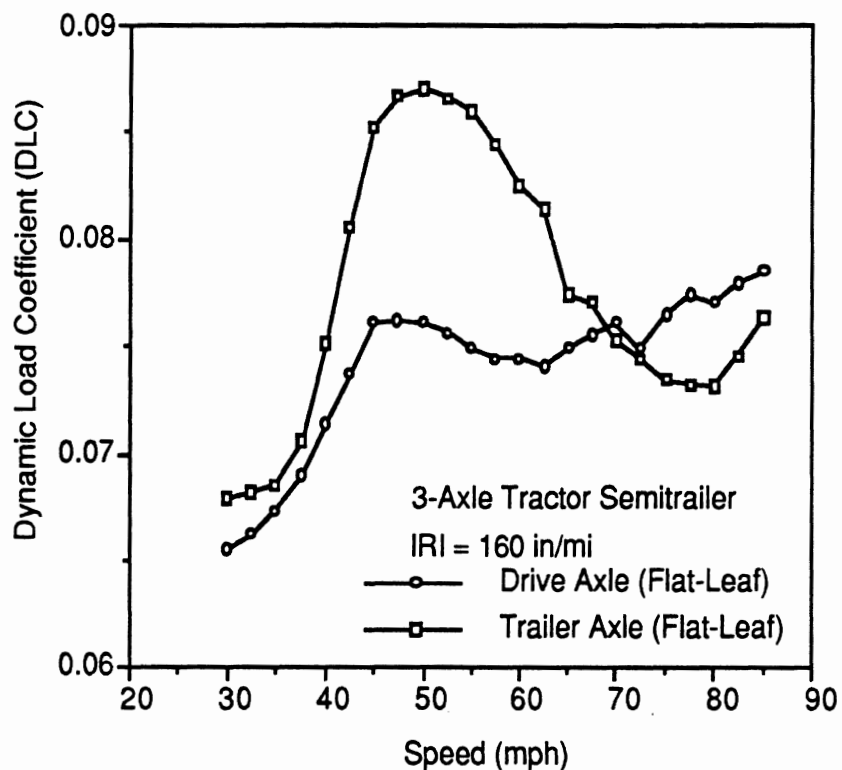
Figure 24. Example of a vehicle "tuning" to a road.

Rigid Pavement Fatigue

The effect of speed on rigid pavement fatigue is purely a consequence of load variations arising from dynamics of the vehicle, as described above, and the effect is not severe. There are no well-established damage mechanisms inherent to rigid pavements that are speed sensitive.

Speed affects rigid pavement fatigue by increasing the peak wheel loads applied to the pavement, which in turn elevate peak stresses and damage. The nonlinear relation between stress and fatigue implies that instances of high loading create more damage than can be compensated by instances of low loading. Thus, dynamic load changes increase the damage of the pavement when averaged along its length. This is demonstrated in Figure 25, which shows the relative fatigue damage caused by all axles of a 5-axle tractor-

semitrailer traveling at 55 mph over a 400 ft length of pavement of moderate roughness (IRI = 160 in/mi). The mean and "static" damage level are indicated with horizontal lines. They look to be about the same, but the mean damage level is actually 7% higher than the damage caused by the same truck with the axle loads held to their static values.

The pavement in Figure 25 is a continuous reinforced concrete pavement. If a jointed pavement was used, the "static" fatigue would vary along the length of each slab. This effect will be explained in the section on Rigid Pavement Factors. Because road roughness is spread more or less randomly over consecutive slabs, dynamic loading in response to that roughness is greater for some slabs than for others. Fatigue damage in the areas where high dynamic loads are imposed can be much greater than fatigue in other areas of the pavement.
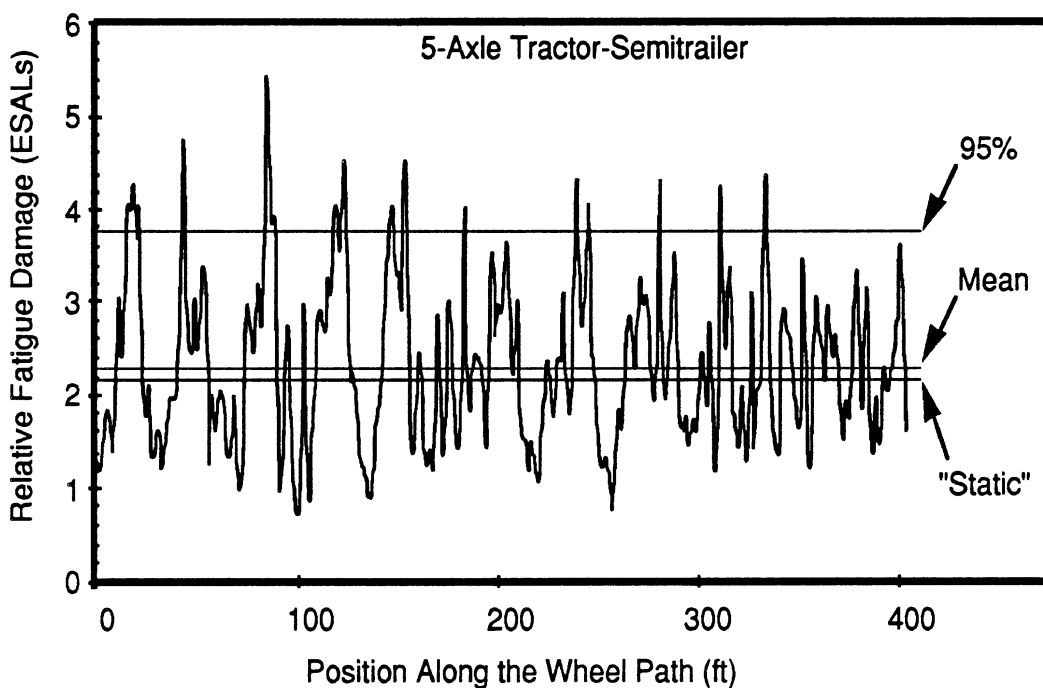
Figure 25. Fatigue damage along a continuous rigid pavement.

The effect of dynamic loads on fatigue was evaluated by considering the pavement locations that are subjected to the most severe loads. This is done by calculating pavement fatigue at regular intervals along the wheeltrack and compiling a probability distribution of the calculated fatigue values. The 95th percentile of the probability distribution was used for comparison of fatigue caused by variations in vehicle design, speed, and roughness. This represents the fatigue damage level sustained by the 5% of the pavement locations that are subjected to the most severe truck loads. Such a small portion of the overall pavement length was chosen because only 5% of the road surface area needs to fail before the road becomes unserviceable. In Figure 25, the 95th percentile damage level is indicated with a horizontal line. The implications of this criteria depend on the spatial repeatability of dynamic loads.

38

Figure 26 shows an example of the effect of speed on DLC, and Figure 27 shows the corresponding effect on relative fatigue. The different lines represent various drive axle suspensions on a 5-axle tractor-semitrailer. In Figure 26, the DLC characterizes the response over the entire simulated test. In contrast, Figure 27 shows the effect on damage to the worst 5% of the pavement. The 95% damage shown is given in ESALs and the damage from the same axles with its loads held at their static (non-dynamic) values is indicated by a horizontal line at the bottom of the plot.

The systematic increase in fatigue with speed simply reflects the fact that increases in DLC with speed are compounded by a power law relationship to fatigue. All suspensions are comparable in damage at speeds below 30 mph with relative damage levels 30 to 45% greater than a suspension at static loads. At higher speeds the difference in dynamic behavior of the various suspensions becomes more apparent. At 65 mph the relative damage ranges from 1.9 to 2.5. Thus, the roughness in the road (at the 160 in/mi) causes a 90% increase in damage at the most severely loaded pavement locations from axles with the best dynamic properties and 150% increase from axles with the worst dynamic properties.

The level of peak stress in a rigid pavement caused by wheel load is particularly sensitive to location on the slab. Near the slab edges (at joints or along the sides), peak stresses are higher for a given load. This complicates the study of dynamic loading. A very small dynamic load component applied near a joint may be as damaging as larger dynamic component applied at center slab. This phenomena is discussed more completely in the Rigid Pavement section of this chapter.

Flexible Pavement Fatigue

Fatigue damage to flexible pavements may decrease with speed on smooth roads, but increase with speed on rough roads. This arises from the fact that the peak tensile strains under the wear course decrease with vehicle speed when the pavement is assumed to behave like a linear viscoelastic material. Higher speed decreases loading time. At the same time, higher speeds increase dynamic loads, particularly on rough roads. The trend with speed, therefore, depends on which mechanism is stronger in a given case.

Figure 28 shows the damage to a flexible pavement (3-in wear course) caused by a tandem drive axle on a 5-axle tractor-semitrailer with different suspensions, operating on a moderately rough road (IRI = 150 in/mi). Fatigue damage is expressed in equivalent single axle loadings (ESALs), where an ESAL is the damage caused by a single pass of an 18-kip axle at 55 mph. It is necessary to specify the speed in this case, because the damage caused by an 18-kip axle will vary with speed on a viscoelastic material even though the load is held at its "static" value.

The viscoelastic behavior of the pavement causes the fatigue from the static loads to decrease a full 7.3% for an increase in speed from 55 to 65 mph. This would be highly beneficial on a smooth road. However, over a road of moderate roughness, the increase in dynamic load with speed diminishes the benefit. The trends with different suspension systems are somewhat complex due to the interaction of (1) diminishing pavement response arising from viscoelastic behavior of the pavement material, (2) increasing dynamic loads

excited by the road roughness, and (3) the fourth-power relationship between strain and fatigue.
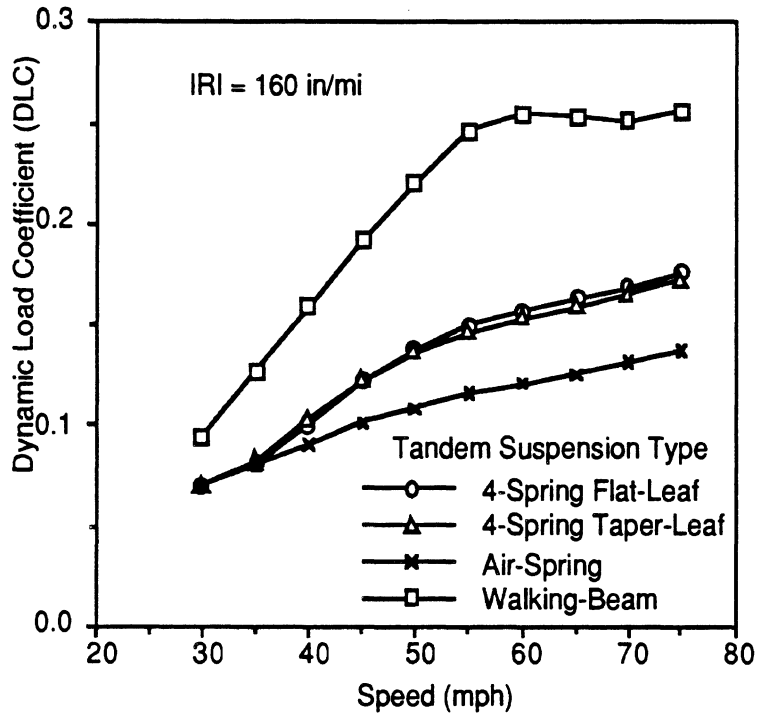
Figure 26. Influence of speed and tandem suspension type on DLC for rigid pavement.
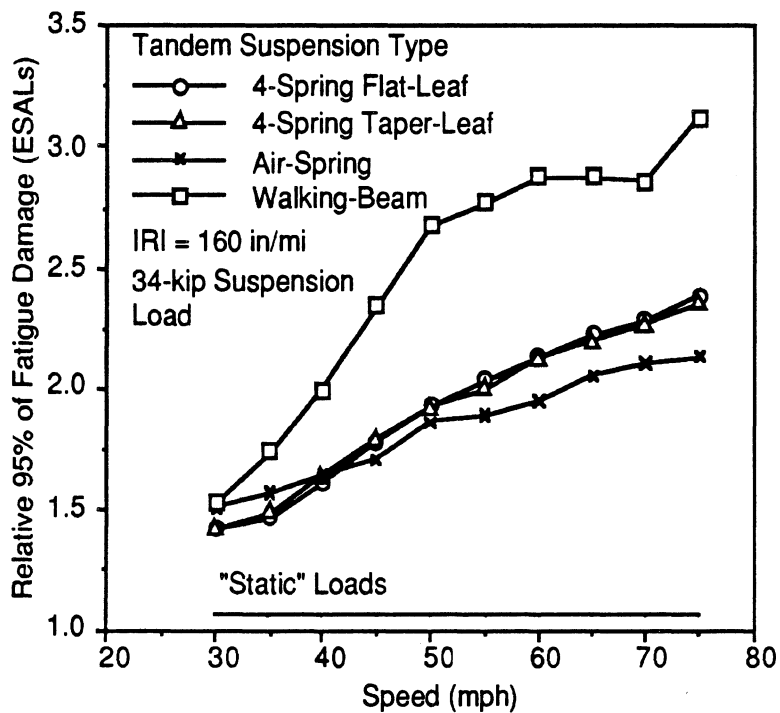
Figure 27. Influence of speed and tandem suspension type on rigid pavement fatigue.
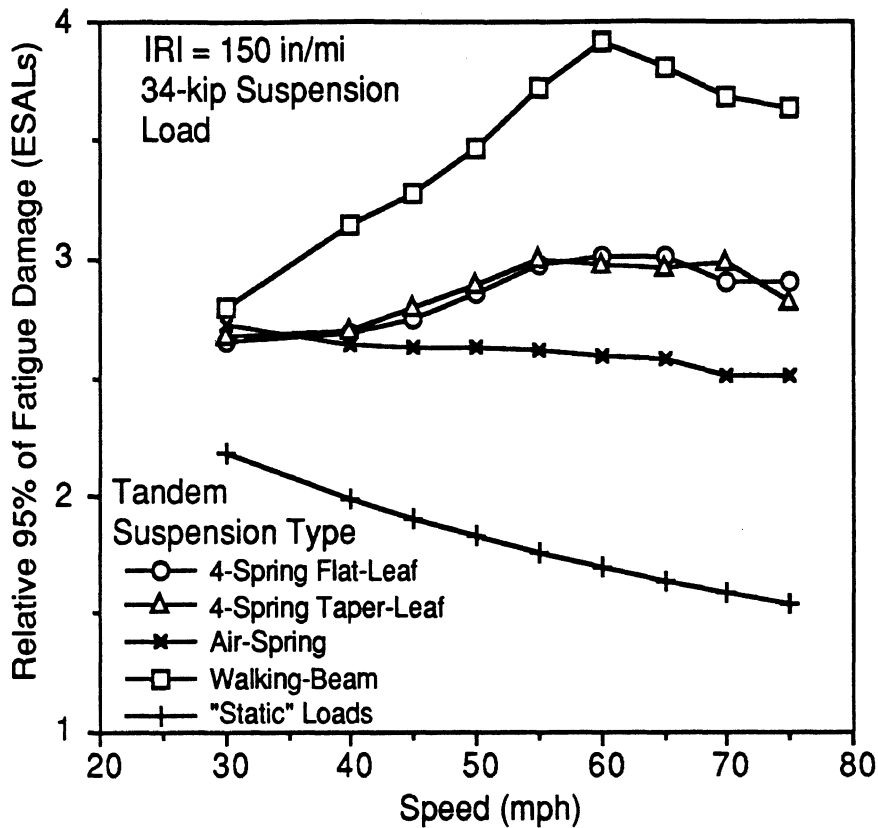
Figure 28. Influence of speed and tandem suspension type on flexible pavement fatigue.

Figure 29 shows the speed sensitivity for a 4-spring flat-leaf tandem drive axle of a 5-axle tractor-semitrailer on a smooth (80 in/mi), intermediate (160 in/mi) and rough (240 in/mi) road. In the absence of dynamics the damage would decrease with speed in accordance with the curve for zero roughness, because the response of a viscoelastic material decreases as the loading times shorten at high speed. In the presence of roughness, the increase in DLC offsets this benefit. On the smooth road the effects approximately offset each other, such that the fatigue varies little over the speed range. On roads with intermediate and high roughness levels the increase in dynamic loads at higher speeds is great enough that the damage increases slightly with speed.

Rutting

Speed interacts with rutting through its influence on the time for which a spot on the pavement is exposed to wheel loads. At high speed the wheel passes over a specific location on the road more quickly, reducing the time available for plastic deformation to occur. The deformation is calculated by integrating the influence function for deformation rate over the time interval required for the wheel to pass by; thus, deformation will be proportional to wheel load and inversely proportional to speed.

41
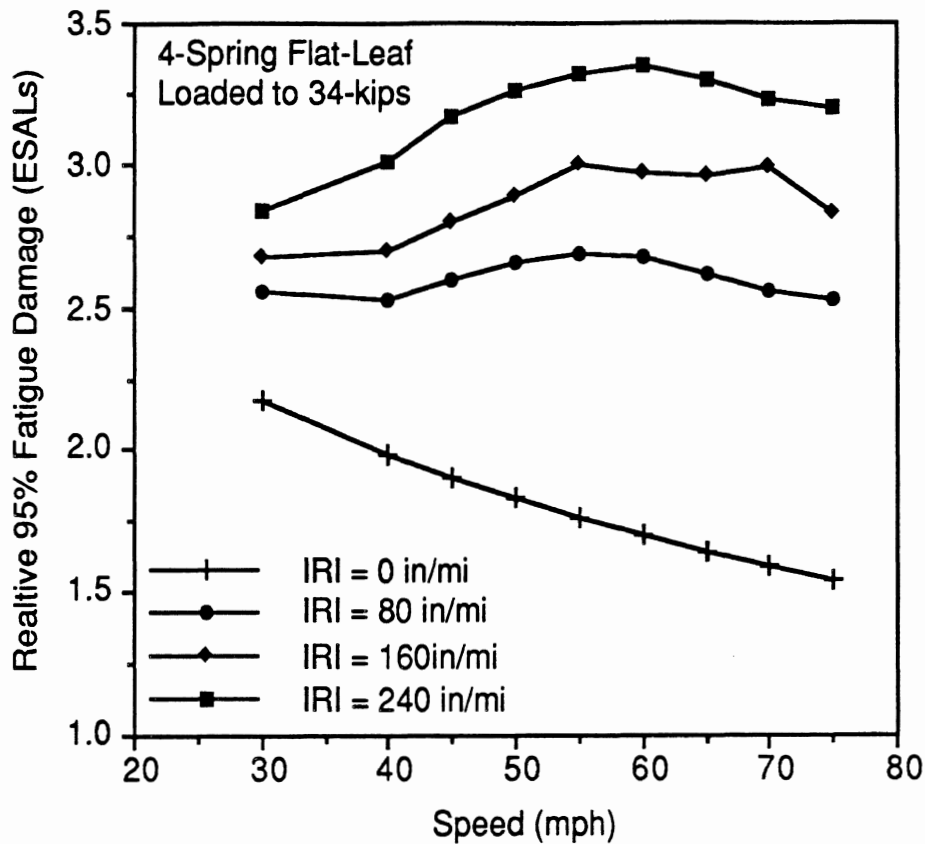
Figure 29. Relative flexible pavement fatigue damage (55 mph ESALs) vs. speed at three levels of road roughness.

Up to this point in the discussions, permanent deformation has been characterized as rutting because truck dynamics have not been involved and the deformation is thus uniform along the length of the pavement. When dynamics are considered, two characteristic forms of deformation will occur. There will be average deformation along the pavement, which is clearly rutting, and localized deformations at locations of high dynamic loads. The interpretation of the localized deformation depends on the assumptions made. Some researchers postulate that many trucks are dynamically similar enough that they are likely to apply their peak forces in the same general location relative to road bumps. In that case, the localized deformations will contribute to generation of road roughness. On the other hand, if the dynamic deformations are randomly distributed as a result of variations in the dynamic properties of trucks, they will simply contribute to average rut depth.

The truth is most likely somewhere in between, but the consequences are relatively minor. This can be seen when the rutting damage is evaluated for different suspension types as shown in Figure 30. The figure shows how the 95% rut depth caused by a 34-kip tandem axle on a 5-axle tractor-semitrailer varies with speed. Relative rut depth is given in ESALs based on the rut depth caused by a single pass of an 18-kip axle at 55 mph. The rut damage caused by a "static" 34-kip tandem axle corresponds to the constant rut depth that would be produced in the absence of any dynamics. Rut depth varies inversely with speed because the pavement loading time, which affects rutting, varies inversely with speed. The damage under dynamic loading from the various suspension types is evaluated on the 5% of the pavement where it is most severe. Yet, for a given speed, the difference in damage

42

caused by static loads and the damage at the locations suffering the most severe dynamic loading is generally only about 10% in the figure. Damage over the normal range of highway operating speeds (45-65 mph) varies by up to 31%, strictly as a result of decreased loading time.

Overall, rutting exhibits a strong speed sensitivity favoring higher speeds. For example, rutting decreases by 16% when vehicle speed increases from 55 to 65 mph .
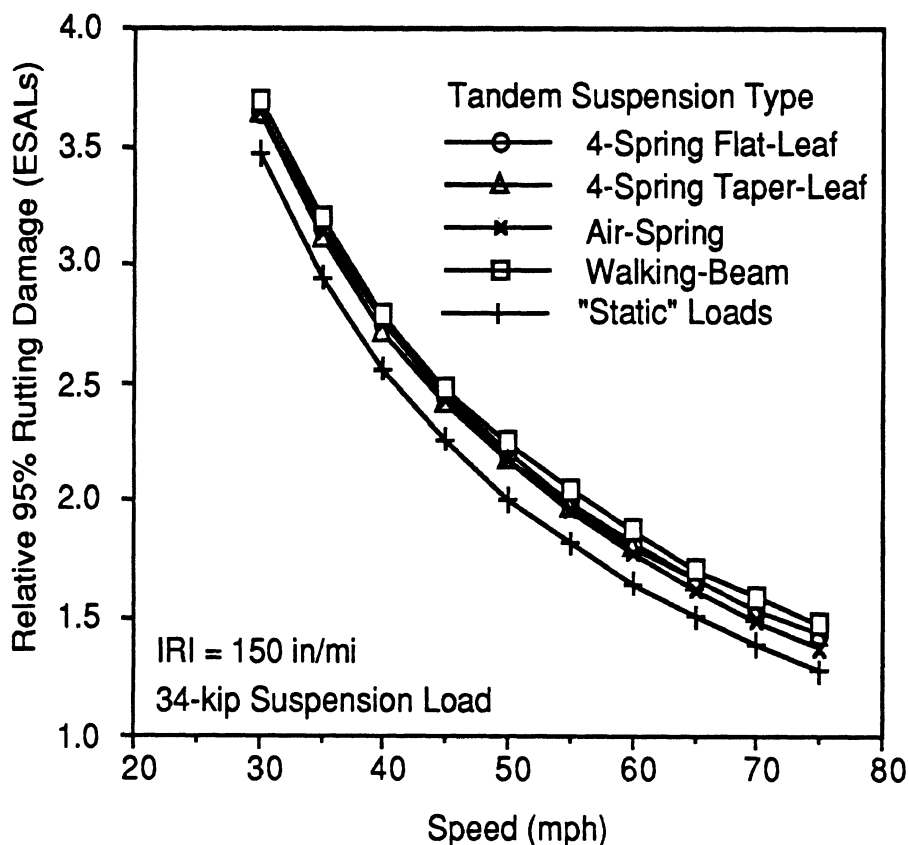
Figure 30. Relative rut depth caused by various tandem suspension types at IRI 150 in/mi.

Single Axle Suspension Type

Trucks in the medium and heavy classes have solid axles at both the front and rear. The suspension systems connecting the axles to the frame vary in design. The components of most significance to the dynamic interactions of the truck with the pavement are the types of springs and dampers. In the case of tandems, the additional property of dynamic load sharing is also important, and is discussed in the later section on tandems.

Suspension Types

Flat and Taper Leaf Springs—Most suspensions are of leaf-spring type with either flat or tapered leaves. The dynamics of road interaction are dependent on the load on the axle (sprung mass), weight of the axle (unsprung mass), the nominal stiffness of the springs,

43

the coulomb friction level, the "beta parameter" characterizing the spring force behavior in cyclic deflections (see Appendix D), and the damping from shock absorbers.

The spring properties are characterized by the force-deflection characteristics whose form is shown in Figure 31. Over large displacements, the spring exhibits a nominal stiffness that is determined by mission characteristics. In general, to maintain uniform loading heights for trucks and fifth wheel heights for tractors the spring rates must be high enough to limit loaded deflections to only a few inches.

Over small displacements typical of ride motions, the effective spring rate may be 3 to 10 times the nominal rate (13). The coulomb friction and beta parameter (which affect the ride stiffness) can be varied in design of the spring. Tapered leaves normally have lower levels of coulomb friction resulting in better ride on the vehicle.

Trucks with leaf spring suspensions rely on damping from the friction of the springs. By virtue of their higher coulomb friction, flat-leaf springs provide enough damping that shock absorbers are often not required. Taper-leaf springs generally have lower friction and may require auxiliary damping from shock absorbers.
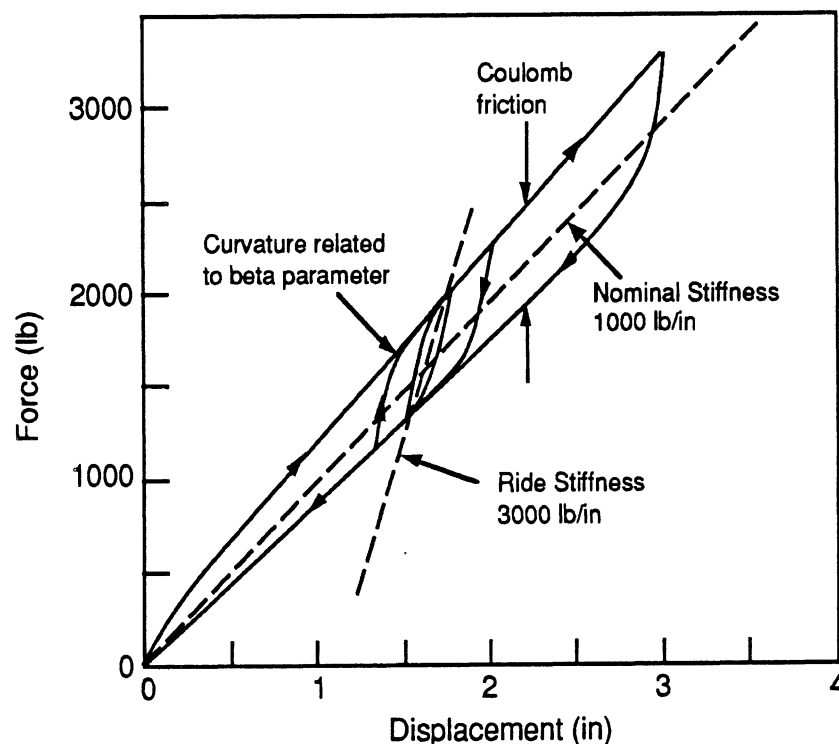
Figure 31. Force-deflection characteristic of a leaf spring.

Air Springs—The primary alternative to leaf springs on truck suspensions is the air spring (see Appendix D). An air spring is an elastomeric bag that is pressurized to provide the lift force. Air-spring suspensions incorporate height control systems which adjust the air pressure (lift force) in the spring to maintain the suspension at the proper ride position despite changes in static load. This ability to adapt to load changes allows the suspension to have the minimum practical spring rate because it operates about the mid-stroke position and can utilize the full suspension travel available for absorbing road bumps. Further, the

44

change in pressure with increasing static load changes the stiffness of the suspension in proportion to load, thereby maintaining the same natural frequency (1-1.5 Hz) at all loads. Air-spring suspensions usually have low internal friction and require hydraulic shock absorbers to obtain adequate suspension damping.

Optimal Passive Suspension—For purposes of comparison, an optimal passive suspension was formulated and simulated in parallel with all other single axle suspensions. A passive suspension consists of elements that can only store or dissipate energy (springs and dampers). An optimal passive suspension is obtained when the spring rate is reduced to the lowest practical minimum and the linear damping coefficient is chosen to achieve the minimum road damage.

The lowest spring rate practical on a motor vehicle is determined by the available suspension travel. (As the rate is reduced, more suspension travel is required to absorb the vertical accelerations of the vehicle. In the limit the suspension hits the "bump stops," and degrades the ride performance.) The spring rate of the air-spring suspension is taken to be the lowest practical for the optimal suspension. Damping was then adjusted to obtain the lowest dynamic wheel loads, defining the optimal passive suspension for these studies.

Active Suspensions—Active suspensions, which replace springs and dampers with hydraulic actuators, have been the subject of considerable study in recent years as a means to improve ride and dynamic loading behavior of motor vehicles. The overall performance is limited by the available suspension travel and trade-offs between ride and dynamic loading phenomena. The limits are well illustrated in a study by Chalasani (*14*).

An active suspension can provide benefits in ride and dynamic loading by control of the low-frequency motions near the sprung mass resonance (1-2 Hz). However, reducing the dynamic load variations associated with high-frequency wheel-hop resonances (10-20 Hz) degrades ride performance. This is illustrated by the comparison of response characteristics for active and passive systems shown in Figure 32. The passive system is representative of a generic motor vehicle, while the active system is optimized for ride. Lower response is obtained at the sprung mass resonance, but response at the unsprung mass resonance is unchanged. In order to reduce dynamic motions at the wheel-hop frequency the active suspension must exert control forces on the axle that are reacted against the sprung mass, adding to the ride vibrations. In effect, the active suspension would transmit road inputs to the sprung mass at high frequency rather than isolating it from those inputs as intended.

With these constraints the improvement achievable in ride and dynamic loading performance with active suspensions will be limited to approximately 10% to 20% over the best passive suspensions. The cost and durability of the sensors, actuators, and high-power hydraulic supply needed to implement active suspensions are additional barriers to their adaptation. As a consequence, most of the current development effort in the automotive industry focuses on solutions which have intermediate capability with much reduced cost and complexity, (e.g., low-bandwidth systems and systems which function in the dissipative mode only). Inasmuch as these systems are still evolving, it is too early to predict yet what benefits will be available with practical active suspensions (or hybrids), but it is likely to be no more than 10% to 20% in dynamic loading performance.
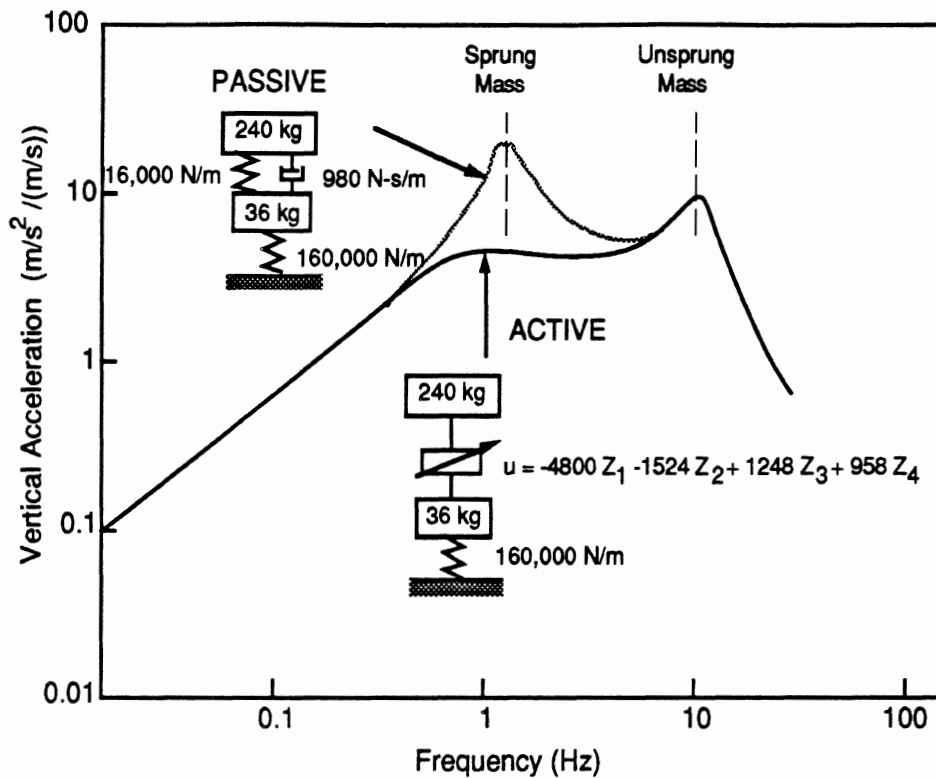
Figure 32. Comparison of vertical acceleration response of active and passive suspension systems (*14*).

Suspension Properties—Although suspension system properties differ on every truck, suspension properties were assembled to be representative of each suspension type for purposes of characterizing their influence on road damage. Properties for flat-leaf, taper-leaf and air-spring suspensions were obtained from experimental measurements of suspension properties on the UMTRI Suspension Parameter Measurement Facility (*15*) and the truck literature. These were used to prepare analytical models of each suspension type where the differences between suspensions were chosen to reflect their generic distinctions. For example, the nominal spring rate of flat-leaf and taper-leaf springs is dictated by external constraints of the truck mission, so they should not be given different stiffness. Rather, the distinctions between the properties of these two types of springs are their coulomb friction levels and values for the beta parameter. On the other hand, air springs can satisfy mission requirements with a much lower spring stiffness because of their height adjustment capability. Therefore, air spring suspensions have a lower spring rate.

Rigid Pavement Fatigue

Fatigue in rigid pavements is elevated by dynamic loads excited by road roughness in some locations. The dynamic properties of the suspension influence the magnitude of these loads and the damage. Figure 33 shows the damage in ESALs as a function of roughness for the single drive axle of a 4-axle tractor-semitrailer. Under a static load the damage would be slightly more than 1.5 ESALs. Compared to the static case, the fatigue damage nearly doubles with roughness on the roughest roads (240 in/mi IRI). All suspensions are subject to this effect, although the flat leaf is worst and the air spring is best.
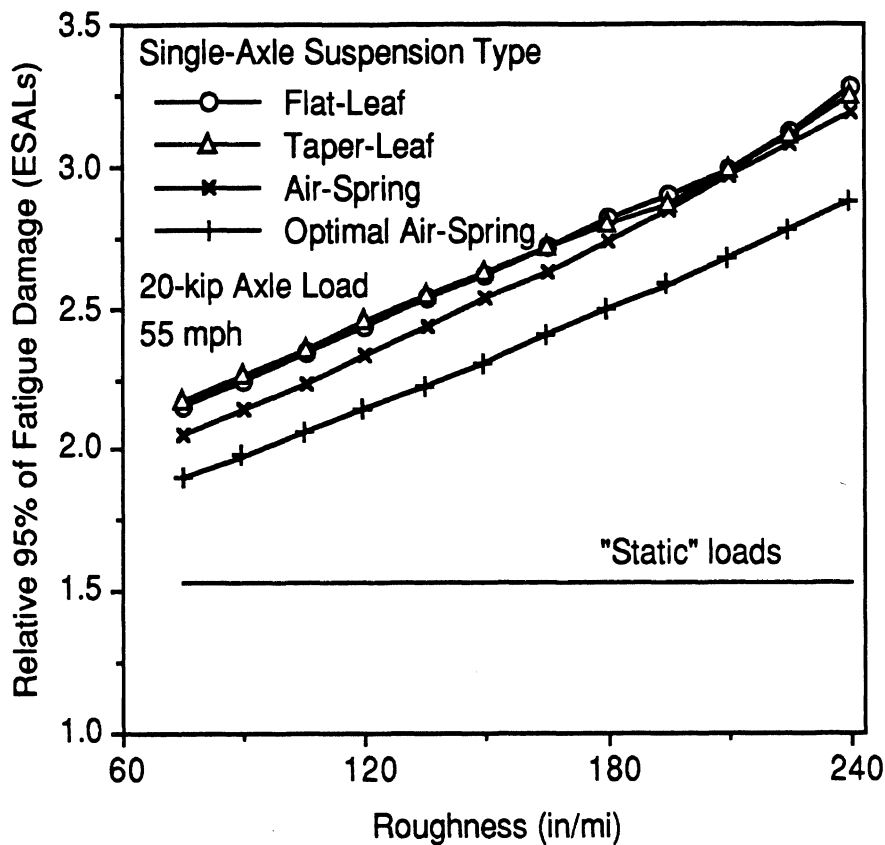
Figure 33. Influence of single-axle suspension type on rigid pavement fatigue.

It is evident that the difference in damage attributable to suspensions is much smaller than that due to roughness in the road. Between the smoothest (75 in/mi) to roughest (240 in/mi) roads the damage increases by 52%, whereas at any given level of roughness the difference between the leaf- and air-spring suspensions is only 5%. Optimizing the damping of the air-spring suspension provides about a 15% reduction in damage.

These results vividly illustrate the importance of damping to the dynamic load performance of truck suspensions. Most of the damping with leaf-spring suspensions derives from friction in the springs, whereas air-spring suspensions are more dependent on shock absorbers for damping. The damping value assumed for the air-spring suspensions in these calculations was selected on the basis of an experimental test on only one suspension, so it is not known how representative this is of the truck population in general. The comparative performance of air suspensions on actual trucks in use will vary with damping in the suspension. One might expect that the best (well-designed suspensions with shock absorbers in good condition) will approach the performance of the optimal suspension, whereas others in poorer condition (e.g., with worn-out shock absorbers) may perform comparable to the leaf-spring suspensions. Overall, it may be concluded that road damage can be reduced about 20% by use of well-designed and maintained air-spring suspensions in place of leaf-spring suspensions on trucks, and perhaps another 20% improvement can be realized from development of active suspensions.

Flexible Pavement Fatigue

Fatigue damage to flexible pavements as seen in Figure 34 closely follows the pattern of that for rigid pavements. Although stress levels and fatigue laws may differ for the two pavement types, the dynamic behavior of the suspensions is comparable on both road types, leading to similar results. That is, small variations in road roughness affect damage much more than differences in dynamic behavior among various single-axle truck suspensions. The potential improvements in flexible pavement damage possible with optimal passive suspensions and active suspensions is comparable to that seen for rigid pavements previously.
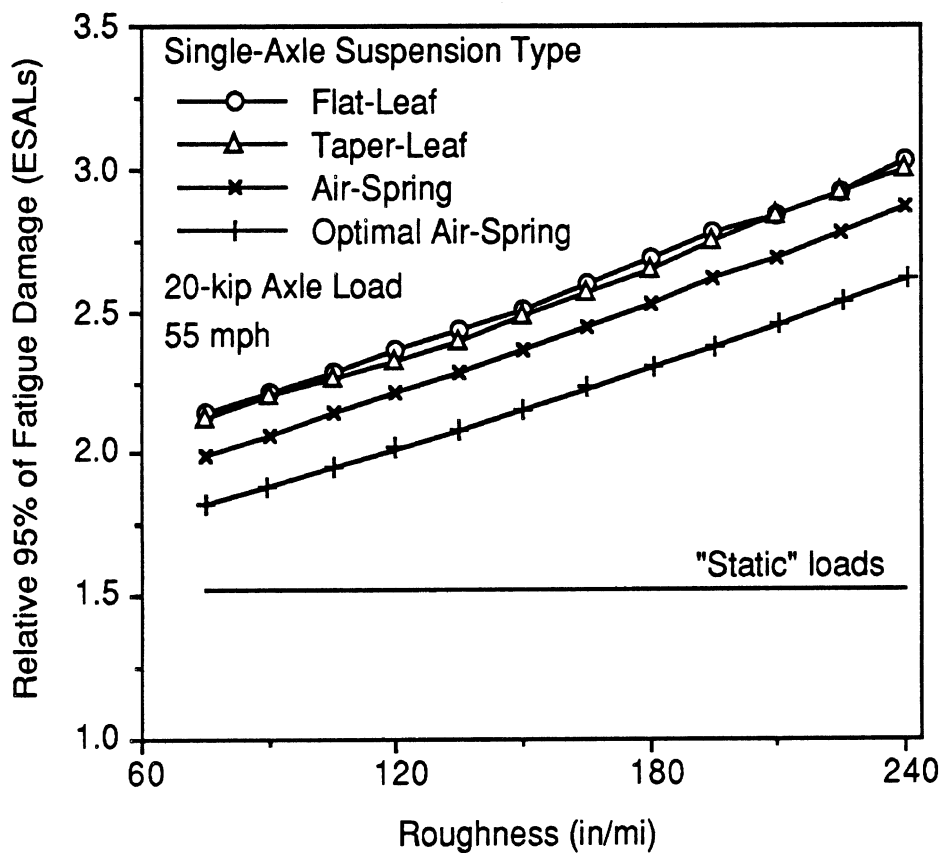
Figure 34. Influence of single-axle suspension type on flexible pavement fatigue.

Rutting

The dynamic behavior of truck suspensions has little effect on rutting damage as was demonstrated in Figure 30. This conclusion derives from the assumption of the linear-elastic behavior of the pavement, together with the fact that the average load on the truck axles are not altered by dynamics. At most, rutting is accentuated where dynamic loads increase in the vicinity of road bumps; however, it must be reduced commensurately elsewhere.

48

Tandem Dynamics

Multiple-axle suspensions may have dynamic properties that affect road loads and damage. The performance varies with suspension design. Some behave like independent axles with interaction occurring only as a result of common connection to the same sprung mass. Others exhibit dynamic behavior influenced by the mechanisms provided for axle load equalization under static conditions.

The three most common tandem suspensions are the 4-spring (flat or taper), the air spring and the walking-beam. More detail on their function and dynamic behavior is given in Appendix D. The air-spring suspension behaves largely like two independent air suspensions because of the slow action of the pneumatic load equalization system employed. Four-springs have an equalizer beam between the ends of the two springs located on same side of the vehicle. The equalizer beam allows some load adjustment and dynamic interaction during bump encounters on the road at high speed, but is hampered by high friction in the process. The walking-beam has a beam on each side of the vehicle connecting the leading and trailing axles. Springs on each side of the vehicle connect to pivots on the centers of the walking-beams. The walking-beam suspension is very good at static load equalization, but is prone to "tandem-hop" vibrations at highway speeds.

Figures 26 through 30 illustrate the degree to which dynamic load coefficient (DLC) and damage depend on roughness, speed, and suspension type. All of the suspensions show a general tendency for DLC to increase with speed, due mainly to the increased excitation from road roughness. The rate of increase also depends on stiffness and damping properties of the suspensions. The leaf-spring and walking-beam suspensions exhibit substantial coulomb friction, in contrast to the air-spring suspension which has viscous damping from shock absorbers. At low speeds (representing low roughness excitation) the suspensions are comparable. As the excitation level increases with speed, the viscous damping forces of the shock absorbers on the air suspension produce larger forces to maintain about the same damping ratio. Damping in the 4-spring suspensions is determined by the available coulomb friction, and will vary with vibration amplitude.

The walking-beam tandem suspension shows the highest DLC mainly because it is subject to a lightly damped mode of vibration in which the front and rear axles bounce out of phase at about 10 Hz without deflecting the leaf spring that connects the walking beam to the rest of the vehicle (16). In the absence of spring deflection there is little damping of the tandem hop vibration. Due to wheelbase filtering, this mode of vibration receives maximum input for a wavelength of twice the axle spacing (8.5 ft). Thus, the 10 Hz resonance receives maximum input from spatial filtering excitation when 8.5-ft wavelengths are seen at 10 Hz, which occurs at 85 ft/sec (58 mph). The high DLC near 60 mph, shown in Figure 26, is due mainly to this effect. The tuning is reflected in the damage curve for the walking-beam suspension (Figure 27) by the high level of damage at this speed.

Other generic types of tandem suspensions are used on a limited basis. The torsion-bar tested by Sweatman (8) was not studied because it is no longer available in the United States. In past studies, it fell in the performance range between the air-spring and 4-spring designs. Walking-beams with rubber-block springs are also used in severe-duty

applications. Based on its mechanics, it is expected to perform much like the walking-beam with a leaf spring.

Rigid Pavement Fatigue

The damage arising from dynamics of tandem suspensions is caused directly by road roughness excitation. Figure 35 shows the damage in ESALs as a function of road roughness for various drive axle suspensions on a 5-axle tractor-semitrailer. The damage indicated by the static loads serves as the reference point against which the effects of suspension and road roughness should be compared.
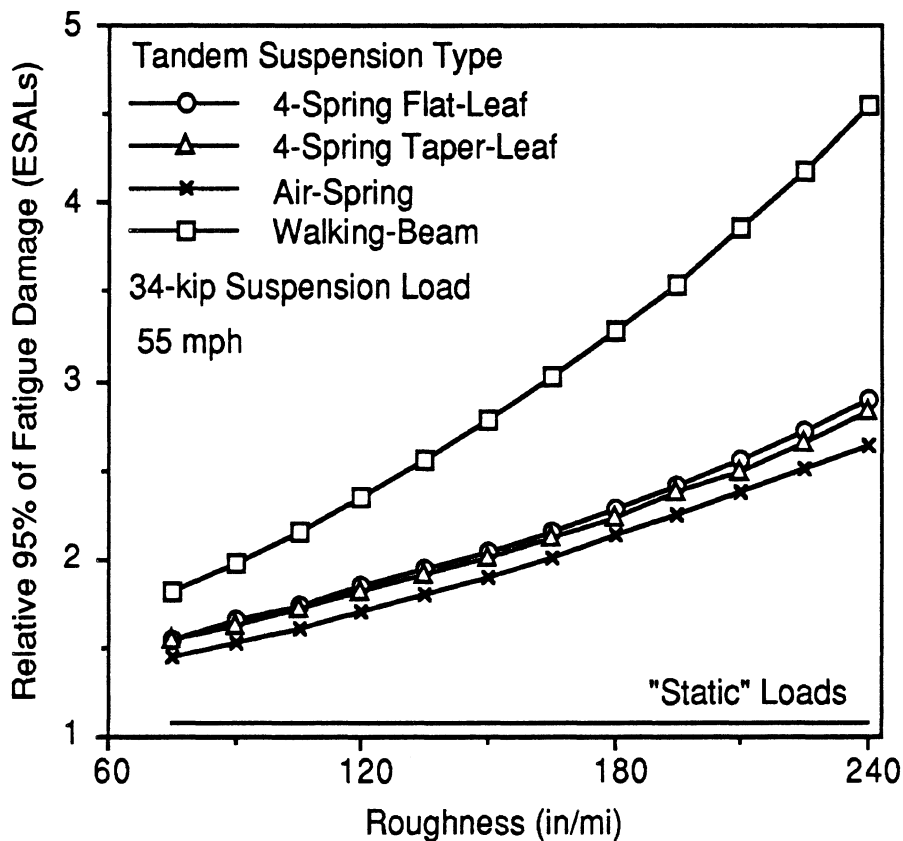
Figure 35. Influence of tandem suspension type on rigid pavement fatigue.

Road roughness is clearly a primary factor affecting damage levels, but the suspensions have a strong influence as well. The air-spring tandem is the least damaging, and the 4-spring (with flat-leaf or taper-leaf) is only slightly worse. However, the dynamics of the walking-beam distinguishes it from all other suspensions, such that the damage is nominally twice that of the other suspensions. It is substantially worst because of the dynamic loads caused by the tandem-hop vibration mode. With free articulation at the center point on the walking-beams the axles can hop vertically out-of-phase with little damping. Shock absorbers acting directly on the axles could damp this vibration mode, but are rarely incorporated in this type of suspension.

50

Flexible Pavement Fatigue

Flexible pavement fatigue closely follows the pattern shown for rigid pavements above. Figure 36 shows the damage in ESALs as a function of road roughness for various drive axle suspensions on a 5-axle tractor-semitrailer. The damage indicated by the static load serves as the reference point against which the effects of suspension and road roughness should be compared. Although stress levels and fatigue laws applicable to flexible pavements may differ from that of rigid pavements, the dynamic behavior of the suspensions is comparable on both road types. Under the most severe conditions (walking-beam suspension, 240 in/mi roughness) the tandem damage approaches 4 times that caused by the static axle loads.
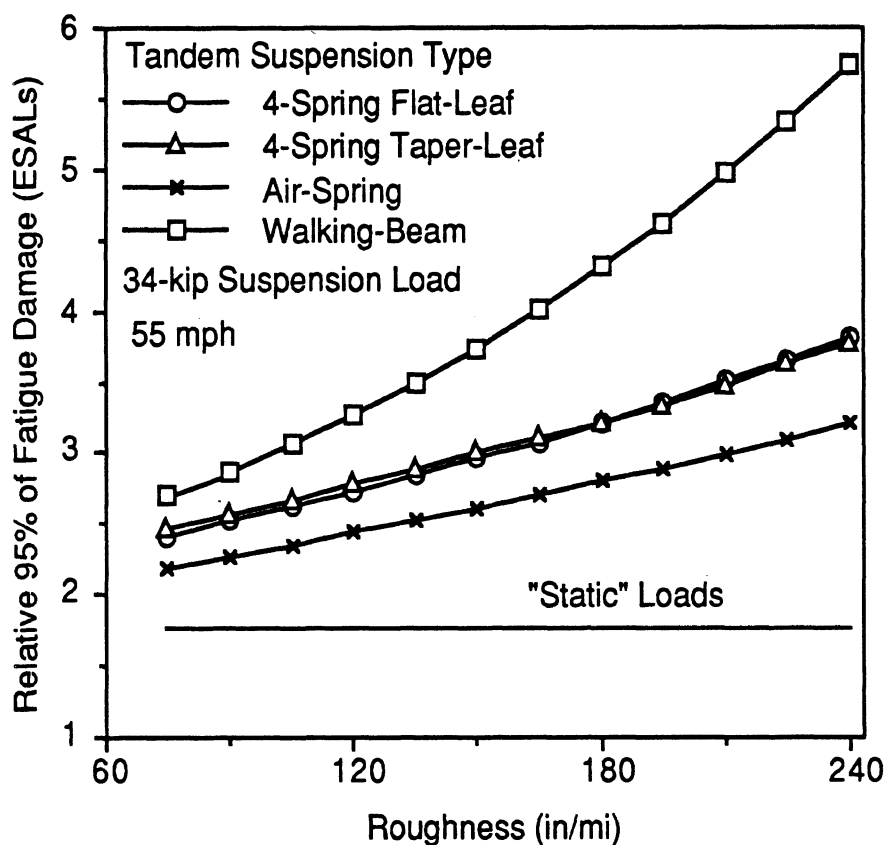
Figure 36. Influence of tandem suspension type on flexible pavement
fatigue.

Rutting

The overall rutting damage to flexible pavements is little affected by dynamic loads of truck suspensions as was seen previously in Figure 30. This conclusion derives from the assumption of the linear-elastic behavior of the pavement material, together with the fact that the average load on the truck axles are not changed by the dynamics. At most, rutting is accentuated where dynamic loads increase in the vicinity of road bumps; however, it must be reduced commensurately elsewhere.

Maneuvering

Accelerating, braking and cornering maneuvers place additional stress on a pavement surface. In accelerating and braking maneuvers the weight of the vehicle shifts longitudinally. In cornering, the weight shifts laterally. Thus, the maneuvers change wheel loads affecting the normal stresses on the pavement. The tire traction and cornering forces necessary to accomplish the maneuvers impose additional shear stresses on the road surface as well. Although pavement distress obvious near intersections and sharp turns offers anecdotal evidence that shear stress can accelerate pavement damage, the tire traction and cornering forces are not addressed in this report because the available pavement structural models do not accommodate shear stresses at the surface.

Accelerating

Loaded trucks are very limited in the acceleration levels that can be achieved. Figure 37 shows estimates of the acceleration capability of typical heavy trucks as a function of speed (*17*). At low speed (start-up accelerations at intersections, or slow pulls up steep grades) accelerations are limited to approximately 0.15 g's, but over the normal range of driving speeds maximum accelerations are 0.05 g's or less. The magnitude of the load transfer in the fore-aft direction for an accelerating straight truck is given by:

$$\Delta W = W \frac{h}{L} a_x \qquad (2\text{-}4)$$

where

ΔW = Fore/aft load transfer from front to rear axles
W = Total weight of the truck
h = Center of gravity height
L = Wheelbase
a_x = Longitudinal acceleration (in g's)

The h/L ratio for trucks is at most 0.5. Thus, the longitudinal load transfer under maximum acceleration at low speeds (0.15 g's) will at most be 7.5% of the total vehicle weight. On straight trucks this corresponds to a load increase on the rear axle(s) of approximately 10%. At highway speeds the longitudinal load transfer will be no more than 2.5% of the weight, causing about a 3% increase in load on the rear axle(s).

By this same rationale the primary load transfer effects on tractor-semitrailers will occur on the tractor, where load transfers of the approximately the same magnitude will occur.

In low-speed acceleration areas the 10% increase in rear axle loads will increase fatigue damage (due to the 4th power relationship) by 45% on the rear axles, but reduce that from the front axle. At high speeds the additional damage from rear axles is about 10%. Recognizing that these are the worst-case estimates, and that trucks undergo significant accelerations over only a fraction of their mileage, it does not appear that acceleration is a very important influence on fatigue damage except in areas where acceleration is prevalent (i.e., near intersections or in hill-climbing lanes).
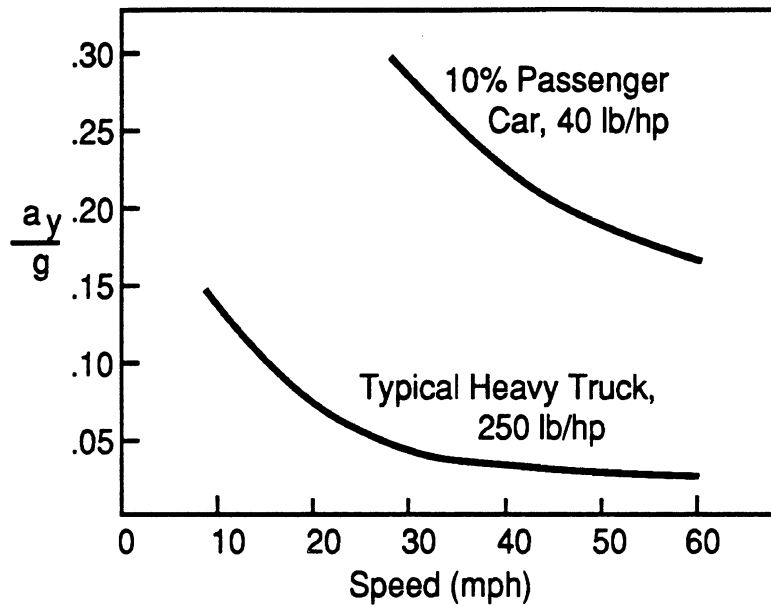
Figure 37. Acceleration capabilities of typical trucks.

Since flexible pavement rutting has been related to gross weight and is insensitive to load distribution among axles, no change in rutting damage is anticipated as a direct result of truck accelerations.

Braking

The longitudinal acceleration levels achievable in braking are much greater than in accelerating, and thus greater load transfer effects can occur. Maximum braking deceleration levels of trucks are nominally 0.5 g's, although in routine braking the deceleration levels are likely to be no greater than for passenger cars. Experimental studies of braking behavior in the literature indicate that most braking occurs at about 0.1 g's (*18*). Figure 38 shows the distribution of braking levels found in routine driving by a number of researchers.

At the 0.1g deceleration level (the average braking deceleration), straight trucks experience load transfer onto the front axle on the order of 5% (h/L = 0.5, a_x = 0.1) of the gross vehicle weight, while tractor-trailer combinations will be somewhat less. A 12,000 lb front axle may carry 13,000 to 14,000 lb during routine braking maneuvers. The additional load on the front axle will increase fatigue damage from that axle by perhaps 50% to 100%. During severe braking maneuvers at 0.5 g's the front axle damage may increase by a factor of 500% to 1000%.

On rigid pavements the front axle static loads are much less damaging than rear axle loads, hence, rigid pavement fatigue damage decreases during braking. On the other hand, front axles are more damaging than rear axles on flexible pavements even at their static load limits because they are fitted with single tires. Thus, forward load transfer during braking increases flexible pavement fatigue damage. Although rutting damage is not directly affected by load transfer in braking, the implication that speeds will be lower in areas where braking is prevalent suggests that rutting damage will be more severe in these areas of
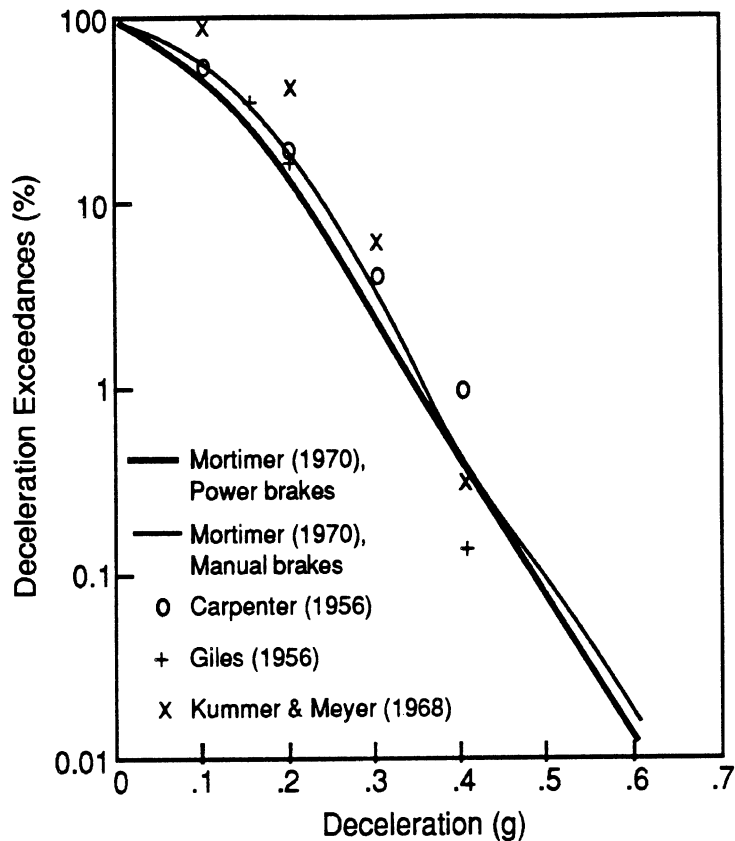
Figure 38. Cumulative distribution of braking deceleration in normal driving (*18*).

roadway (see Figure 30). Shear stresses under truck tires during braking may also lead to accelerated pavement wear by causing corrugation of the pavement surface, and hence, increased road roughness in roadway areas where braking predominates, such as approaches to intersections.

Cornering

Under cornering conditions, load is transferred laterally to the wheels on the outside of the turn. The magnitude depends on the roll moment balance on the vehicle. The exact magnitude of lateral acceleration depends on the speed, radius of turn and whether there is any superelevation on the curve. Speed and radius of turn combine to determine the lateral acceleration level. The load shift from inside to outside tires in the turn can be found by taking a moment balance on the vehicle. For the case of a symmetrical vehicle operating on a turn with superelevation, shown in Figure 39, the total weight on the outside wheels is approximately:

$$F_{zo} = W \left[\frac{1}{2} + \frac{h}{t} (a_y - \theta) \right] \tag{2-5}$$

where

F_{zo} = Load on the outside wheels of the vehicle
W = Gross vehicle weight
h = Center of gravity height

t = Track width

a_y = Lateral acceleration (in g's)

θ = Superelevation angle of the road surface (positive inward)

The second term on the right hand side of the equation represents the relative proportion of the weight that is transferred in a turn. AASHTO guidelines (*19*) recommend that highways be designed for lateral acceleration and superelevation such that the total of the two is normally in the vicinity of 0.1. Truck center of gravity heights are quite variable, but are nominally equivalent to the tread. Thus, in typical turns the outside wheels will experience a total load of:

$$F_{zo} \approx W [0.5 + 0.1] = 0.6 \, W \qquad (2-6)$$

In general, the distribution of the lateral load shift among axles will vary depending on the specific characteristics of the suspensions, but it is reasonably approximated by assuming equivalent percentages on all axles. Thus, it is concluded that in corners the loads on outside wheels of trucks may typically increase up to 60% of the axle weight, which is a 20% increase in load for the individual wheels.

With respect to fatigue on rigid and flexible pavements, the damage (based on a fourth power law) approximately doubles. Since permanent deformation in the layers of flexible pavements is directly proportional to load, the increase in rutting is 20% under the outer wheels.
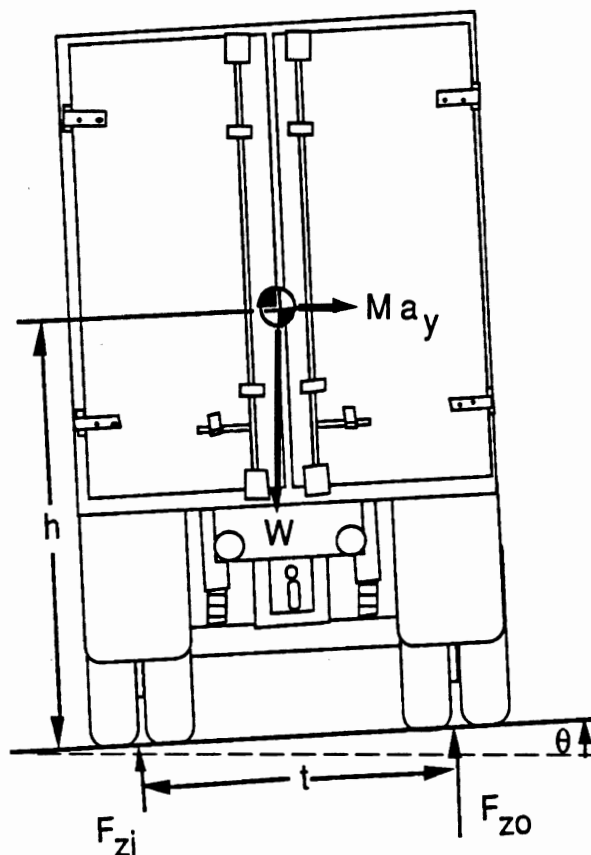
Figure 39. Forces acting to produce a moment balance on a vehicle.

TIRE FACTORS

Single, Dual, Wide-base

In this section the theoretical pavement damaging potential of different tires and mounting configurations are compared. The tires used on modern trucks may be configured in single or dual tire arrangements. Front steering axles use single tires. Tractor drive axles and trailer axles are usually dual tire configurations. Wide-base single tires may be used on tractor front axles when loads exceed 14,000 lb, or on drive or trailer axles in place of dual tires.

The important feature of truck tire sizes is the difference in width, length, and area of the contact patch. To a lesser extent the tires are distinguished by differences in vertical stiffness, although this property is addressed in the comparisons of bias- and radial-ply tires. Tire size, ply rating and inflation pressure determine load capacity. Standard dimensions and load ratings for tires used in the United States are set by the Tire and Rim Association (T&RA) (4).

Three reference tires were selected for primary attention in the analysis; 11R22.5, 15R22.5, and 18R22.5. The tires represent the nominal sizes necessary to carry front axle loads of 12,000, 16,000 and 20,000 lb respectively in a single tire configuration. The 11R22.5 is also suited to service in dual tire applications on 20,000 lb single axles and 34,000 lb tandems. The convenience of having the same tire size on both front and rear axles makes it the tire of choice on most heavy trucks. The 15R22.5 and 18R22.5 tires are wide-base singles that are used for extra-heavy front axles, as well as replacements for duals on rear axles. In this class the 15R22.5 was selected as the tire size typically used on axles intended to carry 16,000 lb, and the 18R22.5 was selected for axles rated at 20,000 lb. Table 6 lists the nominal load capacity and tread dimensions for each of the reference tire sizes. Equivalent tires identified by other size designations are also shown in the table.

Tread width is a very important property of the tires. Maximum tread widths are set by the T&RA at 80% of section width for rib tires and 90% of section width for traction tires; however, the tread widths on typical production tires may vary. Tread widths were noted from the literature and were also measured on a random sample of tires in each size range. These are reflected in the nominal tread width range for each reference tire. For purposes of analyzing pavement responses it was necessary to assign dimensions for the tire contact patch. The assumed width for the contact patch was taken to be the middle of the range of tread widths. The length assumed for the contact patch was based on values given in the literature, from private sources, and from random measurements of actual tires.

Table 6. Tires Selected for Analysis.

Name	Tire Size (and Equivalent)	Axle Load Capacity (kips)		Nominal Tread Width Range[1] (in)	Assumed Contact Dimensions (in)	
		Single	Dual		Width	Length
Conventional	11R22.5 10.00-20 11R24.5 295/75R22.5	12	20	7 - 9	8	9 (single) 8 (dual)
Low-profile	215/75R17.5 245/75R19.5	NA	17	6.5 - 8	7	7
Wide-base single	15R22.5 385/65R22.5	16	NA	10 - 12	11	11
Wide-base single	18R22.5 445/65R22.5	20	NA	13 - 15	14	12

1. Observed range from a random sample of tires

The first row of cells in Table 6 represents the minimum tire sizes used on axles rated to 12,000 lb with single tires and 20,000 lb with dual tires. Any of four tire designations may be used to identify this size; 11R22.5 for the tubeless radial tire, 10.00-20 for the tube-type bias-ply tire, 11R24.5 for the tubeless radial, and 295/75R22.5 for the P-metric series. This tire will be referred to in the analysis as the "conventional" tire, and the findings will apply to tires of any of the size designations shown. Recent changes in the road use laws have allowed front axles to be set back from the front bumper. This design pushes front axle loads upward, typically to about 14,000 lb. At the 14,000 lb loading slightly larger tires (11R24.5 or 12R22.5) are needed. A truck with a 14,000 lb front axle load is included in the truck matrix. Tire contact dimensions for this configuration are assumed to be the same as for the 11R22.5.

The second row in Table 6 lists low-profile tires. Truck fleets that need high cubic capacity in trucks and trailers are attracted to low profile tires. The smallest of these, the 215/75R17.5, has sufficient load capacity to allow its use on 34,000 lb tandem axles, but at tire pressures of 120-125 psi. Used in place of a 295R22.5 the overall tire diameter can be reduced from 40 inches to 30.7 inches. These tires have a tread width on the order of 7 inches wide. The contact patch length varies with tire size. A 7-inch length has been assumed for calculations in this analysis.

The last two rows of Table 6 are the wide-base single tires selected for study.

An analysis of pavement responses and damage was performed using tires of the sizes and loadings listed in the table. The relative damage ascribed to the tires are sensitive to tread width, contact patch length and loading, and may vary with actual tires differing from the assumed parameters.

57

Rigid Pavement Fatigue

The effect of tire configuration on rigid pavement fatigue derives from its influence on peak stress at the bottom of the concrete slab. Influence functions were calculated to determine the stress per pound of load on the tire. Figure 40 shows how the stress in a rigid pavement varies with tire configuration. Pavement response at the bottom of a 10-inch slab is plotted as a function of tire position along the wheel path for conventional single, wide-base single, and dual tires.

Pavement response only varies with tire footprint area when the tire is directly above the point of interest. The portion of the influence function in which the tires are directly above the point of interest is magnified in the figure to more clearly illustrate the effect of tire configuration on peak stress levels. The dual tires produces the lowest peak tensile stress. The wide-base single tire has a peak tensile stress that will be 2 to 9% greater than the dual tires. The single tire (11R22.5) has the highest peak tensile stress (approximately 15 to 20% greater than the dual tires) because of its small contact patch.
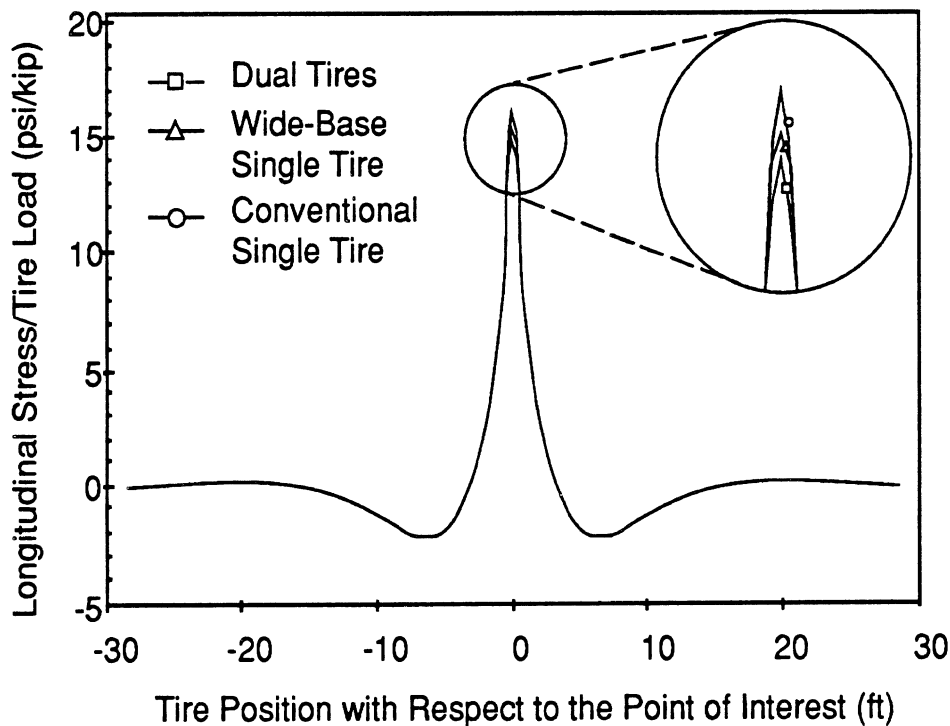
Figure 40. Rigid pavement stress influence functions of conventional single, dual, and wide-base single tires.

The relative degree of fatigue caused by each of the tire configurations depends on the design of the rigid pavement structure. Table 7 shows the relative effect of tire size by comparing the level of pavement stress with each tire size normalized by that of a dual wheel set. The ratio of stresses depends not only on the tire, but on the pavement thickness as well. Generally, a single tire produces 15 to 21% higher stress than a dual wheel set per pound of load, and the wide-base singles elevate stresses by 2 to 9%.

Low profile tires are used only in a dual tire configuration. Although their contact area is slightly smaller than that of the 11R22.5 reference tire, stresses at the bottom of the pavement slab are only elevated a few percent. Inasmuch as their load capacity is limited to 17,000 lb axle load, the overall damage is less than that of an 18-kip axle.

Recognizing that each tire size is rated to carry a different load, an Equivalence Factor (EF) was defined to characterize the relative damage of each tire when operating at its rated load. EF is defined as the number of passes of an 18-kip axle with *dual* tires that are required to consume the same amount of pavement fatigue life as an axle with conventional or wide-base single tires at their rated load. EF is then simply expressed in ESALs.

Conventional single and wide-base single tires are more damaging to rigid pavements relative to dual tires on a per-unit-load basis, particularly on thinner pavements. However, when adjusted for the fact that they carry less load, the Equivalence Factors indicate substantially less damage for the 11R22.5 and 15R22.5 sizes. The 18R22.5 tire is seen to be 62-67% more damaging primarily because it carries 20,000 lb and is compared to an axle at 18,000 lb. Fifty-two percent of the damage is attributable to the higher load, and only 10 to 15% is due to the difference in contact patch size between the 18R22.5 tire and a dual set.

Table 7. Rigid Fatigue Load Equivalence Factors for Single Tires of Various Sizes.

PC Concrete Pavement Thickness (in)	Peak Stress of Single Tire / Peak Stress of 11R22.5 Duals (Per pound of load)			Equivalence Factors[1] for Single Tires at Rated Load (ESAL)		
	11R22.5	15R22.5	18R22.5	11R22.5[2]	15R22.5[3]	18R22.5[4]
7.0^5	1.21	1.09	1.02	0.42	0.88	1.67
8.0^5	1.19	1.08	1.02	0.40	0.86	1.66
9.0^5	1.18	1.07	1.02	0.39	0.84	1.65
10.0^5	1.17	1.07	1.02	0.37	0.83	1.64
12.0^5	1.15	1.07	1.02	0.35	0.81	1.62
7.0^6	1.17	1.07	1.02	0.37	0.83	1.64
8.0^6	1.16	1.07	1.02	0.36	0.82	1.63
9.0^6	1.15	1.07	1.02	0.35	0.80	1.62
10.0^6	1.15	1.06	1.02	0.34	0.80	1.62

1 EFs are defined in these columns as the number of passes of an 11R22.5 dual-tire axle loaded to 18,000 lbs required to consume the same amount of pavement fatigue life as an axle with single tires at rated load.
2. Based on rated load of 12,000 lb per axle.
3. Based on rated load of 16,000 lb per axle.
4. Based on rated load of 20,000 lb per axle.
5. Pavement has an 8-inch thick granular subbase.
6. Pavement has a 4-inch thick cement treated subbase.

Figure 41 demonstrates the typical effect of tire configuration on strains at the bottom of a 6.5-inch asphalt surface layer. The strain per pound of tire load is plotted as a function of position along the wheel path for conventional single, wide-base single and dual tires. Flexible pavement strain is highly dependent on tire configuration when the tire is directly above the point of interest. The conventional single tire has the highest peak tensile strain because it has the smallest contact patch. The wide-base single has a lower peak and dual tires are the lowest.

Because of the compressive strains adjacent to the contact patch of the single tires, the most appropriate measure of strain is not the peak under the tire, but the range from the compressive to the tensile peak. The pavement goes through this strain cycle when the tire passes, and the cycle size is the magnitude of strain used in evaluating damage.
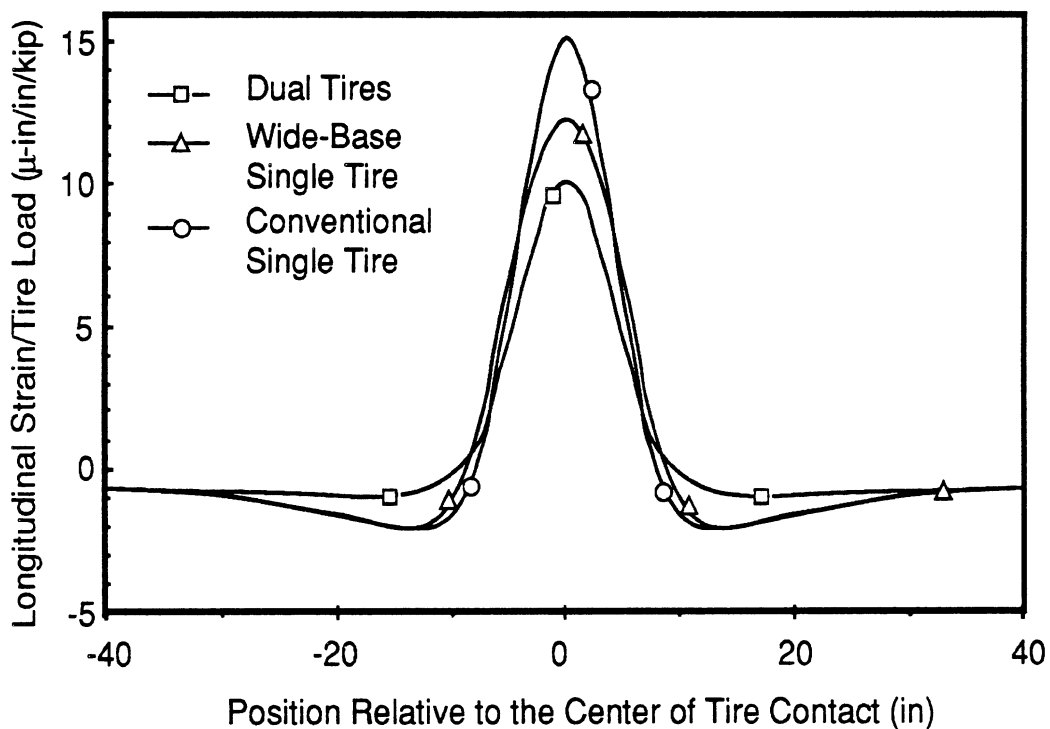
Figure 41. Flexible pavement strain influence functions of conventional single, dual, and wide-base single tires.

Table 8 shows the strain ratios and Equivalency Factors (EFs) for low-profile duals and single tires of various sizes over a range of flexible pavement designs. The EFs are defined as the number of passes of an 18-kip axle fitted with dual tires required to consume the same amount of fatigue life in the wear course as an axle with single tires at their rated load. (Damage to the base, subbase and roadbed soil is not considered here.) The fatigue law applied to the pavements in the table is based on the strain range raised to the 4th power.

Table 8 shows the strain ratios and Equivalency Factors (EFs) for low-profile duals and single tires of various sizes over a range of flexible pavement designs. The EFs are defined as the number of passes of an 18-kip axle fitted with dual tires required to consume the same amount of fatigue life in the wear course as an axle with single tires at their rated load. (Damage to the base, subbase and roadbed soil is not considered here.) The fatigue law applied to the pavements in the table is based on the strain range raised to the 4th power.

Table 8. Flexible Fatigue Load Equivalence Factors for Tires of Various Sizes.

Wear Course Thickness (inches)	Strain Range of Tires Strain Range of 11R22.5 Duals (Per pound of load)				Equivalence Factors[1] for Tires at Rated Load (ESAL)			
	LP duals	11R22.5 single	15R22.5 single	18R22.5 single	LP duals[2]	11R22.5 single[3]	15R22.5 single[4]	18R22.5 single[5]
2.0	1.25	1.74	1.07	0.76	1.95	1.81	0.81	0.51
3.0	1.19	1.74	1.19	0.89	1.61	1.81	1.23	0.95
4.0	1.13	1.70	1.25	0.98	1.29	1.67	1.52	1.43
5.0	1.10	1.64	1.28	1.05	1.17	1.44	1.67	1.86
6.5	1.07	1.55	1.29	1.11	1.04	1.13	1.70	2.28

1. EFs are defined in these columns as the number of passes of an 11R22.5 dual-tire axle loaded to 18 kips required to consume the same amount of pavement fatigue life as an axle with subject tires at rated load.
2. Based on rated load of 17,000 lb per axle.
3. Based on rated load of 12,000 lb per axle.
4. Based on rated load of 16,000 lb per axle.
5. Based on rated load of 20,000 lb per axle.

From the perspective of the strains imposed, the smaller tires result in greater strain per unit load primarily because of their smaller contact areas. Even when adjusted for load as is done when calculating the Equivalence Factors given in Table 8, axles with single tires may be more damaging. Because of complex interactions with the specific design parameters of the pavements, different results are obtained on different pavement thicknesses.

The low-profile tires cause more strain per pound of load than would larger 11R22.5 dual tires. The damage is most pronounced on pavements with thin wear courses. On pavements typical of primary roads (e.g., 5-inch thickness) the strain is 10% higher per pound of load. At 17,000 lb load these tires are about 17% more damaging than an 18-kip axle on a 5-inch pavement. Nevertheless, the low-profile tires are less damaging than a 20-kip axle with 11R22.5 duals on all except the thinnest pavements. Inasmuch as these calculations are based on the smallest of the low-profile tires, less damaging performance would be expected from some of the larger tires classified in the low-profile category.

The conventional single (11R22.5) commonly used on truck front axles is notably more damaging on thinner pavements when carrying 12,000 lb. In order to reduce the damage it imposes to the same level as a 20,000 lb axle with dual tires, the load would have to be reduced to about 11,000 lb. This corresponds to 690 lb per inch of tread width.

The picture is not quite as simple with wide-base single tires because their relative damage is less on thin pavements and greater on thick pavements. (Although damage to the base, subbase and roadbed soil will be higher on the thin pavements.) Compared to an 18-kip axle as used in computation of ESALs, it would appear that they are more damaging than duals on the thicker pavement designs (i.e., 5-inch surface course) typical of major highways. Compared to the damage of the 20,000 lb axle currently permitted, however, the 15R22.5 is only 10% worse. In a comparable sense, the 18R22.5 is 22% worse than a 20,000 lb axle on 5-inch pavement and 52% worse on 6.5-inch pavement. In order to keep the 18R22.5 from being more damaging than a 20-kip dual-tire axle, the load would have to be limited to 18,000 lb. This corresponds to 643 lb per inch of tread width.

The load per inch of tread width provides a much simpler way to quantify the limits discussed above. Load per inch is also easy to monitor on in-service vehicles and takes into account the fact that tread widths will vary on tires of the same size. It should be noted that actual tread width is used here, in contrast to road use laws which specify load per unit width on the basis of the section width of the tire. Using an axle fitted with dual tires and loaded to 20,000 lb as a reference, values for load per unit tread width which produce equivalent damage are given in Table 9. A range of values is given for each single tire size because the damage potential of each tire size changes relative to duals depending on the strength of the pavement. Wear course thicknesses of 2-6.5 inches were considered in development of Table 9.

Table 9. Load per Tread Width to Maintain Flexible Pavement Fatigue Damage within Limits of Current 20-kip Axles with Dual Tires.

Tire Size	Tread Width per Axle (in)	Load per Unit Tread Width[1] (lb/in)
11R22.5 (Duals)	32.0	625
11R22.5 (Single)	16.0	718-806
15R22.5 (Single)	22.0	705-850
18R22.5 (Single)	28.0	643-940

1. Values given over a range of pavement thicknesses based on the damage caused by an 11R22.5 dual-tire axle loaded to 20,000 lb.

In summary, these observations indicate that the single tires on truck front axles are generally more damaging than the 20,000 lb dual-tire axle with regard to fatigue of flexible pavements. The disproportionate damage would be eliminated if front axle loads are kept about 10% below the rated load of the tires. Alternately, the loads could be limited to no more than 650 lb per inch of tread width.

Rutting

The flexible pavement surface rutting caused by axle loading is highly dependent on tire configuration. As rutting is the result of plastic deformation, it is dependent on the magnitude and duration of the load. Rutting damage can be assessed in terms of both the depth of the rut and the volume of material displaced. The criterion used to assess rutting damage affects the conclusions about which tires are best.

Figure 42 shows the rutting influence functions for a flexible pavement with a 6.5-in thick asphalt concrete layer exposed to conventional single, wide-base single, and dual tires. Response is given as the rate of permanent vertical surface deflection per pound of tire load.
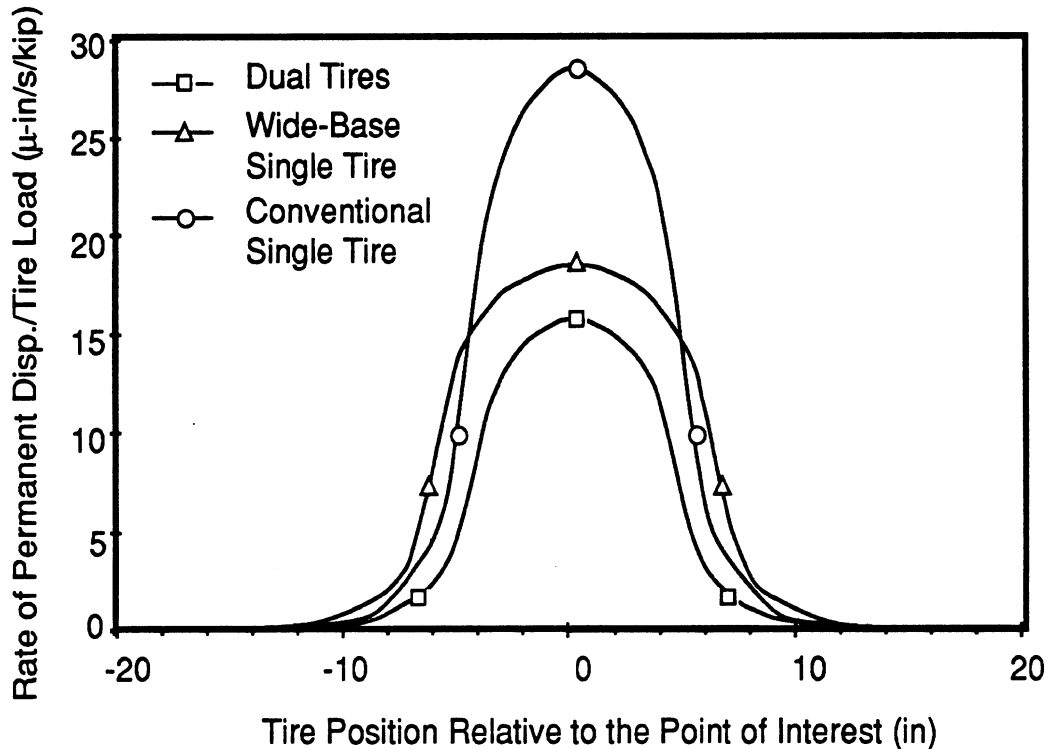
Figure 42. Rutting influence functions of conventional single, dual, and wide-base single tires.

The rutting caused by each tire can be calculated by integrating the response functions shown in the figure with respect to time and scaling the result by the tire load. The relative rut causing potential of each tire configuration can therefore be compared by calculating the area under each response function in the figure. The conventional single tire will rut the pavement nearly twice as deeply as the dual tires for the same load, because only half of the load on the dual tires is passing over the wheel path shown in the figure. The other half is passing over a wheel path located 13 inches in the lateral direction from the one shown. Thus, the duals cause a shallower rut depth, but over a wider area. Because of its greater contact width the wide-base single tire causes a shallower rut depth than the conventional single tire for the same load. The wide-base single tire does, however, cause a wider rut than the conventional single tires.

If the rut depth under an individual tire is the criterion for judging rutting damage, the single tire and wide-base single would be somewhat worse than dual tires, simply based on the influence functions characteristic of each. Table 10 shows the rut depth Equivalence Factors (EFs) for conventional and wide-base single tires over a range of surface layer

Table 10. Rut Depth Equivalence Factors for Conventional and Wide Based Single Tires.

Wear Course Thickness (inches)	Equivalency Factors for Single Tires[1]					
	77°F Surface Temperature			120°F Surface Temperature		
	11R22.5[2]	15R22.5[3]	18R22.5[4]	11R22.5[2]	15R22.5[3]	18R22.5[4]
2.0	1.05	1.21	1.39	1.50	1.40	1.38
3.0	1.11	1.24	1.38	1.57	1.53	1.55
4.0	1.20	1.32	1.45	1.51	1.41	1.40
5.0	1.28	1.38	1.50	1.50	1.43	1.44
6.5	1.38	1.47	1.60	1.59	1.50	1.53

1. EFs equal the ratio of the rut depth caused by an axle with single tires at rated load to that of two (dual) tires on an 18-kip axle.
2. Based on rated load of 12,000 lb per axle.
3. Based on rated load of 16,000 lb per axle.
4. Based on rated load of 20,000 lb per axle.

thicknesses. EFs are the number of passes of an 18-kip axle with *dual* tires that are required to cause the same rut *depth* as an axle with conventional or wide-base single tires at their rated load. Since rutting behavior is very temperature sensitive and most aggravated in hot climates, the EFs are shown at surface temperatures of 77°F and 120°F. At a surface temperature of 77°F, the EFs for all tires tend to increase with surface layer thickness. Although the rutting is generally more severe at 120°F the relative increase with pavement thickness is not significantly altered.

The analysis of low-profile tire performance for rutting showed them to be little different than the 11R22.5 dual tires on an 18-kip axle. The primary reason is the limitation of low-profile tires to 17,000 lb axle ratings.

In the worst cases in the table, single tires at their rated load cause a rut depth that is 50 to 60% greater than that from duals. Yet it is the accumulation of rutting from many axles running in slightly different lateral positions that causes a general depression of the wheeltrack. In this context duals produce twice the rutting volume from the combined effect of the two tires. Thus, rutting volume is a more rational basis for comparing tire effects. The current pavement structural models are not adequate for the precise determination of the volume of material displaced by a tire because the tire contact shape must be modeled as a circle. Hence, rutting cannot be calculated accurately at a location that is not directly under the center of a passing tire. In light of this, the rutting volume must be estimated. The estimations here are based on rut depth times the tread width of the tire. Although this is not likely to be accurate for predicting absolute rutting, it is reasonable for comparing relative rut performance from various tire combinations.

Table 11 shows the rut volume Equivalence Factors (EFs) for conventional and wide-base single tires over a range of surface layer thicknesses. EFs are the number of passes of

an 18-kip axle with *dual* tires that are required to cause the same rut *volume* as an axle with conventional or wide-base single tires at their rated load. When judged on the basis of rut volume, the single tires are less damaging than duals.

Table 11. Rut Volume Equivalence Factors for Conventional and Wide Based Single Tires.

Wear Course Thickness (inches)	Equivalency Factors for Single Tires[1]					
	77°F Surface Temperature			120°F Surface Temperature		
	11R22.5[2]	15R22.5[3]	18R22.5[4]	11R22.5[2]	15R22.5[3]	18R22.5[4]
2.0	.53	.61	.70	.75	.70	.69
3.0	.56	.62	.69	.79	.77	.78
4.0	.60	.66	.73	.76	.71	.70
5.0	.64	.69	.75	.75	.72	.72
6.5	.69	.74	.80	.80	.75	.77

1. EFs equal the ratio of the rut volume caused by an axle with single tires at rated load to the combined volume of two (dual) tires on an 18-kip axle.
2. Based on rated load of 12,000 lb per axle.
3. Based on rated load of 16,000 lb per axle.
4. Based on rated load of 20,000 lb per axle.

Inflation Pressure/Contact Area

Truck tire inflation pressure is a parameter readily set and varied by the truck operator. The observation of inflation pressures well above 100 psi in recent years has increased the concern that the pressure may be affecting pavement damage. It is recognized that inflation pressure does affect the mean contact pressure in the tire contact patch. Equally important is its effect on the size of the contact patch. Inasmuch as the mean contact pressure times the area must equal the tire load, variation in one parameter produces a very predictable change in the other.

Increased inflation pressure has secondary effects of increasing the stiffness of the tire and possibly reducing tire damping. Tire stiffness and damping are only important under the dynamic loading conditions. Variations in tire stiffness resulting from changes in tire inflation pressure were found to have minimal effect on the dynamics of the trucks that were analyzed and does not appear to be significant. Similarly, variations in tire damping are insignificant when adequate suspension damping is present. Thus, this mechanism is not likely to be important in most cases.

Rigid Pavement Fatigue

Finite element models for rigid pavement structures are reasonably well suited for investigating the influence of inflation pressure and the associated changes in contact area. The length of the rectangular contact area in the model can be varied to approximate the change in contact area with pressure (contact width is determined by tire tread width and

does not change significantly with pressure). Elevated pressure (reduced contact length) increases the peak in the influence function at the bottom of the pavement slab by only a few percent, although the associated damage arising from a power relationship to stress increases more. Figure 43 provides an estimate from this model for the change in damage to a 10-inch slab with tire inflation pressure for an axle fitted with 15R22.5 tires loaded to 16,000 lbs and an axle fitted with 11R22.5 dual tires loaded to 20,000 lbs. In each case the damage is normalized by the damage caused by the tire at its recommended inflation pressure for the load specified.

Damage from a 15R22.5 tire increases by 53% over the range of inflation pressures from 75 to 120 psi. That is because the contact length of the tire changes significantly with inflation pressure at constant load. The damage caused by 11R22.5 duals, on the other hand, is not as sensitive to inflation pressure. It only changes by 15% over the range of pressures from 75 to 120 psi, because the contact length of a 11R22.5 tire is not as sensitive to changes in inflation pressure as is the 15R22.5 tire.

Low-profile tires operate at higher inflation pressure than most other truck tires. To accommodate a 17,000 lb axle load, the smallest tires must be inflated to approximately 125 psi. At these elevated pressures the contact areas are reported to be equivalent to larger tires on a per unit load basis. Thus, the contact pressures are not significantly different, despite the higher inflation pressure. Field observations of truck tire pressures rarely exceed 125 psi, so damage factors for low-profile tires at higher pressures were not calculated.
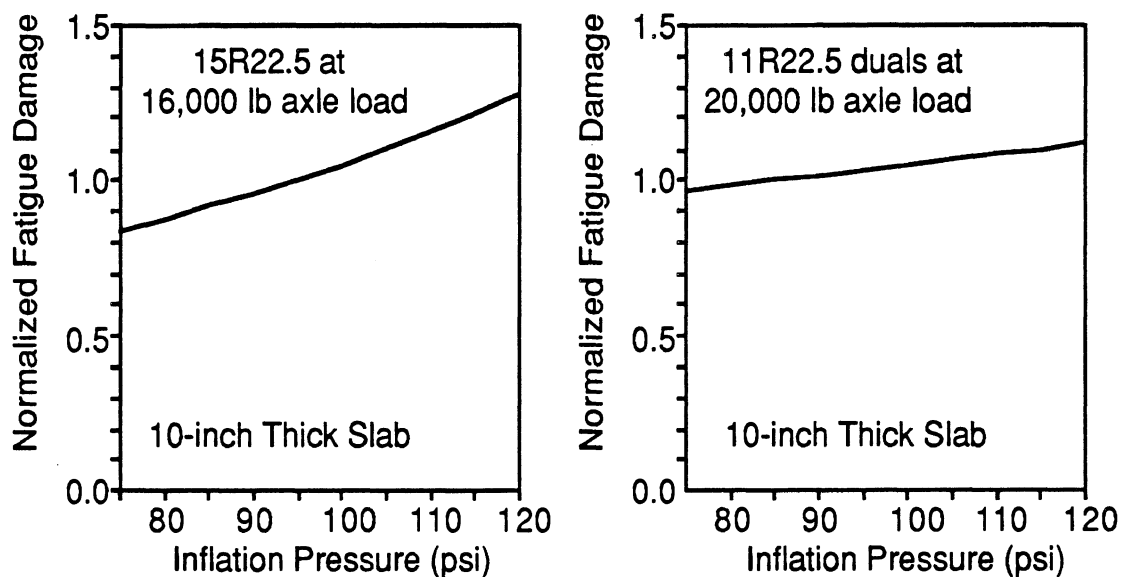
Figure 43. Rigid pavement fatigue damage versus inflation pressure for dual and wide-base tires.

Flexible Pavement Fatigue

The flexible pavement model requires imposition of a circular tire contact patch. Thus it is less precise at duplicating the effects of variations in tire inflation pressure. For that case the area of the circle must be adjusted to equal the contact area of the tire.

Elevated pressure (reduced contact length) increases the range of strains in the influence function at the bottom of the wear course significantly. The associated damage arising from a power relationship to strain causes damage to rise rapidly with inflation pressure. Figure 44 provides an estimate from this model for the change in damage to a pavement with a 5-inch wear course thickness with tire inflation pressure for an axle fitted with 15R22.5 tires loaded to 16,000 lbs and an axle fitted with 11R22.5 dual tires loaded to 20,000 lbs. In each case the damage is normalized by the damage caused by the tire at its recommended inflation pressure for the load specified.

Damage from the 15R22.5 tire increases by a factor of more than 9 over the range of inflation pressures from 75 to 120 psi. That is because the contact length changes significantly with inflation pressure for the same load. The damage caused by 11R22.5 duals, on the other hand, is not as sensitive to inflation pressure. Damage varies by a factor of 2.8 over the range of pressures from 75 to 120 psi. This is because the contact length of a 11R22.5 tire is not as sensitive to changes in inflation pressure as the 15R22.5 tire.

Although low-profile tires routinely operate at higher inflation pressures of approximately 125 psi, at these elevated pressures the contact areas are reported to be equivalent to larger tires on a per unit load basis. Calculations of their damage in previous sections have been based on assumptions of contact area appropriate to the higher pressure. Since field observations of truck tire pressures rarely exceeded 125 psi, damage factors for low-profile tires at higher pressures were not calculated.
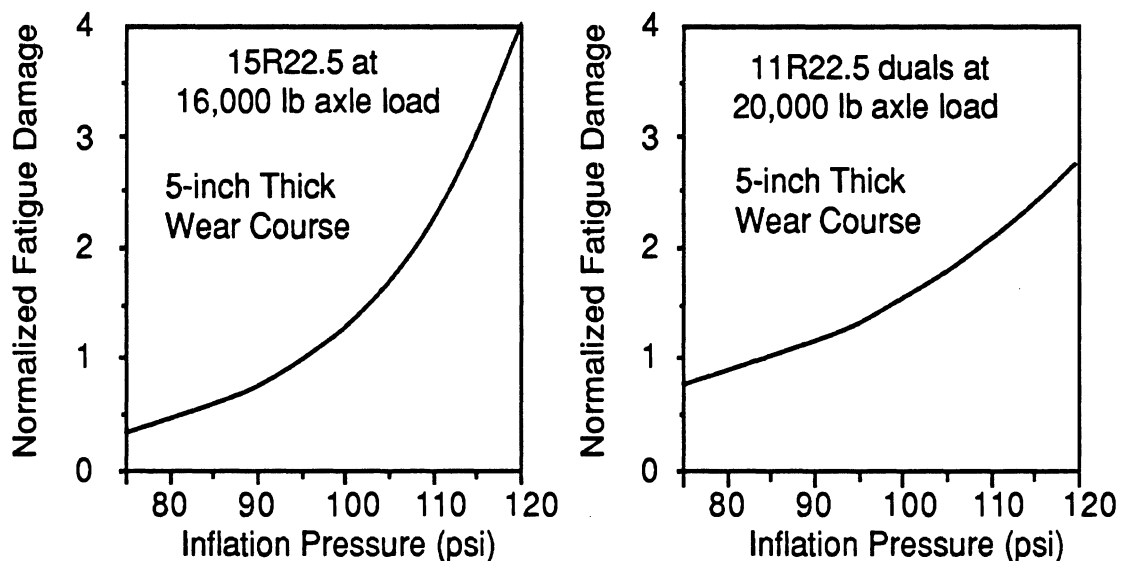
Figure 44. Flexible pavement fatigue damage versus inflation pressure for dual and wide-base tires.

Rutting

Changes in rutting resulting from variations of inflation pressure are difficult to predict accurately with current flexible pavement models. Being limited to a circular contact patch, the diameter must be varied to duplicate changes in contact area arising from pressure

variations. Figure 45 shows the effect of inflation pressure on flexible pavement rut *depth* for dual and wide-base single tires. Increased pressure produces deeper rutting because of the higher plastic deformation when the load is concentrated in a smaller area.
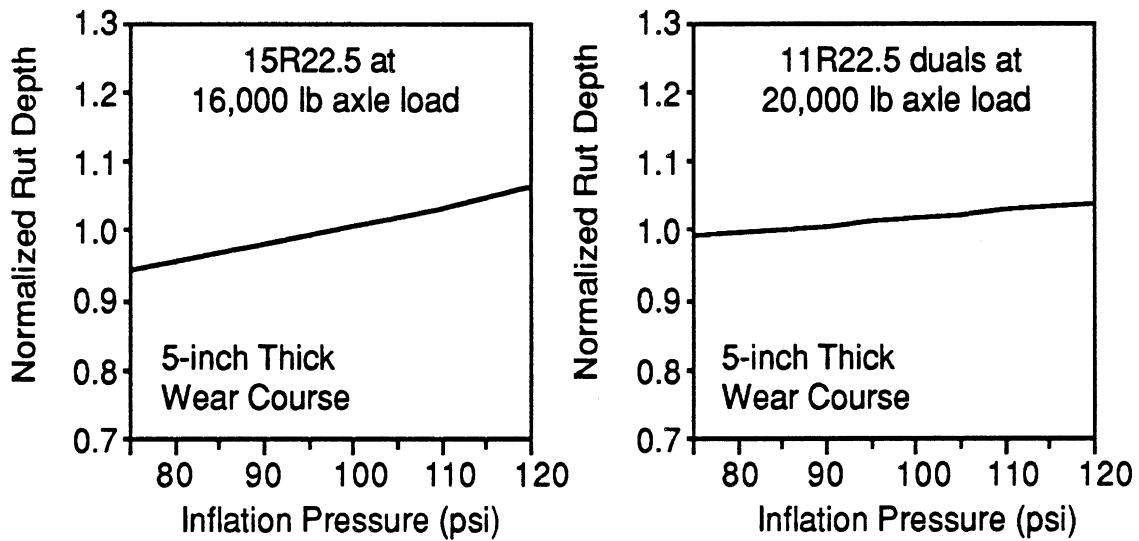
Figure 45. Rut depth versus inflation pressure for dual and wide-base tires.

Generally speaking, the effect of higher pressure is to increase the contact pressure and shorten the contact patch. The higher pressure creates a more intense strain pattern under the tire, but it is concentrated in a shorter length along the direction of travel. Since rutting is linked to the time-based integral of the strain exposure, the shorter time exposure at high inflation pressure will compensate somewhat for the higher strain rate under those conditions. This rationale leads to the conclusion that rutting does not change rapidly with variations in tire inflation pressure, which is in agreement with the findings of (*20*).

Ply Type

Two basic types of tire construction are broadly used; radial-ply and bias-ply tires. The two types are illustrated in Figure 46. Bias-ply tires were the standard in the early years of the American automotive industry until about the 1960's when the advantages of radial tires became recognized and durable designs were developed. Over several decades they gradually displaced bias-ply tires, such that radial tires are used on about one-half of all trucks today.

Radial construction is characterized by parallel plies (rubberized fabric reinforced by cords of nylon, rayon, polyester or fiberglass) running directly across the tire from one bead to the other at a nominal 90 degree angle to the circumference. This type of construction makes for an extremely flexible sidewall. A stiff belt of fabric or steel wire runs around the circumference of the tire between the carcass and the tread to provide directional stability.

In bias-ply tire construction the carcass is made up of plies extending from bead to bead with the cords at high angles (35 to 40 degrees to the circumference) and alternating in direction from ply to ply. Bias construction causes more distortion in the contact patch as

the toroid deforms into a flat shape, causing the tread to squirm in the contact patch (*21*) when rolling as seen in Figure 47.

Bias-ply Tire   Radial-ply Tire
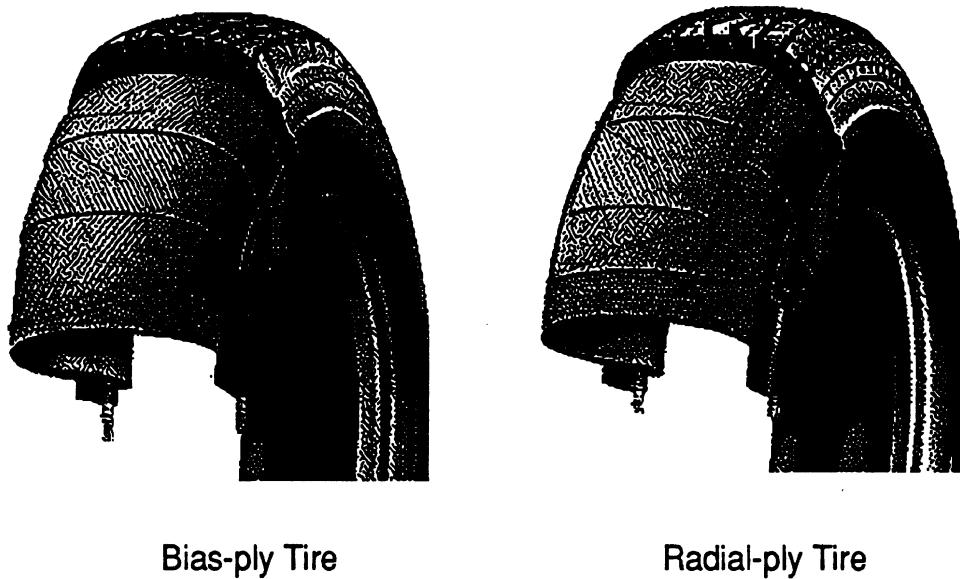
Figure 46. Illustrations of bias and radial-ply tire construction.
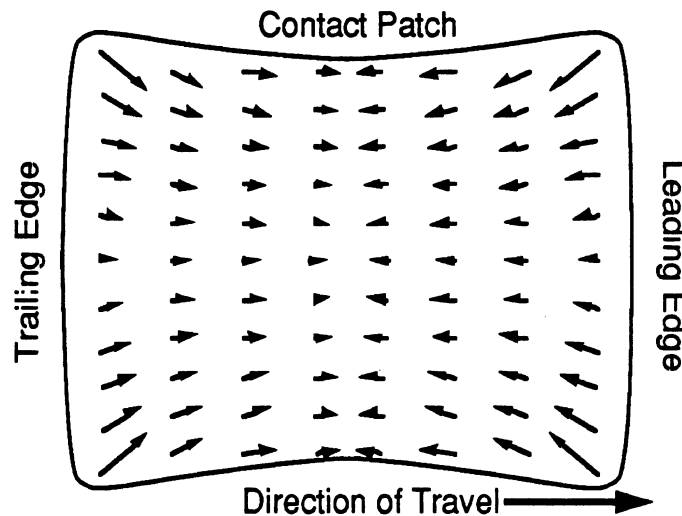
Figure 47. Squirm in the contact patch of a bias-ply tire.

Thus, one of the important distinctions between the two types of tires is the shear stress distribution created in the tire contact patch. While this may potentially influence the tendency for rutting of flexible pavements, current pavement structural models are not adequate for assessing the significance of these properties because they do no provide for shear stress inputs on the road surface.

A second distinction between radial and bias-ply tires is seen in the cornering stiffness properties. Cornering stiffness characterizes the rate at which lateral force builds up as the tire slips at an angle. Although this has no direct influence on pavement damage, it impacts the operating behavior of trucks in a way that could indirectly affect damage. With higher

cornering stiffness, long combination vehicles will track more precisely in a straight line. The off-tracking angles of a long combination vehicle caused by superelevation, crosswinds, and other factors, are only about half as large with radial tires as with bias-ply tires. Further, truck operators must be more diligent in maintaining axles in good alignment with radial tires in order to minimize tire wear. Consequently, vehicles with radial tires will impose their damage on a narrower section of the wheeltrack.

Rigid Pavement Fatigue

Fatigue of rigid pavements is determined by the stresses generated at the bottom of the slab. The stress magnitudes are determined by the wheel load and contact area. Radial and bias-ply tires are similar in contact area. Thus, the fatigue is not directly affected by the ply type of tires, except by the tracking mechanisms described above.

Flexible Pavement Fatigue

Fatigue of flexible pavements is determined by the strains generated at the bottom of the first layer. The strain magnitudes are determined by the wheel load and contact area. Radial and bias-ply tires are similar in contact area. Thus, the fatigue is not directly affected by the ply type of tires, except by the tracking mechanisms described above.

Rutting

One of the distinctions between radial and bias-ply tires that may affect rutting is the shear stress distribution in the contact patch. Specifically, the bias-ply tire creates an inward shear stress distribution in the contact patch as a result of the toroidal shape of the tire conforming to a flat surface. Stresses of this type tend to resist radial stresses which promote material flow and rutting in the pavement material immediately under the tire. Thus, the shear stresses characteristic of bias-ply tires might be beneficial to reducing rutting of the surface layer. While some shear stresses are undoubtedly associated with radial tires, the circumferential belt is purposely intended to reduce these stresses. The available pavement models did not allow evaluation of these mechanisms.

A second distinction between the two types of tires potentially affecting rutting arises from their camber thrust characteristics. Any tire operating at an inclination angle to a surface experiences a lateral force known as camber thrust as illustrated in Figure 48.

The lateral force due to camber angle is characterized by the initial slope of the curve, termed the camber stiffness, C_γ, and is defined by the equation:

$$C_\gamma = \frac{\partial F_y}{\partial \gamma}\bigg|_{\gamma = 0}$$
(2-7)

Where F_y is the lateral force applied to the tire and γ is the camber angle. The camber stiffness normalized by tire load is known as the camber coefficient.

The camber stiffness is a particularly important tire property with regard to how a tire responds to ruts in the wheel path. When a vertically-oriented tire operates on a surface with a cross-slope (such as the side of a rut in the wheel path) the horizontal component of its load acts to push the wheel toward the lowest part of the rut as shown in Figure 49.
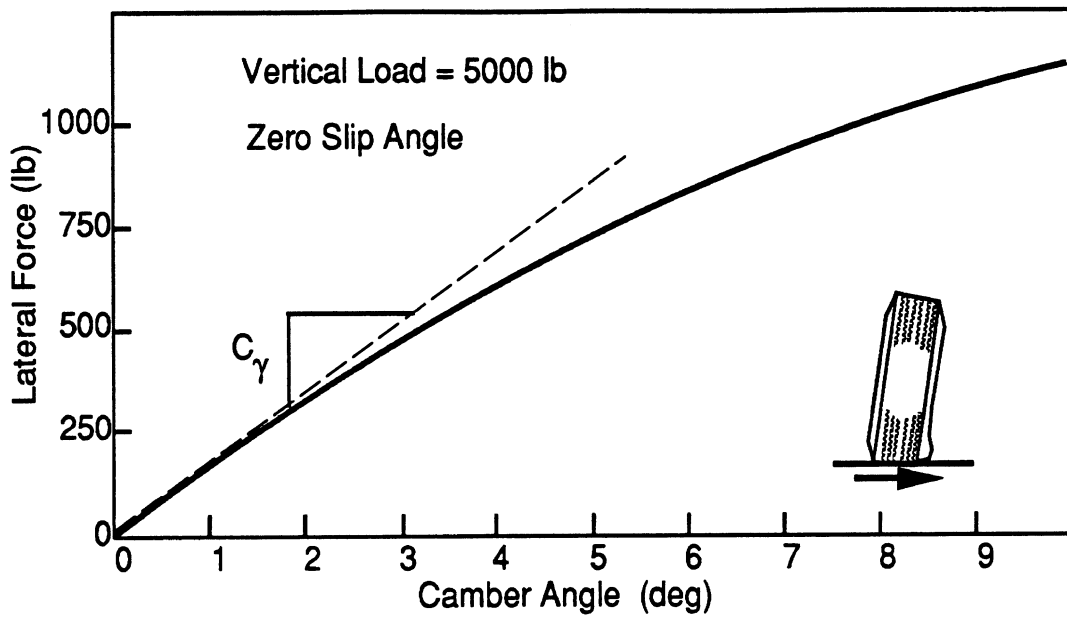
Figure 48. Lateral force (camber thrust) caused by camber of a truck tire.
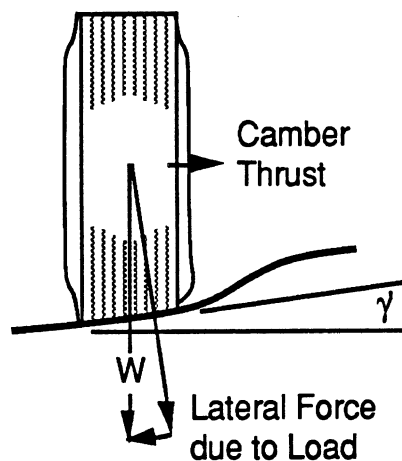
Figure 49. Forces acting on a tire on a cross-slope surface.

The lateral force per unit load is:

$$\frac{F_y}{W} = \sin \gamma' \cong \gamma' \qquad (2\text{-}8)$$

where:

W = Weight on the tire

γ' = Inclination angle of the road surface

Thus at one degree of surface cross-slope angle a lateral force of $1/57.3 = 0.0175$ lb/lb is produced in the "downhill" direction by the gravitational component. On the other hand, the camber thrust from the tire acts to push the tire "up" the slope in proportion to its camber coefficient. If the camber coefficient is greater than 0.0175 lb/lb/deg, the tire will

try to climb out of the rut. If it is less it will tend to run down in the bottom of the rut and track in that position. Thus, a camber coefficient of 0.0175 is a critical value.

Large differences in camber stiffness are associated with differences in tire construction. Figure 50 shows the camber stiffness distributions for a population of radial and bias-ply tires. The camber coefficient for radial tires generally falls about 0.01, while that of bias-ply tires is a little over 0.02.

The significance of this observation relates to the tracking properties that are likely to affect rutting. The camber coefficients for radial and bias-ply tires fall on opposite sides of the critical value. Radial tires will tend to track in a rut, while bias-ply tires will tend to climb out. With the high proportion of radial tires being used on modern trucks, it is hypothesized that this tracking tendency may be one of the primary factors responsible for the dual wheel ruts that frequently develop on asphalt roads.
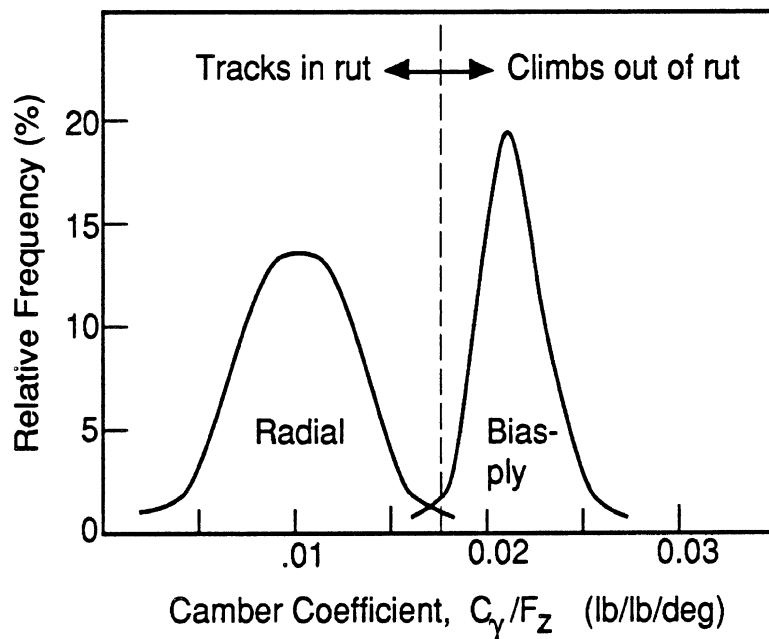
Figure 50. Frequency distribution of camber coefficient for passenger car tires.

Wheel Path Location

Most of the analysis performed in this work has been based on the calculation of damage caused by a single pass of a vehicle. The effect of wheel path location on pavement damage depends on the consideration of all of the vehicles that pass in a lane. If all the vehicles pass in the same wheel path, they will induce damage along the same lateral position with every pass. Vehicles do not always pass in the same lateral position. The wander exhibited by a mix of traffic will increase pavement life by distributing wheel loads across the lane. No effort was made to replicate the random effects of lateral tracking variations in the analysis, because this behavior is not specifically related to truck characteristics.

72

Calculations could be made to illustrate the influence of wheel path location on damage to rigid pavements for a single vehicle pass. However, none were made for flexible pavements because the pavement models use a circular tire contact patch and the layers extend to infinity in the lateral plane (no lane edge effects). This would produce unrealistic estimates of the lateral variation in the strains under a passing tire. However, it should be noted that once ruts begin to form on a flexible pavement, vehicles are more likely follow in the same wheel path.

Rigid Pavement Fatigue

Figure 51 shows the variation in longitudinal stress across a rigid pavement lane induced by a conventional single tire and a set of dual tires. Both tires are placed as if they are mounted on the truck with a maximum overall width of 8 ft that is traveling in the center of a 12 ft wide lane. The single tire has a shallower lateral range of influence than the dual tires. This is a result of the narrower contact width of the single tire. The damage caused by axles with single tires will reduce more significantly with variations in wheel path location.
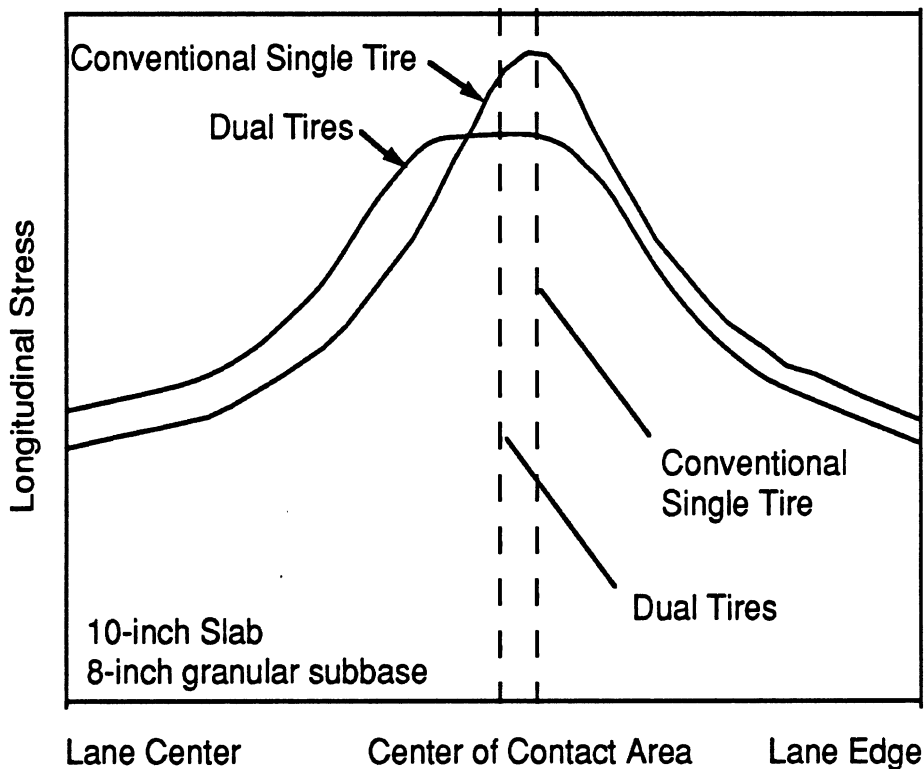
Figure 51. Variation in longitudinal stress across a lane under dual and conventional single tires.

Wheel path location also affects rigid pavement fatigue because of the increase in longitudinal stress response to tire loads near the lane edge. If a tire tracks at the lane edge, the stress under it can be significantly higher than the stress under a tire tracking in the center of the lane. Figure 52 shows how the peak tensile stress under a set of dual tires on a 20-kip axle varies from the lane center to the lane edge for a 10-inch slab, 12-foot lane width. The stress at the edge of the lane is 73% higher for the same load as the stress 42

inches from the edge. (42 inches corresponds to the tracking position of the center of the outer dual tire on a 8-foot wide truck that is centered in a 12-foot lane.) Using the 4th power relationship between fatigue and peak tensile stress, the edge of a lane can sustain damage that is a factor 9 times higher than the lane center for the same loading conditions.

Flexible Pavement Fatigue

The flexible pavement models used in this study are inadequate for evaluating the effects of wheel path location on flexible pavement fatigue because they do not provide for a pavement edge.

Rutting

The flexible pavement models used in this study are inadequate for evaluating the effects of wheel path location on rut generation because they do not provide for a pavement edge.
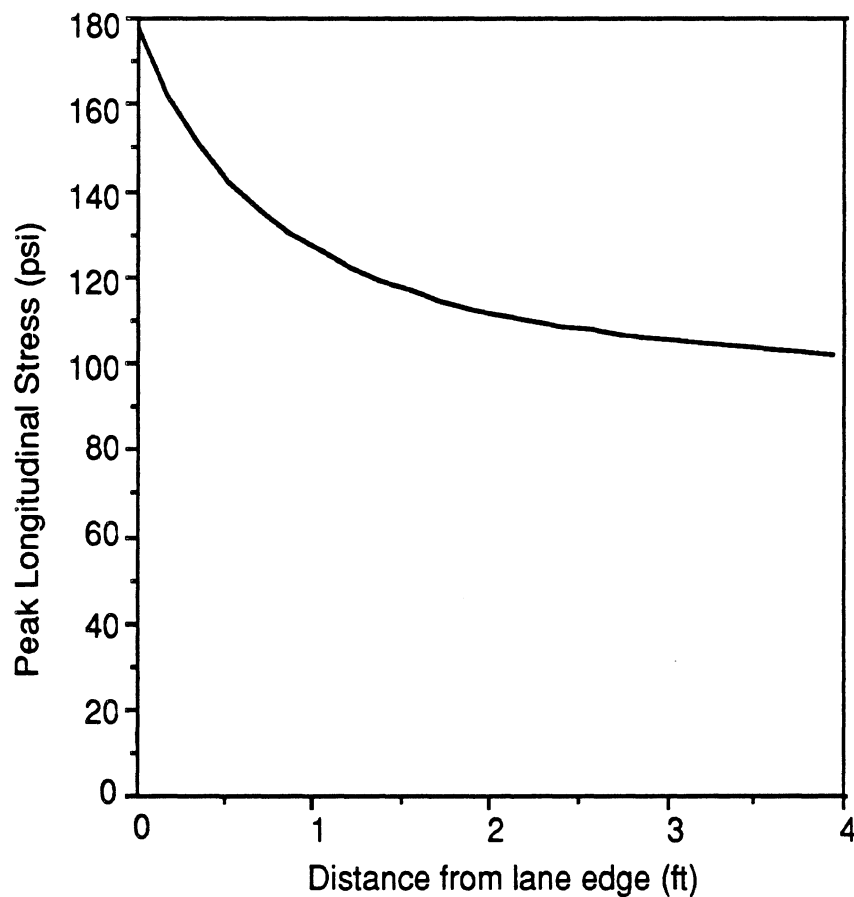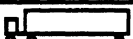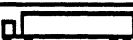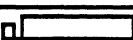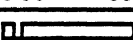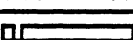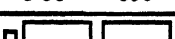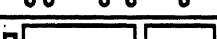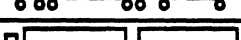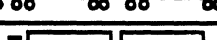
Figure 52. Peak longitudinal stress vs. distance of dual wheel set from lane edge.

RIGID PAVEMENT FACTORS

Trucks with diverse properties have different effects on various pavements. The fatigue life of the family of rigid pavements was investigated with the base matrix of 13 trucks, shown in Table 12. Figure 53 compares the damage of the 13 trucks for the matrix of rigid pavement considered in this study (see Appendix B). Although the trucks have been ordered according to damage predicted by summing their axle loads raised to the fourth power, the relative damage is similar on most other pavements with several exceptions. This is because pavement design variables such as slab thickness, subbase strength, slab length, and joint load transfer level, affect the relative damage potential of various axle spacings and tire contact conditions. These interactions are responsible for the change in damaging potential of one truck relative to another with pavement design.

Table 12. Truck Matrix Sizes, Weights, and Tires.

Truck Num.	Truck Configuration	Configuration Name	GCVW (kips)	Axle Loads (kips)	Tires
1		2 Axle Straight Truck	32	12/20	S/D
3		3 Axle Straight Truck	46	12/34	S/D/D
5		3 Axle Refuse Hauler	64	20/44	W/D/D
9		4 Axle Concrete Mixer	68	18/38/12	W/D/D/D
13		3 Axle Tractor-Semitrailer	52	12/20/20	S/D/D
14		4 Axle Tractor-Semitrailer	66	12/20/34	S/D/D/D
16		5 Axle Tractor-Semitrailer	80	12/34/34	S/D/D/D/D
22		5 Axle Tanker	80	12/34/34	S/D/D/D/D
23		6 Axle Tanker	85	12/34/39	S/D/D/D/D/D
25		5 Axle Doubles	80	10/18/17/18/17	S/D/D/D/D
27		7 Axle Doubles	120	12/34/34/20/20	S/D/D/D/D/D/D
28		9 Axle Doubles	140	12/32/32/32/32	S/D/D/D/D/D/D/D/D
29		Turner Doubles	114	10/26/26/26/26	S/D/D/D/D/D/D/D

75
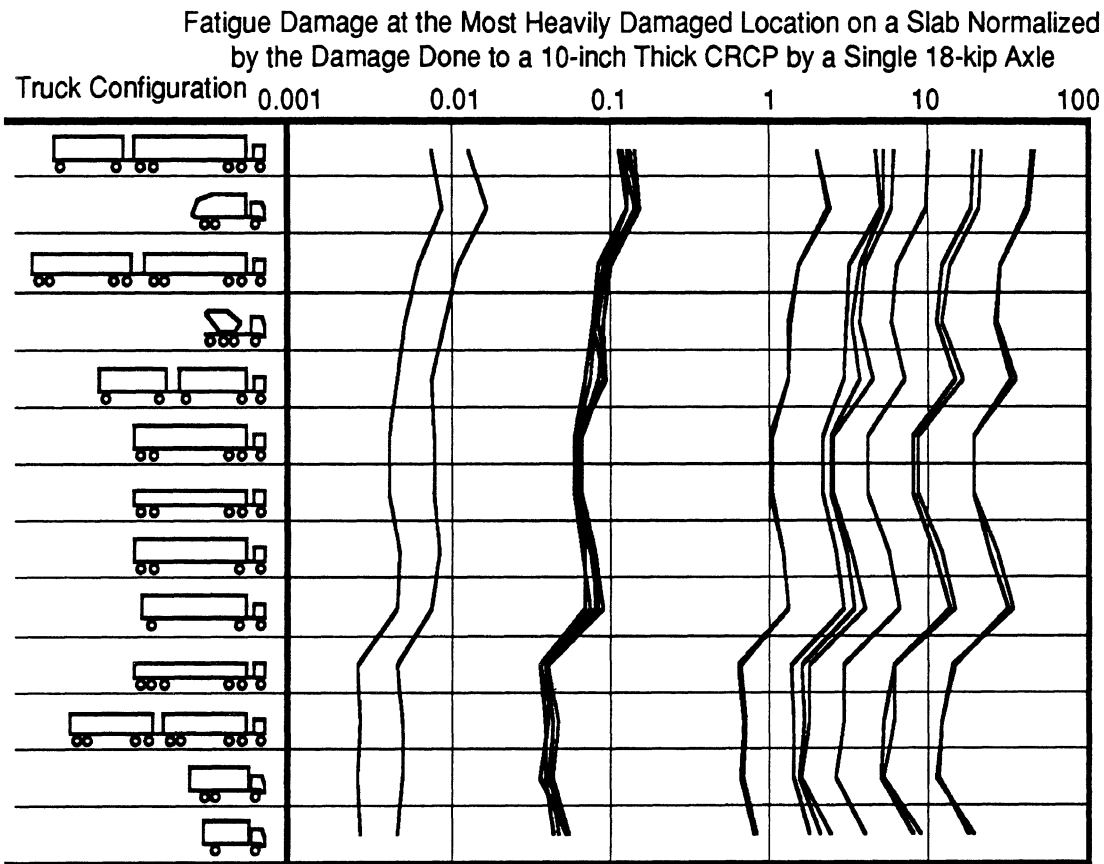
Figure 53. Damage caused by various trucks at their static loads to a mix of rigid pavement designs.

Slab Thickness

Slab thickness and subbase strength are the two most important variables affecting the life of rigid pavements. Thick slabs can endure higher loads for longer duration, but are somewhat more costly to construct. Hence a balance is needed in rigid pavement design to maximize the life to cost ratio.

The maximum tensile stress at the bottom of a slab induced by a single 20-kip axle varies with slab and subbase design as shown in Figure 54. With no base, or a granular base, the slab experiences higher stresses because it is the primary structural member. With a cement treated base, which is assumed not bonded to the slab, slab stress is reduced as a result of the reinforcement from the base. Figure 54 suggests that if fatigue damage is proportional to the peak tensile stress raised to the fourth power, adding an additional inch of thickness to a pavement will increase its fatigue life more than 60% for an 11-inch slab and up to 120% for a 7-inch slab. Use of a higher strength concrete will also increase pavement resistance to damage from trucks. Based on the fourth power law, a 50% increase in ultimate strength would theoretically reduce damage by 80%. Croney and Croney report that with this increase in strength, the service life of a 200-mm slab is doubled (22).
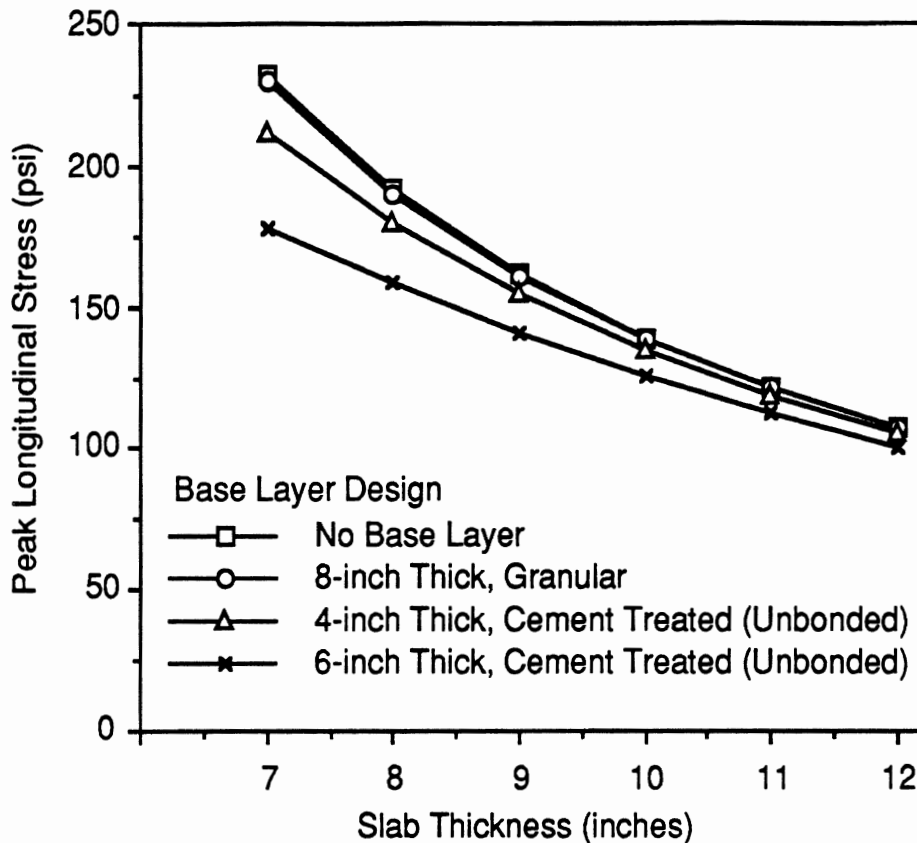
Figure 54. Maximum tensile stress induced by a 20-kip axle under various slab thicknesses and base layer designs.

Slab thickness affects the relative fatigue causing potential of various trucks through its interaction with axle spacing. Figure 55 shows the relative fatigue damage for a set of trucks running on rigid pavements of slab thickness 7, 10, and 12 inches, each with a granular subbase. The damage, given in ESALs, represents one pass of each vehicle with the axle loads at their static values. The trucks are arranged in descending order of damage to the pavement with a 7-inch slab. In the figure, the relative damage caused by some of the trucks increases with slab thickness while others decrease.

The ones that decrease are those whose damage is mostly caused by axles in single axle groups. Those that increase in damage with thickness are the ones whose damage is caused mostly by multiple axle groups. This is because the relative damage of a closely-spaced (51 inches) multiple axle group decreases with slab thickness as shown in Figure 56. The relative damage in ESALs caused by a 34-kip tandem axle is given as a function of axle spacing for the pavements included in Figure 55. The figure shows that, at a spacing of 51 inches, a 34-kip tandem axle induces 0.87, 1.12, and 1.35 ESALs to the pavement of slab thickness 7, 10, and 12 inches, respectively. This effect is responsible for the increase in relative damage with slab thickness for tandem-axle trucks.

Figure 55 also shows a decrease in relative damage with slab thickness for trucks with all single axle groups. This is caused by the increased range of influence of one axle on the peak stress under another for thicker slabs. This is also demonstrated in Figure 56, where
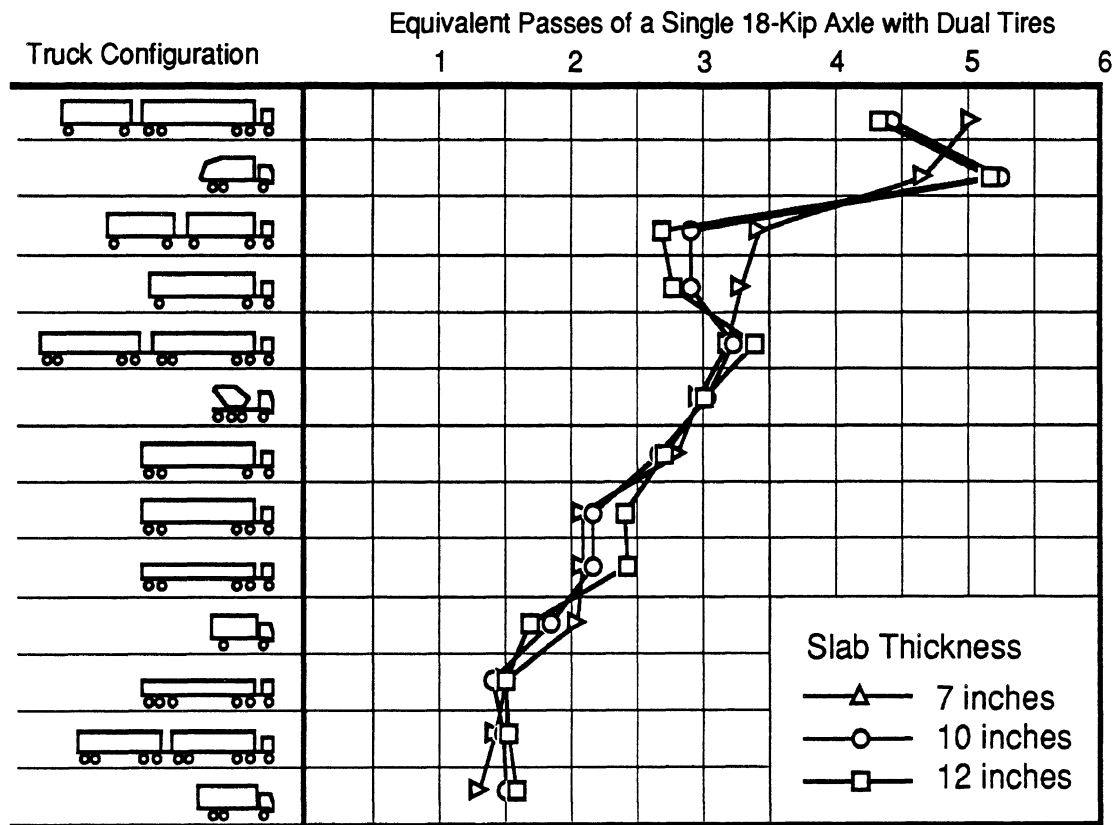
Figure 55. Influence of slab thickness on relative rigid pavement fatigue.
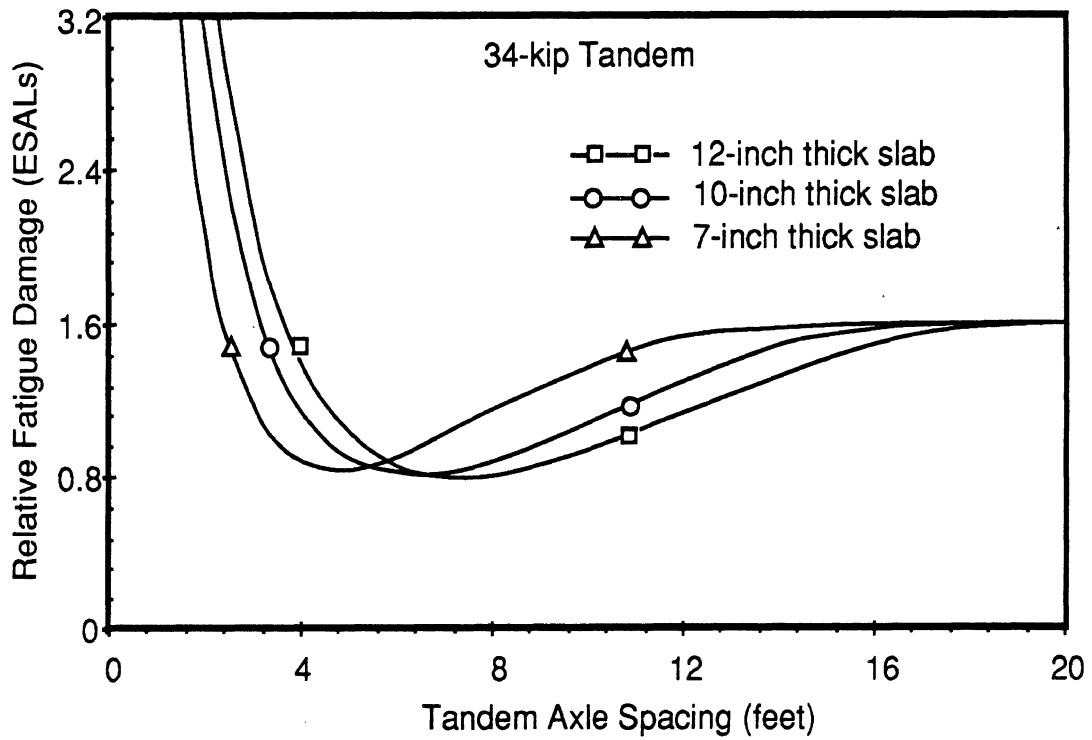
Figure 56. Influence of slab thickness and axle spacing on damage.

the 12-inch slab shows the lowest relative damage in the range of axle spacings from 10 to 20 feet. This means that when steer and drive axles are separated by 10 to 15 feet, they will diminish the peak stresses under each other. The same is true for the axles near a hitch for the doubles combinations (axles are separated by 10 feet across a hitch). This effect is responsible for the significant decrease in relative damage caused by, for example, the 5-axle doubles. It is also responsible for canceling out the increase in relative damage of the tandem axles of the 5-axle tractor-semitrailer, leaving the damage caused by it to remain fairly constant with slab thickness.

Figure 55 shows that the *relative* damage for a set of vehicles is dependent on slab thickness in some cases because of its interaction with axle spacing. The *absolute* damage, on the other hand, changes vastly with slab thickness. For example, the single pass of an 18-kip axle used as a basis for calculating relative damage in Figure 55 represents more than 22 times more damage to the pavement with a 7-inch slab compared to the 12-inch slab.

Subbase Strength

The relative damage caused by the 13 trucks shown in Table 12 changes with subbase strength as a result of an interaction with axle spacing similar to the one explained in the Slab Thickness section. Once again, due to the fact that subbase strength has a strong influence on the overall strength of a rigid pavement, it dictates the range of influence of an axle on the stresses at other locations. This is particularly true in cases where a cement treated subbase is substituted for a granular subbase.

Figure 54 indicates that a slab with a cement treated subbase will be more resistant to truck induced fatigue than the same slab with a granular subbase. This is, however, a theoretical result as the analysis assumes the cement treated subbase maintains its integrity and provides uniform support to the slab. In practice this may not be the case. The rigidity of the cement treated subbase prevents it from conforming to changes in the shape of the slab (as arise from temperature gradients, etc.) as well as a granular base, thus leading to stress concentrations that degrade both the slab and the subbase. Further, with cracking of the weaker subbase, stress concentrations are imposed on the slab. These and other factors not included in the modeling are undoubtedly the reason that designs with cement treated subbases do not performed as well in practice as would be suggested by the analysis.

Subgrade Strength

As the subgrade contributes very little to the overall strength of the rigid pavement designs studied, subgrade strength had minimal influence on the fatigue damage caused by trucks, both relative or absolute.

Joint Load Transfer

Concrete expands with an increase in moisture or temperature. As these conditions are not uniform throughout the slab, the slab warps or curls, such that there is nonuniformity of contact and support. This expansion and contraction, especially due to temperature, is resisted by friction with the underlying layer. If the volume change in concrete structures is constrained, then damage in the form of cracking or crushing of concrete can occur due to

excessive stresses or strains. Joints are provided in concrete slabs to control where cracks will occur in response to the internal stresses caused by; (1) initial shrinkage arising from moisture loss, (2) frictional resistance against the subbase or subgrade during longitudinal expansion and contraction arising from temperature changes, and (3) thermal and moisture gradients between the top and bottom of the slab.

Load transfer at joints plays an important role in fatigue analysis of rigid pavements. Fatigue of concrete pavements is dependent on the peak tensile stresses imposed. Different load transfer conditions provide different stress/strain levels. The interactions of load transfer and axle spacing are seen in the influence functions in the vicinity of a joint. Figure 57 shows influence functions at a point 5 feet from the end of a slab for joints with aggregate interlock, doweled joints, and a continuous pavement (no joint). The most obvious difference between the influence functions is the compressive peak as the tire crosses the joint. The weaker the load transfer (e.g., the aggregate interlock), the higher the compressive peak.

Another effect of load transfer is an increase in peak tensile stress in locations near a joint. The worst location is generally in the range of 3 to 7 feet from the joint depending on slab thickness and load transfer level. The presence of a joint elevates the peak tensile stress at this location by 10% for a doweled joint and 3.3% for aggregate interlock.
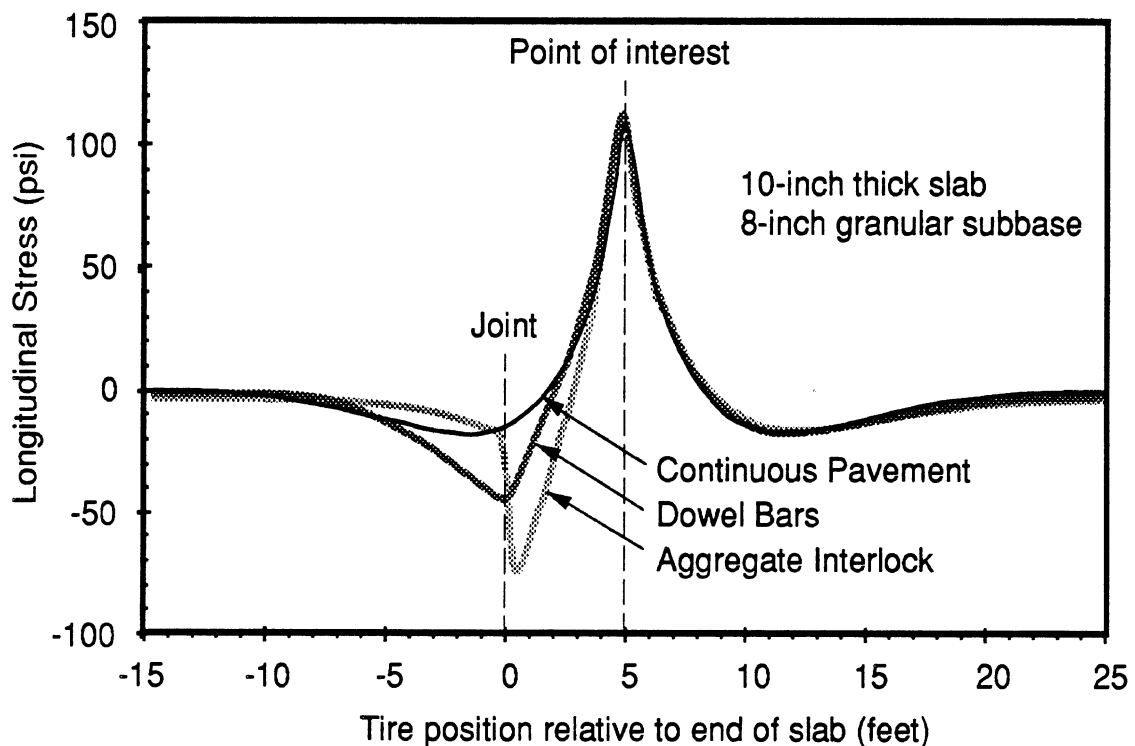
Figure 57. Effect of load transfer level on influence function shape.

The presence of a joint elevates the peak tensile stresses, and hence, damage, caused by a single axle when near the end of the slab. The elevated compressive stresses in the region near the end of the slab can actually reduce the damage caused by tandem axles. This is demonstrated in Figure 58, which shows the stress pattern induced at a location 5 feet aft of

a joint, for a doweled joint and a joint with aggregate interlock. A time history for a continuous pavement is also included to show the stress pattern that would prevail in the theoretical case of a joint with perfect load transfer. As the second axle passes over the point of interest, the third axle traverses the joint. The tensile stress induced by the second axle of the truck is significantly reduced by the large compressive influence of the third axle. This is particularly significant in the case of aggregate interlock, in which the compressive influence of the third axle on the peak under the second is very large at that instant.

Figure 59 shows the portion of fatigue life consumed by a single pass of various truck layouts along the length of a 40-foot slab. All trucks show a fairly constant damage level at points in the interior of the slab because they are not subjected to the slab end effects described above. The 3-axle tractor-semitrailer and 2-axle straight truck show a damage level that increases smoothly near the slab edge in the region where the peak tensile stresses are elevated by the effects of the load transfer device. The Turner doubles, turnpike doubles, and 5-axle tractor semitrailer do not show the highest damage level at the same locations. This is caused by the tandem axle spacing effect described above. In the figure, the damage level is diminished in areas that are in the vicinity of 4 feet from the slab edge. This is where one axle of a tandem set will have a large compressive influence on the stress under the other, and diminish the contribution of the tandem axle to the overall damage caused by the truck. As all of the axles of the three vehicles mentioned are tandem with the exception of the steer axle, this effect is a strong one.
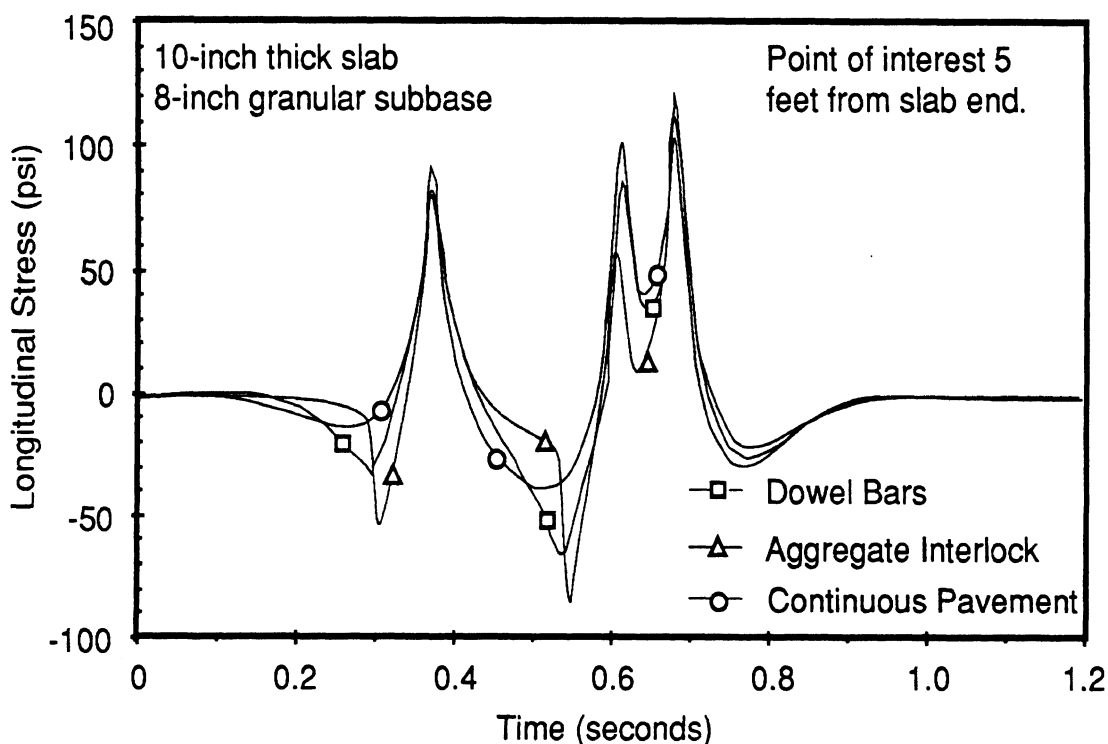
Figure 58. Effect of load transfer at a joint on theoretical stress cycles under a rigid pavement slab induced by a 3-axle straight truck.
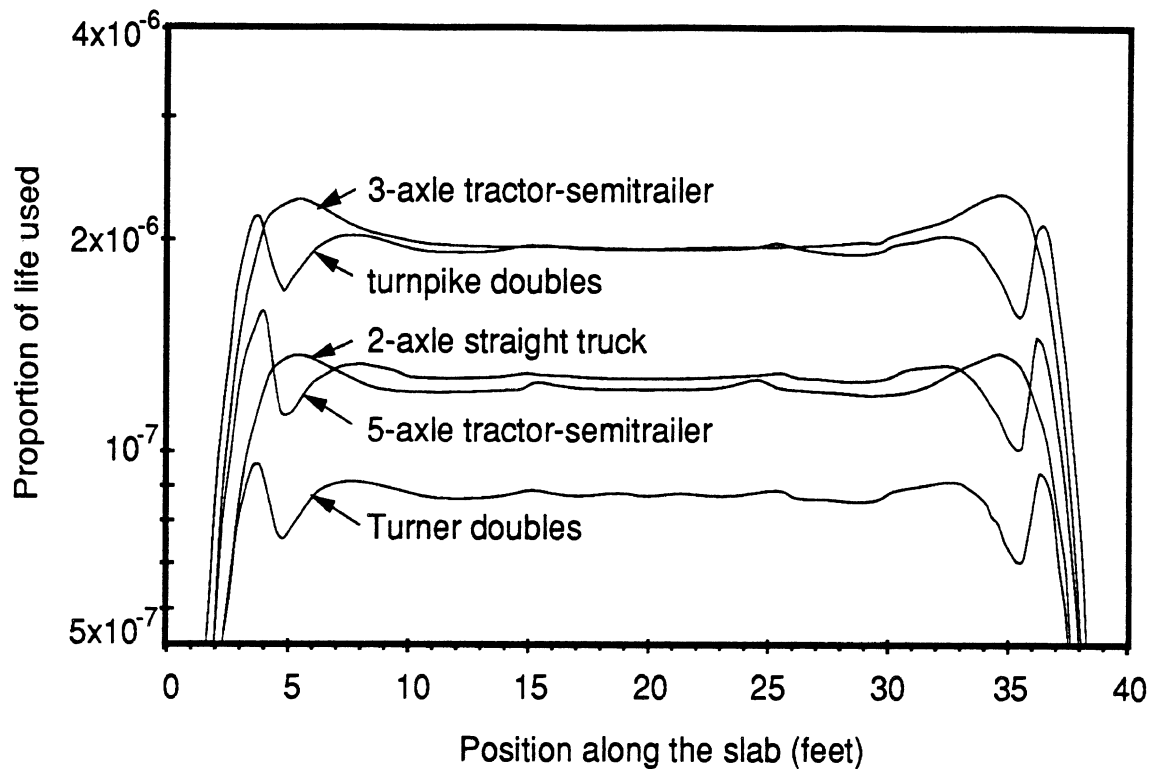
Figure 59. Damage along a slab with doweled joints caused by various truck layouts.

Slab Length

Slab length plays a major role in pavement's life and construction cost. Longer slabs end up with fewer joints thus reducing the cost of joint construction and saving the time of construction. However, long slabs are likely to develop cracks near the center, reducing the effective lengths of the slab to half of the original length or less (*23*). An argument for using short slab lengths is that the effectiveness of aggregate interlock varies inversely with the joint openings, and joint openings have been found experimentally to be less severe with shorter slab lengths (*23*). In normal practice, slab lengths ranging from 12 to 20 feet are used for Plain Jointed Concrete Pavements (PJCP) (*24*).

In this research it has been found that short slabs prove to be slightly more sensitive to fatigue damage. Figure 60 shows results of a study in which all design variables were held fixed except for slab length. One curve shows damage at the mid-slab location and the other is the 95th percentile damage level. Performance decreases significantly for slab lengths less then 20 feet, while there is negligible effect for lengths over 30 feet.

Although fatigue was the primary focus in this research effort, which was limited to the pavement models that were available, rigid pavements failure is seldom purely a result of fatigue. The most common failure experienced at the AASHO Road Test (*1*), and throughout the nation today, is pumping of slabs which causes faulting and loss of support at joints. Slab length plays an even more critical role in this distress mode.
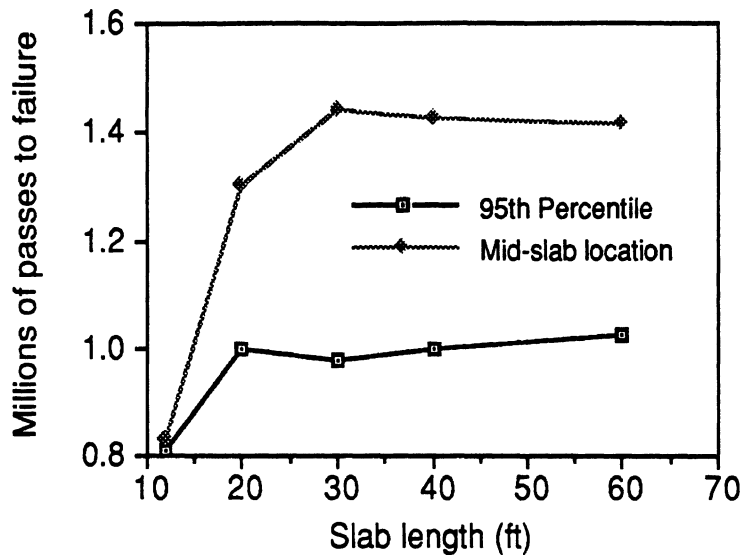
Figure 60. Effect of slab length on rigid pavement fatigue damage.

Temperature Gradient

Transverse cracking in rigid pavements is mainly a result of; (1) internal stresses from drying shrinkage coupled with friction between the bottom of the slab and the underlying layer, and (2) the internal forces associated with temperature gradient causing curling of slabs and moisture gradient causing warping of slabs, and (3) the stresses caused by external loading. The combined effect of vehicle loading and internal stresses will accelerate pavement fatigue when stresses from the two effects are additive. Given that fatigue damage tends to vary with the fourth power of stress, the addition of thermal-induced stress in the pavement can be an extremely important factor in its performance.

A pavement slab subjected to a positive temperature gradient (higher temperature at the surface) curls downward at the edges. A slab subjected to a negative temperature gradient curls upward at the edges. In the case of a slab that is curled downward, a thermally induced tensile stress will be present that, when superimposed on the stress induced by a truck axle, will elevate fatigue damage significantly. In this study, the temperature is assumed to vary linearly with depth based on an experimental study conducted by Richardson et al, in which the authors conclude that nonlinearity of the temperature gradient in a PCC pavement did not have a significant impact on its performance (25).

Figure 61 shows how the proportion of fatigue life used by a single pass of a 5-axle tractor-semitrailer varies along a 40-foot slab with temperature gradients of 0, 1, and 3°F/inch (slab edges curled downward). A thermal gradient of 1°F/inch increases damage at center slab by an order of magnitude and a temperature gradient of 3°F/inch increases damage at center slab by more than 2 orders of magnitude. Thus, the change in damage due to increase in temperature gradient is not linear. Another aspect of the elevation in damage with temperature gradient is that the location of maximum damage shifts from a point near the end with no gradient, to center slab with a gradient.
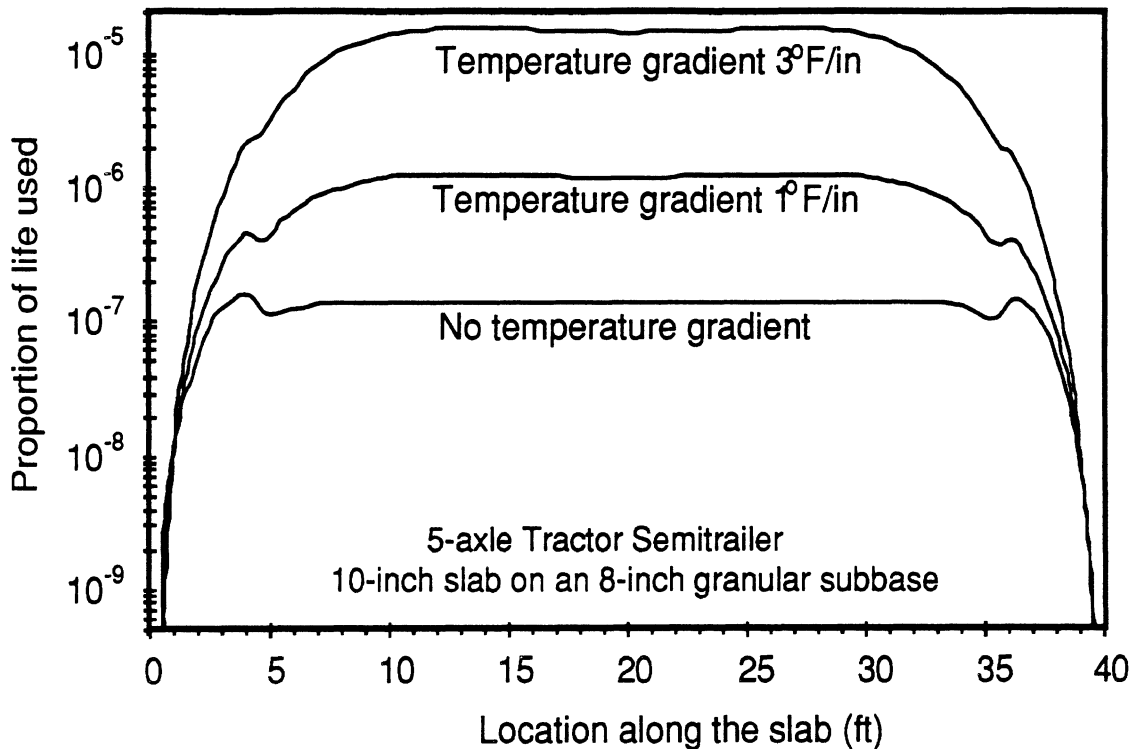
Figure 61. Effect of temperature gradient on fatigue life along the length of a PCC slab.

The elevation in damage with temperature gradient is not the same for every truck. Figure 62 shows how the damage caused by a 2-axle straight truck and Turner doubles varies along a slab with no temperature gradient and a temperature gradient of 1°F/inch. The damage caused by the 2-axle straight truck is elevated considerably less with a temperature gradient than that caused by the Turner vehicle. The reason for the difference is that the thermal stresses are simply superimposed on the peak stresses under each axle of the trucks, with the result that trucks whose damage derives from many axles are more sensitive to temperature gradients. The damage caused by the Turner vehicle is caused by 8 axles loaded to 13 kips and one axle loaded to 10 kips. The damage caused by the 2-axle straight truck is primarily caused by the 20-kip drive axle. Superimposing the thermal stress on the peak stress caused by each of these axles elevates the stress under the 20-kip drive axle by a less significant fraction than the stress under the axles of the Turner vehicle. Thus, the damage caused by Turner vehicle is elevated more than the damage caused by the 2-axle straight truck.

Roughness

Roughness was seen to have a moderate influence on rigid pavement fatigue in the discussions of speed and suspension effects. Truck dynamics increase steadily with roughness. The roughness of rigid pavements has a random component, like that of all other roads, but may also have a periodic component arising from the characteristic shape of slabs. The periodic component may tune to vibration modes of certain trucks and tractor-trailers causing them to be disproportionately damaging at certain speeds. Slab curl and slab tilt are the shape features with the greatest potential to tune to truck vibrations.
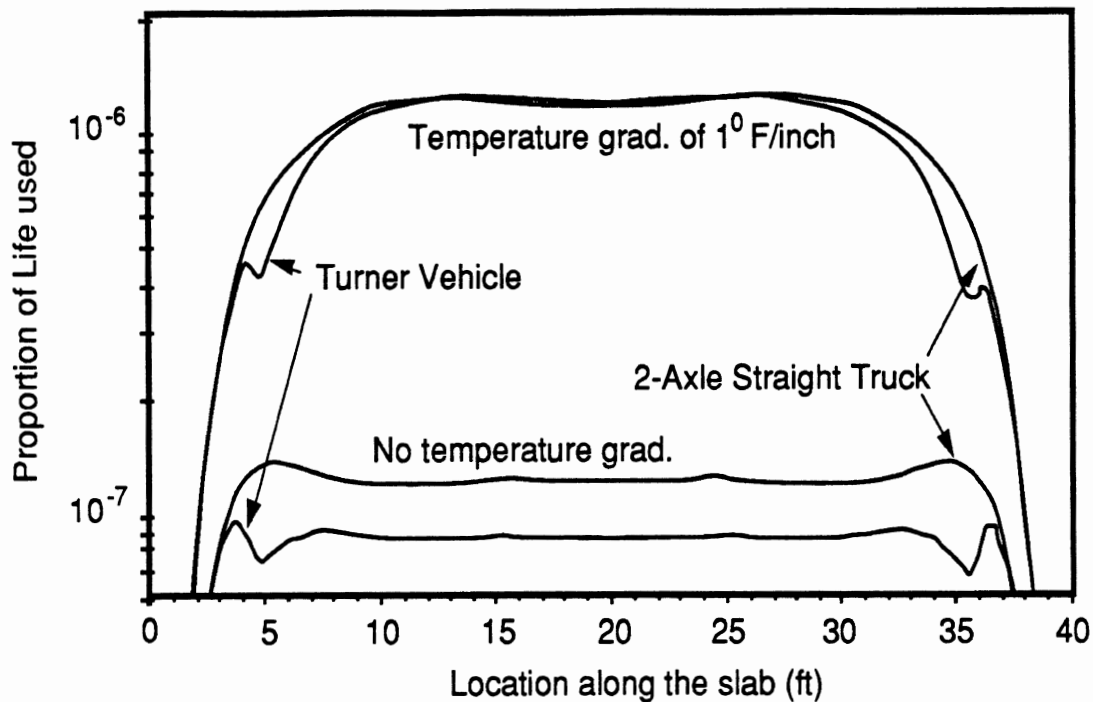
Figure 62. Comparison of the elevation in damage caused by a temperature gradient for various trucks.

The potential for tuning in a truck is dependent on many factors: wheelbase, axle locations, suspension properties, load distribution, speed, slab length and type of pavement distress, making a broad-based assessment of this behavior complex to characterize. Although instances of tuning were observed in some of the analyses, the incremental damage arising from the phenomenon is small relative to other factors, and does not warrant the effort it would take to fully characterize the truck population and operating conditions at which tuning is likely.

FLEXIBLE PAVEMENT FACTORS

The specific characteristics of trucks that are most damaging to flexible pavements, and the nature of the damage, vary with pavement design. Common vehicle and pavement matrices were used for calculating fatigue damage and rutting damage.

Wear Course Thickness

Fatigue

The fatigue damage caused by trucks is highly dependent on the thickness of the wear course. Figure 63 shows fatigue damage by truck configuration for a range of wear course thickness normalized by that of a single 18-kip axle with dual tires on a pavement with a 5-inch wear course. The damage represents one pass of each vehicle with the axle loads at their static values. The pavements in Figure 63 correspond to pavements 1, 2, 5, 8, and 11 described in the Flexible Pavement Matrix section of Appendix C. The figure shows that

damage delivered to a pavement by each of the trucks varies greatly with wear course thickness. For example, the fatigue caused by a single pass of a 5-axle tractor-semitrailer is 14.6 times more on the 2-inch asphalt concrete pavement than on the 6.5-inch pavement. In contrast, on a given pavement, the fatigue damage was found to vary by a factor of about 2.8 over the range of truck designs shown in the figure.

Truck Configuration | **GCVW (kips)** | **Fatigue Damage Normalized by that caused by a Single 18-kip Axle on a Pavement with a 5-inch Thick Wear Course**

GCVW (kips)
120
64
140
68
80
80
80
66
52
85
114
46
32

Wear Course Thickness
—+— 2.0
—▢— 3.0
—○— 4.0
—▷— 5.0
—✕— 6.5
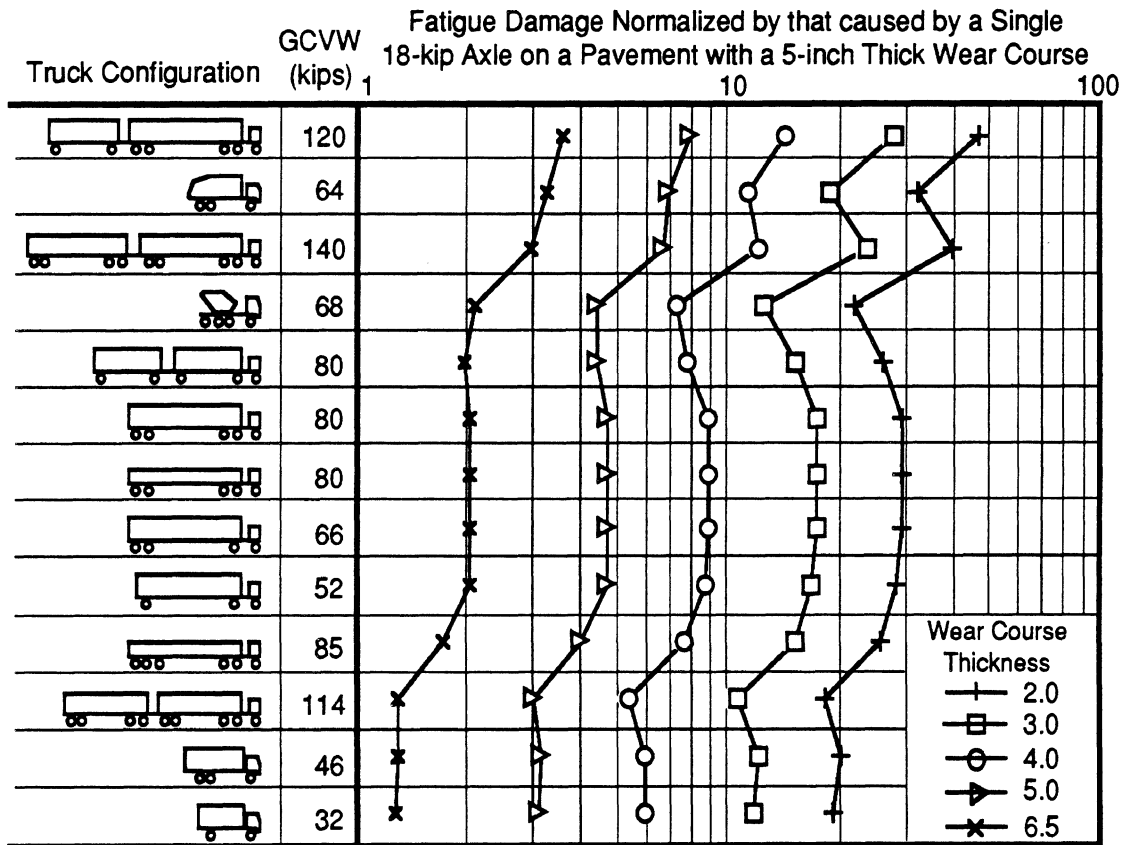
Figure 63. Fatigue damage to flexible pavements with a range of wear course thicknesses.

The trucks in Figure 63 are arranged in descending order of damage predicted by summing the axle loads raised to the 4th power. The damage caused by the trucks relative to each other changes with wear course thickness primarily due to the differences in damaging potential of conventional single and wide-base single tires compared to dual tires over the range of thicknesses. For example, the fatigue damage caused by the 3-axle refuse hauler and the 4-axle concrete mixer relative to other trucks increases with wear course thickness. This is because they each have steer axles fitted with wide-base single tires. As explained in the Tire Factors section of this chapter, wide-base single tires are less damaging relative to dual tires on weaker pavements. The relative contribution of the steer axle of the 3-axle refuse hauler and 4-axle concrete mixer therefore diminishes with wear course thickness. This is a significant effect because the steer axle of each of these vehicles contributes to a significant portion of the overall damage by virtue of their load.

Rutting

The levels of rut depth caused by truck traffic changes significantly with wear course thickness. That is, a single pass of an 18-kip axle on a pavement with a 6.5-inch wear course corresponds to 1.41 times the rut depth of the same axle on a 2-inch wear course. The difference is simply due to the fact that a thicker wear course means the presence of more material that is prone to plastic flow. This is demonstrated in Figure 64, in which the rut depth per vehicle pass is given for various truck configurations and wear course thicknesses. The damage given in the figure is normalized by the damage caused by a single pass of an 18-kip axle with dual tires on a pavement with a 5-inch thick wear course. The figure demonstrates that wear course thickness has a strong influence on plastic flow rutting. For example, a 5-axle tractor-semitrailer will cause 50% more plastic deformation in the layers of the pavement with a 6.5-inch thick wear course than it will cause in the pavement with a 2-inch wear course. In contrast, on a given pavement, the rut depth per vehicle pass was found to vary by a factor of up to 3.9 over the range of truck designs shown in Figure 64. It should be noted that the results given in the figure are for plastic flow of the pavement layers only, and do not include compaction of the base, subbase, and subgrade layers. Although this analysis predicted that thinner layers reduce rutting, a model that includes compaction would favor a thicker asphalt concrete layer and would be necessary to arrive at optimum pavement layer thicknesses.
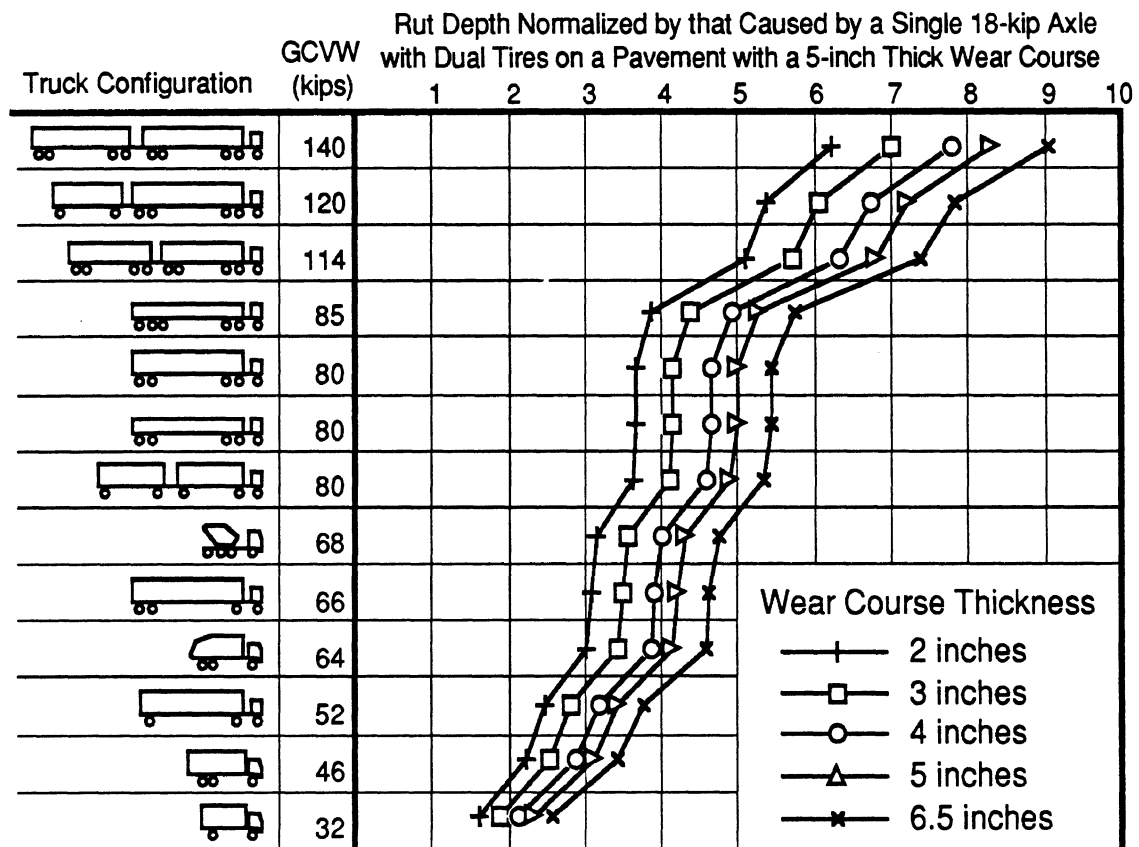
Figure 64. Rut depth caused by a range of trucks and pavement wear course thickness.

Figure 65 shows how the relative rut depth caused by various truck layouts changes with wear course thickness. The rut depth from one pass of each vehicle with the axle loads at their static values is plotted in terms of ESALs for a range of wear course thicknesses. Unlike Figure 64, this figure shows the relative damage to a pavement normalized by a single pass of an 18-kip axle on that pavement. The gray band shown in the figure represents the relative damage caused by each vehicle over a range of wear course thicknesses from 2 to 6.5 inches. The relative damage caused by each truck changes with wear course thickness primarily due to the differences in damaging potential of conventional single and wide-base single tires compared to dual tires. As explained in the "Tire Factors" section of this chapter, the rut depth caused by single tires relative to dual tires increases with wear course thickness.

Truck Configuration	GCVW (kips)	Equivalent Passes of a Single 18-Kip Axle with Dual Tires
	140	
	120	
	114	
	85	
	80	
	80	
	80	
	68	
	66	
	64	
	52	
	46	
	32	
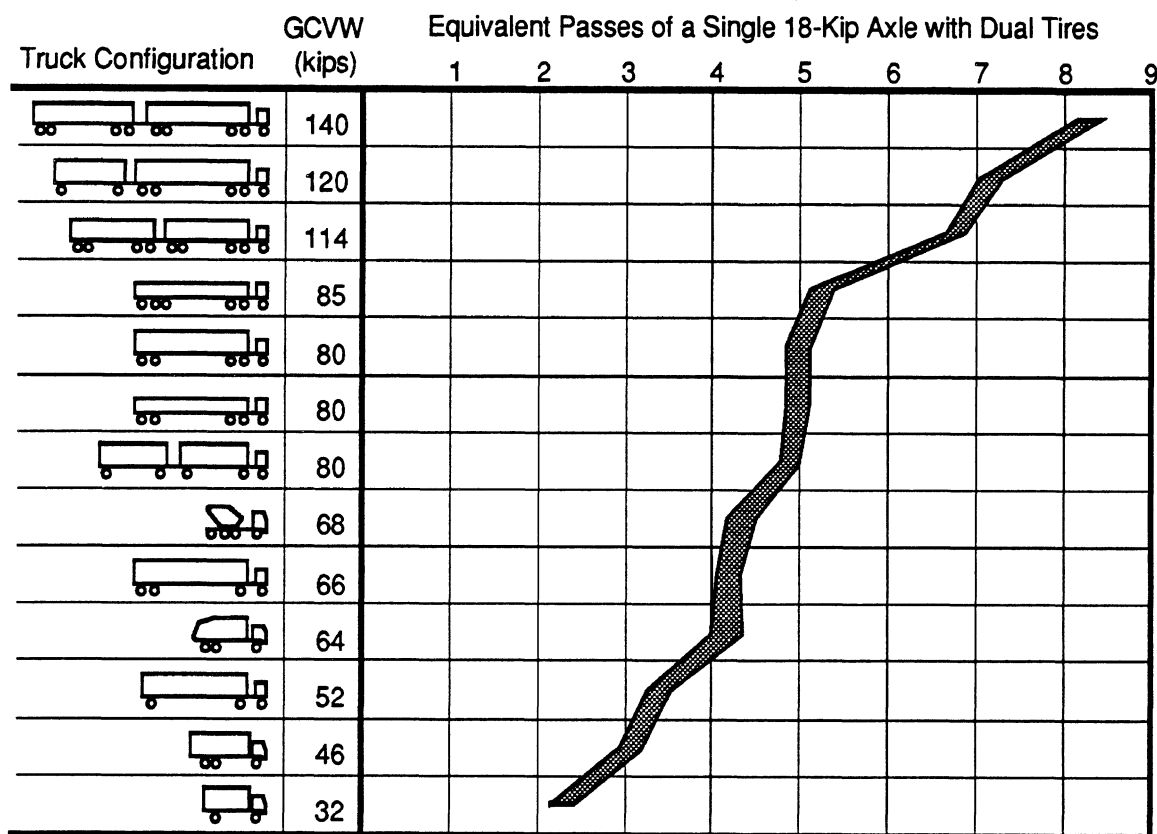
Figure 65. Rut depth production expressed as ESAL exposure per pass deriving over a range of trucks and pavement wear course thickness.

Since the relative rutting damage given in the figure is based on a reference axle with dual tires, the contribution of axles with dual tires to relative damage is constant with wear course thickness. For example, the drive axle of the 2-axle straight truck (bottom of the figure) is loaded to 20 kips and is fitted with dual tires. It is responsible for 1.1 ESALs on all of the wear course thicknesses considered. The steer axle, which has conventional single tires and is loaded to 12 kips, is responsible for 1.3 ESALs on a pavement of 6.5 inch wear course thickness and only 1.0 ESAL on a pavement of 2-inch wear course thickness. Thus, the relative damage caused by the entire vehicle ranges from 2.1 to 2.4 ESALs for the thicknesses considered. Despite the fact that the relative damage caused by

the 2-axle straight truck is higher on pavements with a thinner wear course, it is still the least damaging of the trucks included by virtue of its small gross weight. This is because the axles with single tires on all of the other trucks cause a similar increase in relative damage. The 9-axle doubles (top of the figure), for instance, also has a steer axle loaded to 12 kips with single tires and is 0.3 ESALs more damaging to the pavement of 2 inch wear course thickness than the pavement with a 6.5 inch wear course thickness.

Base and Subbase Thickness

Fatigue

Changes in base and subbase thickness has a modest effect on flexible pavement fatigue damage. For example, a pavement with a wear course thickness of 5 inches, an 8-inch base, and a 13-inch subbase sustains 15% more fatigue damage per pass of an 18-kip axle than a pavement with the same wear course thickness with a 11-inch base and a 16.5-inch subbase.

On the other hand, thickness of the base and subbase layers has a very minor effect on the fatigue damage potential of trucks relative to each other. The same mechanisms that change relative damage potential of trucks on pavements of various wear course thickness are present. The interactions are minimal, however, because the base and subbase are more removed from the truck, and contribute much less to the overall strength of a pavement than the asphalt concrete layer.

Rutting

The base and subbase thicknesses cause very minor changes in the amount of plastic flow rutting induced by truck traffic. For example, on a pavement with a 5-inch thick wear course, reducing the base layer from 11 inches to 8 inches and the subbase from 16.5 inches to 11 inches only decreased rutting by 9%. In the case of the base layer, the lack of influence is due to the fact that it undergoes only a small portion of the overall plastic flow experienced by the flexible pavement designs considered. Significant deformation does occur in the subbase. Although the thickness of the base and subbase layers has little effect on rutting from plastic flow, thicker base and subbase layers would help mitigate subgrade compaction.

Subgrade Strength

Fatigue

As the subgrade has little effect on the strains in the wear course of a flexible pavement, subgrade strength had minimal influence on the fatigue damage caused by trucks. As expected, fatigue damage to thinner pavements depends more heavily on the strength of the subgrade. It should also be noted that a pavement with a subgrade that has undergone significant compaction will be more prone to fatigue cracking.

Rutting

Subgrade strength was found to have negligible influence on rutting in flexible pavement layers from plastic flow. Optimal compaction of the subgrade material was assumed. To the extent that any compaction occurs, it will be most pronounced in pavements with thinner wear course layers.

Surface Temperature

Fatigue

Figure 66 shows the effect of temperature on relative fatigue damage of different truck configurations caused by the reduction in modulus at elevated temperatures. (In these calculations the same damage law is used at both temperatures.) The relative fatigue is given in ESALs on a pavement with a 5-inch wear course at surface temperatures of 77° and 120°F. The trucks are arranged in descending order of relative damage caused to the pavement at 77°F.
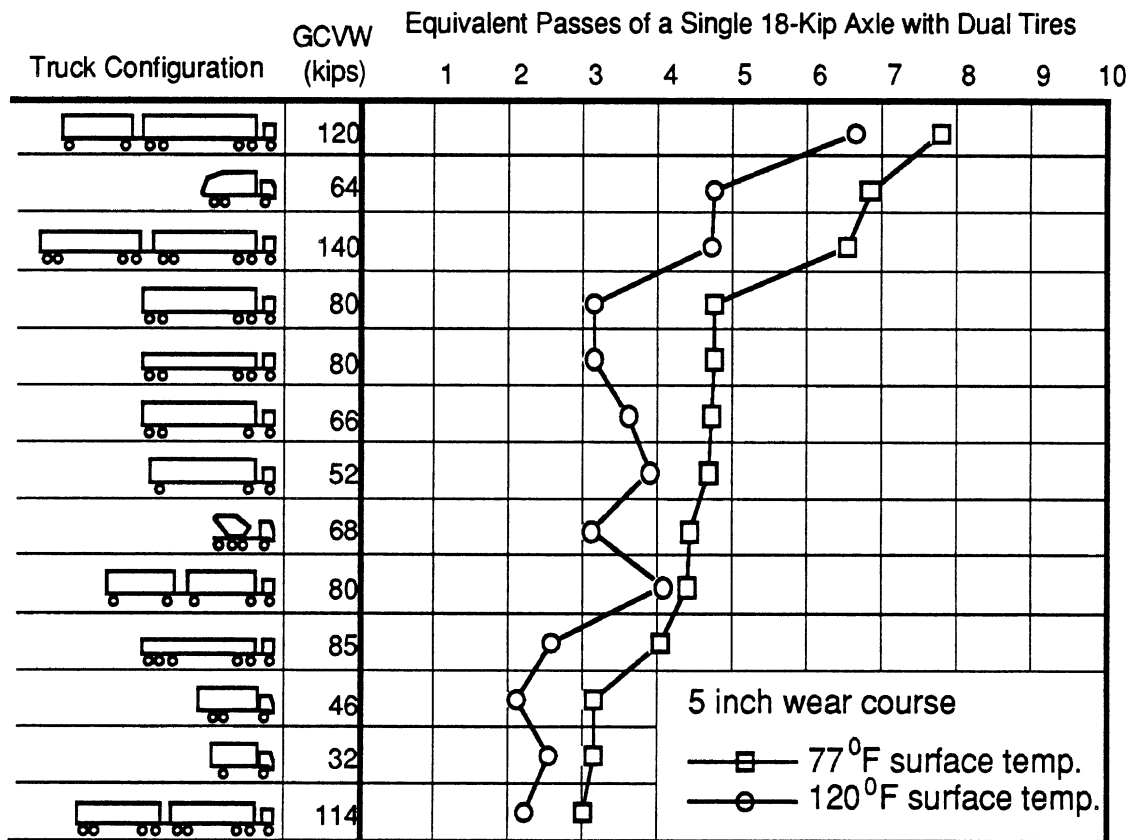
Figure 66. Influence of surface temperature on relative flexible pavement fatigue damage.

At a surface temperature of 120°F the damage (relative to an 18-kip axle) is lower in every case, although it is reduced most for truck configurations with closely-spaced tandem axles. At 120°F pavement surface temperature the strain under single axles increases markedly (an 18-kip axle induces strain that is 1.8 times higher than at 77°F). However,

the lower modulus associated with higher temperatures produces more interaction between closely-spaced axles (similar to that seen on rigid pavements) with the benefit of lower relative strains. Therefore, the relative damage from a 5-axle tractor-semitrailer is lower than that of a 3-axle tractor-semitrailer at elevated temperature.

These conclusions about the relative damageability of truck configurations are based solely on the temperature effects on strain. At high temperatures it is known that asphalt has the ability to heal itself, and is therefore less likely to develop cracks. However, there was no simple and convenient means to include healing in the damage law used in this study.

Rutting

Figure 67 shows how the relative amount of permanent deformation of the pavement layers caused by various truck layouts changes with surface temperature. The relative plastic deformation caused by various truck layouts is given in ESALs for a pavement with a 5-inch wear course at surface temperatures of 77° and 120°F. The additional relative plastic deformation at a surface temperature 120°F is attributed to the increase in damaging potential of conventional single tires compared to dual tires at elevated temperatures.

As explained in the Tire Factors section of this chapter, the rut depth caused by single tires relative to dual tires per pound of load changes with surface temperature. The overall
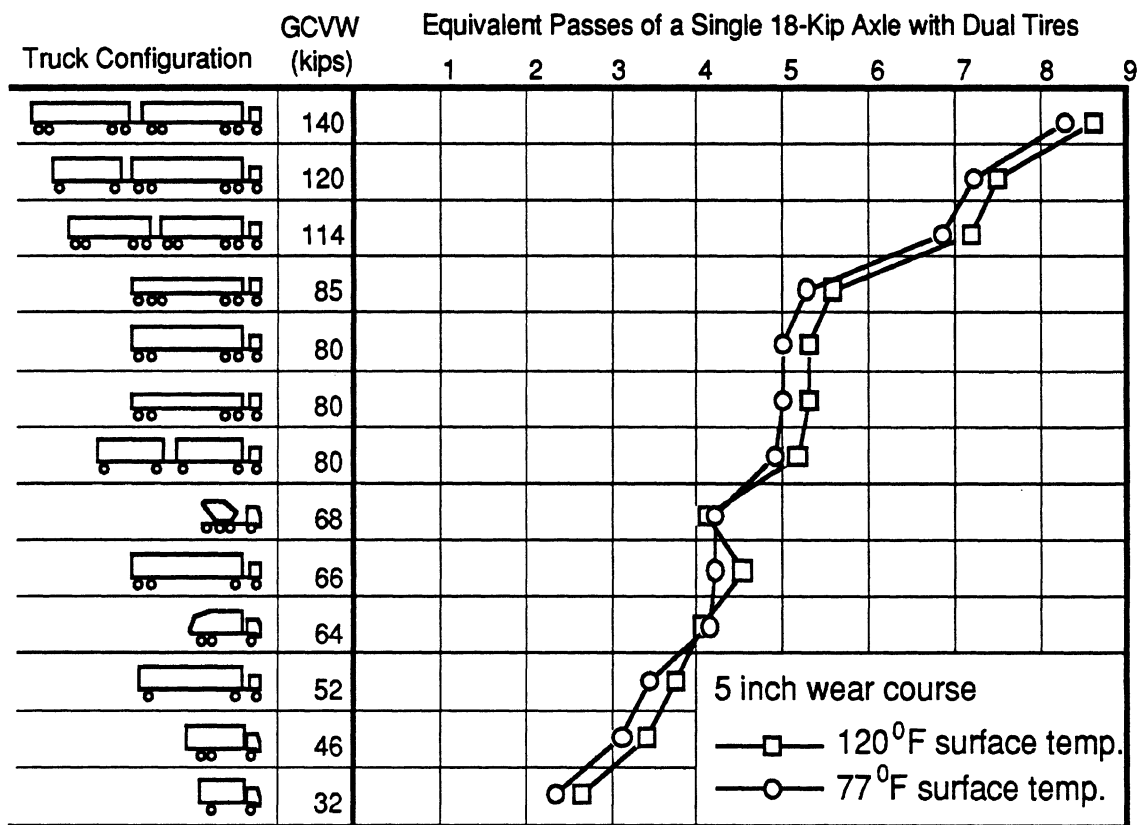
Figure 67. Influence of surface temperature on relative rutting damage.

effect is a modest one. Most of the trucks show an increase in relative damage of about 0.3 ESALs. The exceptions (the 3-axle refuse hauler and the 4-axle concrete mixer) have steer axles fitted with wide-base single tires.

Although the relative rut depth caused by a particular truck layout changes only modestly with surface temperature, the absolute levels of rut depth change dramatically. That is, a single ESAL on a pavement at a surface temperature of 120°F represents up to 17 times as much rutting damage as the same pavement at a surface temperature of 77°F.

Roughness

Roughness in the surface of a flexible pavement directly affects the dynamics of the trucks using the roadway. With increasing roughness the dynamic loads increase, thereby increasing fatigue. Over the typical range of roughness (80 to 240 in/mi IRI) the dynamic load coefficient will vary by a factor of 3 (see Figure 22), and the relative damage (in ESALs) will increase by 20% (roughly the same order of magnitude as variations among truck suspensions). Consequently, trucks that are more dynamically active, particularly those with walking-beam tandem suspensions, will be more damaging on low strength pavements with high roughness.

Roughness has only minimal influence on the aggregate rutting damage to a flexible pavement. While regions experiencing high dynamic loads will experience more rutting, nearby regions of low dynamic load will see proportionately less. While these mechanisms contribute to an increase of roughness the overall rut depth along the wheeltracks is not affected.

INTERPRETATION, APPRAISAL, APPLICATION

As evidenced by the exposition in Chapter 2, the analytical study of truck-pavement interactions has produced many insights on how truck wheel loads damage pavements. The analytical approach has the benefit that it allows investigation of the phenomena involved to aid in understanding how specific truck characteristics affect pavement damage. Although there are uncertainties in the analysis methods, most of them are mitigated by the fact that the findings are expressed in terms of relative damage. Where that is not true, the discussion attempts to qualify the results and to suggest where better information is needed.

The major standards, specifications, policies and procedures related to highways and truck operations have been reviewed with an eye toward identifying changes that may be advised as a consequence of the findings from the research. Areas in which the results may be applied are presented in this chapter organized under topical headings.

HIGHWAY DESIGN

The American Association of State Highway and Transportation Officials (AASHTO) is the umbrella group serving as the national voice of state highway organizations, and the Federal Highway Administration (FHWA) represents the federal establishment. FHWA and AASHTO establish guidelines for design of pavement structures (5,26), their maintenance (19,27) and design of highway geometrics (19). These recommendations are considered authoritative and are used as well by many state, county, and municipal authorities. In addition, AASHTO and FHWA influence policy-making through the recommendations they make to the President and Congress (28-30). The findings from this research have numerous applications relevant to the guidelines and policy recommendations that emanate from these organizations. Specific areas are addressed below.

Rigid Pavement Design Issues

The edges of rigid pavement slabs experience stresses that are up to 75% greater than the levels when the truck tracks in the center of the slab. The region of sensitivity generally extends 2 to 3 feet from the edge. Pavement design standards should take this variable into consideration in one of two ways:

> Lane Width—Most medium and heavy trucks are currently 8 feet in width to the outer extremes of the wheels. (Trucks up to 8.5 feet overall width are permitted on designated highways.) On narrow lanes of 10 to 12-feet in width the truck wheels will encroach onto the sensitive regions. This effect may be mitigated by use of higher-strength or thicker pavements for narrow lane widths. Long-combination vehicles may generally be expected to increase exposure of the edges to truck wheel loads due to their potential for greater off-tracking. Thus, higher-strength or thicker designs are warranted on roads exposed to long-combination vehicles. Straight road sections with lanes of 14 to 16 feet in width are wide enough that truck wheels are less likely to track on the sensitive edge regions.

Edge Treatment—On road sections where truck wheels are likely to track within 2 to 3 feet of the edge, durability can be increased by providing additional strength or thickness along the edges. Tying the slab to a concrete shoulder is another way to enhance design in this area.

Analysis of rigid pavement structures has shown that stresses near a joint (or crack) in a PCC pavement are greater than those in the interior region. In the area about 5 to 6 feet from the joint, damage levels are elevated by 10% to 25% above those at the middle of the slab (see Chapter 2, Rigid Pavement Factors). The higher stresses in the near-joint region provide a potential explanation for persistent problems of corner breaking common with rigid pavements. In order to achieve better consistency of strength and durability throughout the pavement, design changes to ameliorate these conditions may be considered.

Joint Load Transfer—The elevated stresses in the near-joint region are dependent on shear- and moment-transfer properties of the joint. The ideal joint design obviously would be one with the same shear transfer and bending stiffness as the slab, thereby eliminating the discontinuity responsible for the high stress region. Future studies of joint design should focus on the relationship between joint properties and the stresses identified here.

Slab Thickness—Peak stresses in the near-joint region could be reduced by increases in slab thickness. Selectively increasing thickness near the joints would result in a tapered slab design with better durability at the joints, but might prove impractical for other reasons (higher construction costs, greater propensity for mid-slab cracking, etc.). Since temperature steel does not reduce stress levels in a slab, additional "reinforcing" will not solve this problem (although the additional steel may help to maintain slab integrity once cracks occur).

Slab Length—Variations in the design length of the slab do not offer direct means to alleviate the high-stress end conditions. Slabs shorter than 20 feet generally result in elevated stress throughout the mid-slab region because the end effects extend into the mid-slab region. For slabs 30 feet or longer the mid-slab region is free of elevated stress arising from end effects, but are prone to mid-slab cracking due to shrinkage and moisture effects. The more significant interaction of slab length comes from the potential influence on truck dynamics. The characteristic shapes of slab curl due to thermal and moisture gradients can tune to the resonances of trucks, elevating dynamic loads. The incremental damage from these mechanisms is likely to reach magnitudes of 50% to 100%. While these phenomena were modeled in the analysis, no systematic answers to this complex problem were discovered.

Inasmuch as rigid pavement fatigue is most directly linked to the maximum axle loads on trucks, the performance of these pavements will continue at current levels if road use laws do not permit any increase in these limits. The damaging flexural stresses caused by truck wheels diminish with an increase in the modulus of rupture of the concrete, and even more rapidly with an increase in the thickness of rigid pavement slabs. On roads where higher axle loads (or a higher percentage of high axle loads) are anticipated, increased

thickness is the single, most important means to achieve better pavement performance; fatigue damage varies by a factor of 20 from thin to thick pavements. To a lesser extent, the highway engineer can minimize road damage by maintaining roads in a smooth condition; damage increases by a factor of 3 on rough (2.5 PSI) roads.

Flexible Pavement Design Issues

The major issue in flexible pavement performance today is rutting. Rutting is manifest as either a general depression of the wheeltrack, or distinct dual-tire marks in the wear course.

Rutting, in the nature of a general depression of the wheeltrack, is the result of compaction and plastic flow of one or more layers of the pavement. The analysis suggests that the amount of rutting is proportional to the total weight of all the trucks using the highway. This factor is determined by the amount of freight that must be moved, and thus cannot be controlled by the highway designer. There is also reason to believe that the radial tires becoming more widely used on modern trucks may contribute to dual-tire rutting because of their unique ability to follow in a wheeltrack depression. There is no evidence to suggest that control over truck properties (such as gross weight, wheel load, or tire pressure) will yield any significant change in rutting experience. Consequently, this rutting problem can only be alleviated by developing asphalt mixes that are more resistant to rutting. Further, it is known that compaction of the lower layers, however, is mitigated to a certain extent by thicker overlying layers.

Fatigue damage in flexible pavements is determined primarily by individual axle loads. Therefore, current design methods based on axle load are appropriate, although they do not directly take into account the dynamic loads. The highway engineer has means to influence and control dynamic loads by specification of acceptance criteria for roughness in new construction, and the road roughness level at which maintenance is warranted on existing pavements. Damage increases by approximately 50% on rough roads (2.5 PSI) in comparison with smooth roads (above 4 PSI). Management practices that emphasize smoothness to satisfy the driving public, also promote longevity of pavement structures.

The flexible pavement models used in this study did not allow investigation of pavement performance near discontinuities, specifically near the edges of the pavement structure. It is reasonable to expect that flexible pavements experience elevated strains when truck wheels operate near the edges much as was discussed above for rigid pavements. Flexible pavements, however, have a much narrower influence function so the region of sensitivity is smaller. Nevertheless, design features that provide edge support will undoubtedly add to the durability of flexible pavements under heavy truck loads.

FEDERAL AND STATE REGULATIONS

Road use laws defining dimensional and weight limitations on trucks operating on the highway network are established by Federal law for the Interstate and Designated Highway Systems, and by the individual states for most other roads. Modifications to those laws could reduce truck damage to the highway system.

Steering Axle Loads

By necessity the front steer axles on trucks utilize single tire configurations. Although loads to 20,000 lb are permissible, most trucks operate at about 12,000 lb. Tires rated to accept this load (the 11R22.5 size) create high stresses in pavement structures. Steering axle tires are more damaging in fatigue of flexible pavements than a 20,000 lb load on an axle with dual tires. To keep the damage within the same limits tolerated for the 20,000 lb axle, steering axle loads with these tires would have to be reduced to the range of 10,000 to 11,000 lb. Road damage from vehicles currently operating at the 80,000 lb gross weight limit would be decreased approximately 10% by modifying road use laws to favor a load distribution of 10,000 lb on the steering axle with allowance for 35,000 lb on tandems.

Wide-base singles tires in the size range of 15R22.5 to 18R22.5 are used on front steer axles required to carry more than 14,000 lb. Despite their larger size, these tires are quite damaging to flexible pavements when operated at their rated loads, because of the high stresses created. In order to keep damage to the same level as a currently tolerated with 20,000 lb axles, it would be necessary to limit loads to 14,000 lb for the 15R22.5 tire and 18,000 lb for the 18R22.5 tire.

Many states attempt to control road damage by specifying the maximum load per unit width of tire tread. The 20,000 lb, dual-tire axle corresponds to approximately 625 pounds of load per inch of tread width (450 lb/in based on tire section width). On wide-base singles, loads to 650 lb/in of tread width (488 lb/in based on tire section width) can be tolerated without increasing strains above that experienced with the 20,000 lb axle.

Rear Axle Loads

Current road-use laws tolerate up to 20,000 lb on a single rear axle. Although most trucks use a dual tire arrangement on such axles, wide-base singles are permitted. As discussed above, this creates extra damage to flexible pavements. In order to limit damage to that characteristic of the dual tire axles, rear axles with wide-base singles should be limited in loads to 14,000 lb for the 15R22.5 tire and 18,000 lb for the 18R22.5 tire.

Truck Speeds

Truck operating speed has a minor and variable influence on the amount of damage imposed on the pavement. Generally, higher speeds are slightly more damaging to rigid pavements, and slightly less damaging to flexible pavements. It may be concluded that on pavements in good condition there is no rationale for limiting truck speed for reasons of pavement wear. Only when a road has experienced substantial deterioration producing severe roughness would speed limitation yield any significant benefit in reduced road wear.

Truck Configurations

Recognizing that one of the essential functions of the highway system is to provide routes of transport for the nation's industrial goods, the larger and heavier truck configurations appear most desirable. From an efficiency of transport perspective, the large multi-vehicle combinations with low axle loads produce less road wear per ton-mile of transport. Among the vehicle configurations examined, the Turner truck and similar combinations are least damaging to the roads. Multiple axles at lighter loads reduce fatigue

in both rigid and flexible pavements. Although gross weight most directly determines flexible pavement rutting, the larger combinations are, nevertheless, least damaging on a ton-mile basis because of the higher proportion of cargo to tare weight with these combinations.

Tire Pressures

There has been considerable concern that elevated tire pressures on heavy trucks may be contributing to road damage (*31*). Tire pressure has a small effect on fatigue of rigid pavements, but a large effect on fatigue of flexible pavements. A 20 psi increase in pressure can increase fatigue damage on flexible pavements by 200 to 300%.

Road use laws should be amended to limit tire inflation pressures on trucks to the recommended cold setting (printed on the sides of the tire) plus a 15 psi allowance for pressure buildup when hot. Including a tire pressure check in weight enforcement activities would be a quick and effective means to reduce the road damage attributable to this cause.

Weight Enforcement

Truck-weight enforcement is routinely implemented by roadside weigh scales and truck inspections by motor-carrier enforcement officers. Practices vary among the various organizations performing the weighing. Load equality between tandem axles is essential to minimize road damage, but is not usually monitored. Damage increases at an accelerating rate when load disparities exceed 10% (individual axle loads 10% greater than the average). Consideration should be given to routine monitoring of tandem load distributions in weight enforcement activities to determine the significance of this factor as a cause of road wear. If warranted, the loads on each axle of a tandem set should be regulated.

TRUCKING OPERATIONS

Truck operators have a vested interest in seeing the highway network, which is the source of their livelihood, remain in good condition. The operators and their drivers can take a number of steps as follows to minimize road damage:

1) Wherever possible, trucks should be loaded to achieve uniformity of loads among rear axles of comparable types. For example on a 3-axle tractor-semitrailer, road damage can be minimized by distributing the load in the trailer so as to achieve comparable loads on the tractor rear axle and the semitrailer axle. On a 5-axle tractor-semitrailer the goal should be to achieve comparable loads on the tractor rear tandem and the semitrailer tandem.

2) On truck combinations where the load is distributed between a single axle and a tandem set, the load should be positioned to keep the load on the single axle no higher than the load on each of the tandem axles.

3) Steering axle loads should be kept to the minimum possible with due consideration for safety and stability. Steering axle loads in excess of 650 lb per inch of tire tread width are more damaging than the more heavily loaded rear axles.

4) Elevated tire pressure can be very damaging to flexible pavements. An extra 20 psi can double or triple fatigue damage that causes cracking. Drivers and service personnel

should be required to not exceed the inflation pressure specifications printed on the side of the tires.

5) Drivers should be encouraged to avoid driving in a lane position that places the tires near the edges of pavements, except when necessary.

6) Wide-base single tires are more damaging than dual tires at comparable loads. Thus, dual-tire axle configurations are preferable to the use of wide-base singles on rear axles.

7) Insufficient damping in suspension systems can add unnecessarily to road damage, as well as suspension and tire wear. Shock absorbers need to be maintained in proper working condition.

8) Walking-beam suspensions are particularly damaging to roads, because of the absence of shock absorbers. If a walking-beam suspension is specified, shock absorbers on the axles should be specified.

TRUCK AND TIRE DESIGN

Several aspects of truck and tire design can be identified as areas where improvements can be made to reduce road damage.

1) Equality of load sharing among tandem axles reduces road damage. Designers should strive to achieve no more than 5% load difference between tandems. This goal should be evaluated not only under idealized circumstances, but also under the influence of driving and braking torques, and under varying load conditions. Designers should strive to maintain good load sharing even when the frame is not level. For example, it has been observed (15) that only minor variations in the truck frame pitch angle can disturb the equality of loads on some tandem suspensions.

2) Road damage can be reduced by development of suspensions with improved dynamic performance. Air-spring suspensions can achieve performance comparable to the optimal passive suspension by giving attention to selection of the shock absorber damping level. Use of these suspensions in lieu of leaf-spring suspensions has the potential to reduce road damage by about 20%. Active suspensions could potentially yield another 20% improvement. The walking-beam tandem suspension generates high dynamic loads that are unnecessarily damaging to roads because of the poor damping of its "tandem-hop" vibration mode. This mode of vibration can be readily reduced by installing shock absorbers between the axles and the truck frame. Truck manufacturers and users with a concern for road damage must specify shock absorbers on walking-beam suspensions.

3) The low-frequency vibrations that degrade ride of trucks and increase cargo damage also contribute to road damage. Truck manufacturers should be encouraged to continue development of trucks with improved ride. The use of air-spring suspensions is one of the most effective means to improve dynamic behavior with benefits of reduced road damage.

4) Tires with a wider tread are generally less damaging to roads. Tire manufacturers developing new truck tire profiles should strive for greater tread width in order to bring tire loads down to 650 lb per inch of tread width. Especially in the case of truck steering axle

tires, maximizing the tread width is important because steering axle tires consistently operate at high loads in single tire configurations. Wider treads are also important on the new low-aspect ratio tires.

CONCLUSIONS AND SUGGESTED RESEARCH

Engineering models of trucks and pavement structures were adapted to allow simulation of the interaction between trucks and the roadway. These tools were then used for a systematic analysis of the way in which road responses to truck wheel loads are affected by truck, roadway, and environmental characteristics. The objective of this exercise was to determine quantitatively which truck characteristics most affect fatigue and rutting damage and how these relationships might be sensitive to roadway and environmental conditions. The exercise was successful at identifying relationships that are rational according to the current knowledge of the mechanics involved. But, at the same time the process has revealed areas in which the current knowledge is deficient and warrants additional research.

This chapter summarizes the conclusions from the project and highlights areas in which further research is needed.

CONCLUSIONS

The mechanistic analysis of road damage from trucks assessed multiple factors in truck design and operating practices that influence damage. The load distribution among axles and types of tires on those axles establishes a "loading footprint" for the vehicles which has the most direct and powerful influence on damage potential. Dynamic factors incidental to the vehicle, its speed, resonance properties, and suspension characteristics exert second-order influences on damage. Thus, the loading footprint can be used to obtain the first-order estimate of the damage potential of a given truck design. Fatigue and rutting damage of flexible pavements are not sensitive to the same vehicle characteristics. Therefore, damage equivalence in rutting and fatigue is dependent on different vehicle properties.

Among the various combination vehicles currently proposed or in use, the Turner combination (with a 10,000 lb front axle load limit) is the most transport productive with the least pavement damage. A Turner combination at 114,000 lb gross weight causes only one-half the fatigue damage of a 5-axle double at 80,000 lb, and only 60% of the damage of a 5-axle tractor-semitrailer at 80,000 lb.

The maximum axle load is the strongest determinant of fatigue damage on both rigid and flexible pavements. Truck steer axles with over 10,000 lb on conventional single tires (11R22.5 or equivalent) are more damaging than 20,000 lb axles on dual tires. Wide-base single tires are more damaging than dual tires at the same load. In order to keep damage to levels equivalent or less than 20,000 lb on a single axle with dual tires, axles with wide-base singles should be limited to loads of 650 lb per inch of *tread* width (488 lb/in based on tire section width).

The damage from closely-spaced tandem axles (48 to 52 inches of spread) is reduced by load interactions on rigid pavements. Flexible pavements do not have significant load interaction. Tandem axle loads, currently limited to 34,000 lb, could be increased to as much as 40,000 lb with no greater damage than would be imposed by two widely-

separated 20,000 lb axles. Tridem axles are a very effective means to increase truck load capacity while reducing road damage. Tridem axles on a semitrailer (limited to 39,000 lb) would permit up to 85,000 lb on a tractor-semitrailer with less damage that a 5-axle tractor-semitrailer at 80,000 lb.

Front axles with single tires can be a major contributor to flexible-pavement fatigue damage. Revising the road-use laws to allow the common 5-axle tractor-semitrailer to operate at 10,000 lb on the front axle and 35,000 lb on the tandems would reduce road fatigue damage by 10% for these vehicles.

The primary determinant of flexible pavement rutting is gross vehicle weight. However, there would be no benefit from limiting gross vehicle weight in light of the fact that it would only force more trucks on the road to meet commercial transport needs (assuming there is no modal shift of commercial transport). No evidence was found to suggest that specific truck characteristics (which are practical to control) could reduce rutting damage.

Good static-load equalization on multiple-axle suspensions is essential to minimize road fatigue damage. Load equalization within 5% among the axles is a reasonable limit for minimizing fatigue.

The dynamic loads arising from the interaction of road roughness with truck dynamics increase fatigue damage of rigid and flexible pavements. At a minimum (the best trucks on the best roads) dynamics increase damage by 25% to 50% above the static, and in the worst case the damage is multiplied by a factor of four. Among relevant truck properties, the dynamic behavior of suspensions is the most important and amenable to control. Air-spring suspensions (both single and tandem) appear to provide the least damaging dynamic performance. Leaf-spring suspensions (single and tandem) are generally more damaging than air springs. Optimized passive suspensions (air springs and shock absorbers) would reduce road damage by about 20% from that of typical leaf-spring suspensions. Active suspensions could yield another 20% benefit. Among the tandem suspensions, the walking beam is unique in that it can be nearly twice as damaging as air springs. Walking-beam suspensions, however, could be rendered much less damaging by installation of shock absorbers on the axles.

The primary tire variable affecting road stress and fatigue damage, particularly on flexible pavements, is the contact area. Tread width and inflation pressure have the most direct influence on contact area. Regulation of truck axle loads in terms of pounds of load per inch of tread width is a practical means to control road damage. While there is no absolute value that is tolerable, the 20,000-lb axle on dual tires serves as a reference against which other alternatives can be judged. On that basis, the limit is approximately 625 lb per inch of *tread* width for conventional tires, and 650 lb per inch of *tread* width for wide-base singles. Equally important is the need to control inflation pressure. Checks of inflation pressure could be added to truck enforcement activities to ensure that pressures are within reasonable range of the load capacity of the axle. Limiting all axles thusly will effectively ensure that road damage from other tire configurations will not exceed current tolerances.

SUGGESTED RESEARCH

The research methodology employed in this project was specifically limited to utilization of available models of trucks and pavement structures in order to avoid diverting effort to development and validation of new models. In the course of the work, the shortcomings of modeling and the state of the knowledge related to trucks and pavements became acutely obvious. A number of areas in which additional research is warranted can be suggested.

Throughout the study, fatigue-damage evaluation focused on stresses and strains at the bottom of the top layer of pavement. This location was chosen because of its acceptance as the primary region of damage, despite the fact that failure at this location is not well supported by evidence from field observations (see Appendix A, Prediction of Road Damage). While there were no discoveries to suggest that the bottom of the layer was an inappropriate location for assessing damage, a more thorough method would be to search the pavement structure to ensure that alternative failure modes were not being generated under each condition analyzed. Ultimately, this points out the need for major studies of fatigue damage in flexible and rigid pavements in order to better establish the modes of failure from field observations and to rationalize those failure modes with the analytical models used.

The degree to which trucks vary in lateral position in a lane will affect the absolute level of both rutting and fatigue damage. Only the relative damage had to be assessed for the purposes of this study, so it was assumed that all trucks tracked in the center of the lane. However, better absolute prediction of pavement life using these analysis methods will require that lane tracking variations be modeled, particularly to assess the potential for accelerated damage when truck wheels track near the edges of the pavement structure.

Temperature plays an important role in damageability of both rigid and flexible pavements, albeit by different mechanisms. Rigid pavements are distorted by temperature gradients through the slab, while flexible pavements change material properties with temperature. The effects of temperature were approximated in analysis of both pavement types to determine their general level of significance. Temperature is seen to be an important variable in both cases. Further research to better model temperature effects and quantify their influence would be beneficial.

Rigid Pavements

Rigid pavements are treated via a finite-element model of the slab on an elastic base. The ILLI-SLAB model used in the research also allows specification of the properties of the joints connecting the slabs. Nevertheless, many issues arose in the study which could have been better addressed with enhancements of the model or more complete data for characterizing typical pavement properties.

Shear- and moment-transfer properties at rigid pavement joints have an influence on stresses in the areas near the end of the slab. A more thorough understanding of the modeling and properties of pavements in use would enhance the ability to assess actual stress levels caused by trucks.

Further shortcomings in the modeling of rigid pavements arise from the uncertainty about bonding between the slab and base course. The models can represent bonded or unbonded conditions, but do not cover partial bonding derived from the friction lock between layers. Bonding helps reduce stresses in the slab, but places greater load on the weaker base course. Early failure of the base course then imposes stress concentrations in the slab. These mechanics warrant further research.

Fatigue of Portland Cement Concrete road surfaces by trucks is the cumulative result of the cyclic stresses imposed. The state of knowledge of PCC fatigue under cyclic (reverse) stress conditions is embryonic. Most empirical fatigue data is derived from experiments that do not involve stress reversals. Additional research into fatigue under conditions comparable to truck wheel loading is needed to establish valid ways to evaluate the stress cycles and relate them to damage.

It would appear that temperature gradients in rigid pavements and the slab distortions that result have a strong influence on the damage resulting from truck wheel loads. Current models are deficient at representing the mechanics involved. In particular, loss of support under curled slabs is a major factor in damage causation that cannot be addressed adequately with these models.

Flexible Pavements

The multi-layer elastic model for flexible pavements used in the study has several limitations that affect its ability to address issues of interest. The model is limited to application of a tire load over a circular area. This allowed only an approximation of the effects of variations in the contact area of tires to reflect different tire sizes, inflation pressures, and loads.

The multi-layer, flexible-pavement model does not provide for calculation of behavior near the pavement edge. Improvement of the model to incorporate edge conditions would allow more thorough study of the damage effects of truck wheel loads when they encroach on the edges of flexible pavements. Since edge failure is a common problem with flexible pavements, enhancements to the model would provide a valuable tool for studying pavement damage in this region.

Rutting damage was estimated by ascribing linear, viscoelastic properties to the asphalt materials. While this is a good first approximation, the conclusions of the study could be altered if the properties are sufficiently non-linear. Additional research for characterizing the viscoelastic properties of asphalt materials are needed to improve predictions of rutting behavior.

Finally, the analytical methods for predicting fatigue damage are not well validated. The emphasis on strains at the bottom of the wear course as the indicator of fatigue is not justified by field observations. Core samples taken in Britain showed that cracks almost invariably originate at the top surface and extend downward (see Appendix A). Also, while it is accepted that strain and damage are related by a power law, the suggested exponent values range from 1.9 to 5.5. The exponent value has a strong influence on the relationship of truck characteristics to damage. With a low exponent, truck gross weight becomes the

most important factor affecting damage, whereas with a high exponent, the maximum axle load is the critical factor.

Truck Properties

Pitch-plane models were used to replicate the behavior of trucks in the study. While there is a good library of properties from which to generate generic truck models, the same is not true for truck suspension systems. The UMTRI suspension library is mostly limited to quasi-static properties of leaf-spring suspensions. Dynamic properties of truck suspensions are not well-known. Dynamic tests should be conducted on a representative sample of each type of truck suspension so that typical properties can be established for purposes of evaluating their influence on road damage, and to establish the range of variation of properties among generic suspension types to determine how broadly the findings may be generalized.

Because of the nearly infinite variety of trucks, it is difficult to characterize their dynamic performance in a systematic fashion. In addition to the multiple combinations of axles, suspensions, and dimensions, the dynamic behavior will vary with every load distribution, speed and pavement profile.

There is evidence (32) to suggest that under some circumstances, putting a road-friendly suspension on the tractor drive axle of a combination vehicle can increase the dynamic wheel loads on the trailer axles. Under these circumstances it is not possible to say that one suspension is more road friendly than another, but only that the entire vehicle is more or less road friendly. This has the difficult implication that to devise procedures for testing the damageability of combination vehicles it may be necessary to test tractors with a standard trailer, and trailers with a standard tractor.

The matter of spatial repeatability of wheel loads among trucks (the tendency for all trucks to "hammer" the pavement in the same general areas) needs to be examined via field research in order to improve the ability to predict road damage on an absolute basis.

More empirical studies of these types are needed to improve the knowledge about truck characteristics, if advances are to be made in understanding truck-pavement interactions.

REFERENCES

1. American Association of State Highway and Transportation Officials, *The AASHO Road Test. Report 7, Summary Report.* Highway Research Board Report 61G (1962) 59 p.

2. Irick, P.E., "Characteristics of Load Equivalence Relationships Associated with Pavement Distress and Performance." *ARE Inc. Engineering Consultants* (1989).

3. Nasim, M.A., et al., "The Behavior of a Rigid Pavement Under Moving Dynamic Loads." *Transportation Research Record,* No. 1307 (1991) pp. 129-135.

4. Tire and Rim Association Inc., *The Tire and Rim Association Inc. Year Book,* Tire and Rim Association, Copley, Ohio (1989).

5. American Association of State Highway and Transportation Officials, *The AASHTO Guide for Design of Pavement Structures.* AASHTO, Washington, D. C. (1986) 653 p.

6. Treybig, H.J., et al., "Overlay Design and Reflection Cracking Analysis for Rigid Pavements. Volume 1. Development of New Design Criteria Phases II and III." *Fedral Highway Administration, FHWA-RD-77-76* (1977) 245 p.

7. Cebon, D., "Vehicle-Generated Road Damage: A Review." *Vehicle System Dynamics,* Vol. 18, No. 1-3 (1989) pp. 107-150.

8. Sweatman, P.F., "A Study of Dynamic Wheel Forces in Axle Group Suspensions of Heavy Vehicles." *Australian Road Research Board Special Report 27* (1983) 65 p.

9. Ervin, R.D., et al., "Influence of Truck Size and Weight Variables on the Stability and Control Properties of Heavy Trucks." *University of Michigan Transportation Research Institute UMTRI-83-10/2, Federal Highway Administration FHWA-RD-83-030* (1983) 179 p.

10. Gillespie, T.D., et al., "Calibration of Response-Type Road Roughness Measuring Systems." *National Cooperative Highway Research Program Report 228, University of Michigan Transportation Research Institute, UMTRI-80-30* (1980) 81 p.

11. Sayers, M. and Gillespie, T.D., "Dynamic Pavement/Wheel Loading for Trucks with Tandem Suspensions." Seventh IAVSD Conference on the Dynamics of Vehicles on Roads and on Tracks, Cambridge, MA. *Proceedings* (1984) pp. 517-533.

12. Sayers, M.W., "Dynamic Terrain Inputs to Predict Structural Integrity of Ground Vehicles." *Wright-Patterson Air Force Base, University of Michigan Transportation Research Institute, UMTRI-88-16,* (1988) 114 p.

13. Gillespie, T.D., "Heavy Truck Ride." *Society of Automotive Engineers SP-607,* (1985) 68 p.

14. Chalasani, R.M., "Ride Performance Potential of Active Suspension Systems - Part I: Simplified Analysis Based on a Quarter-Car Model, - Part II: Comprehensive Analysis Based on a Full-Car Model." Symposium on Simulation and Control of Ground Vehicles and Transportation Systems, *Proceedings*. AMD-Vol. 80, DSC-Vol. 2, American Society of Mechanical Engineers (1986) pp. 187-226.

15. Winkler, C.B. and Hagan, M., "A Test Facility for the Measurement of Heavy Vehicle Suspension Parameters." *Society of Automotive Engineers Paper No.800906* (1980) 29 p.

16. Sayers, M. and Gillespie, T.D., "The Effect of Suspension System Nonlinearities on Heavy Truck Vibration." Seventh IAVSD Conference on the Dynamics of Vehicles on Roads and on Tracks, Cambridge, U.K. *Proceedings* (1981) 13 p.

17. St. John, A.D. and Kobett, D.R., "Grade Effects on Traffic Flow Stability and Capacity." *National Cooperative Highway Research Program NCHRP 3-19* (1972) 173 p.

18. Ervin, R.D. and Winkler, C.B., "Estimation of the Probability of Wheel Lockup." *International Journal of Vehicle Design*, Vol. 9, No. 4-5 (1986) pp. 423-437.

19. American Association of State Highway and Transportation Officials, *Geometric Design for Resurfacing, Restoration, and Rehabilitation (R-R-R) of Highways and Streets*. AASHTO, Washington, D. C. (1977) 16 p.

20. Smith, H.A., "Truck Tire Characteristics and Asphalt Concrete Pavement Rutting." *Transportation Research Record*, No. 1307 (1991) pp. 1-7.

21. Meyer, W.E. and Kummer, H.W., "Mechanisms of Force Transmission Between Tire and Road." *Society of Automotive Engineers 490A* (1962) 18 p.

22. Croney. D and Croney, P., *The Design and Performance of Road Pavements*, Second Edition. Chapter 18. "Performance Studies Incorporated in In-Service Highways in the United Kingdom." McGraw-Hill, London (1991).

23. DeYoung, C., "Spacing of Undoweled Joints in Plain Concrete Pavement." *Highway Research Record*, No. 112 (1966) pp. 46-54.

24. McBride, J.C., Decker, M.S. "Performance Evaluation of Utah's Concrete Pavement Joint Seals." *Transportation Research Record*, No. 535 (1975), pp. 35-50.

25. Richardson, J.M.and Armaghani, J.M., "Stress Caused by Temperature Gradient in Portland Cement Concrete Pavements." *Transportation Research Record*, No. 1121 (1987) pp. 7-13.

26. American Association of State Highway and Transportation Officials, *The AASHTO Interim Guide for Design of Pavement Structures. 1972 [Revised]*, AASHTO, Washington, D. C. (1981) 132 p.

27. American Association of State Highway and Transportation Officials, *AASHTO Maintenance Manual 1976*. AASHTO, Washington, D.C. (1976) 329 p.

28. American Association of State Highway and Transportation Officials, *Guide for Maximum Dimensions and Weights of Motor Vehicles and for the Operation of Nondivisible Load Oversize and Overweight Vehicles*. AASHTO, Washington, D. C. (1988) 28 p.

29. American Association of State Highway and Transportation Officials, *Transportation Policy Book*. AASHTO, Washington, D. C. (1989) 141 p.

30. United States Department of Transportation, *Moving America. New Directions, New Opportunities. A Statement of National Transportation Policy. Strategies for Action*. U.S. DOT (1990) 136 p.

31. Thompson, M.R., "Analytical Methods for Considering Tire Pressure Effects in Pavement Design." Symposium/Workshop on High Pressure Truck Tires, Austin, Texas. *Proceedings* (1987).

32. Cebon, D., "Assessment of the Dynamic Wheel Forces Generated by Heavy Road Vehicles." ARRB/FORS Symposium on Heavy Vehicle Suspension Characteristics, Canaberra, Austrailia. *Truck Designers Sprung?* (1987) pp. 143-162.

APPENDIX A
REVIEW OF PREVIOUS STUDIES

INTRODUCTION

This review begins with a brief discussion of the modes of failure of pavement systems and the methods typically used for their analysis. This information is necessary background before the influence of various vehicle features on road damage can be discussed.

The review then examines the three aspects of pavement loading that can be considered to have a "static" influence on road damage: (1) the arrangement of axles (number and location); (2) the average (static) load on each axle; and (3) the tire contact conditions. The effects of these factors can, to a first approximation, be examined independently of vehicle dynamics. The review then considers the effects of vehicle design on dynamic wheel loads and finally considers the influence of dynamic wheel loads on road damage.

Throughout the review it will be assumed that the vehicles are traveling in a straight line at constant speed, so that the wheel loads are primarily vertical with no appreciable lateral or longitudinal components. The review will not include discussion of the forms of road damage which are essentially caused by environmental factors alone.

Background to Road Surface Wear

Road surfaces (or pavements) may be classified as flexible, composite or rigid. A flexible pavement consists of one or more layers of flexible (asphalt) material supported by a granular subgrade. Composite pavements consist of a flexible surface layer supported by a stiff Portland Cement Concrete (PCC) base and rigid road surfaces consist of a layer of PCC on a granular foundation. Rigid pavements can further be classified according to their arrangement of steel reinforcement and joints.

Each of these road types has a number of characteristic failure mechanisms. According to Rauhut, Roberts and Kennedy (1,2) and Jackson (3), the most important of these are:[1]

- Fatigue cracking for all types of pavements.

- Permanent deformation (longitudinal rutting) for flexible and composite pavements.

- Reduced skid resistance for flexible and composite pavements.

- Low temperature cracking for flexible pavements.

- Reflection cracking for composite pavements.

---

[1] Pavement damage terminology is defined by Kennedy et al. (1).

- Faulting, spalling, low temperature and shrinkage cracking, blow-ups, punchouts and steel rupture for rigid pavements, depending on their structural category.

Each failure mechanism is affected by many factors including the roadway design and construction methods, the material properties of each constituent layer, the traffic loading and the environmental conditions throughout the service life (1).

Prediction of Road Damage

Current mechanistic pavement design practice in many countries is to optimize resistance to fatigue and rutting (4). Analytical models are used to determine the "primary responses" (stresses, strains and displacements) of a layered road structure due to a static, standard wheel load (often 40kN). The "fourth power law[2]" is frequently used to convert the estimated traffic during the service life into an equivalent number of standard wheel loads. Experimental fatigue and permanent deformation characteristics of the road materials[3] are then combined with the calculated primary responses to evaluate suitable pavement layer thicknesses and material property specifications (4).

For the analysis of fatigue damage, the most commonly used primary responses are the horizontal tensile stress or strain at the bottom of the asphalt or PCC surface layer, since analytical models generally predict that maximum tensile strains occur at this location on the axis of the load. Pavement designers consequently infer the upwards propagation of fatigue cracks from the layer interface. Thrower (12) noted, however, that this failure mechanism is not well supported by observations of core samples taken from roads in Britain, where cracks almost invariably originate at the top surface and extend downward.

Rutting damage in flexible pavements is the result of permanent deformation in each of the pavement layers. In the AASHO road test (6) approximately 68% of the permanent deformation occurred in the granular foundation layers, while 32% occurred in the asphalt surface and subgrade compressive strain was found to correlate well with rutting damage (13). In tests performed by the Transport and Road Research Laboratory (TRRL) in the UK (14) these proportions were approximately 46% and 54% respectively. Pavement designers often attempt to minimize deformation of the granular layers by limiting the compressive stress or strain at the top of the subgrade. In other design procedures, the

---

[2] The "fourth power law" stems from the AASHO road test (1958-60) (5, 6) from which it was deduced that the decrease in pavement "serviceability" caused by a heavy vehicle axle can be related to the fourth power of its static load. A static load P is assumed to be equivalent to $(P/P_0)^4$ applications of the standard axle load P_0. Pavement serviceability was assessed using the "Present Seviceability Index" (PSI) which was determined by a panel of highway experts. It was found that the PSI could be expressed as a multiple regression of "cracking and patching," rut depth and surface roughness.

[3] The damage characteristics of pavement materials are very sensitive to stress or strain amplitudes, typically displaying power relationships with exponents in the range 1-8, depending on the material and the mode of distress (see, for example, (7-11)).

elastic vertical deflection of the surface, or the sum of the theoretical permanent deformations of each layer are used as design criteria.

Although considerable research effort has been concentrated on predicting pavement failure, agreement between theory and experiment is often unsatisfactory (*12*). There are numerous complicating factors including "healing" of asphalt materials in rest periods between load pulses (*8,12,15*), the distribution of wheel paths across the road (*4,12,15-17*), extreme sensitivity of material properties to climatic conditions, particularly temperature (*4,12,15,18,19*), inaccuracy of the "fourth power law" (*12,20*), variations in tire types (*19,21,22*), inadequacies of pavement response and damage models (*12*) and the variable nature of the applied loads. It is not uncommon for such analyses to underestimate pavement fatigue lives by a factor of 100 (*4,12,15*).

Criteria for evaluating the road damaging effects of various vehicle features must inevitably be based on the current understanding of road surface failure. As illustrated above, this is an area of considerable uncertainty.

EFFECTS OF AXLE ARRANGEMENT

There is considerable civil engineering literature concerned with the relative road damaging effects of various axle group arrangements (single/tandem/triaxle) and it is not possible to present a comprehensive review here. Most studies either simulated (*13,23-26*) or measured (*18,27-31*) the "primary" response of the pavement (stress, strain, deflection) to a variety of axle configurations. Empirical road damage relationships (rutting and fatigue) were used to estimate relative pavement damage. One typical result by Southgate and Deen (*26*) is shown in Figure A-1.

It is generally concluded that for equal damage to flexible pavements, tandem and triaxle groups can carry more weight than the same number of widely spaced single axles, and that an optimum axle spacing exists (around 48 inches), depending on the road structure, assumed mode of failure and damage criterion (*32*). This fact is reflected by current axle load/geometry regulations in a number of countries (see, for example (*28,33*)).

Recent literature in this field was reviewed by Morris (*32*) and this will not be repeated here.
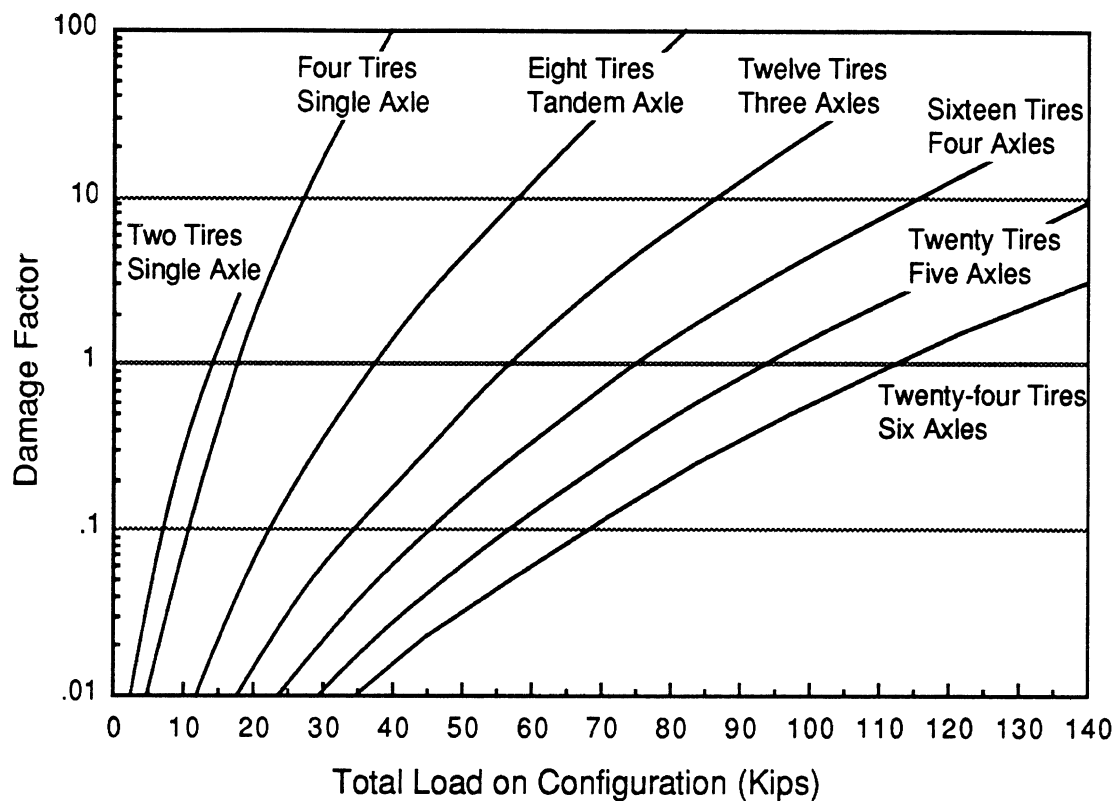
Figure A-1. Effects of total axle group static load on relative pavement damage. After Southgate and Deen (26).

EFFECTS OF STATIC LOAD SHARING

Uneven Wheel Loads

Most tandem and triaxle truck suspension systems are designed to equalize the static loads carried by the axles in a group. In practice, the effectiveness of load equalization on moving vehicles varies significantly among suspensions.

Mitchell (34) made a slow-speed axle weight survey of 259 vehicles in the UK in 1985. He noted that for triaxle groups with leaf spring suspensions, the lightest axle was typically observed to be 60-70% of the heaviest and sometimes only 30-40%. Air suspensions were observed to equalize much better, the lightest axle typically being 90% of the heaviest. Tandem suspensions were also observed to equalize better than triaxles.

Sweatman (35) introduced the "Load Sharing Coefficient" (LSC) which he defined as:

$$LSC = \frac{\text{Mean measured wheel load}}{\text{(Total group static load/Number of wheels in group)}}. \qquad \text{(A-1)}$$

The LSC is theoretically unity for perfect load sharing, but Sweatman's road tests, for a variety of speeds, yielded values in the range 0.791 - 0.983 for tandem suspensions, i.e. 21% - 1.7% equalization error respectively.[4]

Sweatman observed some interesting anomalies, in particular that the worst tandem suspension was of the walking-beam type (which is designed for good static load sharing) and the best was a 4-spring tandem which Mitchell (*34*) reported to be poor.[5] The air spring tandem fell between these two. Sweatman attributed the poor performance of the particular walking-beam suspension to bad installation practice and incorrect torque rod location. He also noted that road roughness had little effect on the relative performance of the different suspensions, but that approximately 2% variation occurred due to speed and up to 4% variation could be attributed to road camber and cross fall, which resulted in lateral load shifting.

Woodrooffe et. al. (*36*) performed quasi-static pitch tests on a trailer and concluded that their tandem walking beam suspension performed best, followed by the air-spring tandem and then the 4-spring suspension.

Simmons and Mitchell (*34,37*) performed an extensive study of load sharing on tandem and triaxle, air and leaf-spring suspensions. The work included pitch tests and road tests on a number of humped bridges, with vehicles that were instrumented to record dynamic wheel loads as well as the forces in the suspension components (torque rods, springs, etc.). They drew the following main conclusions:

- Poor load sharing is largely a quasi-static phenomenon which is independent of speed, depends mainly on the pitch angle of the vehicle, but is also strongly dependent on the geometry of the suspension components.

- On humped bridges the load on the leading axle of a 6-spring triaxle trailer suspension can be 1.47-1.82 times the nominal load (i.e. LSC = 1.47-1.82). For these conditions, most of the load normally carried by the third (trailing) axle of the group is transferred to the first (leading) axle, while the center axle load remains relatively constant. Under the same conditions, the triaxle air suspension yielded LSC = 1.16-1.31.

- Poor load sharing in 4-spring and 6-spring suspensions is mainly due to friction at the "slipper" ends of the springs. It can be improved considerably by introducing a low friction material in the sliding contact or by utilizing shackles instead of slipper connections.

---

[4] For a tandem suspension with LSC=0.79, the lighter axle will generate an average load which is 0.79x100/(1+0.21) = 65% of the heavier one, (assuming no difference between left and right wheel paths). This can be compared with Mitchell's results (*34*).

[5] See Appendix D and Sweatman (*35*) for a description of these suspensions.

Predicted Road Damaging Effects of Uneven Load Sharing

Gordon (*38*) analyzed unevenly loaded tandem suspensions using an elastic layer pavement model and determined that for permanent deformation (rutting) failure, a suspension with LSC = 0.8 (as per Sweatman's measurements) is twice as damaging as a suspension with perfect load sharing. Southgate and Deen (*39,40*) performed a similar analysis for fatigue damage. Using their results: LSC = 0.8 corresponds to a factor of 2.9 increase in predicted damage. O'Connell et. al. (*25*) predicted 23% increase in cracking damage and 43% increase in rutting for the LSC = 0.8.

Southgate and Deen also analyzed the measured static wheel loads of 670 tandem suspensions and 1951 triaxle suspensions and used this data to simulate the influence of uneven load sharing on road damage. They predicted that fatigue damage due to the tandem suspensions was 1.4 times worse than for perfect load-sharing suspensions, and damage for the triaxle suspensions was 2.3 times worse.

EFFECTS OF TIRE FACTORS

During the thirty years or so since the AASHO road test, cross-ply tires have largely been replaced by radial-ply tires on heavy trucks (*41,42*), and average inflation pressures have increased from 550 kPa (80 psi) to 690-760 kPa (100-110 psi) (*32,39,41,43*). Wide-base single tires are replacing dual tires in Europe, although they are not widely used in the USA, except on heavily loaded steering axles (*32,39*).

There is concern in the pavement engineering community that these changes in operating patterns may increase pavement damage, particularly rutting (*22,32,41,43-45*).

Contact Pressure Distribution

Most pavement analysts have assumed that the normal component of the contact pressure between tire and road surface is uniform, acts over a circular area and is nominally equal to the inflation pressure (see, for example (*2,4,39,44,46-49*)). Considerable experimental evidence exists to suggest that this is not the case. Pressures are observed to increase around the edges of the contact area, particularly in the "shoulder" areas at either side, due to the bending stiffness of the side walls and tread band (*22,41,42,45,50-52*). Under normal inflation and loading conditions, the maximum shoulder pressure is typically observed to exceed the inflation pressure by a factor of two (*41,42,45,51,53*), although the contact pressure distribution is found to be more uniform for higher inflation pressures and/or lower vertical loads (*41,42,51,53*). The contact area is also found to decrease with increased inflation pressure and to increase with total load. Marshek et. al. (*51*) reported typical results for truck tires: 8-20% decrease in area for 50% increase in pressure; 30-35% increase in area for 50% increase in load.

Effect of Tire Contact Conditions on Flexible Pavement Response and Damage

A number of authors have calculated (*39,43-45,54,55*), or measured (*18,19,22,27,54*), the influence of tire contact conditions on stresses and strains in the road surface.

The general consensus is clear: the details of the contact conditions, such as the exact area, pressure and pressure distribution, affect stresses and strains near to the surface of the pavement, whereas the response in the lower layers depends mainly on the overall load (*41,44,45,54*). For example, Haas and Papagiannakis (*44*) showed that increasing tire inflation (contact) pressure from 415 to 830 kPa at constant load increased the theoretical vertical compressive strain near to the surface of a 200 mm thick asphalt layer by up to a factor of eight, but hardly affected the strain at the bottom of the layer. Conversely, doubling the axle load at constant pressure increased subgrade compressive strain by a factor of two, but made little difference to compressive strain in the asphalt layer. These trends were corroborated by Marshek et. al. (*56*). Similarly, Roberts et. al. (*43,45*) and Marshek et. al. (*56*) applied relatively realistic (axisymmetric) contact pressure distributions to elastic layer pavement models. Both studies established that assumptions about contact conditions can alter predicted horizontal strains in thin surface layers (< 50 mm) substantially, particularly for under-inflated tires which have large shoulder contact pressures. The effects of non-uniform loading are much less significant for vertical subgrade strains and for thicker pavements.

Research into pavement *damage* confirms the localized influence of contact conditions (*32,41*). Theoretical studies by Southgate and Deen (*39*) indicated that fatigue damage due to tensile strain of thin asphalt pavements is likely to increase rapidly with average contact pressure. This was confirmed by Marshek et. al. (*56*) and O'Connell et. al. (*25*). Both of these studies, however, reported that inflation pressure has little effect on subgrade rutting. Roberts et. al. (*43,45*) and Haas and Papagiannakis (*44*) estimated rut formation by summing theoretical permanent deformations of the pavement layers and both ascertained that rutting damage is sensitive to contact pressure. In view of the localized influence of contact pressure on compressive strain observed in (*44*) (see above), this was presumably due to near-surface effects. On the basis of asphalt pavement strain measurements, Addis (*27*) reported that a 40% increase in tire pressure would increase fatigue damage by 26%. Laboratory measurements by Eisenmann et. al. (*54*) on a 225 mm thick asphalt road surface model showed that rut depth development was approximately linearly related to the average contact pressure, (independent of load), and proportional to the square root of the number of load applications.

Tire contact conditions (pressure and area) vary dynamically with dynamic wheel loads. No analysis of road damage which accounts for this effect has been found in the literature. On the basis of the static analyses and measurements presented above, it seems reasonable to speculate that these dynamic effects will make some difference to stresses and strains in

the upper pavement layers, and probably have negligible influence in the lower layers, where the overall dynamic load level will be the most important factor.

Effect of Tire Configuration on Flexible Pavement Response and Damage

Several authors have considered the influence of the number and type of tires on an axle.

Experimental measurements by Christison et. al. (18) for a variety of axle and tire configurations indicated that asphalt layer interfacial strains and vertical surface deflections were equivalent for 27 kN carried on a single tire or 40 kN carried on a dual pair. Analysis of the measured strains in terms of pavement damage indicated that a single tire is theoretically 7-10 times worse than a pair for equal load. This was confirmed theoretically by Treybig (13). Zube and Forsyth (19) presented very similar results in an experimental comparison of wide-base single tires and dual wheels. Eisenmann et. al. (54) and Addis (27) both reported that the measured strains under wide single tires were 50% greater than those under dual tires carrying the same total load. Addis reported that this would increase pavement fatigue damage by as much as a factor of 2.5.

On the basis of asphalt strain measurements, Huhtala (22) reported that wide-base single tires are likely to cause 3.5 to 7 times more damage than dual tires, and that the worst conditions are for thinner asphalt layers. He also noted that the contact pressures under each tire in a pair can be quite different due to a number of factors, including differential inflation pressures or temperatures, tread wear, axle bending or transverse road profile. He reported that a wide-base single tire is 1.5 times more damaging than an unevenly inflated dual pair with 500 kPa in one tire and 1000 kPa in the other.

An OECD report (21) recommended that relative to dual tires, wide-base single tires should be considered to be 2.1 times more damaging and conventional single tires to be 2.9 times more damaging.

It is important to note that the large pavement damage factors cited above were derived from a two-stage process. First, strains in the road were measured (or predicted) under dual and wide single tires. These strains were typically 1.5 to 2 times greater for the wide single tires than the duals. Second, relative pavement damage was estimated using a power-law damage relationship (typically with a fourth power) to weight the strains. This raises the important question of whether a fourth power is appropriate, or whether it may bias the results excessively.[6]

---

[6] The validity of the "fourth power law" is questionable (20), particularly for current axle loads and configurations, tire pressures and road constructions, all of which are substantially different from the AASHO road test conditions (6, 57). More recent research has indicated that the damage exponent may take a wide range of values; for flexible pavements: 2–6 (20), 1.3–4.1 (12) and for composite or rigid pavements: 8–12 (18,21) and 11–33 (28). An extensive discussion of the fourth power law is provided in (57).

Most evidence suggests that when fatigue cracking is the dominant mode of failure, a fourth power is a reasonable average value for the exponent n in the fatigue relation for asphalt:

$$N = k \left(\frac{1}{\epsilon} \right)^n \qquad (A\text{-}2)$$

where N is the number of cycles to failure at strain level ϵ (see (7,9) for typical asphalt fatigue data). Therefore, for fatigue cracking of thin pavements, the high power in the damage law, and hence high relative damage factors (of 3.5 to 7) for wide single tires, appear to be reasonable. For thicker pavements, sub–surface tensile strains are less affected by the tire contact conditions and more strongly influenced by the total load, so it is likely that the relative fatigue damage factors for wide single tires will be less than cited above.

The situation is less clear in the case of permanent deformation, particularly for thicker asphalt pavements. There is considerable evidence to suggest that permanent deformation in asphalt is *proportional* to the elastic stress or strain level, rather than some high power of it (4,10,44,58,59).[7] If permanent deformation is proportional to elastic stress, then use of the fourth power law to weight stress levels cannot be justified, and the relative increase in rutting damage for wide single tires is likely to be a factor of 1.5 or 2 at most.[8]

Tests performed by the FHWA with an accelerated pavement loading facility (ALF) seem to bear out these conclusions. According to Kenis (66), wide single tires increased strain levels by a factor of two compared with dual tires (for the same total load); increased rutting damage by a factor of two; and increased fatigue cracking by a factor of four.

Collecting the above evidence together, the following tentative conclusions may be drawn about the influence of wide single tires on road damage:

1. For relatively thin asphalt pavements that fail by fatigue cracking, wide single tires are likely to cause up to 7 times more damage than dual tires carrying the same total load.

2. For thicker pavements, where permanent deformation is the main mode of failure, wide single tires are likely to cause 1.5 to 2 times more damage than dual tires carrying the same total load.

---

[7] This would be exactly true if asphalt could be regarded as a linear visco-elastic material (60,61).

[8] If rut formation is proportional to the stress or strain level, and hence approximately proportional to the applied load, then dynamic load variations would be expected to be relatively unimportant, compared with the static loads. The depth of ruts would therefore be expected to be relatively constant along a road, as is generally observed on the highway. Conversely, fatigue damage would be expected to be much more sensitive to the magnitude of the applied loads and hence fatigue cracking may be expected to occur in localized areas where the dynamic loads are consistently high (62-65).

INFLUENCE OF VEHICLE DESIGN ON DYNAMIC WHEEL LOADS

In 1984, Magnusson et al. (*50*) presented a review of literature concerned with dynamic axle loads. They concluded (largely on the basis of the theoretical publications) that soft suspension springs and tires of low vertical stiffness are desirable for minimizing dynamic loads. However, important implications of low suspension and tire stiffness for handling and roll stability were not addressed. Furthermore, that an optimal level of viscous damping usually exists depending on the conditions, and that any dry (Coulomb) friction in the suspension usually increases dynamic wheel loads. Aurell (*67*) presented the results of experimental and theoretical parametric studies on suspension systems which agreed with Magnusson's results. Heath (*68*) performed a large parametric study of dynamic wheel loads for four linearized vehicle models traveling on random road surfaces. He corroborated the view that soft suspensions and tires are desirable, but noted that for very low tire stiffness it is possible for the low frequency force components due to sprung mass motion, and hence the RMS force levels, to increase. Heath's results also indicated the existence of optimal suspension damping levels and he noted that it is usually better to have too much rather than too little suspension damping.

There have been a number of major experimental studies of dynamic loads in recent years: Whittemore et al. (*69*) and Ervin et al. (*70*) in the USA, Leonard et al. (*71*), Addis et al. (*72*) and Mitchell, Gyenes and Simmons (*37,73*) in the UK, Sweatman (*35,74*) in Australia, Woodrooffe et al. (*36*) in Canada and a West German study reported by Gorge (*75*) and Hahn (*76*). These studies have mainly examined RMS dynamic wheel loads for various suspensions, tires and operating conditions, and they are summarized in Table A-1.

In general, the researchers have drawn broadly similar conclusions about the effects of suspension and tire types on dynamic wheel loads, and these conclusions corroborate the trends predicted in the theoretical studies described above.

- Dynamic wheel loads were found by all studies to increase with speed (although not necessarily monotonically) and road roughness.

- Centrally-pivoted tandem drive axle suspensions such as walking-beam and single-point suspensions[9] were always found to generate the highest dynamic loads because of their lightly damped pitching modes at around 8-10 Hz (see, for example, (*70,73*)). Hahn (*76*) noted however, that these suspensions can be improved considerably by suitable use of hydraulic dampers. Four-spring tandem suspensions were generally found to generate smaller dynamic loads than walking beams. Torsion-bar and air suspensions generated the lowest loads. Figure A-2 from (*35*) shows typical results for various suspensions.

---

[9] See Appendix D and Sweatman (*35*) for description of suspension types.

- Hahn (76) noted that modern single-spring parabolic suspensions with good hydraulic damping are "not significantly worse" than stiff air suspensions. Conversely, Aurell (67) reported that air suspensions without hydraulic dampers could generate significantly higher dynamic loads than leaf spring suspensions.

- Sweatman (35) noted that reducing suspension stiffness generally reduces wheel loads.

LEGEND

D1	Walking-beam RT 340	T1	Four-spring
D2	Walking-beam RT 380	T2	Six-spring
D3	Torsion bar	T3	Air-bag tandem
D4	Single-point ("Big 6")	T4	Air-bag triaxle
D5	Dynalastic		
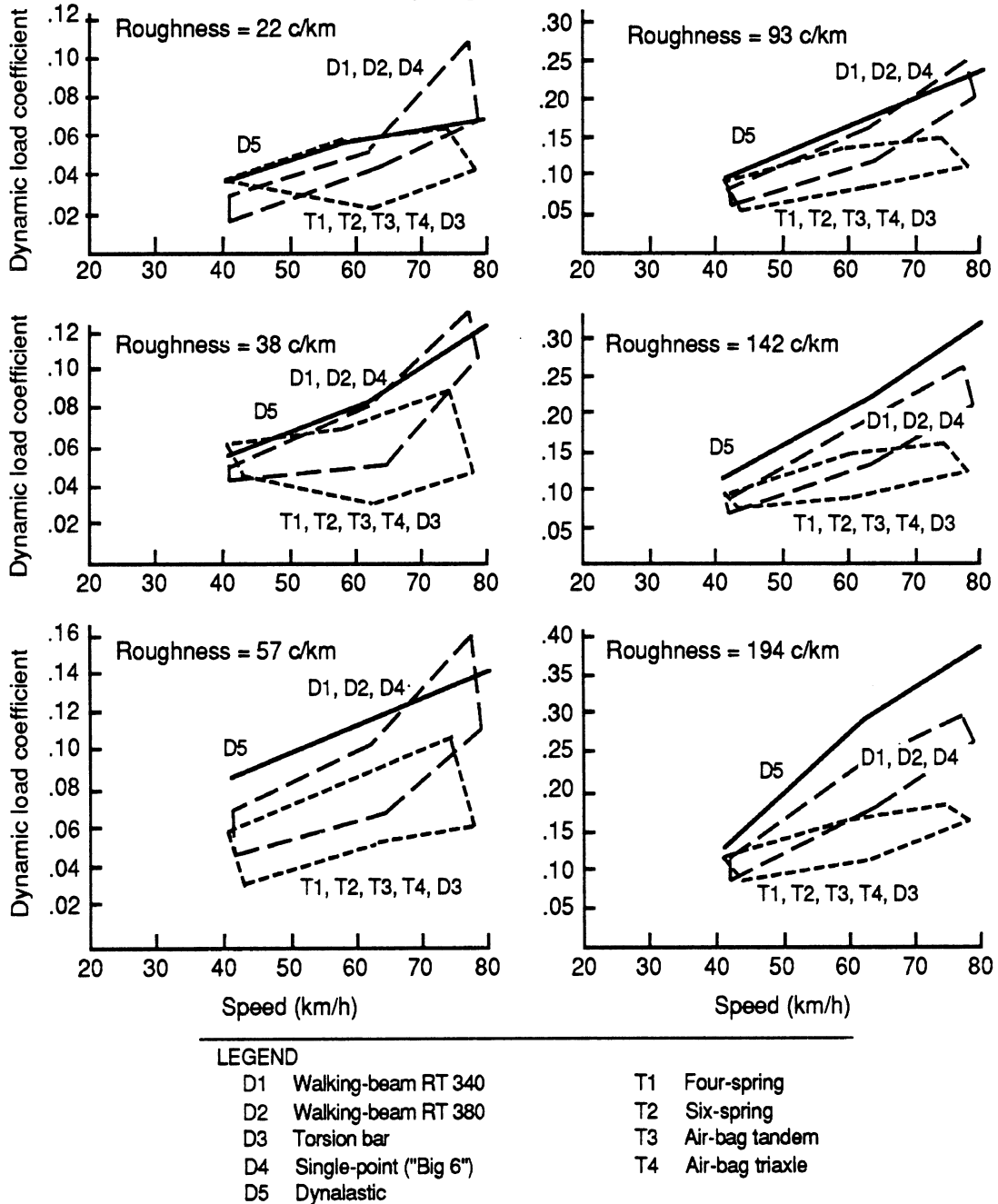
Figure A-2. Effects of speed on the dynamic load coefficients (DLC) generated by a variety of suspension systems. After Sweatman (35).

Table A-1. Summary of Major Dynamic Wheel Load Measurement Studies.

Source	Force Measurement Method (i)	Vehicles (ii)	Test Suspensions (iv)	Road Surfaces	Speeds (km/h)	Other Variables/ Notes (v)
Whittemore et. al. (6), 1970, USA	• Hub • Strain • Tire pressure	• 1 x Rigid • 2 x Artic	• 2 x Leaf spring single • 1 x Walking beam tandem	• 9 x Highway sections • Planks	54, 88, sweep 32, 48, 64, 80	• Tire pressure • Fully laden
Leonard et. al. (71), 1974, UK	• Weigh scale • (Ground vibration)	• 8 x Artic	• Leaf spring single • 4 - spring tandem • Single point tandem • 6 - spring triaxle	• 5 x Planks of different profiles	16, 32, 48, 64	• Fully laden
Sweatman (35,74), 1983 Australia	• Hub	• 9 x Artic	• 3 x Walking beam • Torsion bar tandem • 4 - spring, 6 - spring • Air tandem & triaxle • Single point tandem	• 6 x Highway sections	40, 60, 80	• 2 Tire pressures • RTRRMS roughness • Fully laden • Static load sharing
Ervin et. al. (70), 1983, USA	• Hub	• 3 x Artic	• Walking beam tandem • 4 - spring tandem • Torsion bar tandem	• 3 x Highway sections	72, 88	• RTRRMS roughness • Fully laden
Gorge (75) 1984 Hahn (76)1987 West Germany	• Weighted accns • Hub • (Pavement strains)	• 9 x Artic • 2 x Buses	• 3 x Leaf spring single • 1 x Air single • 4 - spring, 6 - spring • Air tandem & triaxle • 1 x Single point tandem	• 3 x Test track sections • 3 x Highway sections	30, 50, 70, 80, 90	• Fully laden
Woodrooffe et. al. (36) 1986 Canada	• Strain • (Pavement strains & deflections)	• 1 x Artic (iii)	• 2 x Walking beam • Air single, 2 xair tandem • 2 x 4 - spring tandem	• 2 x Highway sections • Planks • Railway crossing	40, 60, 80 18, 40 40, 60, 80	• Axle spread • Static load • RTRRMS roughness
Addis et. al. (72), 1986, UK	• Laser tire deflection • Strain • (Pavement strains)	• 1 x Artic	• 2 x Leaf spring single • 4 - spring (wide) tandem	• 1 x Test track section	32, 48, 64	• Tyre type • Static load
Mitchell et. al. Simmons et. al. (34,37,73) UK, 1989	• Strains (all axles) • (Strain-gauged suspension components)	• 1 x Rigid • 2 x Artic (iii)	• 1 x Leaf spring single • 1 x Single point tandem • 2 x 4-spring,1x6-spring • 4 x Air tandem • 1 x Walking beam • 1 x Air triaxle	• 3 x Test track sections • 25mm plank • 6 x Highway bridges • 7 x Humped bridges	32, 48, 64, 80, 96 64-96	• Fully laden • Static load sharing

Notes: (i) Hub = Instrumented hub transducer, Strain = Strain gauged axles housing, (ii) Artic = Articulated tractor and semitrailer, (iii) Interchangeable subframes, (iv) See (35) for description of suspension types, (v) RTRRMS = Response Type Road Roughness Measurement System.

- Triaxle suspensions were found to be better than tandem suspensions in several studies (35,36,76). Woodrooffe et al. (36) found that varying the axle spacing of an air-spring tandem suspension had negligible effect on the dynamic loads, whereas the Dynamic Load Coefficient (DLC) generated by a four-spring tandem suspension varied considerably with axle spacing, depending on the speed and road roughness.

- Mitchell and Gyenes (73) found that their test suspensions ranked in the same order of DLC's, regardless of road roughness and speed. Other researchers, however, have not found this to be the case (35,76,77).

- On smooth road surfaces, friction was found effectively to lock some leaf-spring suspensions (72,76). This can lead to relatively large and lightly damped vibration of the vehicle mass on the tire "spring" stiffness.

- Most research has indicated that lower tire pressures usually result in reduced wheel loads (69,70,78). Sweatman (35,74), however, reported that for some suspensions the opposite was true. According to Ervin et al. (70) this anomaly could be because Sweatman did not correct his measured wheel loads for accelerations of the outboard mass, or due to "tuning" of one of the test vehicle's vibration modes to the particular road profile. A third possible explanation is the increase in the sprung mass contribution (to the wheel loads) ascertained theoretically by Heath (68) and described above.

- Wide-based tires were found by Hahn (76) to generate slightly lower loads than dual tires and Addis et al. (72) noted that radial ply tires are slightly preferable to bias-ply tires. Both of these conclusions are consistent with the observed reduction of wheel loads with lower stiffness tires.

EFFECTS OF DYNAMIC WHEEL LOADS

There have been two main approaches to assessing the road–damaging effects of dynamic wheel loads. The first involves statistical analysis of the loads and use of the "fourth power law" to relate the loads to road damage. This is known as the "road stress factor" approach. The second involves calculating the theoretical damage incurred by a road model due to passage of one or more vehicles. This requires calculation of the response of a road model to moving dynamic loads. Both approaches are discussed in this section.

Before considering either approach, it is important to address the issue of "spatial repeatability" of dynamic wheel loads.

Spatial Repeatability

Despite being a "stochastic" process, there is considerable evidence to show that for any given testing speed, the wheel load time histories generated by a particular heavy vehicle are repeated closely on successive runs over a given stretch of road (65,72,75,76,79,80). This may be expected since the vehicle encounters the same road profile, and hence excitation, on each run. This phenomenon has been termed "spatial repeatability'.

Figure A-3, from Addis et al. (72), illustrates the effect. It shows the wheel loads measured on the axles of a tandem leaf-spring suspension, when driven over the same section of test track three times. The loads are plotted as a function of distance and it can be seen that the same locations along the road incur the maximum loads on each run.

A similar effect was observed by Ervin et al. (70) who noted that three vehicles with different suspensions were all excited by the same roughness feature and consequently applied peak wheel loads to the same localized area in the vicinity of that feature.

Hahn (65) noted that "Since all heavy commercial vehicles have approximately the same natural frequencies and are driven at approximately the same speed on motorways and long distance roads, it may be concluded that for a given pavement the dynamic wheel load peaks always occur within relatively narrowly defined road sections."

A recent theoretical study by Cole (63) investigated Hahn's hypothesis. Cole simulated the road damage done by a family vehicles of the same basic configuration, with parametric differences and speed variations typical of the highway vehicle fleet. He showed that there is a strong correlation between the spatial distribution of damage done by approximately 70% of all vehicles in a particular class.

The spatial repeatability issue is central to the interaction between vehicles and roads because some locations along the road can incur very large damage as a vehicle passes. If this damage is repeated for most vehicles in a given class, then the overall road damage caused by dynamic wheel loads at these locations will be much worse than most analytical studies have predicted. The spatial repeatability of dynamic wheel loads might be expected to vary around the world, depending on the road surface roughness, the local size and weight regulations and the homogeneity of the vehicle fleet.
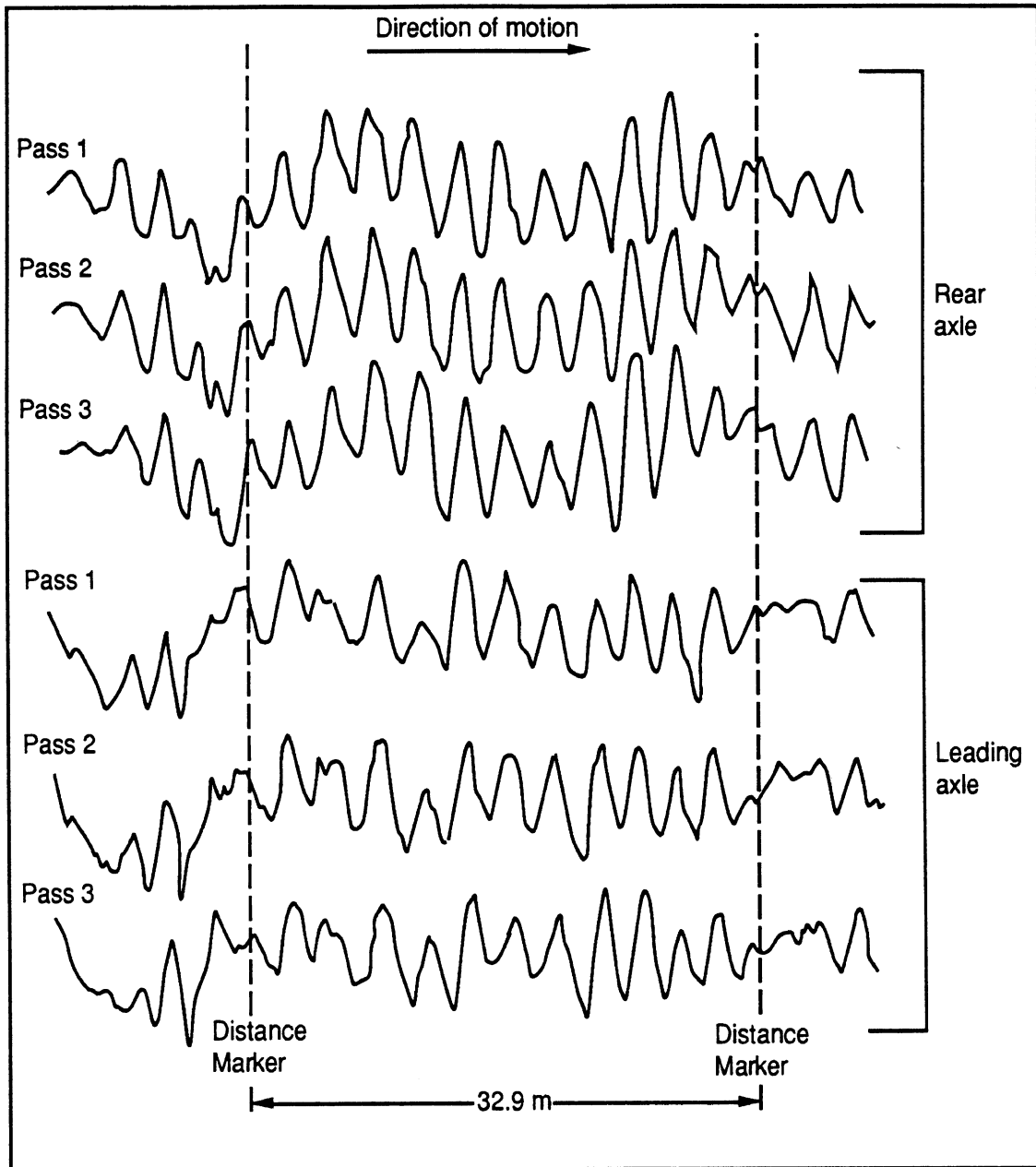
Figure A-3. Measured wheel load variations on each axle of a leaf-spring tandem plotted as a function of distance for three runs at 32 km/h. (72).

Road Stress Factor Approach

In 1975, Eisenmann (81) derived a quantity known as the "road stress factor", Φ, using the assumption that road damage depends on the fourth power of the instantaneous wheel load. Assuming that dynamic wheel loads are Gaussian (normal distribution), Eisenmann showed that the expected value of the fourth power of the instantaneous wheel load is given by:[10]

$$\Phi = E[P(t)^4] = (1 + 6\bar{s}^2 + 3\bar{s}^4)\, P_{stat}^4 . \tag{A-3}$$

Where:

$P(t)$ = Instantaneous wheel load at time t.
$P_{stat} = E[P(t)]$ = Static (average) wheel load.
$\bar{s}$ = Coefficient of variation of dynamic wheel load = (Standard Deviation/Mean)
    (essentially the Dynamic Load Coefficient DLC, see Sweatman (35))
$E[]$ = Expectation operator.

In 1978, Eisenmann (82) proposed a modified version of Eq. A-3 which accounted for the effects of wheel configuration and tire pressures:[11]

$$\Phi' = \nu\, (\eta_I\, \eta_{II}\, P_{stat})^4 . \tag{A-4}$$

Where:

$$\nu = 1 + 6\bar{s}^2 + 3\bar{s}^4. \tag{A-5}$$

ν is the "dynamic road stress factor" (Sweatman (35)),

η_I accounts for wheel configuration (single or dual tires), and

η_{II} accounts for tire contact pressures.[12]

Eq. A-4 underpinned a substantial body of research in West Germany during the 1980's by the "Road Stress Committee" (21,54,75,83,84). The equation has the desirable (although not necessarily justifiable) effect of decoupling the road damage problem into three sub-problems which can be studied separately.

---

[10] Sweatman (35) generalized Eq. A-3 to account for departure of the wheel load probability distribution from Gaussian, but showed that the effects of skewness and kurtosis on Φ were negligible for his measured tire force data.

[11] Sometimes written as $\Phi' = (\eta_I\, \eta_{II}\, \eta_{III}\, P_{stat})^4$ where $\eta_{III} = \nu^{1/4}$ (21,83).

[12] An additional factor is sometimes included to account for the type of axle group (single/tandem/triaxle) (21,83).

Considerable research effort has gone into quantifying η_I, η_{II} and ν for a variety of suspensions and tire contact conditions. Values for η_I and η_{II} can be found in several papers $(54,75,83,84)$[13] but will not be discussed here.

For typical highway conditions of roughness and speed, Sweatman (35) measured ν in the range 1.11 to 1.46 depending on the suspension system. Other researchers have published similar results $(70,73,75)$. (It is expected that suspensions should rank in the same order whether the wheel loads are compared in terms of road stress factor or DLC.)

Mitchell and Gyenes (73) used the road stress factor to analyze their measured wheel loads and those presented by Hahn (76). They estimated that widespread replacement of steel and rubber suspensions with air suspensions in the UK would reduce overall damage due to drive axles by 8% and damage due to semitrailer axle groups by 10-20%. Their analyses of the UK and West German wheel load data yielded qualitatively similar conclusions.

The road stress factor approach was used to analyze the West German research results for buses (65). This provided the information for West German legislation, introduced in 1984, which allows two-axle buses to carry eleven tonnes rather than ten tonnes on air-suspended rear axles with dual wheels, providing the sprung mass "natural frequency" is less than 1.5 Hz, and the "damping ratio" is greater than 0.25 (85).

A similar regulation is currently being implemented by the European Community (86). Single drive axles of articulated vehicles will be allowed to carry an additional tonne of payload (taking the total axle load to 11.5 tonnes) providing the natural frequency, measured in a step test, is less than 2.0 Hz; the "damping ratio" greater than 0.2; and the axle has two pairs of dual tires.[14]

It is worth noting that the West German Road Stress Committee developed a nomograph for determining Φ' graphically, depending on the road roughness, speed, static axle load and vehicle characteristics. It assumes a quarter-car representation of the vehicle (84). The committee used this method to compare a number of different vehicle configurations and recommended several 42 tonne articulated combinations which might be expected to do less damage than existing 38 tonne combinations (84).

---

[13] It is interesting to note that η_I and η_{II} are considered to be "penalty" factors or "bonus" factors depending on the author. For example, the OECD report: "Impacts of heavy freight vehicles" (21) recommended $\eta_I = 1.0$ for twin tires and 1.3 for single tires, i.e. a 30% "penalty" for single tires, whereas Eisenmann et. al. (54) recommended $\eta_I = 1.0$ for single tires and 0.9 for twin tires, i.e. a 10% "bonus" for twin tires.

[14] Note that the step test proposed for measuring *the* natural frequency and damping ratio of a suspension for the EC test is flawed, because it does not account for many of the important characteristics of suspension dynamics and dynamic loads. See (64) for details.

Magnusson et. al. (*50*) criticized use of the road stress factor. They noted that the fourth power law arose from measurements of the overall loss of serviceability of the AASHO road test sections due to vehicles that applied wheel loads which included a dynamic component. As a result, the fourth power law implicitly accounts for dynamic wheel loads. "Eisenmann's supplementing of the formula (fourth power law) consequently appears somewhat dubious" (*50*).

The road stress factor approach incorporates all of the uncertainties inherent in the fourth power law, which has itself been the subject of considerable criticism (*12,20,57*). It has three other questionable features:

1. It assumes that strain in the road surface is directly proportional to the instantaneous wheel load and neglects the sensitivity of road surface response to the speed and frequency of the applied loads (see Hardy and Cebon (*87,88*)).

2. It assumes that road damage is spread randomly over the surface and does not account for any concentration of damage which may occur in the vicinity of particular roughness features (see Spatial Repeatability section).

3. It assumes that each suspension system on a vehicle does not influence the wheel loads, and hence road damage, generated by other axles. Thus suspensions are compared through analysis of the wheel loads generated by individual axles or axle groups, rather than through analysis of road damage done by the whole vehicle. (See (*64*)).

According to Morris (*32*), the road stress factor is "a plausible rule of thumb that can serve as a bench-mark for comparison with more analytical approaches."

Analytical Models of Vehicle/Road Interaction

A number of theoretical studies of the interaction between vehicles and road surfaces have been performed in recent years. They are summarized in Table A-2. These studies can be divided into two distinct classes denoted in the table as "whole-life models" and "single vehicle pass" calculations.

Whole-life models of flexible pavements

"Whole-life models" (*15,46,79*) attempt to predict the deterioration of a pavement's structural integrity and surface profile with time due to the applied dynamic wheel loads. This requires an empirical relationship between the wheel loads and the change of road surface profile. This is an area of considerable uncertainty. The calculations also attempt to include the complex affects of environmental/seasonal factors (temperature, frost, etc.) on road strength and the statistical variation of structural properties along the road.

Table A-2. Summary of Theoretical Vehicle-Pavement Interaction Studies.

Source	Vehicle Models (i)	Pavement models	Vehicle model parameters examined	Pavement parameters examined	Pavement damage criteria (ii)	Interaction assumptions
Ullidtz et. al. (15), 1983, Denmark	• 1/4 Car • Linear	• Flexible • Elastic layer • Random property changes every 0.3m	• Static load	• 180 AASHO road test sections • Detailed inclusion of climatic factors	• Cracking • Rutting • Serviceability (PSI)	• Whole life model • Damage calculated weekly • Profile degradation with time.
Cebon, (89,90), UK, 1985-7	• 3 x Artic • 1 x Rigid (6x4) • 1 x 4-spring tandem • Nonlinear	• Flexible • Beam on damped elastic foundation • Dynamic	• Road roughness • Speed • Linear/Nonlinear	• Fixed pavement model	• Fatigue • Rutting • Simplified criteria using wheel forces only	• Single vehicle pass • Damage starts at a few locations which experience large strains
O'Connell, Abbo et. al. (23,25) USA 1986	• 1 x Artic with 3 tandems (4-spring, walking beam, air spring) • Nonlinear	• Flexible: elastic layer • Rigid: plate on Winkler foundation (FE)	• Road roughness • Speed • Suspension type and parameters (stiffness, damping, friction) • Axle spacing • Load sharing	• Fixed pavement models, flexible and rigid	• Cracking • Rutting • PSI • DLC	Flexible: • Single vehicle pass • Modified road stress factor Rigid: • Whole life model • Joint fault degradation
Brademeyer et. al. (46)- USA, 1986	• AASHO road test vehicles (single axles)	• Flexible • Elastic layer • Statistical variation of material properties • Modified VESYS IIIA	• Static load	• 23 AASHO road test sections • 4 climatic seasons • Several roughness levels	• Cracking • Rutting • PSI • Slope variance (roughness)	• Whole life model • Damage calculated weekly • Road profile spectrum degradation with time
Monismith et. al. (16), USA, 1988	• Measured tire forces, from (70)	• Flexible • Elastic layer • Frequency dependent stiffness	• Suspension type • Torsion bar • 4-spring • Walking beam	• Fixed pavement model	• Fatigue	• Single vehicle pass • Each point on road subjected to the full spectrum of tire forces
Papagiann-akis et. al. (79), Canada 1989	• Statistics of dynamic loads	• Flexible • Elastic layer • Statistical variation of material properties • Modified VESYS IIIA	• Suspension type • Rubber tandem • Air tandem	• 10 AASHO road test sections • 5 climatic seasons • 3 roughness levels	• Cracking • Rutting • Slope variance • PSI	• Whole life model • Spatial repeatability in AASHO road test • Road profile degradation due to cracking

(i) Artic = Articulated tractor and semitrailer. *(ii)* PSI = Present Serviceability Index, from AASHO road test (6), DLC = Dynamic Load Coefficient.

A—19

The three whole-life flexible pavement analyses were all validated using data from the AASHO road test (*6*). Predictions of rutting and cracking by Ullidtz et. al. (*15*) and Papagiannakis et. al. (*79*) reproduced the AASHO test results well. Papagiannakis et. al. found that the dynamic analysis improved the accuracy of their damage predictions considerably. Brademeyer et. al. (*46*) also achieved relatively convincing agreement of rutting and serviceability predictions with AASHO test data. In this case, however, the improvement in accuracy was relatively small over the results presented by Kenis et. al. (*48*) who performed a similar analysis of the AASHO road test, (using the same VESYS analysis program), without including dynamic loads. Fatigue cracking predictions in (*46*) were inaccurate. Neither (*46*) nor (*15*) drew any conclusions about the influence of vehicle design on road damage because the main emphasis of these studies was prediction of pavement degradation with time. Papagiannakis et. al. (*79*) deduced that rubber suspensions (walking-beam type) cause 17-22% additional theoretical damage due to dynamics, and air suspensions cause an additional 6-8%.

Single Vehicle Pass Calculations

"Single vehicle pass" calculations (*16,25,89,90*) determine the incremental change in road wear due to one passage of a vehicle over a particular road. There are two substantive differences in the assumptions made by O'Connell et. al. (*25*) and Monismith et. al. (*16*), on one hand, and Cebon (*89,90*), on the other.

1. O'Connell et. al. and Monismith et. al. used pavement models based on elastic layer theory. Monismith et. al. recognized the importance of the frequency dependence of road response and modified the elastic modulus of the asphalt according to the "predominant" loading frequency (wheel load resonant frequency + 5Hz to account for the speed of 90 km/h).

   Cebon (*90*) accounted for the influence of speed and frequency of the applied loads by calculating the dynamic response of an idealized road model consisting of a beam supported by a damped elastic (Winkler) foundation.

2. There is an important difference in the assumed relationship between the wheel loads and road deterioration. Monismith et. al. and O'Connell et. al. assumed that the wheel loads are randomly distributed over the road surface so "any single point in the wheel path is likely to sustain the same level of loading as any other point ... (and hence) ... may be subjected to the full spectrum of loads that a given truck might apply" (*16*). Thus they calculated the average value of the particular road damage criterion by assuming that each axle or axle group damages the road independently. O'Connell et. al. achieved this by calculating a modified "road stress factor" (similar to Eq. 3) based on theoretical pavement strain instead of the dynamic wheel loads. Monismith et. al. analyzed the wheel loads generated by one axle only of a tandem group.

Conversely, based on considerations discussed in the Spatial Repeatability section, Cebon (90) calculated the accumulated damage at particular points along the road due to all of the axles of a vehicle and then assumed that the road is likely to become unserviceable when a relatively small proportion of the surface area is damaged.

Monismith et. al. (16) concluded that for their particular conditions, the theoretical increase in damage done by dynamic wheel loads of three tandem suspensions compared with damage due to static wheel loads alone was: Torsion-bar - 19%, 4-spring - 22%, Walking-beam - 37%.

O'Connell et. al. (25) performed a large parametric study of vehicle and pavement variables (see Table A-2). One typical result is shown in Figure A-4. They concluded that:

- Dynamic wheel loads can cause a significant increase in theoretical pavement damage, typically up to 25% depending on the conditions, but this can be improved by careful suspension design.

- Air suspensions were found to be the least damaging and walking-beam suspensions the most damaging (see Figure A-4).

- Although dynamic loads and theoretical cracking damage were found to increase slightly with tandem axle spacing, rutting damage was found to decrease dramatically because of reduced compressive strains in the subgrade.

Cebon (89,90) concluded that dynamic wheel loads are likely to have a significantly greater influence on pavement fatigue life than predicted in the other studies because he asserted that road deterioration is governed by damage at the worst locations (95th percentile) rather than the average value over the road surface. This assertion is consistent with the observations described in the Spatial Repeatability section of this appendix because it assumes that particular locations will be damaged significantly more than others by all vehicles in the "fleet." Gordon (38) postulated the same damage mechanism and calculated that dynamic loads were up to 14 times worse than static loads, for the worst suspensions. This damage hypothesis is also discussed by Sweatman (35) and Mitchell and Gyenes (73). Cebon also concluded that:

- Theoretical fatigue damage was found to be up to four times that due to moving static loads at the worst locations, for typical conditions of highway speeds and surface roughness.

- Theoretical road damage done by articulated vehicles was found generally to increase with speed. Certain "critical" speeds exist at which increased damage occurs due to pitch coupling between the axles and increased excitation of the modal responses on the vehicle. One typical result from (90) is shown in Figure A-5.
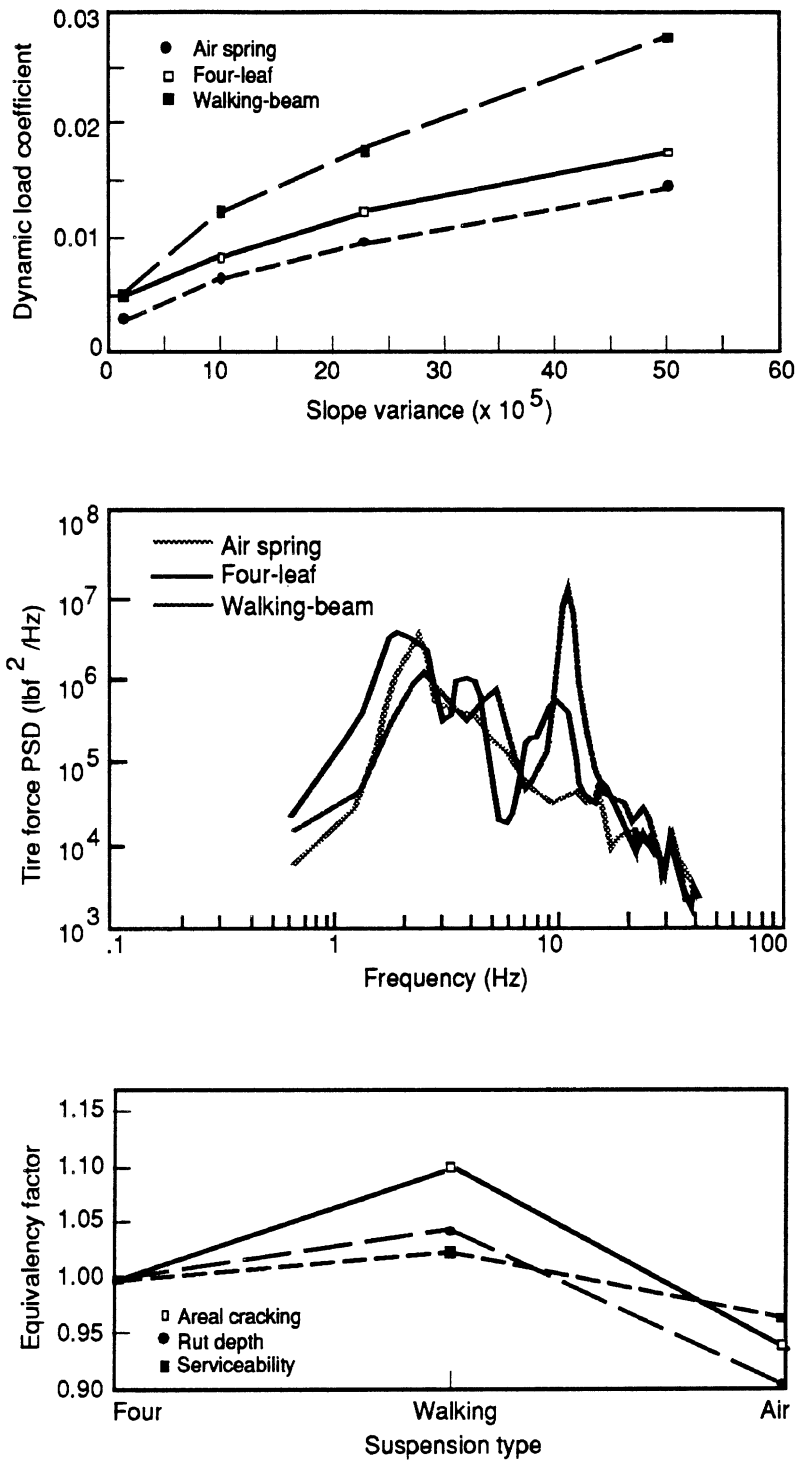
Figure A-4. The effect of suspension type on simulated wheel loads and flexible pavement damage. After O'Connell et. al. (25).
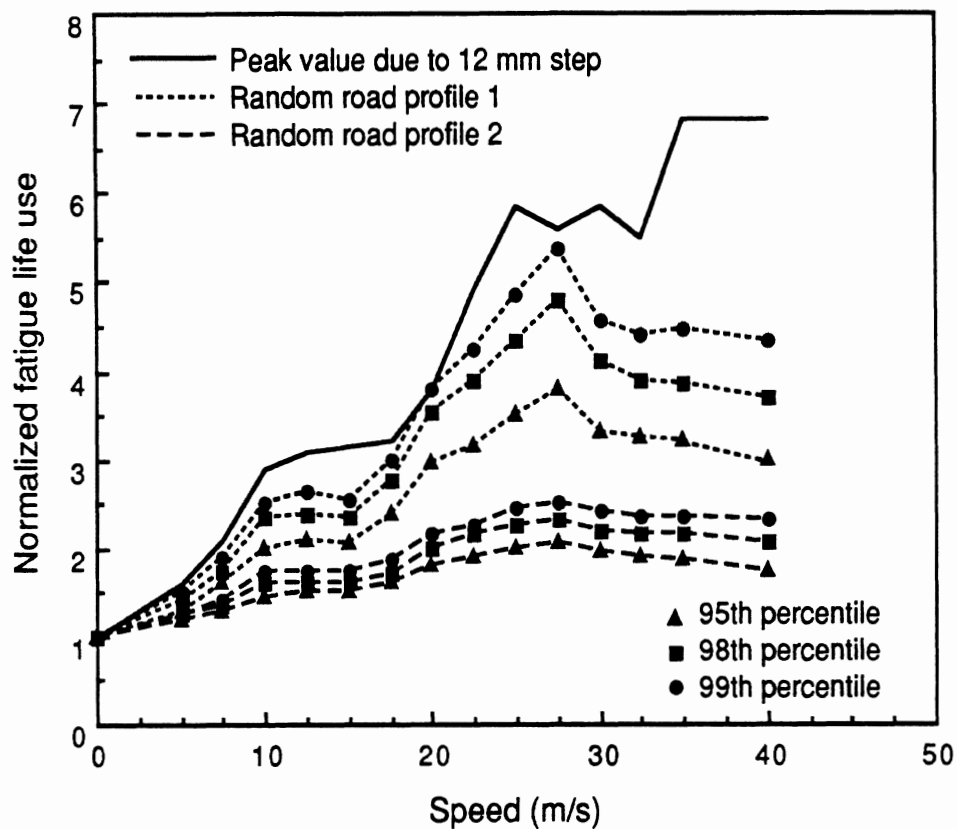
Figure A-5. Variation of normalized theoretical fatigue damage with speed, due to one pass of a two axle vehicle model with a 4-spring tandem suspension system. After Cebon (90).

- On roads with relatively smooth surface profiles, at highway speeds, the increase in dynamic wheel loads with speed may be outweighed by the decrease in dynamic response of the road surface. The net effect may be a reduction in fatigue damage with speed. This effect can be seen in Figure A-5.

Rigid Pavements

The jointed rigid (PCC) pavement analysis by Abbo et. al. (23,91) is a special case because it is largely a "single vehicle pass" analysis but it includes a model of joint fault degradation with time. This study concluded the following:

- Under static vehicle loads, the ends of concrete slabs are more prone to fatigue damage than the mid-slab region, due to the discontinuity in bending strength at the joints. Under dynamic loading, however, excitation of the sprung mass modes of the vehicle by joint faults can increase significantly the fatigue damage predicted for the mid-slab regions.

- Suspensions ranked in order of increasing damage:

single axle < 4-spring tandem < walking-beam tandem.

• Reducing the spacing of the 4-spring tandem increased the predicted pavement strains and damage slightly, whereas reducing the walking-beam spacing reduced dynamic loads substantially at highway speeds (depending on the speed, because of wheelbase filtering effects) and hence reduced predicted damage.

• Suspension spring characteristics (stiffness, hysteresis) were found to be important, but tire pressure was not.

Finally, Savage (92) described an interesting mechanism for the occurrence of cracks near to the downstream edge of slabs in jointed PCC pavements. He postulated that when an axle drives off a slab, large rebound accelerations of the slab end can occur. These result in horizontal cracks which propagate along the reinforcing mesh. The ingress of loose particles into the crack faces may then allow large bending stresses to occur in the concrete surface when it is loaded subsequently, resulting in vertical cracks and spalling. Analysis of this damage mechanism would require a dynamic model of the slab.

COMPARISON OF VEHICLE EFFECTS ON ROAD DAMAGE

The conclusions of this chapter regarding the importance of various vehicle features on relative road damage are collected together in Figure A-6. The vertical axis indicates road damage relative to that caused by a "baseline" condition of tandem axles, dual tires, perfect static load sharing, and no dynamic wheel loads. Each dark bar in the chart represents the results published in one or more papers. The conclusions summarized in the chart are: (1) applying a tandem suspension load to a single axle can be expected to increase road damage by a factor of up to 25 (first bar of chart)[15]; (2) replacing dual tires with wide-base single tires is likely to increase road damage by a factor of 1.5 to 10 (second bar of chart); (3) unequal static load sharing between axles in a tandem suspension can increase the damage by a factor of up to 3 (third bar of chart).

The fourth bar summarizes the literature on the road-damaging effects of dynamic wheel loads. The *average* increase in damage caused by dynamic loads, compared to static loads alone is approximately 10%-40% ("mean damage" on the fourth bar of the chart, as calculated by the road stress factor). This is small compared with the effects of tire type and unequal static load sharing. If the assumption of uniformly distributed damage is correct, then discouraging the use of the popular wide-base single tires and improving static load sharing (both of which would be straightforward to enforce) may be much more effective than encouraging the use of particular suspension types.

---

[15] This is not a particularly realistic scenario, but is included for comparison purposes.
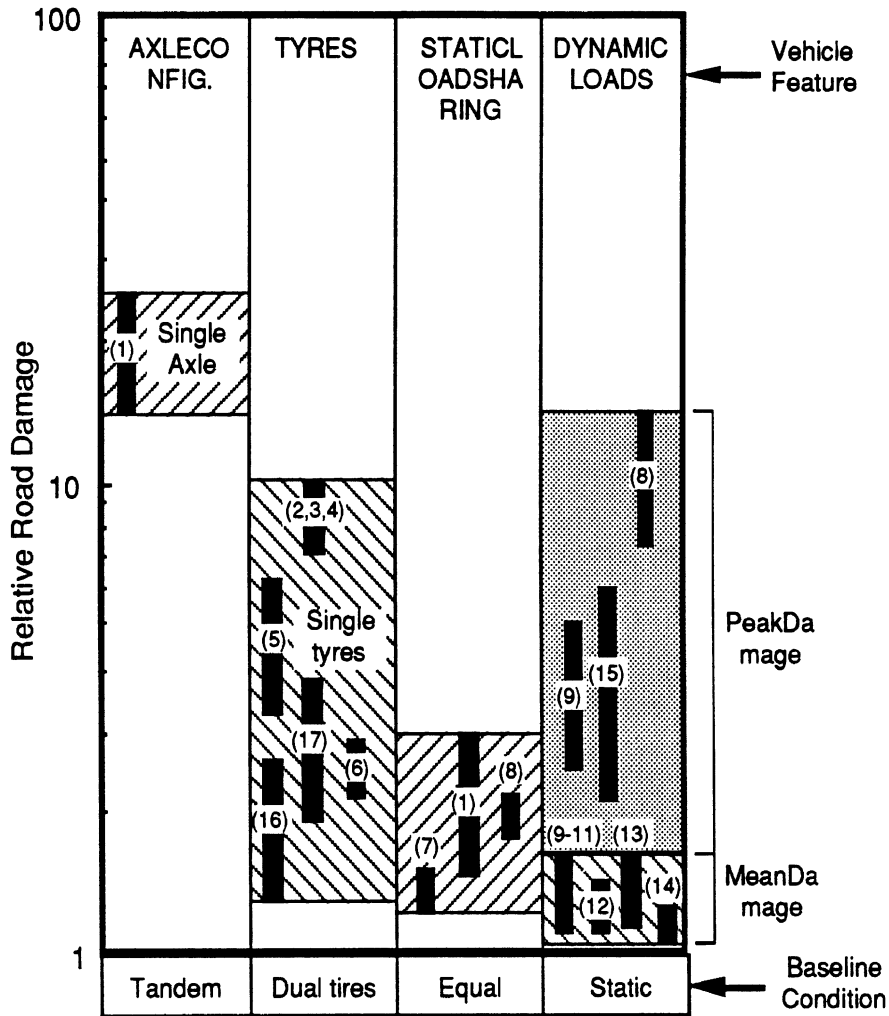
References:

1 Southgate and Deen, USA, (1983,1984), *(26,40)*
2 Zube and Forsyth, USA, (1965), *(19)*
3 Christison et al, Canada, (1978), *(18)*
4 Treybig, USA, (1983), *(13)*
5 Huhtala, Finland, (1988), *(22)*
6 OECD (1982), *(21)*
7 O'Connell et al, USA, (1986), *(25)*
8 Gordon, Australia, (1987), *(38)*
9 Sweatman, Australia (1983), *(35)*
10 Eisenmann, Germany, (1975), *(82)*
11 Gorge, Germany, (1984), *(75)*
12 Mitchell and Gyenes, UK (1989), *(73)*
13 Monismith et al, USA, (1988), *(16)*
14 Papagiannakis et al, Canada, (1989), *(79)*
15 Cebon, UK, (1985), *(89,90)*
16 Addis, UK, (1991), *(27)*
17 Kenis, USA, (1991), *(66)*

Figure A-6. Survey of literature on the effects of vehicle features on road damage.

A—25

Assuming a high degree of "spatial repeatability", the relative increase in *peak* road damage caused by dynamic loads is in the range 2-14 ("peak" damage in the fourth bar of the chart), which is comparable with the effects of tires and unequal static load sharing. It should be noted that the higher value of 14 is for walking-beam and pivoted-spring tandem suspensions (*38*).

These results show that dynamic wheel loads are only an important cause of road damage (compared to other effects such as tires and unequal load sharing) *if* the loads applied to the road surface by the heavy vehicle fleet are "spatially repeatable". It is most important to account for this behavior when analyzing or measuring the road-damaging potential of heavy vehicles.

CONCLUSIONS

1. Static analyses have shown that optimum tandem and triaxle group spacing exists. These minimize road damage for given static loading conditions.

2. The physics of uneven load sharing in some axle group suspensions is relatively well understood. Depending on the assumptions, theoretical road damage is increased by a factor of 1.2 to 3.0 for tandem suspensions with (typical) load sharing error of 20% (LSC = 0.8).

3. Variations in tire contact conditions, including the number and type of tires on an axle, contact area, pressure and pressure distribution mainly influence fatigue and rutting damage just below the surface of flexible pavements, particularly for thin, wearing courses. Subgrade rutting and fatigue damage in thicker pavements is largely governed by the total dynamic wheel load.

4. Various experimental and theoretical studies have indicated that single and wide-base single tires can be a factor of 1.5 to 10 times more damaging to roads than dual tires.

5. Viscous damping and soft spring and tire stiffness are desirable for minimizing dynamic loads, dry (Coulomb) friction is undesirable. Multiple-axle suspension systems generally rank in the following order of increasing dynamic loads:

   (Air-spring, torsion-bar) < (4-spring, 6-spring) < (walking-beam, single-point).

   This order depends to a certain extent on the particular suspension system and test conditions.

6. Analyses of dynamic wheel loads based on *mean* damage levels predict that dynamic wheel loads increase road damage by approximately 10%-40% for typical vehicles and operating conditions. Analyses based on *peak* damage and the hypothesis of "spatial repeatability" predict much higher damage at specific locations along the road, typically a factor of 2 to 4, but it may be as much as 14.

7. Theoretical road damage increases with road roughness and speed, but it may decrease at higher speeds due to decreasing dynamic response of the road structure.

8. According to some theoretical road damage analyses, suspension systems rank in approximately the same order as in (5) above.

REFERENCES

1. Kennedy, T.W., et al., "Distress and Related Material Properties for Premium Pavements." *Transportation Research Record*, No. 715 (1979) pp. 15-21.

2. Rauhut, J.B., et al., "Response and Distress Models for Pavement Studies." *Transportation Research Record*, No. 715 (1979) pp. 7-14.

3. Jackson, N.C., "Pavement Performance - A State DOT Perspective." *Society of Automotive Engineers Paper No. 881843* (1988) 11 p.

4. Peattie, K.R., *Developments in Highway Pavement Engineering*. Chapter 1. "Flexible Pavement Design." P. S. Pell ed., Applied Science Publishers Ltd, London. (1978).

5. American Association of State Highway and Transportation Officials, *The AASHO Road Test. Report 6, Special Studies* Highway Research Board, Washington D.C., 61E (1962).

6. American Association of State Highway and Transportation Officials, *The AASHO Road Test. Report 5, Pavement Research* Highway Research Board Report 61E (1962) 352 p.

7. Brown, S.F., *Developments in Highway Pavement Engineering.*" Chapter 2. Material Characteristics for Analytical Pavement Design." P. S. Pell ed., Applied Science Publishers Ltd, London (1978).

8. Francken, L., "Fatigue Performance of a Bituminous Road Mix Under Realistic Test Conditions." *Transportation Research Record*, No. 712 (1979) pp. 30-37.

9. Francken, L. and Verstraeten, J., "Methods for Predicting Moduli and Fatigue Laws of Bituminous Road Mixtures Under Repeated Bending." *Transportation Research Record*, No. 515 (1974) pp. 114-123.

10. Majidzadeh, K., et al., "Evaluation of Permanent Deformation in Asphalt Concrete Pavements." *Transportation Research Record*, No. 715 (1979) pp. 21-31.

11. Maupin, G.W., "Test for Predicting Fatigue Life of Bituminous Concrete." *Transportation Research Record*, No. 659 (1977) pp. 32-37.

12. Thrower, E.N., "A Parametric Study of a Fatigue Prediction Model for Bituminous Road Pavements." *Transport and Road Research Laboratory, Laboratory Report LR892* (1979) 19 p.

13. Treybig, H.J., "Equivalency Factor Development for Multiple Axle Configurations." *Transportation Research Record*, No. 949 (1983) pp. 32-44.

14. Lister, N.W., "The Transient and Long Term Performance of Pavements in Relation to Temperature." Third International Conference on the Structural Design of Asphalt Pavements, Ann Arbor, *Proceedings* (1972).

15. Ullidtz, P. and Larsen, B.K., "Mathematical Model for Predicting Pavement Performance." *Transportation Research Record,* No. 949 (1983) pp. 45-55.

16. Monismith, C.L., et al., "Modern Pavement Design Technology Including Dynamic Load Conditions." *Society of Automotive Engineers Paper No. 881845* (1988) pp. 33-52.

17. Thrower, E.N., et al., "Methods for Predicting Permanent Deformation - Flexible Pavements." *Transport and Road Research Laboratory, Contracts Report CR38* (1986) 36 p.

18. Christison, J.T., et al., "In Situ Measurements of Strains and Deflections in a Full-Depth Asphaltic Concrete Pavement." *Proc. Assoc. Asphalt Paving Technology,* Vol. 47 (1978) pp. 398-430.

19. Zube, E. and Forsyth, R., "An Investigation of the Destructive Effect of Floatation Tires on Flexible Pavement." *Highway Research Record,* No. N71 (1965) pp.129-150.

20. Addis, R.R. and Whitmarsh, R.A., "Relative Damaging Power of Wheel Loads in Mixed Traffic." *Transport and Road Research Laboratory, Laboratory Report LR 979* (1981).

21. *Impacts of Heavy Freight Vehicles.* OECD, Paris (1982).

22. Huhtala, M., "Field Tests to Compare Tires." FHWA Load Equivalence Workshop, McLean VA. *Proceedings* (1988) 12 p.

23. Abbo, E., et al., "Analysis of Moving Dynamic Loads on Rigid Pavements." ARRB/FORS Symposium on Heavy Vehicle Suspension Characteristics, Canberra, Austrailia. *Truck Designers Sprung?* (1987) pp. 51-70.

24. Majidzadeh, K. and Ilves, G.J., "Methods for Determining Primary Response Load Equivalency Factors." FHWA Load Equivalence Workshop, McLean VA. *Proceedings* (1988) 20 p.

25. O'Connell, S., et al., "Analyses of Moving Dynamic Loads on Highway Pavements, Part I: Vehicle Response." International Symposium on Heavy Vehicle Weights and Dimensions, Kelowna, British Columbia. *Proceedings* (1986) pp. 363-380.

26. Southgate, H.F. and Deen, R.C., "Variations of Fatigue Due to Unevenly Loaded Axles Within Tridem Groups." *University of Kentucky, Research Report UKTRP-84-11* (1984) 22 p.

27. Addis, R.R., "The Effect of Wheel Loads on Road Pavements." *IMechE Conference on Road Wear: The Interaction Between Vehicle Suspensions and the Road*, London (1991).

28. *Heavy Trucks, Climate and Pavement Damage*. OECD Road Transport Research, Paris (1988) 175 p.

29. Christison, J.T., "Pavements Response to Heavy Vehicle Test Program: Part 2 - Load Equivalency Factors." *Vehicle Weights and Dimensions Study, Vol. 9. Canroad Transportation Research Corporation* (1986) 79 p.

30. Huhtala, M., "The Effect of Different Trucks on Road Pavements." International Symposium on Heavy Vehicle Weights and Dimensions, Kelowna, British Columbia. *Proceedings* (1986) pp 151-159.

31. Tayabji, S.D., et al., "Effect of Frozen Support and Tridem Axles on Concrete Pavement Performance." *Transportation Research Record*, No. 954 (1984) pp. 38-51.

32. Morris, J.R., "Effects of Heavy Vehicle Characteristics on Pavement Response - Phase 1." Transportation Research Board, Prepared for NCHRP Project 1-25 (1987).

33. Schacke, I. and Barenholdt, E., "Heavy Vehicles - Some European Observations." International Symposium on Heavy Vehicle Weights and Dimensions, Kelowna, British Columbia. *Proceedings* (1986) pp 11-16.

34. Mitchell, C.G.B., "The Effect of the Design of Goods Vehicle Suspensions on Loads on Roads and Bridges." *Transport and Road Research Laboratory, Research Report 115* (1987) 15 p.

35. Sweatman, P.F., "A Study of Dynamic Wheel Forces in Axle Group Suspensions of Heavy Vehicles." *Australian Road Research Board Special Report 27* (1983) 65 p.

36. Woodrooffe, J.H.F., et al., "Effects of Suspension Variations on the Dynamic Wheel Loads of a Heavy Articulated Highway Vehicle." *Vehicle Weights and Dimensions Study, Vol. 11. Canroad Transportation Research Corporation* (1986).

37. Simmons, I.C.P. and Mitchell, C.G.B., "The Equalisation of Truck Bogie Axle Weights." Second International Symposium on Heavy Vehicle Weights and Dimensions, Kelowna, Canada. *Proceedings* (1989).

38. Gordon, R.G., "Influence of Vehicle Suspensions on Pavement Costs and Performance." ARRB/FORS Symposium on Heavy Vehicle Suspension Characteristics, Canberra, Australia. *Truck Designers Sprung?* (1987) pp 391-405.

39. Southgate, H.F. and Deen, R.C., "Effect of Load Distributions and Axle and Tire Configurations on Pavement Fatigue." *University of Kentucky Research Report UKTRP-85-13* (1985) 37 p.

40. Southgate, H.F., et al., "Strain Energy Analysis of Pavement Designs for Heavy Trucks." *Transportation Research Record,* No. 949 (1983) pp. 14-20.

41. Chan, G.P., et al., "Laboratory Measured Tire-Pavement Contact Pressures." FHWA Load Equivalence Workshop, McLean VA. *Proceedings* (1988) 35 p.

42. Yap, P., "A Comparative Study of the Effects of Truck Tire Types on Road Contact Pressures." *Society of Automotive Engineers Paper No. 881847* (1988) pp. 53-59.

43. Roberts, F.L., "Overview: Tire Types Pressures and Models to Evaluate Pressure Effects." FHWA Load Equivalence Workshop, McLean VA. *Proceedings* (1988) 38 p.

44. Haas, R.C.G. and Papagiannakis, A.T., "Understanding Pavement Rutting." Special Workshop on Rutting in Asphalt Pavements, Toronto, Roads and Transport Association of Canada. *Proceedings* (1986) 30 p.

45. Roberts, F.L., et al., "Effects of Tire Pressures on Flexible Pavements." *Texas Transportation Institute Research Report 372-IF* (1986) 245 p.

46. Brademeyer, B.D., et al., "Analysis of Moving Dynamic Loads on Highway Pavements. Part II: Pavement Response." International Symposium on Heavy Vehicle Weights and Dimensions, Kelowna, British Columbia. *Proceedings* (1986) pp. 381-393.

47. Brown, S.F., et al., "The Structural Design of Asphalt Pavements by Computer." *Journal of the Institution of Highway Engineers* (1980) 8 p.

48. Kenis, W.J., et al., "Verification and Application of the VESYS Structural Subsystem." Fifth International Conference on the Structural Design of Asphalt Pavements, *Proceedings* (1982) pp. 333-345.

49. Lai, S., "Probabilities Solution for Viscoelastic Layered Systems." *Int. Conf. on Statistics and Probability in Soil and Structural Engineering,* Vol. 1 (1979) pp. 390-401.

50. Magnusson, G., et al., "The Influence of Heavy Vehicles' Springing Characteristics and Tyre Equipment on the Deterioration of the Road." *VTI Report 270* Translated by TRRL as WP/V&ED/86/16, 1986 (1984).

51. Marshek, K.M., et al., "Experimental Investigation of Truck Tire Inflation Pressure on Pavement-Tire Contact Area and Pressure Distribution." *University of Texas Center for Transportation Research Research Report 386-1* (1985) 62 p.

52. Seitz, N. and Hussmann, A.W., "Forces and Displacement in Contact Area of Free Rolling Tires." *Society of Automotive Engineers Paper No. 710626* (1971) 7 p.

53. Tielking, J.T., "Finite Element Tire Model." FHWA Load Equivalence Workshop, McLean VA. *Proceedings* (1988) 10 p.

54. Eisenmann, J., et al., "Effects of Commercial Vehicle Design on Road Stress - Research Results Relating to the Roads." *Strasse und Autobahn*, Vol. 37, No. 6. Translated by TRRL as WP/V&ED/87/29 (1987) pp. 238-244.

55. Roberts, F.L., "Flexible Pavement Strains Caused by Auto Tyres." *American Society of Civil Engineers Journal of Transportation Engineering*, Vol. 113, No. 5 (1987).

56. Marshek, K.M., et al., "Effect of Truck Tire Inflation Pressure and Axle Load on Flexible and Rigid Pavement Performance." *Transportation Research Record*, No. 1070 (1986) pp. 14-21.

57. Kinder, D.F. and Lay, M.G., "Review of the Fourth Power Law." *Austrailian Road Research Board Internal Report AIR000-248* (1988).

58. Eisenmann, J. and Hilmer, A., "Influence of Wheel Load and Inflation Pressure on the Rutting Effect at Asphalt–Pavements – Experiments and Theoretical Investigations." Sixth International Conference on the Structural Design of Asphalt Pavements, Ann Arbor. *Proceedings* (1987) pp.392-403.

59. Van de Loo, P.J., "The Creep Test: A Key Tool in Asphalt Mix Design and the Prediction of Pavement Rutting." *Proc. Assoc. Asphalt Paving Technology*, Vol. 47 (1978) pp. 522–554.

60. Goacolou, H., "Calculation of the Rutting of Structures – Castor Program: Method for Prediction of Permanent Deformations in Asphaltic Structures." Sixth International Conference on the Structural Design of Asphalt Pavements, Ann Arbor. *Proceedings* (1987) pp. 191-199.

61. Thrower, E.N., "Permanent Deformation - A Linear Viscoelastic Model of a Road Pavement." *Transport and Road Research Laboratory, Supplementary Report SR184UC* (1975) 16 p.

62. Cebon, D., "Vehicle-Generated Road Damage: A Review." *Vehicle System Dynamics*, Vol. 18, No. 1-3 (1989) pp. 107-150.

63. Cole, D.J., "Measurement and Analysis of Dynamic Tyre Forces Generated by Lorries." PhD dissertation, Cambridge University, Engineering Department (1990).

64. Cole, D.J. and Cebon, D., "Assessing the Road–Damaging Potential of Heavy Vehicles." *IMechE Conference on Road Wear: The Interaction Between Vehicle Suspensions and the Road*, London (1991).

65. Hahn, W.D., "Effects of Commercial Vehicle Design on Road Stress - Vehicle Research Results." Institut fur Kruftfahrwesen, Universitat Hannover. Translated by TRRL as WP/V&ED/87/38 (1985).

66. Kenis, W.J. *Personal Communication.*

67. Aurell, J., "The Influence of Different Suspension Parameters on Dynamic Wheel Loads." *IMechE Conference on Road Wear: The Interaction Between Vehicle Suspensions and the Road*, London (1991).

68. Heath, A.N., "Heavy Vehicle Design Affecting Road Loading." ARRB/FORS Symposium on Heavy Vehicle Suspension Characteristics, Canberra, Australia. *Truck Designers Sprung?* (1987) pp 251-270.

69. Whittemore, A.P., et al., "Dynamic Pavement Loads of Heavy Highway Vehicles." *National Cooperative Highway Research Project Report 105* (1970) 94 p.

70. Ervin, R.D., et al., "Influence of Truck Size and Weight Variables on the Stability and Control Properties of Heavy Trucks. Volume II." *University of Michigan Transportation Research Institute UMTRI-83-10/2, Federal Highway Administration FHWA-RD-83-030* (1983) 179 p.

71. Leonard, D.R., et al., "Loads and vibrations caused by eight commercial vehicles with gross weights exceeding 32 tons." *Transport and Road Research Laboratory, Laboratory Report 582* (1974).

72. Addis, R.R., et al., "Dynamic Loading of Road Pavements by Heavy Goods Vehicles." Congress on Engineering Design, Seminar 4A-03, Institution of Mechanical Engineers, Birmingham. *Proceedings* (1986) 26 p.

73. Mitchell, C.G.B. and Gyenes, L., "Dynamic Pavement Loads Measured for a Variety of Truck Suspensions." Second International Symposium on Heavy Vehicle Weights and Dimensions, Kelowna, Canada. *Proceedings* (1989).

74. Sweatman, P.F., "Effect of Heavy Vehicle Suspensions on Dynamic Road Loading." *Australian Road Research Board Research Report ARR 116* (1980) 15 p.

75. Gorge, W., "Evaluation of Research Reports Concerning the Influence of Commercial Vehicle Development and Design on the Road Fatigue." English translation by the International Transport Union, Geneva (1984).

76. Hahn, W.D., "Effects of Commercial Vehicle Design on Road Stress - Quantifying the Dynamic Wheel Loads for Stage 3: Single Axles, Stage 4: Twin Axles, Stage 5: Triple Axles, as a Function of the Springing and Shock Absorption System of the Vehicle." *Institut fur Kruftfahrwesen, Universitat Hannover Report No. 453.* Translated by TRRL as WP/V&ED/87/40 (1987).

77. Woodrooffe, J.H.F. and Le Blanc, P.A., "Heavy Vehicle Suspension Variations Affecting Road Life." ARRB/FORS Symposium on Heavy Vehicle Suspension Characteristics, Canberra, Austrailia. *Truck Designers Sprung?* (1987) pp. 71-97.

78. Dickerson, R.S. and Mace, D.G.W., "Dynamic Pavement Force Measurements with a Two-Axle Heavy Goods Vehicle." *Transport and Road Research Laboratory, Supplimentary Report SR688* (1981) 14 p.

79. Papagiannakis, A.T., et al., "Impact of Roughness-Induced Dynamic Load on Flexible Pavement Performance." First International Symposium on Surface Characteristics, Penn. State University. *Proceedings.* American Society of Testing and Materials (1988).

80. Woodrooffe, J.H.F., et al., "Suspension Dynamics - Experimental Findings and Regulatory Implications." *Society of Automotive Engineers Paper No. 881847* (1988) pp. 69-77.

81. Eisenmann, J., "Dynamic Wheel Load Fluctuations - Road Stress." *Strasse und Autobahn,* Vol. 4 (1975) pp. 127-128.

82. Eisenmann, J., "Beuteilung der Strassenbeanspuchung." *Strasse und Autobahn,* Vol. 3 (1978).

83. Walloschek, H.J., "Road Loading as a Function of Vehicle Characteristics." ARRB/FORS Symposium on Heavy Vehicle Suspension Characteristics, Canberra, Austrailia. *Truck Designers Sprung?* (1987) pp. 119-142.

84. Baum, "Comments on Increasing Total Weights of Commercial Vehicles from the Point of View of Road Stress." *Road and Traffic Research Institute Report 99,* Road Stress Working Committee, Cologne Translated by TRRL as WP/V&ED/87/27 (1983).

85. Von Becker, P., "Commercial Vehicle Design - Road Stress: Effect on Transport Policy Decisions." *Strasse und Autobahn,* Vol. 12 Translated by TRRL as WP/V&ED/87/28 (1985) pp. 493-498.

86. Berry, J., *Proposal for a Council Directive, COM(90) 486.* Commission of the European Communities, Brussels (1990) 28 p.

87. Hardy, M.S.A. and Cebon, D., "On the Response of Continuous Pavements to moving Dynamic Loads: Part 1 Theory and Experimental Validation." Submitted to ASCE Journal of Engineering Mechanics (1991).

88. Hardy, M.S.A. and Cebon, D., "On the Response of Continuous Pavements to Moving Dynamic Loads: Part 2 Influence of Vehicle Loading Parameters." Submitted to ASCE Journal of Engineering Mechanics (1991).

89. Cebon, D., "Examination of the Road Damage Caused by Three Articulated Vehicles." 10th IAVSD Symposium on the Dynamics of Vehicles on Roads and on Tracks, *Proceedings.* Prague, Swets and Zeitlinger (1987) pp. 65-76.

90. Cebon, D., "Theoretical Road Damage Due to Dynamic Tyre Forces of Heavy Vehicles. Part 2: Simulated Damage Caused by a Tandem-Axle Vehicle." *Proc. I.Mech.E.,* Vol. 202, No. C2 (1988) pp. 109-117.

91. Markow, M.J., et al., "Analyzing the Interactions Between Dynamic Vehicle Loads and Highway Pavements." *Transportation Research Record,* No. 1196 (1988) pp. 161-169.

92. Savage, R.J., "Dynamic Failure of Joints in Reinforced Concrete Pavements." *Concrete* (1985).

APPENDIX B
RIGID PAVEMENT MODELING

This appendix describes the analytical methods used to include the response behavior of rigid pavements in the study of vehicle/road interactions. An existing computer model called ILLI-SLAB is used to obtain stresses and strains throughout the pavement structure in response to applied loads, such as those arising from vehicle tires.

The appendix begins with a background section that introduces the general methods used to compute the response of a rigid pavement to applied loads. The next section describes the ILLI-SLAB model that was used for this project. The description includes extensions made to support the large-scale simulation activities that were undertaken. Results from a validation activity are presented, in which experimental pavement responses were compared to simulated results. Analytical models used to compute pavement damage are described. The appendix concludes with a section Rigid Pavement Matrix, that presents the full matrix of pavements that were studied, with some discussion of the rationale for selecting pavement designs and parameter values.

To facilitate analysis of the large number of pavement and vehicle combinations of interest in this study additional analysis methods were developed to characterize the response to multiple, time-varying loads from a moving vehicle in a way that is computationally efficient. These methods are described in Appendix F.

BACKGROUND

In the past, rigid pavements have been designed using the Westergaard theory (1). Westergaard developed closed-form analytical equations for stresses in rigid pavement slabs. He developed equations for three loading cases, namely; edge, corner, and center slab. Since the original work done by Westergaard, researchers have improved the methods used for stress calculation. For example, Pickett and Ray developed influence charts which graphically represent the Westergaard equations (2). There are certain problems and limitations with this theory, such as (1) it does not consider load transfer between joints or cracks, (2) only corner, edge, and center slab stresses can be calculated, (3) infinite slab length is not possible.

Finite element analysis has opened a new avenue to rigid pavement analysis. It allows the pavement to be divided into a set of discrete parts and calculates stresses, strains, and deflections at nodal points between these elements. Several pavement analysis programs have been written that apply the method to pavement structures. One of these, called ILLI-SLAB, was used to compute pavement responses in this research. It was chosen for this work because it is suitable for the work, widely used, readily available, well maintained, and frequently updated. Other rigid pavement computer programs that are also in use, and which might be used for the same purpose, are summarized below.

J-SLAB is a finite element program that was developed by the Portland Cement Association for the Federal Highway Administration (*3*). It has capabilities similar to those of ILLI-SLAB except that only a Winkler foundation can be used to model its subgrade support conditions. J-SLAB is also restricted in that it only allows two layers to be modeled as fully bonded. (ILLI-SLAB offers several subgrade models and unbonded layers.)

WESLAYER and WESLIQUID (*4*) are finite element programs developed by the U.S. Army Corps of Engineers Waterways Experiment Station for analysis of rigid pavements. WESLYER uses solid subgrade formulation and WESLIQUID uses Winkler formulation for subgrade support conditions. WESLYER can model up to five subgrade layers. These programs have capabilities similar to ILLI-SLAB in all other respects. ILLI-SLAB is more widely used, however, and appears to be more actively supported by its developer.

PMARP is also a finite element program based on modification of the ILLI-SLAB program. It has an added fatigue damage model. The program is similar to ILLI-SLAB, but some parts may be technically incorrect (*5*).

THE ILLI-SLAB PAVEMENT MODEL

ILLI-SLAB was developed at the University of Illinois in the late 1970s for structural analysis of jointed, one-layer concrete pavements with load transfer systems at the joints (*6,7*). The ILLI-SLAB model is based on classical theory of a medium-thick plate on a Winkler foundation. The program can calculate the structural response of a concrete pavement system with joints and cracks.

The program is capable of representing one or two uniform layers bonded or unbonded above the subgrade. Load transfer mechanisms can be modeled as dowel joints or aggregate interlock or a combination of both between adjacent slabs. However, all adjacent slabs must be modeled with the same level of load transfer. Tire loads can be represented as up to 100 rectangular areas under uniform pressure. The program has the capability to deal with temperature gradients and gap underneath the slab. A variety of subgrade models are available such as Winkler foundation, Vlasov, Boussinesq, and other formulations. The program can use symmetry lines in the longitudinal or transverse directions or both. Uniform or varying slab thickness and elastic modulus for the slab and subbase can be specified.

ILLI-SLAB was modified to generate influence functions, used in this research program to combine pavement response with dynamic truck loading, as described in Appendix F and Reference (*8*).

VALIDATION

Field tests were conducted at Carlyle, Illinois to validate the ILLI-SLAB pavement model. The PACCAR Technical Center prepared a loaded three-axle truck with instrumentation to measure dynamic axle loads (strain gaged axles and axle accelerometers) and body accelerometers. The truck was taken to three rigid pavement test sites built by the State of Illinois on route US 50. The University of Illinois provided instrumentation for measuring and recording pavement strains. The combined instrumentation systems were configured to record dynamic loads on each of the truck axles simultaneously with the pavement strains, using a common marker signal to synchronize the records. Static tests were performed on all three pavement sites. Dynamic tests over the speed range of 0 to 55 mi/h were conducted on two sites, accumulating a total of 39 test runs. Measured responses obtained by PACCAR and the University of Illinois were provided to UMTRI for processing. Plots were made of all test results and assembled into an informal document entitled "Model Validation Studies: Raw Pavement Response Data," distributed to the principals involved.

Test Pavement and Instrumentation

The rigid pavement test site is located on US 50 between Carlyle and Lebanon in southern Illinois. Experiments were performed on 40-ft test sections which have thicknesses of 9.5 and 7.5 inches. The instrumented sections contain a number of imbedded strain gauges and thermocouples, located near the top and bottom surfaces of the PCC slab and laid out as shown in Figure B-1. The outputs of eight strain gauges were recorded for each vehicle pass. The thermocouple outputs were logged immediately prior to each test.

In order to ensure accurate amplitude and frequency resolution of the dynamic pavement response data, the strain gauge amplifier outputs were low-pass filtered at
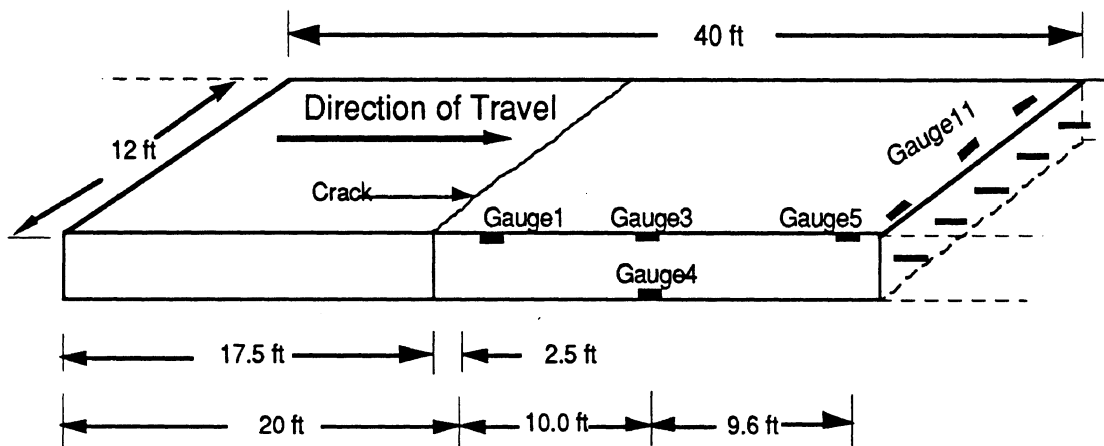
Figure B-1. Layout of strain gauges.

approximately 100 Hz and subsequently sampled at frequencies in the range of 200 to 400 Hz using the University of Illinois data acquisition system. Copies of the pavement response data, obtained by Illinois, were provided to UMTRI. The data files were converted to a standardized format for engineering data used at UMTRI, so that data is well documented and can be automatically processed by existing data analysis and plotting programs. (Files in this format are called "ERD files.)

Test Vehicle and Instrumentation

The test vehicle used in the tests was a three axle Peterbilt model 359 tractor with a 220 inch wheelbase and four-spring tandem drive axle suspension. It was provided and instrumented by The PACCAR Corporation. The vehicle was chosen to be representative of a major class of US vehicles. For the purpose of the rigid pavement validation study, the tractor was operated without an attached semi-trailer, but was equipped with a loading frame and weights on the fifth wheel to provide the correct static axle load distribution. All of the axles were instrumented for the measurement of dynamic wheel loads. Instrumentation arrangements are shown in Figure B-2.

The simplest method for measuring dynamic wheel forces is to strain-gauge the axle housing between the spring mounting and brake back-plate to measure bending moments due to vertical wheel loads (9-15). Assuming that lateral movement of the tire contact center of pressure is small compared with the distance between the static center of pressure and the strain gauge installation, the bending strain is proportional to the shear force carried by the axle. It is necessary to correct the measured shear force for the inertia (linear and angular) of all wheel and axle components "outboard" of the load cells (axle housing, brakes, wheel and tire) (9,12). Mitchell and Gyenes (12) claimed a probable measurement accuracy of 3.5% with their similar system of wheel load measurement. All three axles of the test vehicle were instrumented this way to measure the wheel loads generated by five of the six wheels (four wheels of the tandem drive axle group and one steering tire).

The vehicle was equipped with a 14 channel FM tape recorder. One channel was used for tape speed regulation, one was used for voice, and the remaining 12 channels were available for logging test data. Measurement of the dynamic wheel loads required 11 channels of instrumentation: 5 for strain gauge bridges and 6 for accelerometers. The remaining data channel was used to record the longitudinal position of the vehicle relative to the test section, to synchronize the pavement-based and vehicle-based instrumentation systems.

Longitudinal position was detected with an infrared transceiver carried by the vehicle. The transceiver detected strips marked on the pavement at the beginning, middle and end of the test section. A pulse was therefore recorded on the vehicle-based tape recorder when the vehicle passed each of these locations. A telemetry link between the vehicle and roadside instrumentation systems enabled identical pulses to be recorded by the roadside data logger to synchronize the two recording systems. Calibration of the axle strain gauges was
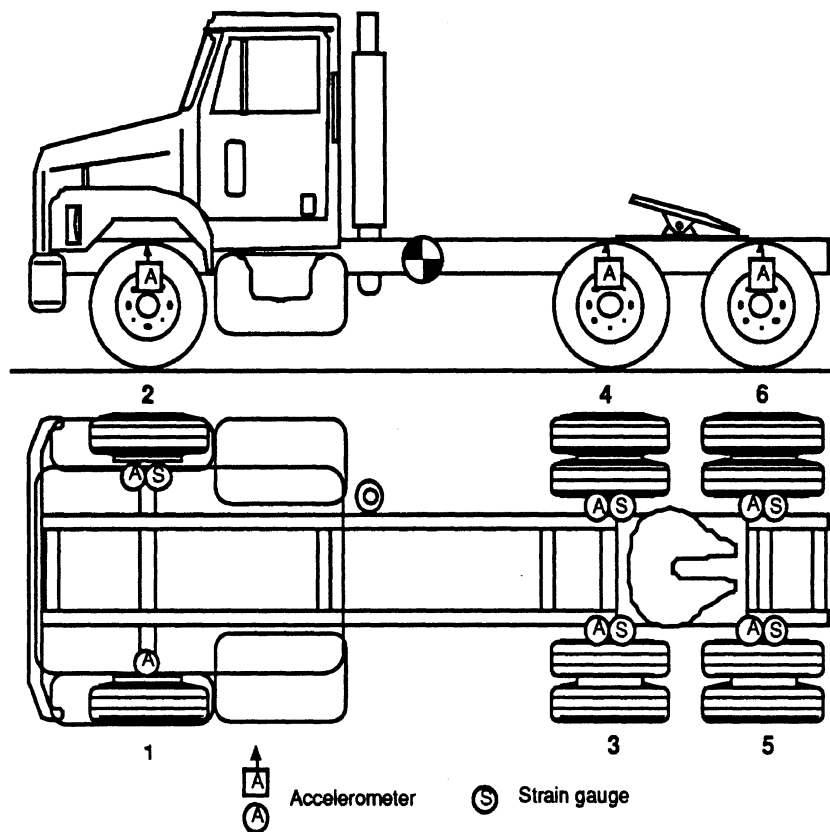
Figure B-2. Instrumentation on the truck.

performed quasi-statically on the PACCAR road simulator. The vehicle was placed on the simulator with the body fixed to ground and hydraulic actuators were used to vary the axle loads slowly for each axle in turn. At the completion of the tests PACCAR engineers reduced the truck data and converted the results into the standardized ERD files, which they provided to UMTRI.

Rigid Pavement Model Validation

The ILLI-SLAB rigid pavement response program was used to determine theoretical influence functions for the primary response variables of interest at the points corresponding to the strain gauge locations on the test pavements. These functions were subsequently combined with the measured wheel force time histories to generate simulated primary response time histories at the measurement points. The method of calculating the influence functions and pavement response time histories is described in Appendix F. These simulated responses were compared with measured pavement strain responses. Figure B-3 compares simulated and measured strains for a strain gauge in the interior of the test pavement slab. As evidenced by this graph, very good agreement is possible, particularly in prediction of the shape and magnitudes of the tensile strains. The main disparities in Figure B-3 occur in prediction of the compressive strains, but because they are generally of low level and are not damaging to the slab, the agreement here is less critical.
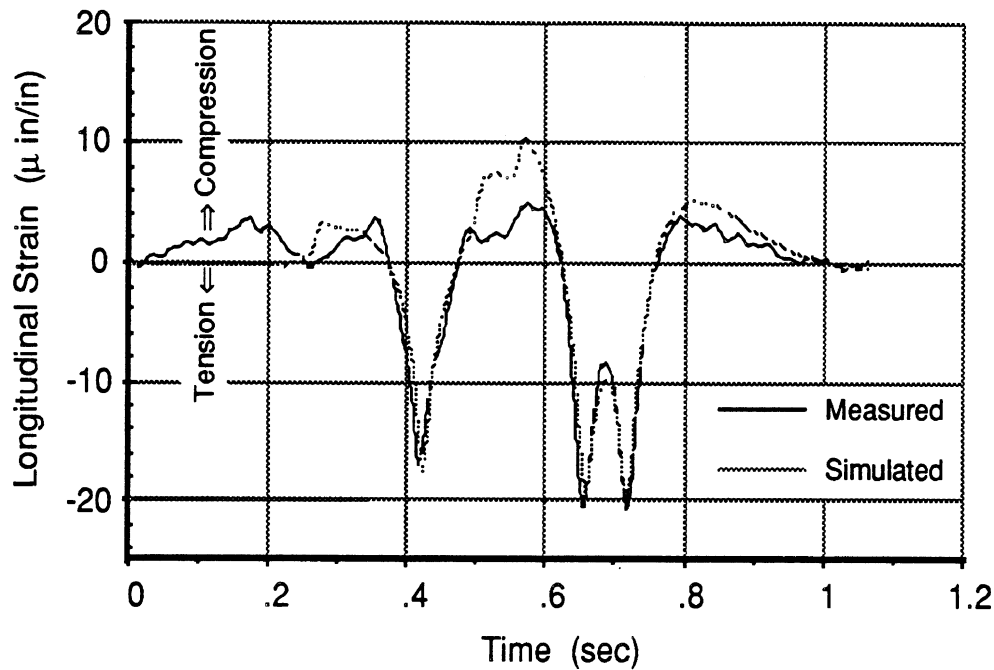
Figure B-3. Comparison of measured and calculated responses at gauge 4 (see Figure B-1), 50 mph.

PAVEMENT DAMAGE CALCULATION

The only form of rigid-pavement damage that was considered in this study is the fatigue damage that accrues from repeated vehicle loads. Several methods of calculating fatigue damage to rigid pavements are available in the literature. Some of these fatigue laws will be described here, including the Vesic fatigue model that was chosen for damage analysis in this study. In general, the fatigue laws relate the number of cycles of loading (N) needed to cause failure to the a ratio of stress (σ) to the modulus of rupture of concrete (MR).

The fatigue of concrete has been studied by many researchers with both experimental and theoretical treatments (*16-24*). Most laboratory studies involve testing in pure compression or pure tension only. A few studies (*25-28*) have examined the effects of stress reversal. Many of the fatigue laws derived from real-world experience, such as the AASHO Road Test (*29*), are implicitly based on reversing stress loadings. Several of these fatigue laws are discussed below and compared graphically in Figures B-4 and B-5.

PCA Fatigue Model

The Portland Cement Association (PCA) is a major source of data appropriate for design of structures using Portland Cement Concrete (PCC). In 1966 the Association developed a fatigue model (*30*) for PCC which exhibits an endurance limit of 0.5.
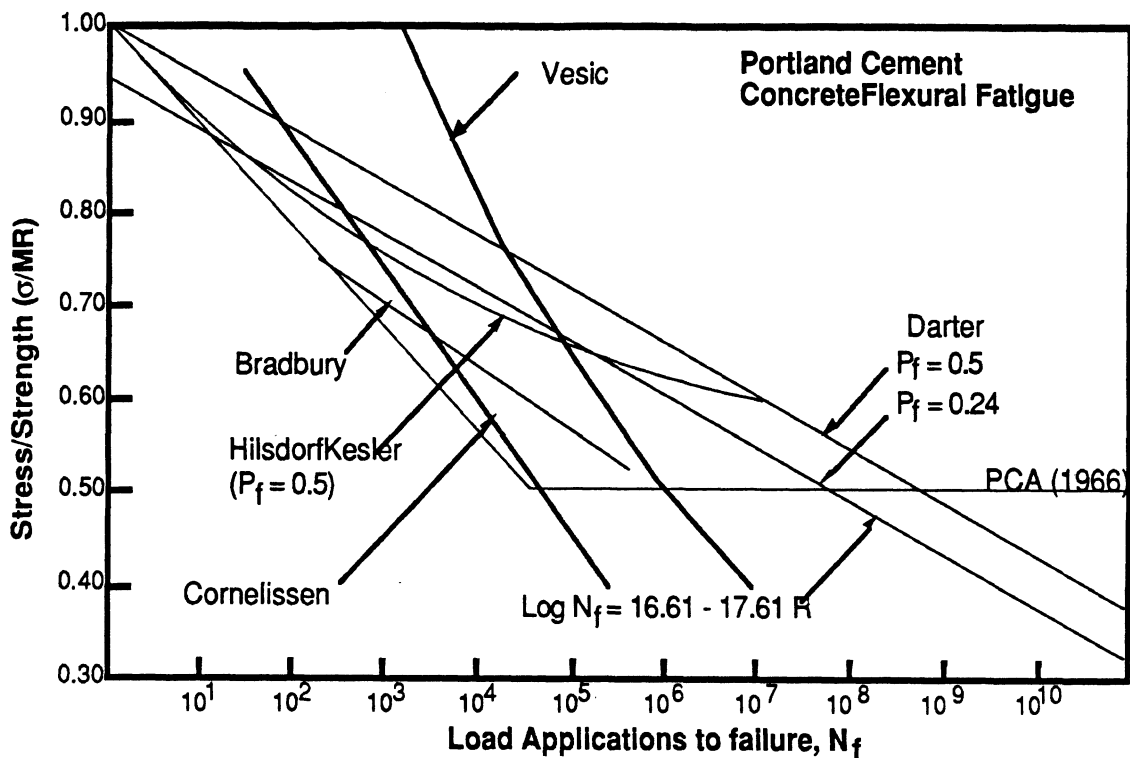
Figure B-4. Fatigue relations derived by different authors.

Consequently, the 1966 PCA curve, shown in Figure B-4, projects infinite life for concrete if the stress/strength ratio is less than 0.5. The mathematical relationship for the 1966 model is:

$$\text{Log N} = 11.78 - 12.11\,\frac{\sigma}{MR} \qquad \text{for } \frac{\sigma}{MR} > 0.5 \qquad \text{(B-1)}$$

$$\text{Log N} = \infty \qquad \text{for } \frac{\sigma}{MR} < 0.5 \qquad \text{(B-2)}$$

Other PCC fatigue models are not consistent with the PCA model in that they do not conclude that PCC has an endurance limit (21,23). PCA corrected this anomaly in 1973 by extending the curve defined by Eq. B-1 and removing the endurance limit (31).

Darter Fatigue Model

Darter (18) developed a fatigue model for use in a design procedure for zero maintenance plain-jointed concrete pavements. Fatigue data was obtained from three studies (16,32,33) and an S-N curve of 140 tests was plotted from these studies. The following fatigue equation resulted from a least square regression of the data:

$$\text{Log N} = 17.61 - 17.61\,\frac{\sigma}{MR} \qquad \text{(B-3)}$$

This equation represents a confidence interval of 50%. A more conservative probability of failure limit, 24%, was selected for development of the zero-maintenance design procedure for plain jointed concrete pavements. This limit is given as:

$$\text{Log N} = 16.61 - 17.61 \frac{\sigma}{\text{MR}} \tag{B-4}$$

Eq. B-4 is shown graphically in Figure B-4.

The Cornelissen Model

Cornelissen (25-27) conducted an experimental study in order to find the fatigue strength of plain concrete in uniaxial tension and in cyclic tension-compression loading. Special testing equipment was designed to overcome normal problems associated with tension-compression testing. Details of the test can be found in (27). Cornelisson (25) conducted 189 repeated tension tests. Multiple linear regression analysis produced the following equation for uniaxial tension:

$$\text{Log N} = 14.81 - 15.52 \frac{\sigma_{max}}{f_t} + 2.79 \frac{\sigma_{min}}{f_t} \tag{B-5}$$

After analyzing the results of 144 compression-tension tests, he derived the equation:

$$\text{Log N} = 9.36 - 7.93 \frac{\sigma_{max}}{f_t} - 2.59 \frac{\sigma_{min}}{f_c} \tag{B-6}$$

where f_c corresponds to the compressive strength of concrete and f_t corresponds to the tensile strength of concrete (effectively the modulus of rupture).

The corresponding S/N curves are shown in Figure B-5 for repeated tension and compression-tension tests. He concluded that stress reversal causes more damage than tests with zero minimum stress. The Cornelissen model treats the case in which pavement stress returns to zero from a tensile peak inconsistently. If a cycle size occurs in which σ_{max} has a positive value and σ_{min} approaches zero from the compressive side (Eq. B-6), the Cornelissen model will treat it as much more damaging than a case in which σ_{min} approaches zero from the tensile side (Eq. B-5). Given that the stress between the axles of a tandem set exhibit this pattern, the Cornelissen model is not appropriate for the evaluation of fatigue due to longitudinal pavement stress.

ARE Fatigue Model

Austin Research Engineers (ARE) analyzed data from the AASHO Road Tests and developed a fatigue model (34) in the form of a power law. In the analysis actual load applications were converted into 18-kip single axle loads (ESALs) employing equivalency factors for a terminal serviceability index of 2.5, and maximum mid-slab stresses were calculated using elastic layer theory. A fatigue equation based on regression of the data was obtained as follows:
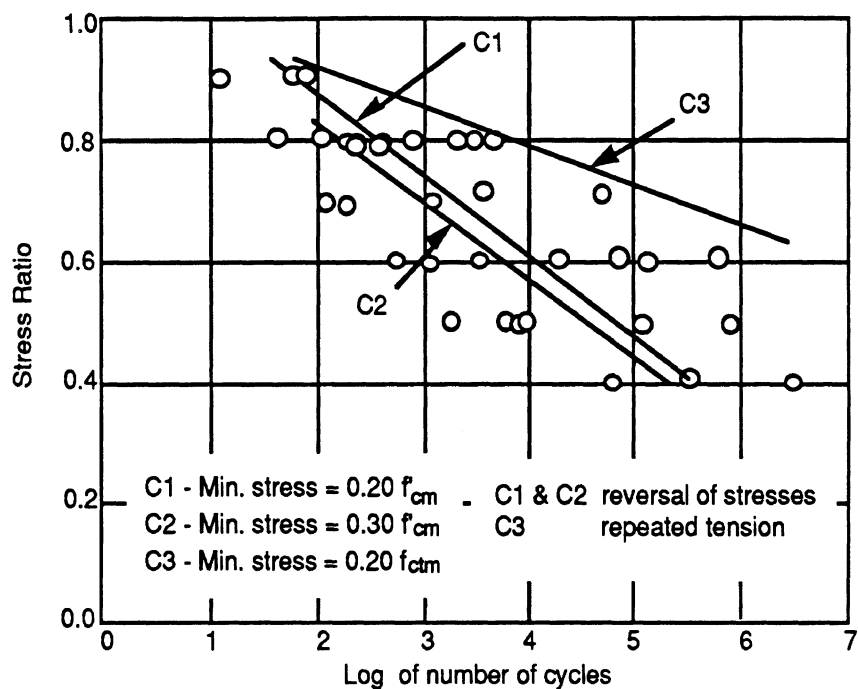
Figure B-5. Cornelissen's fatigue curves for reversal of stresses and repeated tension only.

$$\text{Log } N = \text{Log}(23440) - 3.21 \text{ Log} \frac{\sigma}{MR} \qquad \text{(B-7)}$$

Inasmuch as the actual load cycles on which the analysis is based were truck loadings, this fatigue law is implicitly based on cyclic loading and stress reversals.

RISC Distress Model

The RISC distress model is a power law developed by Ilves and Majidzadeh (35) through analysis of the AASHO Road Test data. They calculated stresses using plate theory, where the plate is supported on a multi-layered elastic solid subgrade, and obtained the following relationship:

$$\text{Log } N = \text{Log}(22209) - 4.29 \text{ Log} \frac{\sigma}{MR} \qquad \text{(B-8)}$$

The number of passes to failure, N, represents the number of 18-kip ESALs which will produce terminal serviceability of 2.0.

Vesic Distress Model

The Vesic distress model (36) is a fatigue law in the form of a power law. Vesic used Westergaard plate theory (1) to calculate stresses in the wheel path in conjunction with analysis of the AASHO Road Test data. The relationship found was as follows:

B—9

$$\text{Log } N = \text{Log}(22500) - 4 \text{ Log } \frac{\sigma}{MR} \qquad \text{(B-9)}$$

σ represents the maximum combined tensile stress caused by loads placed on the assumed wheel path position. For AASHO slabs the modulus of rupture was taken as 790 psi. According to Vesic, pavement life varies as the fourth power of the concrete strength. This relationship operates similarly to the RISC distress model and the ARE fatigue model, described above.

Comparison of Fatigue Equations

The fatigue models described above are shown in Figures B-4 and B-5, where σ is maximum stress and MR is modulus of rupture of concrete. The Darter and PCA models are based on fatigue research studies which do not allow for reversal of stresses. The ARE, Vesic, and RISC methods of calculating critical stresses are all similar in that they all relate fatigue life usage to strength ratio raised to a power near 4 (which is consistent with the fourth power law). They each have distinct terminal serviceability limits but yield approximately the same relative pavement damaging potential for truck and pavement design characteristics. Findings presented in this report are based on the Vesic fatigue model.

RIGID PAVEMENT MATRIX

Many factors are considered in the design of rigid pavement slabs. Designs are based on traffic, weather, and regional factors. In this research, the matrix of designs was intended to include practical designs that are in use in the United States. Table B-1 shows the matrix of pavement designs assembled for the study. Considerations underlying the selection of parameters and options in the table are described below.

Pavement Type

Rigid pavements are generally divided into three broad categories. The first category is Jointed Plain Concrete Pavement (JPCP), constructed without temperature steel (often called reinforcement) for highways that carry fewer heavy axle loads. JPCP is also used with a cement treated subbase placed between the slab and the subgrade. It consists of short slabs ranging from 12 ft to 30 ft in length. The slab thickness ranges from 6 to 12 inches. The joints usually do not contain dowels, and if there are no dowels to to transfer the loads, the slab length should be a maximum of 15 feet. The joints are provided to control slab cracking.

Table B-1. Rigid Pavement Matrix

ID No.	Pavement Type	Slab Thickness (in)	Subbase Thickness (in)	Stabilized	Joint Load Transfer	Length (ft)
1	JPCP	8	0		Good	12
2	JPCP	7	0		Good	15
3	JPCP	10	0		Poor	15
4	JPCP	7	4	Yes	Poor	20
5	JPCP	10	4	Yes	Good	20
6	JPCP	8	6	Yes	Poor	20
7	JPCP	12	6		Good	20
8	JRCP	7	4		Poor	30
9	JRCP	7	4	Yes	Good	30
10	JRCP	8	6		Poor	30
11	JRCP	9	4		Poor	30
12	JRCP	8	4	Yes	Good	40
13	JRCP	9	4	Yes	Good	40
14	JRCP	10	8		Poor	40
15	JRCP	9	4	Yes	Good	60
16	JRCP	10	6	Yes	Good	60
17	JRCP	12	8		Good	60
18	CRCPB	8	4	Yes	Continuous	–
19	CRCPU	10	8		Continuous	–

The second category is Jointed Reinforced Concrete Pavement (JRCP), used for highways that carry high volumes of traffic, such as freeways and interstate highways. The pavement consists of slabs containing temperature steel mesh. Slab length typically ranges from 25 to 100 feet and slab thickness ranges from 6 to 10 inches. The steel is provided to resist temperature effects and hold cracks together so that high aggregate interlock will exist across cracks. While often refered to as "reinforcement," the steel is not intended to take tensile stresses from traffic loading. The transverse joints are provided with smooth dowel bars for load transfer. The subbases are normally granular, however, some may be stabilized with asphalt or cement.

The third category is Continuous Reinforced Concrete Pavement (CRCP). CRCP structures have continuous longitudinal, relatively heavier, temperature steel reinforcement than that in JRCP. CRCP has no transverse joints except construction joints. Sufficient steel is provided in CRCP to hold the temperature and shrinkage cracks together tightly.

Pavement Thickness

Data on the thicknesses of pavements in the United States have been studied in a recent FWHA report (*37*). Table B-2 shows a mix of different pavements all over the United States. The thickness of pavements used in this study were chosen by considering the thicknesses described in Table B-2.

In JPCP pavements thicknesses of 8, 10, 12, and 15 inches represent the whole range of pavements seen in practice. Common thicknesses of JRCP and CRCP built in the United States are 8, 9, and 10 inches. Thicknesses of 8 to 10 inches were selected for the study as representative of JRCP and CRCP.

Table B-2. Design Data for Selected U.S. Highways. (*37*)

Project Location (Year construction)	Slab Thickness (in)	Subbase Thickness (in)	Length (ft)	Pavement Type	% Steel JRCP
I-94 Rothsay, MN WB (1970)	9	6 (AGG)	27	JRCP	0.08
	8	6 (AGG)	27	JRCP	0.09
	9	5 (CTB)	27	JRCP	0.08
I-94 Rothsay, MN WB (1969-control)	9	6 (AGG)	39	JRCP	0.04
I-90 Albert Lea, MNEB (1977)	8	6 (AGG)	13-19	JPCP	-
	9	5 (AGG)	13-19	JPCP	-
	9	5 (AGG)	27	JRCP	0.09
RT-360 Phoenix, AZ, WB & EB (1972)	9	6 (CTB)	13-17	JPCP	-
	13	none	13-17	JPCP	-
	11	none	13-17	JPCP	-
US-10 Clare, MI, WB & EB (1975)	9	4+10 (AGG)	71.2	JRCP	0.15
	9	4+10 (AGG)	13-19	JRCP	-
I-94 Marshal, MI, WB (1986)	10	4+3 (AGG)	41	JRCP	0.14
I-69 Charlotte, MI, NB (1972)	9	4+10 (AGG)	72.2	JRCP	0.15
I-94 Paw Paw, MI	10	4+21 (PAGG)	41	JRCP	0.14
RT 23 Catskill, NY,EB&WB (1965)	9	3+8 (ATB)	20	JPCP	-
	9	4+8 (AGG)	60.8	JRCP	0.20
I-88 Otego, NY, EB&WB (1975)	9	6 (AGG)	20	JPCP	-
	9	4+8 (AGG)	63.5	JRCP	0.20
I-95 Rocky Mount, NC, NB&SB (1967)	9	4 (AGG)	30	JPCP	-
	8	4 (AGG)	60	JRCP	0.17
I-75 Tampa, FL, NB (1986)	13	6 SAND	12-19	JPCP	-

The design thickness of a subbase depends on the soil condition or subgrade. Normally it ranges from 4 to 12 inches. In this study 4, 6, and 8 inch thicknesses were selected. Both stabilized and unstabilized subbases were considered. Subbases are stabilized by treatment with portland cement, asphalt or lime. Subbases which are not stabilized are normally granular material laid and compacted. The typical range of values for the static stress-strain modulus E_s for selected soils are shown in Table B-3 (38). The modulus of elasticity for non-stabilized subbases ranges up to 5000 ksf.

Some of the stabilized subbases in the study were assumed to be bonded to the underside of the slab. The unstabilized subbases were assumed to be unbonded.

Joint Load Transfer

Three levels of load transfer were considered in this study: good, poor, and perfect. Good load transfer provides shear and moment transfer between slabs and was modeled as dowel joints with thick dowel bars. Poor load transfer was defined as a low level shear transfer and was modeled as weak aggregate interlock between slabs. Pavements with perfect load transfer were modeled as continuous reinforced concrete.

Table B-3. Static Soil Modulus Data. (38)

Soil Type	E_s	
	ksf	MPa
Clays		
Very soft	50-250	2-15
Soft	100-500	5-25
Medium	300-1000	15-50
Hard	1000-2000	50-100
Sandy	500-5000	25-250
Glacial till		
Loose	200-3200	10-153
Dense	3000-15000	144-720
Very dense	10000-30000	478-1440
Loess	300-1200	14-57
Sand		
Silty	150-450	7-21
loose	200-500	10-24
Dense	1000-1700	48-81
Sand and gravel		
Loose	1000-3000	48-144
Dense	2000-4000	96-192
Shale	3000-30000	44-14400
Silt	40-400	2-20

Length of Slab

For JPCP three representative lengths of 12, 15, and 20 ft have been selected. The criteria for the selection of the minimum length of a slab is the width of a traffic lane on a normal highway. Normally the width of a traffic lane is 12 ft. Hence to keep a slab at least a square, the minimum length is selected as 12 ft. A maximum slab length of 20 feet has been selected for JPCP based on the fact that slabs of JPCP longer than 20 ft crack in the middle due to temperature and shrinkage.

Slab lengths for JRCP range from 30 to 100 feet in practice. A minimum length of 30 ft and maximum length of 60 feet were selected for the study.

Modulus of Subgrade Reaction

The modulus of subgrade reaction (K) varies from soil to soil in different parts of the country. Typical values of the modulus are given in Table B-4 (*21*). Yoder and Witczak (*38*) in their book *Principles of Pavement Design* indicate that the modulus of subgrade reaction is not critical to choice of thickness for concrete pavements, so use of average values appears warranted. Thus, a single value of 200 ksi (in the midrange of the values found in practice) was selected as the modulus of subgrade reaction for all designs in the pavement matrix.

Table B-4. Typical values for modulus of subgrade of reaction. (*21*)

Soil Type	Modulus of Subgrade Reaction (pci)
Plastic clays	50-100
Silts and silty clays	100-200
Sands, clayey gravels	200-300
Gravels	300+
Average, used for study	200

Finite Element Mesh Size

A special study was conducted to determine the largest mesh size that would capture the peak stresses in the pavement structure in the vicinity of joints under exposure to rapidly varying truck wheel loads. Three inches was found to be sufficient and was selected as the standard finite element mesh size for analysis of rigid pavements using ILLI-SLAB.

Tire Contact Conditions

Tire contact area plays an important role in pavement deflection and stress response. Conventional single, dual, and wide-base single tires each have a different contact patch sizes. The contact area was defined as the total area within the perimeter of the contact patch without regard to openings in the tread.

A typical truck tire contact patch is not precisely rectangular in shape (39,40), but a rectangle is a reasonable approximation of the shape for truck tire contact area. It is also known that the contact pressure is not uniform throughout the contact patch (40-42). However, the computed stress distributions in the PCC pavements were not significantly affected by changes in the distribution of the tire contact pressure. Thus, for PCC fatigue analysis, the tire pressure can be assumed uniform throughout the tire footprint. In this study, the tire contact patch was modeled as rectangular in shape with uniform pressure to compute influence functions with ILLI-SLAB.

Influence functions were computed for three types of tires: dual, conventional single, and wide-based (super) single. The contact patch dimensions and lateral placement used for these three cases are shown in Figure B-6. The rationale behind the selection of tire contact dimensions is given in Appendix D.
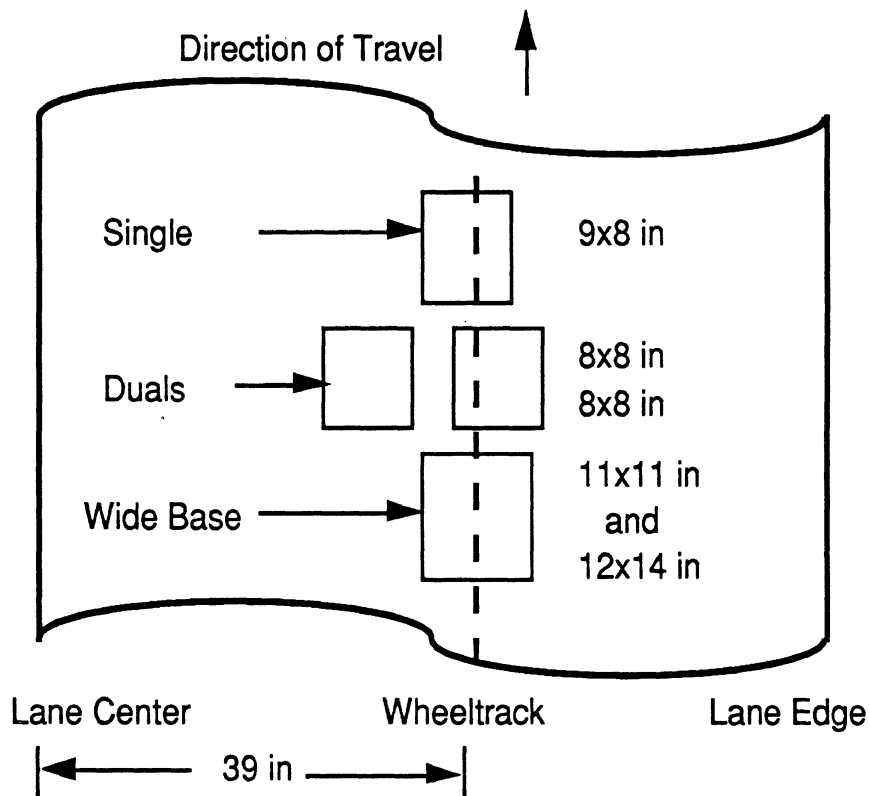
Figure B-6. Contact patch for different tires and their lateral position in a traffic lane.

Lateral Position on the Road

The longitudinal strip on which all the influence functions were computed has a lateral placement that is 39 inches from the center of the lane, as shown on Figure B-6. This position was selected to capture the maximum stress under the tires of a truck with a maximum overall width of 96 inches as it travels down the center of the lane. However, the

location of the peak stresses changes depending on the distance between wheels and the width of the traffic lane. Figure B-7 shows how the tensile stress varies laterally under each type of tire. The wide-based single tire, shown in the figure, is the only case in which the chosen track misses the maximum stress. Even in the weakest pavement, the stress under the chosen track is only 1.5% below the maximum stress under the tire.
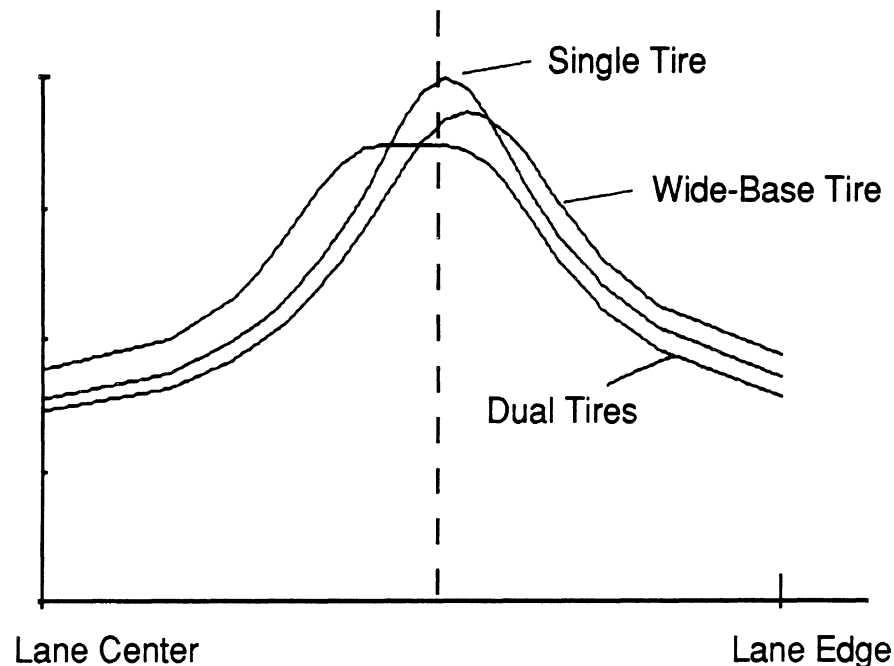
Figure B-7. **Pavement stress level verses lateral position for conventional single, wide-base single, and dual tires.**

REFERENCES

1. Westergaard, H.M., "Stresses in Concrete Pavements Computed by Theoretical Analysis." *Public Roads,* Vol. 8, No. 3 (1926) pp. 25-35.

2. Pickett, G. and Ray, G.K., "Influence Charts for Concrete Pavements." American Society of Civil Engineers, *Transactions.* Paper No. 2452, Vol. 116 (1951) pp. 49-73.

3. Tayabji, S.D. and Colley, B.E., "Analysis of Jointed Concrete Pavements." *Federal Highway Administration, FHWA/RD-86/041* (1986).

4. Chou, Y.T., "Structural Analysis Computer Programs for Rigid Multi-Component Structures with Discontinuities - WESLIQID and WELAYER." *U. S. Army Waterways Experiment Station, Technical Report GL-80*, Vicksburg, Miss. (1980).

5. Smith, K.D., et al., "Performance of Jointed Concrete Pavements. Volume II - Evaluation and Modification of Concrete Pavement Design and Analysis Models." *Federal Highway Administration, FHWA-RD-89-137* (1990) 301 p.

6. Tabatabaie, A.M. and Barenberg, E.J., "Finite-Element Analysis of Jointed or Cracked Concrete Pavements." *Transportation Research Record*, No. 671 (1978) pp. 11-19.

7. Tabatabaie, A.M. and Barenberg, E.J., "Structural Analysis of Concrete Pavement Systems." *American Society of Civil Engineers*, Vol. 106, No. TE5 (1980).

8. Nasim, M.A., et al., "The Behavior of a Rigid Pavement Under Moving Dynamic Loads." *Transportation Research Record*, No. 1307 (1991) pp 129-135.

9. Cebon, D., "An Investigation of the Dynamic Interaction Between Wheeled Vehicles and Road Surfaces." PhD dissertation, Cambridge University, Engineering Department (1985) 251 p.

10. Cole, D.J. and Cebon, D., "Simulation and Measurement of Vehicle Response to Road Roughness." *Proceedings of the Institute of Acoustics*, Vol. 10, No. 2 (1988) pp 477-484.

11. Mitchell, C.G.B., "The Effect of the Design of Goods Vehicle Suspensions on Loads on Roads and Bridges." ARRB/FORS Symposium on Heavy Vehicle Suspension Characteristics, Canberra, Austrailia. *Truck Designers Sprung?* (1988) pp. 99-118.

12. Mitchell, C.G.B. and Gyenes, L., "Dynamic Pavement Loads Measured for a Variety of Truck Suspensions." Second International Symposium on Heavy Vehicle Weights and Dimensions, Kelowna, Canada. *Proceedings* (1989).

13. Whittemore, A.P., et al., "Dynamic Pavement Loads of Heavy Highway Vehicles." *National Cooperative Highway Research Program, Report 105* (1970) 94 p.

14. Woodrooffe, J.H.F. and LeBlanc, P.A., "The Influence of Suspension Variations on Dynamic Wheel Loads of Heavy Vehicles." *Society of Automotive Engineers Paper No. 861973* (1986).

15. Woodrooffe, J.H.F., et al., "Effects of Suspension Variations on the Dynamic Wheel Loads of a Heavy Articulated Highway Vehicle." *Vehicle Weights and Dimensions Study, Vol. 11. Canroad Transportation Research Corporation* (1986).

16. Ballinger, C.A., "Cumulative Fatigue Damage Characteristics of Plain Concrete." *Highway Research Record*, No. 370 (1972) pp. 48-60.

17. Crepps, R.B., "Fatigue of Mortar." American Society for Testing and Materials *Proceedings*, Vol. 23, Part II (1923) pp. 329-330.

18. Darter, M.I., "Design of Zero-Maintenance Plain Concrete Pavements, Vol 1 - Development of Design Procedures." *Federal Highway Administration, Department of Transportation, Report DOT-FH-11-8474* (1977).

19. Hatt, W.K., "Researches in Concrete." *Purdue University Bulletin 24* (1924) pp. 44-55.

20. Hilsdorf, H.K. and Kesler, C.E., "Fatigue Strength of Concrete Under Varying Flexural Stresses." Americam Concrete Institute, *Proceedings*. Vol. 63 (1966) pp. 1059-1076.

21. Kesler, C.E., "Effect of Speed of Testing on Flexural Fatigue Strength of Plain Concrete." *Highway Research Board*, Vol. 32 (1953) pp. 251-258.

22. McCall, J.T., "Probability of Fatigue Failure of Plain Concrete." American Concrete Institute, *Proceedings*. Vol. 55, No. 2 (1959) pp 233-244.

23. Murdock, J.W. and Kesler, C.E., "Effect of Range of Stress on the Fatigue Strength of Plain Concrete Beams." American Concrete Institute, *Proceedings*. Vol. 30, No. 2 (1958) pp 221-231.

24. Tepfers, R., "Tensile Fatigue Strength of Concrete." American Concrete Institute, *Proceedings*. Vol. 76, No. 8 (1979) pp. 919-933.

25. Cornelissen, H.A.W., "Constant-Amplitude Tests on Plain Concrete in Uniaxial Tension and Tension-Compression." *Delft University of Technolog,y Report 5-84-1* (1984).

26. Cornelissen, H.A.W. and Siemes, A.J.M., *Plain Concrete Under Sustained Tensile or Tensile and Compressive Loadings*. Behavior of Offshore Structures. (1985) Elsevier Science Publishers B. V. Amsterdam.

27. Cornelissen, H.A.W. and Timmers, G., "Fatigue of Plain Concrete in Uniaxial Tension and Alternating Tension-Compression." *Stevin Laboratory, Delft University of Technology, Report 5-81-7,*(1981).

28. Tepfers, R., "Fatigue of Plain Concrete Subjected to Stress Reversal." American Concrete Institute, *Proceedings*. ACI-SP-75 (1982) pp. 195-215.

29. American Association of State Highway and Transportation Officials, *The AASHO Road Test. Report 5, Pavement Research*. Highway Research Board, Report 61E (1962) 352 p.

30. Portland Concrete Association, *Thickness Design for Concrete Pavements*. PCA (1966) 32 p.

31. Packard, R.G., "Design of Concrete Airport Pavement." *Portland Cement Association* (1973) 61p.

32. Nordby, G.M., "Fatigue of Concrete: A Review of Research." American Concrete Institute, *Proceedings*. Vol. 30, No. 2 (1959) pp 191-220.

33. Raithby, K.D. and Galloway, J.W., "Effects of Moisture Condition, Age, and Rate of Loading on Fatigue of Plain Concrete." American Concrete Institute, *Proceedings*. (1974)

34. Treybig, H.J., et al., "Overlay Design and Reflection Cracking Analysis for Rigid Pavements." *Federal Highway Administration, FHWA-RD-77-67* (1977).

35. Majidzadeh, K. and Ilves, G.J., "Evaluation of Rigid Pavement Over Lay Design Procedure, Development of the OAR Procedure." *Department of Transportation, DTFH11-9489* (1983).

36. Vesic, A.S. and Saxena, S.K., "Analysis of Structural Behavior of Road Test Rigid Pavements." *Highway Research Record,* No. 291 (1969) pp 156-158.

37. Smith, K.D., et al., "Performance of Jointed Concrete Pavements. Volume I - Evaluation of Concrete Pavement Performance and Design Features." *Federal Highway Administration, FHWA-RD-89-137* (1990) 200 p.

38. Yoder, E.J. and Witczak, M.W., "Principles of Pavement Design." Second Edition, (1975).

39. Ford, T.L. and Charles, F.S., "Heavy Duty Truck Tire Engineering." *The Society of Automotive Engineers, SP 729* Warrendale, PA. (1988) 54 p.

40. Ford, T.L. and Zekoski, J., "Impact of Truck Tire Selection on Contact Pressures." *Good Year Tire & Rubber Company, Paving and Transportation Conference, Symposium on Pavement Rutting at the University of New Mexico (1988).*

41. Akasaka, T., "Two-Dimentional Contact Pressure Distribution of a Radial Tire." Tire Science and Technology, *Transactions*. Vol. 18, No. 2 (1990) pp. 80-103.

42. Yap, P., "A Comparative Study of the Effect of Truck Tire Types on Road Contact Pressures." *Society of Automotive Engineers Paper No. 881846* (1988).

APPENDIX C
FLEXIBLE PAVEMENT MODELING

This appendix describes the analytical methods used to investigate the response of flexible pavements to heavy truck wheel loads. The appendix begins with a background section that describes the general methods used to compute the response of a flexible pavement to applied loads. The next section describes the VESYS model for the flexible pavement structure. Past validation activities are cited, in which experimental measures were compared to responses predicted by the model. Analytical methods used to compute rutting and fatigue damage are described. The appendix concludes with a discussion of the matrix of pavements that were studied and the rationale for selecting pavement designs and parameter values.

To facilitate the large number of pavement and vehicle combinations of interest in this . study, additional analysis methods were developed to characterize the response to multiple, time-varying loads from a moving vehicle in a way that is computationally efficient. These methods are described in Appendix F.

BACKGROUND

In the past, the approach to design of flexible pavements has been mostly empirical, based on engineering judgments and field experience. The factors considered while making design decisions were primarily soil-strength properties obtained from specified soil tests, properties of pavement layer materials, and performance of pavement thickness components with traffic characteristics. In recent years, more emphasis has been placed on a mechanistic approach to pavement design. This approach includes multi-layer elastic theory or finite element analysis. Both methods have been successfully used to develop flexible pavement design procedures. Multi-layered linear elastic theory is now commonly used for the calculation of primary responses in flexible pavement systems.

A number of computer programs have been developed for calculating the generalized load responses of flexible pavements. Some of the more well-known are BISAR (*1*), ELSYM5 (*2*), WESLEA (*3*), ILLI-PAVE (*4*), and VESYS (*5*).

THE VESYS PAVEMENT MODEL

VESYS is a family of programs for mechanistic analysis of asphalt concrete pavement performance developed at MIT under sponsorship of the Federal Highway Administration. Its development started in 1974 and the program has been updated frequently since then.

The version VESYS-DYN was chosen for use in this study based on its capabilities and its wide acceptance in the highway community. The program handles elastic and viscoelastic analysis of any number of pavement layers with any combination of elastic or

viscoelastic behavior among layers. The viscoelastic model is identical to an elastic layer theory model, with the extension that the material properties may be characterized as time-dependent. All layers have finite thicknesses except the bottom layer, which has infinite thickness, and all layers are infinite in the horizontal direction. The loading is represented by a circular area with uniform pressure. The program offers several different types of analysis which include changing climactic conditions, simultaneous loading from multiple axles, and a damage model to predict pavement performance. For the purpose of this research, VESYS was used to compute primary responses to applied tire loads. The program was modified to compute responses at points specified in Cartesian coordinates to tire loads of uniform contact pressure applied over a circular contact area (two circular areas are used to model dual tires). The program was also modified to generate influence functions, used in this research program to combine pavement response with dynamic truck loading, as described in Appendix F.

VALIDATION

The VESYS pavement model was validated in past studies by (6-8) in which the experimental work was performed on the Transport and Road Research Laboratory test track. In the tests, instrumented vehicles were driven over instrumented sections of flexible pavement and the response of the pavement and vehicles were logged simultaneously. The vehicle responses were then combined with influence functions that were measured from the test pavement and the resulting calculated pavement response time histories were compared favorably with the measured time histories over a wide range of speeds. In a subsequent study (9), influence functions calculated using VESYS were satisfactorily fitted to the measured pavement responses for a wide range of speeds.

DAMAGE MODEL

Two primary responses of flexible pavements are used in this study to determine the damage incurred. The imposition of stresses/strains in the pavement layers promote fatigue which eventually leads to cracking and breakup of the pavement structure. Similarly, permanent deformation arising from compaction and flow of the asphalt materials produces ruts in the wheel paths which eventually constitutes failure of the pavement.

Fatigue

The most common hypothesis in the literature concerning fatigue damage of flexible pavements is that cracks are initiated at the bottom of the bound layers, where the tensile strains under wheel loads are greatest. The cracks are then expected to propagate vertically to the surface (5,10-13). The current authors do not know of experimental evidence that supports this hypothesis. Indeed, Thrower (12) noted that this failure mechanism is not well supported by observations of core samples taken from roads in Britain, where cracks almost invariably originate at the top surface and extend downwards. Nevertheless, the

hypothesis represents the current consensus among pavement researchers, and therefore has been used for assessing fatigue damage in this study.

Primary Response Components

When a steady load with a circular contact area is applied to the surface of a layered elastic system, such as that shown in Figure C-1, the maximum horizontal strains occur at the layer interface directly below the center of the contact area. For a circular contact area, the maximum radial and circumferential (longitudinal and transverse) strains are identical. An example of this is provided in Figure C-2, which shows theoretical radial and circumferential strains at the bottom of the 5-inch thick asphalt surface layer shown in Figure C-1. The contact pressure of 100 psi is distributed over a circular area of radius 4.79 inches. It is important to note that the radial strains become compressive (negative) about 8 inches from the center of the contact area. Twelve inches is typical of measured and calculated longitudinal strains in thicker flexible pavements (*10,14*). Figure C-2 also shows that the compressive vertical strains directly under the load are of similar magnitude to the radial and circumferential strains.
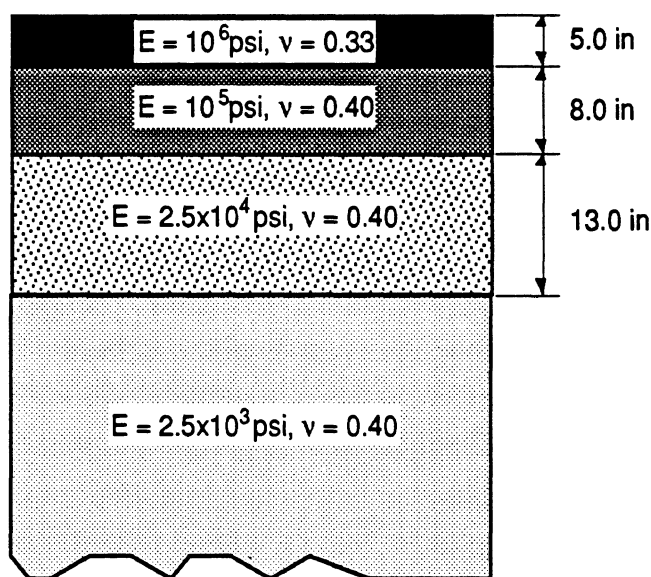
Figure C-1. Elastic layered road model used for influence function calculations.

The situation is different for wheels with dual tires. Figure C-3 shows a plan view of two circular contact areas which model a pair of dual tires. The contact pressure acting over each area is 100 psi. The longitudinal strain and transverse strain along the center of the outer wheel path (A-A) are shown in Figure C-4. The peak longitudinal strains along the wheel path are approximately 50% greater than the peak transverse strains. Furthermore, the *range* of the longitudinal strains, including the compressive (negative) part of the curve, is considerably greater than the range of the transverse strains. It is the strain *range* that governs fatigue damage, as explained later.
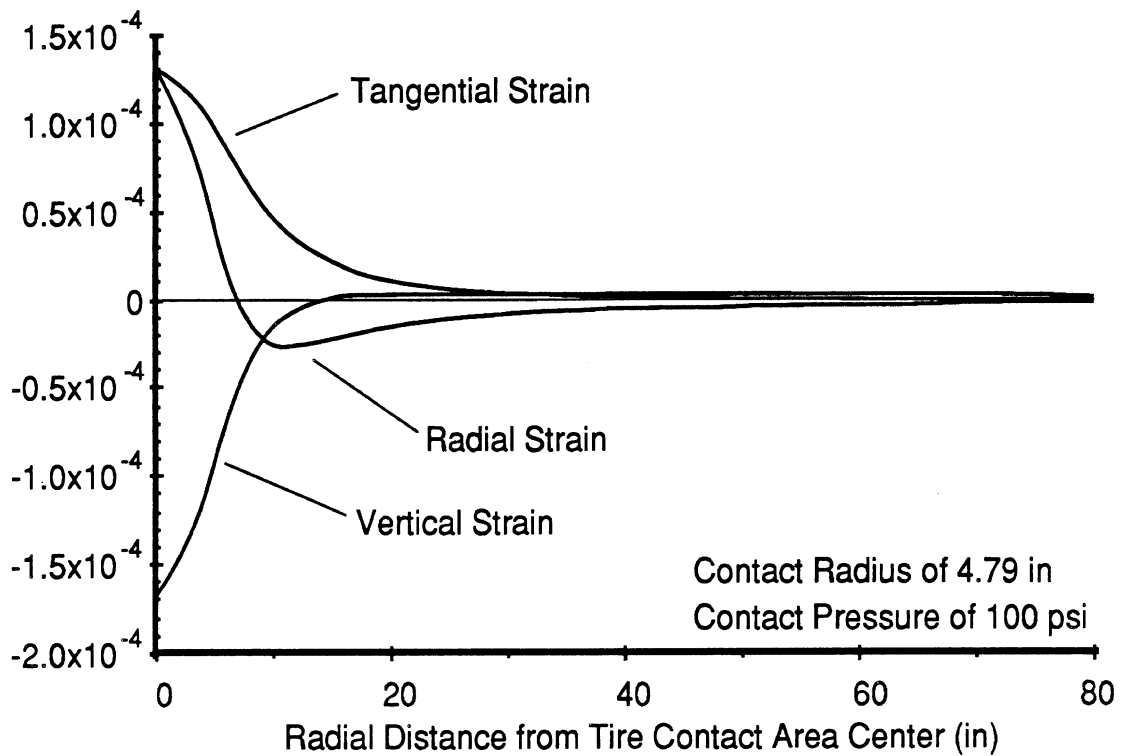
Figure C-2. Radial, circumferential and vertical strains under a 5-inch wear course.
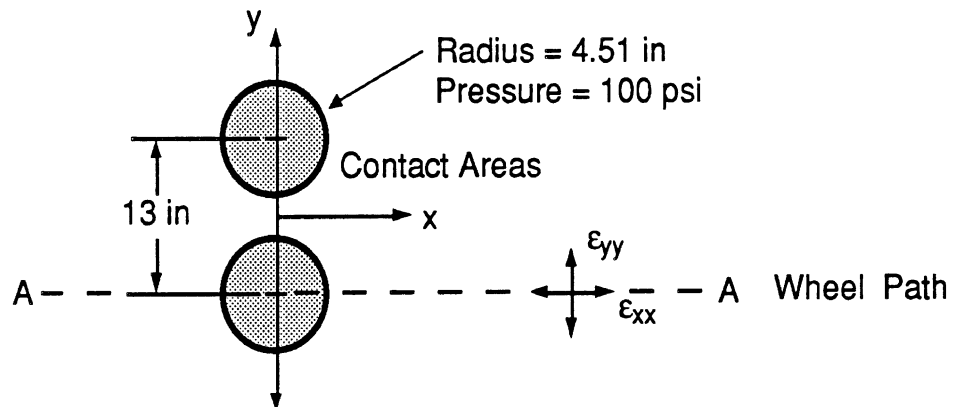
Figure C-3. Plan view of the contact areas of a pair of dual tires.

1.5x10^{-4}

Longitudinal Strain

1.0x10^{-4}

Transverse Strain

Strain

0.5x10^{-4}

0

Contact Radii of 4.51 in

Contact Pressure of 100 psi

-0.5x10^{-4}

0   20   40   60   80

Longitudinal Position (in)
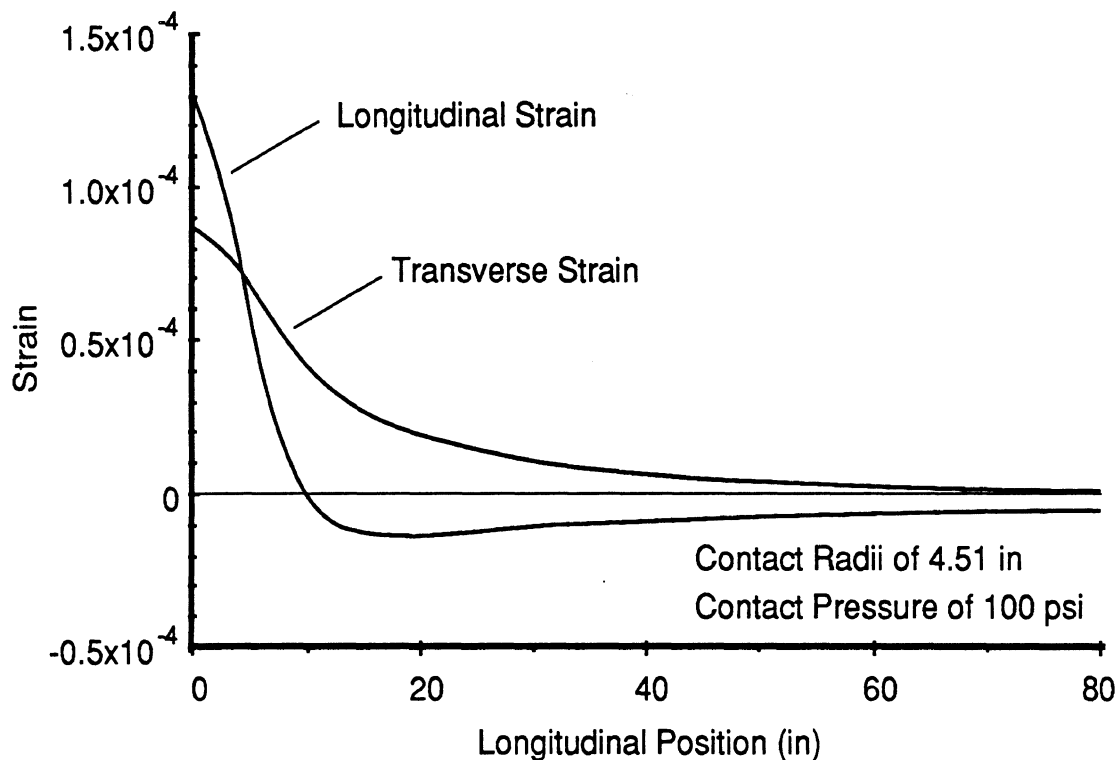
Figure C-4. Longitudinal and transverse strains under a 5-inch wear course (along line A-A in Figure C-3).

Figures C-5 and C-6 show the strains under the wear course induced by a tandem axle with a (typical) spacing of 51 in. In Figure C-5, the two axles in the group have dual tires whereas in Figure C-6, the axles have wide-base single tires. Both axle groups have a total static load of 34 kips. The dual tires have contact radii of 4.51 inches, and the wide-base single tires have contact radii of 6.21 inches. The vehicles are traveling at 55 mph; however, only the static component of the wheel loads are included (no dynamic component).

It is apparent from Figure C-5 that for dual tires, both the *peaks* and the *ranges* of longitudinal strain are greater than the peaks and ranges of the transverse strains. This is mainly a consequence of the shapes of the influence functions shown in Figure C-4. Conversely, for the wide-base single tires shown in Figure C-6, the *peak* transverse strains are slightly larger than the peak longitudinal strains, but the *range* of the longitudinal strains (including the compressive parts) is still greater than the range of the transverse strains.

The relative increase in the peak transverse strains under the wide-base singles is due to the overlapping of the influence functions from the two tires. For the longitudinal strains, the negative part of the influence function from one axle reduces the peak strain generated by the other axle. However, the transverse strain influence function is always positive and therefore the strain from one axle reinforces the peak strain generated by the other.
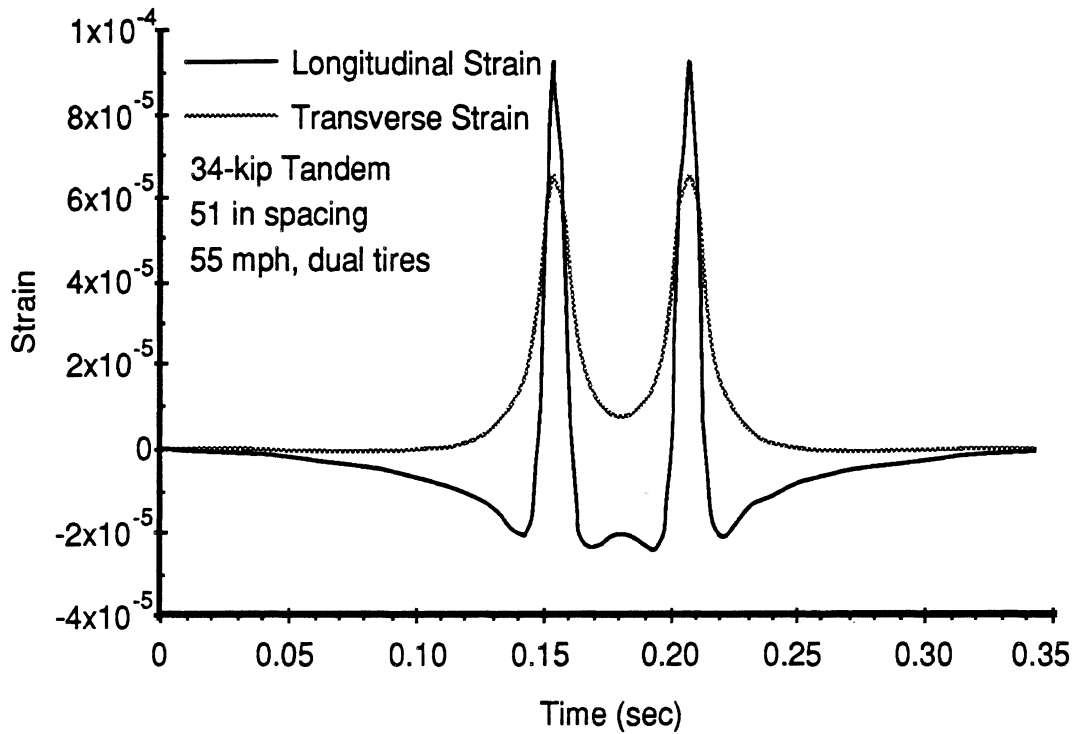
Figure C-5. Strain under a 5-inch wear course induced by a passing tandem axle with dual tires.
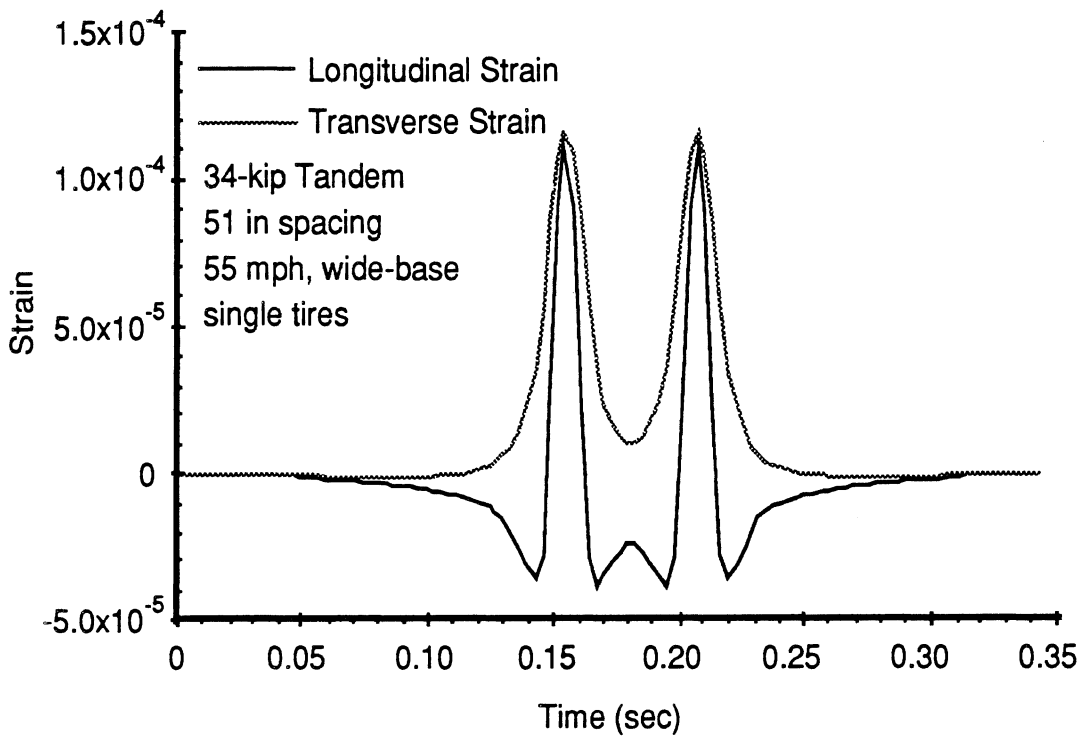
Figure C-6. Strain under a 5-inch wear course induced by a passing tandem axle with wide-base single tires.

The strain time history experienced at any particular point in the road is complex: it is triaxial, and the directions of the principal strains rotate as a wheel load passes by. If the wheel has a single tire and passes directly over the point of interest, then the principal strains rotate in a vertical plane only. If the wheel has dual tires or the wheel path is displaced laterally from the point of interest, then the principal strains rotate in a horizontal plane as well. In either case, the loading conditions are known as 'non-proportional' and they are the subject of considerable research in the fatigue and fracture mechanics literature (15-18).

Fatigue of laboratory specimens of asphalt is known to be "strain-controlled" (19), but Lefebvre, et al (18), noted that very little research has been performed on non-proportional loading in strain-controlled ("low-cycle") fatigue. Furthermore, no information concerned with non-proportional, strain-controlled loading of asphalt was found in the literature during the current study.

There are two main approaches to evaluating fatigue damage in non-proportional loading of *metals* (17):

1.   The plastic yield criteria of Tresca or von Mises can be used to reduce a multi-axial stress or strain state to an equivalent uniaxial stress or strain state. "Reviews by many investigators have shown that these phenomenological criteria are very limited in their predictive capability and are not able to account for variations in life observed under different multi-axial loading conditions" (18).

2.   It can be assumed that there is a 'critical plane' where material failure occurs (15,18). In this approach, crack propagation is generally assumed to occur on the plane of maximum shear stress, in the direction normal to the greatest principal stress (15). In non-proportional loading, it is necessary to evaluate an appropriate damage parameter for all possible planes during each simulation step, and to perform a damage analysis for each plane (16).

Validated mathematical models of the fatigue failure of asphalt pavements due to non-proportional loading do not exist. It was therefore considered that use of such methods for handling the non-proportional loading in this study could not be justified. Instead, it was decided to calculate fatigue damage occurring on transverse vertical planes at the bottom of the asphalt surface layer due to the longitudinal strain component. This decision can be rationalized on the basis that: (1) the longitudinal strain component has the largest *range* for all wheel configurations and the largest *peak values* for most wheel configurations as shown above; (2) the "single-pass" fatigue damage calculation in this study is used to compare vehicles and suspensions (all other factors "remaining equal") rather than to estimate the fatigue lives of pavements; and, (3) the longitudinal strain at the bottom of the asphalt surface layer is the most common measure cited in the road damage literature for estimating the fatigue life of flexible pavements. The initiation of longitudinal cracks is likely to be a reasonable indicator of initial fatigue damage, even if the cracks acquire complex geometry as they grow and the longitudinal strain does not remain the critical component later in the fatigue life.

Fatigue Laws

The relationships between the amplitude of the applied strain ε and the number of cycles to failure N of asphalt laboratory specimens have been shown to take the form (*10-12,19-21*):

$$N = k_1 \, \varepsilon^{-k_2} \qquad\qquad\qquad \text{(C-1)}$$

where k_1 and k_2 are mix constants. The value of k_2 may vary between 1.9 and 5.5 (*19-22*).

Using Miner's hypothesis for the linear accumulation of fatigue damage (*12,19,23,24*), the theoretical "damage" D_k (proportion of the fatigue life used) at measurement station k on the road, due to the passage of the vehicle, can be estimated from:

$$D_k = \sum_{j=1}^{N_c} \frac{1}{N_{jk}}, \quad \text{for } k = 1, 2, 3,\text{........} N_s \qquad\qquad \text{(C-2)}$$

where N_c is the number of strain "cycles" due to passage of the vehicle, and N_s is the total number of measurement stations along the road.

It is apparent from Eq. C-1 and C-2 that the fatigue damage for a given strain cycle is proportional to ε^{k_2}. The constant k_2 can be quite large (typically 4 or 5), and therefore the fatigue damage is very sensitive to the strain level, and hence magnitude of dynamic wheel loads.

Cycle Counting

In this study the pavement strain response at various points along the road was calculated by combining longitudinal strain influence functions (pavement strains per unit tire force, e.g., Figure C-4) with dynamic wheel loads. A typical result for the static wheel loads of a 5-axle tractor-semitrailer[1] traveling at 55 mph is shown in Figure C-7. The strain time history shows a tensile peak and an associated compressive "bow-wave" and "wake" for each axle. In order to determine theoretical fatigue damage (using Eq. C-2) from such a strain time history, it is necessary to reduce the response to a set of equivalent simple strain cycles. Two methods were considered for this purpose: "peak counting", and the "rainflow" method of cycle counting.

---

[1] This vehicle had leaf spring suspensions on all axles; dual tires on both the tractor drive axle and trailer group; and static wheel loads (one side of the vehicle only) of 6550 lbs and 11100 lbs on the tractor, and 18200 lbs total group load on the trailer. The pitch–plane simulation was validated experimentally in an earlier study, see (*25*) for details. This vehicle model is used for the analysis throughout the remainder of this Appendix.
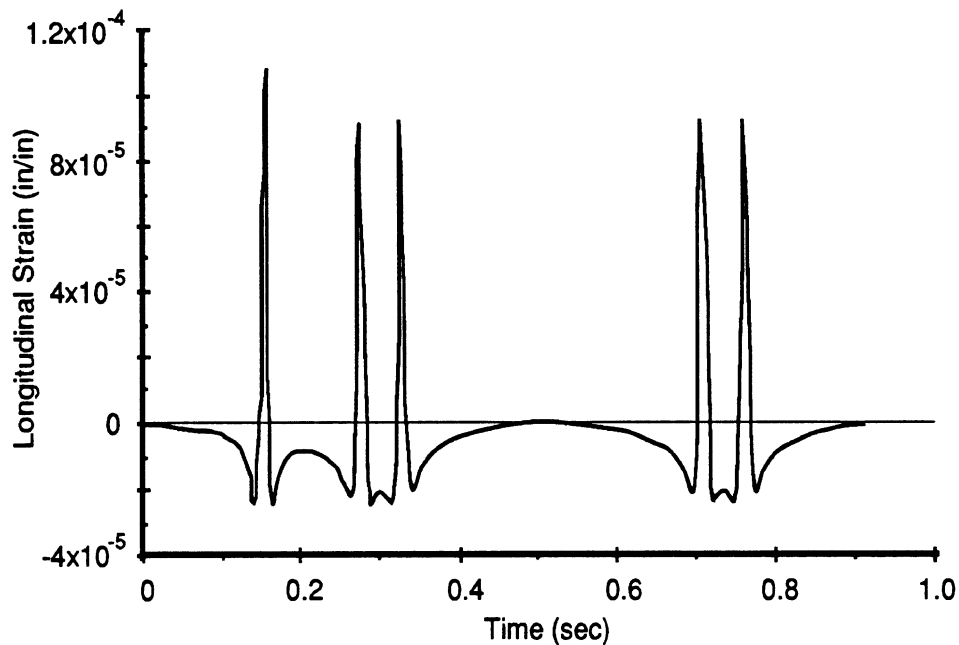
Figure C-7. Longitudinal strain at the bottom of a 5-inch wear course induced by a 5-axle tractor-semitrailer.

The *peak-counting* method uses peak tensile strains under each truck axle as the size of the equivalent strain-cycle. This method was employed by Christison in the Canadian Vehicle Weights and Dimensions Study (*26*) and by Cebon in a previous study of fatigue damage due to dynamic wheel loads (*27*). It is often used when evaluating fatigue due to measured strains (*10,14,28*). The simple peak counting method does not account for compressive strains between tensile peaks, nor does it consider cases in which the strain level does not recover to zero between axles.

The basis of the *rainflow* cycle counting method is that the overall difference between the highest peak and the lowest valley in a strain time history is more important than intermediate small fluctuations (*24*). The method corresponds to counting complete hysteresis loops in the stress-strain curve for the material. The overall range of strain (lowest valley to highest peak) is first found and removed from the time history. The size of this range is used as the first strain "cycle" in Eq. C-1 and the resulting damage is added to Eq. C-2. The next highest range is then found and removed, and the damage added to Eq. C-2. This process is continued until all strain reversals have been considered. This method is commonly employed for analysis of metal fatigue due to complex response time histories and is described in detail in (*10,24,29*).

Sample Results

Figure C-8 shows the theoretical fatigue damage, evaluated by the *rainflow* cycle counting method, for the 5-axle tractor-semitrailer, traveling over a relatively smooth asphalt highway profile at 55 mph. The constants in the fatigue life Eq. C-1 were $k_1 = 2.51 \times 10^{-8}$ and $k_2 = 4.0$. The "damage" that would be caused by purely static loads

traveling at the same speed is shown on the figure by a horizontal line at approximately 4.11×10^{-8}. This number means that the road would undergo $1/(4.11 \times 10^{-8}) = 2.43 \times 10^7$ passes of the static wheel loads to failure. The mean damage level of 4.32×10^{-8} is also shown on the figure.
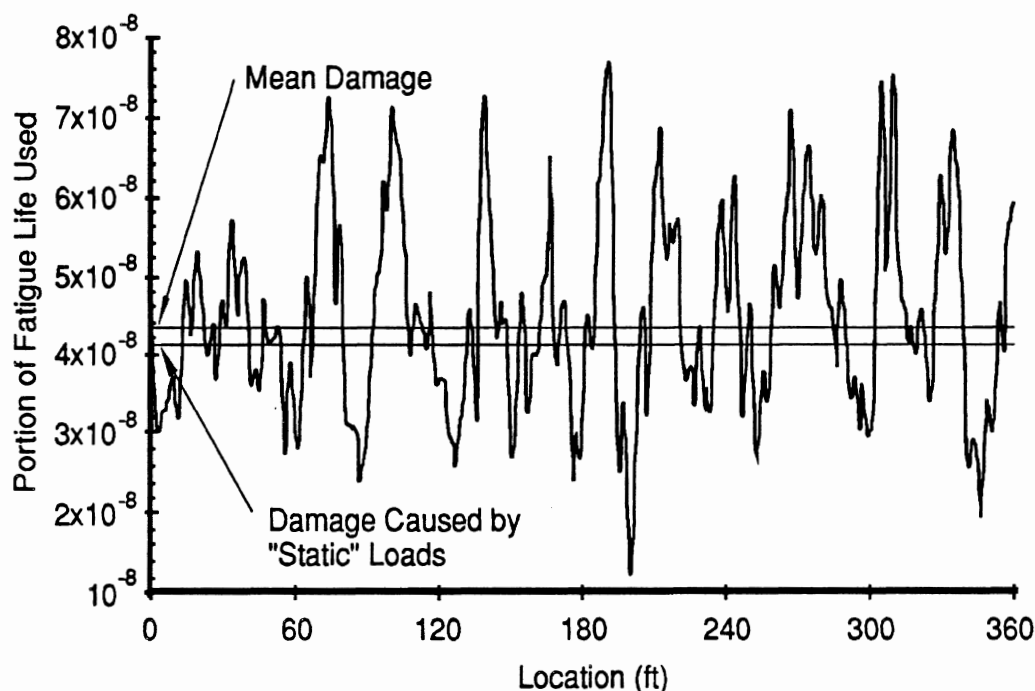
Figure C-8. Theoretical fatigue damage generated by a single pass of the 5-axle tractor-semitrailer traveling over a moderately rough road.

It can be seen that some locations on the road incur large damage levels, due to the dynamic variations in tire load. For example, at approximately 74 ft along the road, the fraction of life consumed is above 7.0×10^{-8}. Therefore at this location the theoretical damage incurred is 1.7 times the damage due to the static loads. The damage level is so high because of the effect of the power k_2 in the fatigue law. This weighs heavily the damage caused by high peak strain levels resulting from dynamic wheel loads.

The damage history in Figure C-8 was normalized by the static damage level, and is re-plotted over the first 120 ft of pavement length in Figure C-9. Also shown in Figure C-9 is the damage distribution calculated for the same primary pavement responses, using the *peak* counting method. It can be seen that in general, predictions of relative damage from the peak-counting method are similar to those of the rainflow method. The absolute damage levels predicted by each method are different, however, as the rainflow method predicts absolute damage levels more conservatively.

In this study it was found that the *ranking* of vehicles was generally not affected strongly by the cycle counting method. It was therefore decided to use the *rainflow* counting procedure, which is generally considered to be more accurate (*24*). It should be

noted, however, that the peak counting and rainflow methods would predict relative damage levels that are very different in cases where the strain under one axle of a truck is significantly affected by the strains induced by a nearby axle (such as the case of transverse strains).
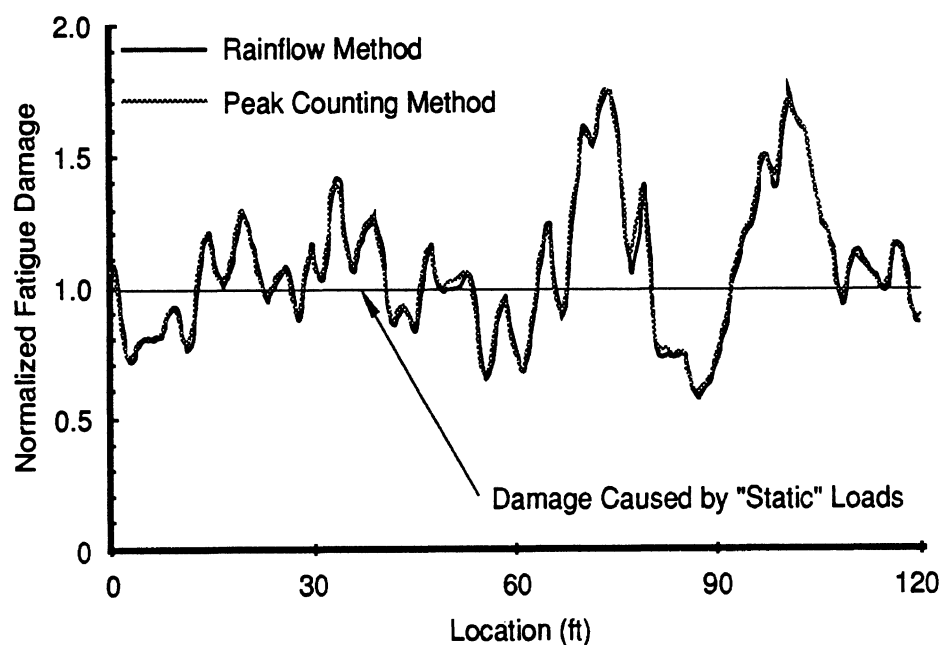
Figure C-9. Expanded view of the first 120 ft of the fatigue damage profile shown in Figure C-8, illustrating the influence of the pavement strain cycle counting algorithm on damage relative to case of "static" wheel loads.

Rutting

Rutting arises from four mechanisms. The first is mechanical deformation, resulting from consolidation in the base, subbase, or subgrade layers. This is usually accompanied by cracking. It can occur because of an inadequate structural section design or poor compaction of the subgrade or the lower layers of the pavement. The second is consolidation rutting of the asphalt surface, caused by poor compaction of the mat during construction or an improper mix design. After construction, traffic continues to compact the mat in the wheel paths, forming single basin-shaped ruts. The third is pavement surface wear caused by studded tires and chains, which can occur on both rigid and flexible pavements. The forth, plastic flow rutting, is a depression at the center of the loaded area with humps on either side of the rut due to the viscoelastic property of hot mix asphalt. Mat stability will affect plastic flow rutting. It is the fourth type of rutting that was studied in this research (*30*).

The rutting model used in this study uses the theory of viscoelasticity and the "Correspondence Principle." This principle says that for a *linear viscoelastic* material the *rates* of permanent stress, strain and displacement can be calculated using *elastic* stress

analysis, but with the elastic material parameters (Young's Modulus and Poisson's ratio) replaced by their *viscous* equivalents. The assumption of linear viscoelasticity is a reasonable approximation for asphalt, clays and soils (*31*). Coarse granular materials can be assumed to display a very high "effective viscosity." The Correspondence Principle and its application to rutting of layered road systems is discussed in detail by Thrower (*31,32*).

The main advantages of using a simple linear viscoelastic model are that:

1. It is based on an exact deformation theory and yields a realistic residual displacement field;
2. It accounts for the permanent deformation in each pavement layer;
3. It is based on easily measured material properties for which data is readily available;
4. It accounts for the correct relationships between vehicle speed and pavement loading time;
5. It accounts correctly for the effects of temperature;
6. It yields realistic results, that display sensible trends for a wide range of conditions.

The main disadvantage of the method is that creep of asphalt is sometimes found to be nonlinear, especially for large strains (*33*). The method may not therefore be accurate for all pavement materials. Nevertheless, the method is very useful for comparing the road damaging potential of heavy vehicles, and evaluating the important trends.

The next section summarizes the theory of the rutting model.

Correspondence Principle

The response $z(t)$ of a linear system to a time-varying input $f(t)$ is given by the convolution integral (*34*):

$$z(t) = \int_{-\infty}^{\infty} h(t-\tau)f(\tau) \, d\tau \qquad \text{(C-3)}$$

where: $z(t)$ is the response at time t,
$f(\tau)$ is the input force at time τ, and
$h(t)$ is the response at time t to a unit impulse at time t = 0.

Assume that $f(t)$ is only non-zero for time T_f:

$$f(t) = \begin{cases} 0 & t < 0 \\ F(t) & 0 \le t \le T_f \\ 0 & t > T_f \end{cases} \qquad \text{(C-4)}$$

Then the integral in Eq. C-3 need only be evaluated up to time T_f.

$$z(t) = \int_{0}^{T_f} h(t-\tau)F(\tau) \, d\tau$$

Now suppose that the impulse response has a permanent offset $h(t) = h_\infty$ for large times, $t > T_h$, as shown in Figure C-10. Then:

$$z(t) = h_\infty \int_0^{T_f} F(\tau)\, d\tau \qquad \text{(C-5)}$$

for all $t > T_h + T_f$.
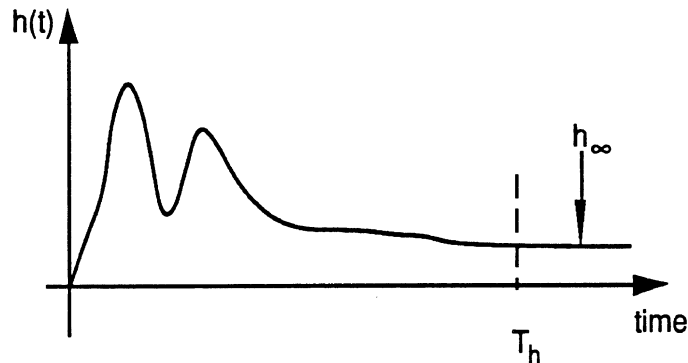
Figure C-10. Schematic diagram of an impulse response h(t) of a flexible pavement.

Therefore the final permanent deformation of the system is proportional to the product of the applied impulse (integral of the input over time) and the final value of the impulse response h_∞.

Now consider how h_∞ can be evaluated for a general linear system, which obeys a differential equation of the form:

$$\sum_{i=0}^{N} \alpha_i \frac{d^i z}{dt^i} = \sum_{j=0}^{M} \beta_j \frac{d^j f}{dt^i} + \gamma. \qquad \text{(C-6)}$$

If $f(t)$ is a transient input which satisfies Eq. C-4, and $z(t)$ is initially at the undisturbed position:

$$z = 0, \text{ for } t < 0,$$

then γ in Eq. C-6 must be zero.

If there is a permanent deformation in the system for $t \gg T_f$, so that

$$z = \delta, \text{ and } \frac{d^i z}{dt^i} = 0,$$

then it must be the case that

$$\alpha_0 = 0. \qquad \text{(C-7)}$$

Integrating Eq. C-6 then gives:

$$\int_{-\infty}^{\infty} \sum_{i=1}^{N} \alpha_i \frac{d^i z}{dt^i} \, dt \quad = \quad \int_{-\infty}^{\infty} \sum_{j=0}^{M} \beta_j \frac{d^j f}{dt^j} \, dt$$

hence

$$\left[\sum_{i=1}^{N} \alpha_i \frac{d^{(i-1)}z}{dt^{(i-1)}} \right] \quad = \quad \left[\sum_{j=1}^{M} \beta_j \frac{d^{(j-1)}f}{dt^{(j-1)}} \right] + \int_{0}^{T_f} \beta_0 F \, dt \qquad \text{(C-8)}$$

The only non-zero term in the two square brackets is the z-term for i = 1, which is $\alpha_1 \delta$. Thus

$$\alpha_1 \delta \; = \; \beta_0 \int_{0}^{T_f} F(t)dt \quad \text{hence} \quad \delta \; = \; \frac{\beta_0}{\alpha_1} \int_{0}^{T_f} F(t)dt \qquad \text{(C-9)}$$

Comparing Eq. C-5 and C-9, it is clear that

$$h_\infty = \frac{\beta_0}{\alpha_1}. \qquad \text{(C-10)}$$

It is possible to calculate h_∞ for a linear *viscoelastic* road model using a linear *elastic* road response calculation. Consider the case when all derivatives terms in Eq. C-6 are zero, i.e., the system is rate-independent (linear elastic). Then the static displacement output z of the system due to a static force input f is

$$\alpha_0 z = \beta_0 f \quad \text{therefore} \quad \frac{z}{f} = \frac{\beta_0}{\alpha_0} . \qquad \text{(C-11)}$$

Now suppose that Eq. C-6 is re-written in terms of z_{dot}, the time derivative of z. Recalling that $\alpha_0 = 0$ (from Eq. C-7), Eq. C-6 becomes

$$\alpha_1 z_{dot} = \beta_0 f \quad \text{therefore} \quad \frac{z_{dot}}{f} = h_\infty = \frac{\beta_0}{\alpha_1}. \qquad \text{(C-12)}$$

Hence, if the elastic material parameter α_0 is replaced with the viscous parameter α_1 in the linear elastic system equations, the output per unit force input is the desired h_∞ from Eq. C-10. This relationship is known as the Correspondence Principle.

Note that there are two limitations to this theory:

1. The material must be linear viscoelastic

2. In general it is necessary to assume that the volumetric and deviatoric stress and strain components are uncoupled.

For asphalt pavement materials it is reasonable to assume that the permanent deformation takes place due to shear flow, without significant volume change (compaction) (*11,35*). For example, in the AASHO Road Test (*36*), it was found that only 20% of the change in thickness of the surface layers and 4% of the change in thickness of the subbase was due to increases in the density of the materials. Subsequent improvement in road compaction methods is likely to have reduced the compaction of asphalt surface layers. Therefore, to a first order, it is assumed that the material undergoes incompressible permanent deformation and the "viscous Poisson's ratio" v is assumed to be 0.5.

The viscosities quoted in the literature refer to shear stress and shear strain, i.e., viscosity η "corresponds" to the Shear Modulus G. To perform the viscous stress analysis using an elastic layered model like VESYS, it is necessary to use the viscous equivalent to the Young's Modulus E.

Now E and G are related by:

$$G = \frac{E}{2(1+v)}, \text{ which for } v = 0.5 \text{ gives } E = 3G.$$

Thus the 'extensional viscosity' λ which corresponds to E is given by $\lambda = 3\eta$. This is the parameter which is used in the influence function calculation.

Application of the Correspondence Principle to Pavement Rutting

It can be shown (*37*) that the response of a road to moving dynamic wheel loads is given by

$$z(x,t) = \int_{-\infty}^{\infty} h(x-V\tau,t-\tau)f(\tau)d\tau = \int_{-\infty}^{\infty} h(x-V(t-\tau),\tau)f(\tau)d\tau, \qquad \text{(C-13)}$$

where

$z(x,t)$ is the response at position x at time t,
   V is the vehicle speed, and
$h(x,t)$ is the response at position x and time t
   to a unit impulse at the origin at time t = 0.

Now substitute t = x/V - (t-τ), and assume that the impulse response is negligible for distances greater than X from the point of application of the impulse, i.e., h(x,t) = 0 for |x| > X. Then Eq. C-13 becomes

$$z(x,t) = \int_{-\frac{x}{V}}^{\frac{x}{V}} h\left(V\theta, \theta + t - \frac{x}{V}\right) f\left(\frac{x}{V} - \theta\right) d\theta. \qquad (C\text{-}14)$$

Finally, let the steady state offset of the impulse response function be given by

$$h(x,t) = h_\infty(x), \text{ for } t \to \infty.$$

Then it is apparent that the permanent deformation (for $t \to \infty$) at longitudinal position x is given by

$$z(x,\infty) = \int_{-\frac{x}{V}}^{\frac{x}{V}} h_\infty(V\theta)\, f\left(\frac{x}{V} - \theta\right) d\theta. \qquad (C\text{-}15)$$

For more than one axle this result can be generalized easily using linear superposition.

The integral in Eq. C-15 can be evaluated to determine the permanent deformation at a particular point on the pavement. The quantity $h_\infty(\cdot)$ is treated as a simple influence function which is combined with the wheel load time history f(t) in the same way as for any elastic primary response component. The resulting time response is integrated throughout the duration of the vehicle passage. The result is the permanent vertical deformation of the road surface. For pavement rutting, $h_\infty(x)$ is the *rate of permanent vertical displacement* of the road surface.

The calculation correctly accounts for the distribution of permanent deformation through the pavement layers, assuming that all layers behave as linear viscoelastic materials. It accounts for the effect of the loading time during the integration stage, and so only one influence function $h_\infty(x)$ is needed (for each tire type), to include the effects of vehicle speed. Therefore it is *not* necessary to generate a new influence function for each speed. The effect of pavement temperature on rut generation can be included in the analysis by using lower viscosities for the layers near the surface, where the temperatures are high.

Results for Non-Dynamic Loads

Now consider the permanent deformation due to a non-dynamic moving load. Assume that the force is constant, f(t) = F, and moving with speed V. The integral in Eq. C-15 then becomes independent of distance x along the road, and it can be re-written

$$z(\infty) = F \int_{-\frac{x}{V}}^{\frac{x}{V}} h_\infty(V\theta)\, d\theta. \qquad (C\text{-}16)$$

If the distance $V\theta$ is replaced by the dummy integration variable $y = V\theta$, then Eq. C-16 becomes

$$z(\infty) = \frac{F}{V} \int_{-x}^{x} h_\infty(y)dy. \tag{C-17}$$

The integral in this equation is simply the area under the graph of the influence function $h_\infty(y)$.

Eq. C-17 is a useful result, because it shows that for a linear viscoelastic pavement model subject to moving static loads, the permanent deformation is directly proportional to the magnitude of the applied loads and inversely proportional to vehicle speed. Therefore deeper ruts can be expected on roads over which heavy vehicles travel slowly.

Sample Results

The road model shown in Figure C-11 was used for the permanent deformation analysis described throughout this appendix. The layer viscosities λ were chosen so that the *proportion* of the overall permanent deformation occurring within each layer (due to a static load) was the same as reported in the AASHO Road Test (*36*). These proportions are shown alongside the pavement model in Figure C-11. It can be seen that in both the AASHO test and in this model, 32% of the overall permanent deformation occurred in the asphalt surface, 14% occurred in the crushed stone road base, 45% occurred in the sub-base and 9% occurred in the subgrade. The viscoelastic Poisson's ratio was set to 0.5 in all the layers as discussed above.

The influence functions $h_\infty(\bullet)$ for each of the pavement layer interfaces are shown in Figure C-12. These were calculated for a single tire with a circular contact area. The area under each of these curves is related to the permanent deformation (at the particular depth) for moving static loads, as indicated by Eq. C-23. The influence function for the surface layer has a larger area than the rest, indicating that the permanent deformation at the surface is larger than the permanent deformation at the interface between surface and road base, etc. The influence function for deformation of the subgrade is quite small, because only 9% of the total permanent deformation occurred there in this model (and in the AASHO test). It can be seen that for radial distances greater than 20 inches, $h_\infty(\bullet)$ is negative, indicating slight *upwards* flow of material. This would manifest itself as a small ridge on either side of the central rut. For pavements with relatively more viscous lower layers and less viscous surface layers, this upwards flow can be quite large.

Figure C-13 shows the rut depth profile for a single pass of the 4-axle articulated vehicle traveling at 55 mph along 360 ft of the smooth asphalt highway. This rut depth profile was generated using the same wheel loads as the fatigue damage profile shown in Figure C-8. The mean rut depth is approximately 4×10^{-6} in for a single vehicle pass, indicating that a rut depth of 1/2 inch would take approximately 1.25 million vehicle passes to form.
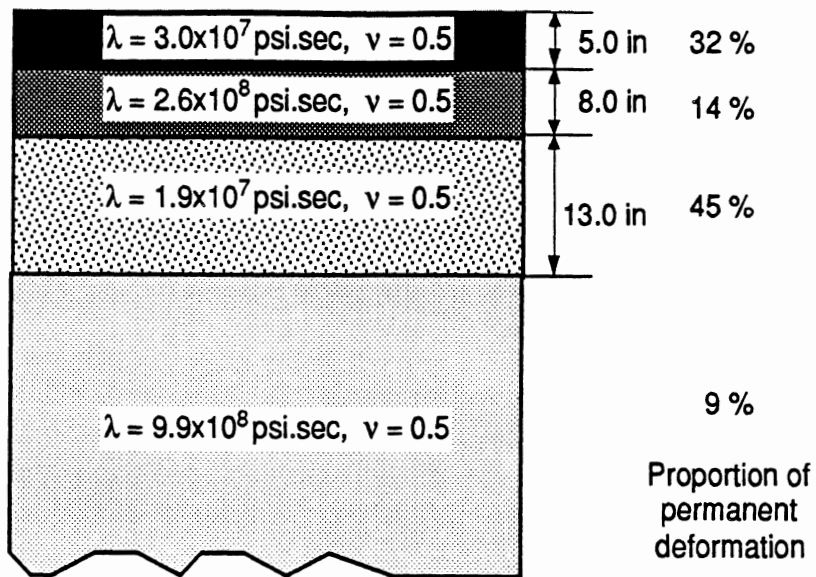
Figure C-11. Viscoelastic layered road model used for permanent deformation calculations.
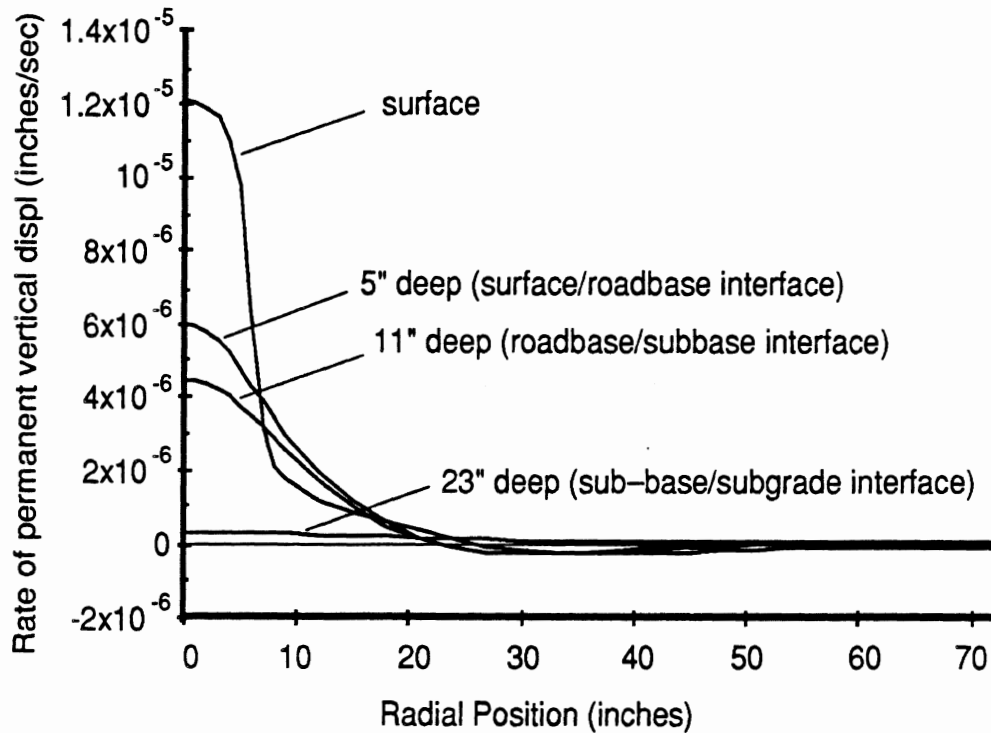
Figure C-12. Influence functions for the rate of permanent vertical displacement, generated by the viscoelastic layered response model.
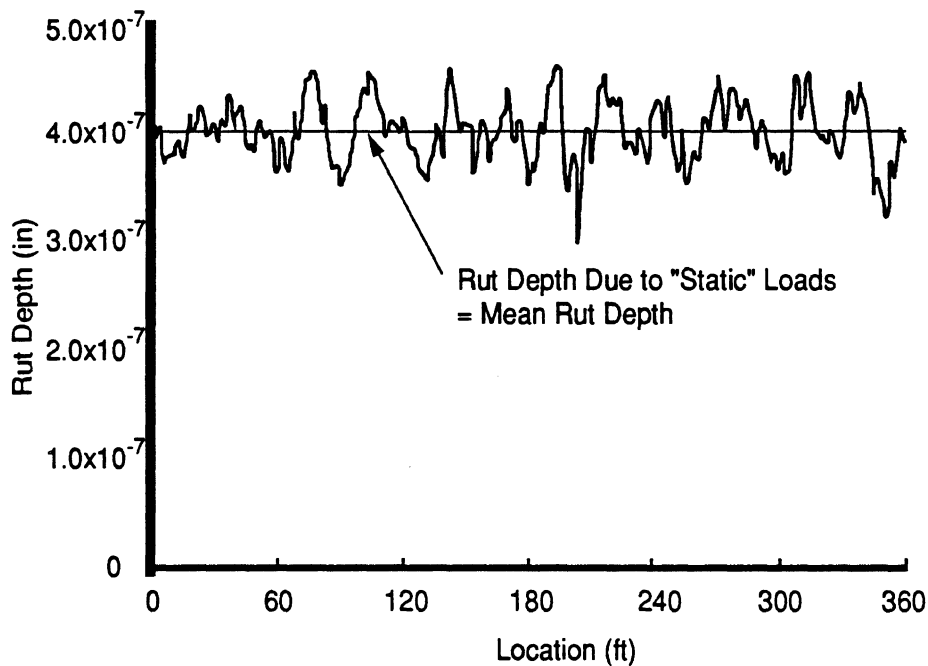
Figure C-13. Theoretical permanent deformation generated by a single pass of the 5-axle articulated vehicle at 55 mph on a smooth asphalt highway.

Comparison of Figures C-8 and C-13 indicates two important differences between the fatigue and permanent deformation criteria:

1. The mean rut depth is equal to the rut depth due to the static axle loads. Conversely, the mean level of the fatigue damage profile is 25% greater than the fatigue damage due to the static axle loads.

2. The variation in rut depth is only about ±20% of the mean, so that the maximum rut depth is approximately 1.2 times the rut depth due to static loads. The rut depth is therefore expected to be reasonably uniform along a road. Conversely, the peaks in the fatigue damage profile are up to a factor of 5 or 6 times the fatigue damage due to the static loads. These peaks are likely to be the cause of localized fatigue cracking (especially if the dynamic wheel loads are 'spatially repeatable'), and in extreme cases they will cause pot-holes.

These effects occur because of the high power k_2 in the fatigue damage Eq. C-7, which weights heavily the effects of dynamic strains (forces). On the other hand, the rut depth is essentially proportional to the magnitude of the wheel loads (Eq. C-21 and C-23), so the variation in rut depth is similar to the variation in the dynamic wheel loads used to generate the damage profiles, i.e., approximately ±20%.

These results agree qualitatively with observations on the highway. Wheel ruts are usually reasonably uniform in depth (with relatively small variations about the mean level), whereas fatigue cracks and the resulting pot-holes, usually occur in localized areas.

DATA ANALYSIS

The damage profiles shown in Figures C-8 and C-13 were classified into 64 discrete damage levels and the resulting "histograms" were converted into probability density functions. These are plotted in Figures C-14 and C-15. In both cases the damage plotted on the x-axis has been normalized by the damage due to the static axle loads. Figure C-14 shows that the fatigue damage distribution is skewed as a result of the weighting effect of the power k_2 in the fatigue damage equation. Conversely, Figure C-15 shows that the rut depth distribution is symmetrical and approximately Gaussian (Normal). This is expected because the dynamic wheel loads are Gaussian (*38-41*), and the rut depth is essentially proportional to the magnitude of the instantaneous wheel loads.

Figures C-14 and C-15 also show that there are a few points on the road which incur very large levels of fatigue damage (normalized fatigue damage of 3 to 6), whereas the normalized rut depth is always less than about 1.3. This is consistent with the observations in the previous section.

The *cumulative* probability distributions can be obtained by integrating the probability density functions (Figures C-14 and C-15) with respect to the damage (x-axis) level. This has the effect of smoothing-out the statistical scatter in the probability density functions. The cumulative probability distributions for both damage criteria are plotted in Figure C-16.
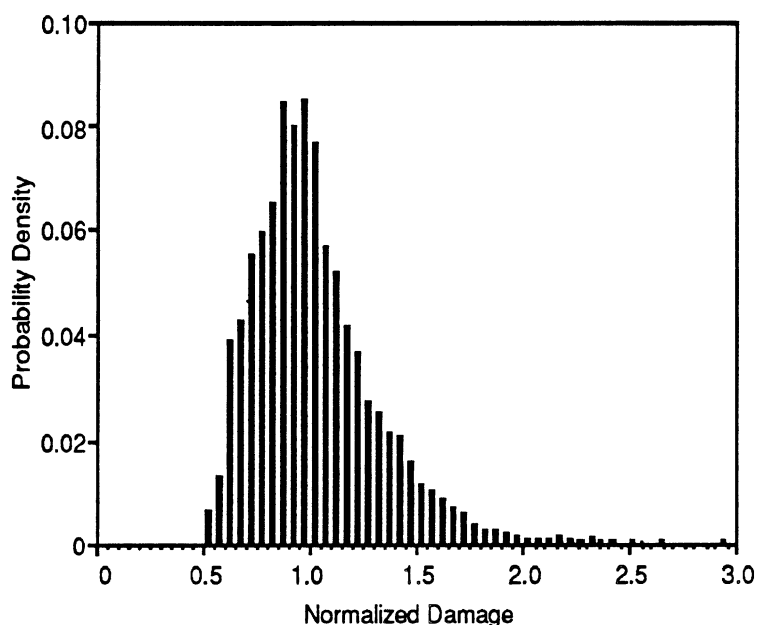
Figure C-14. Probability density functions of the normalized road damage profiles for fatigue.
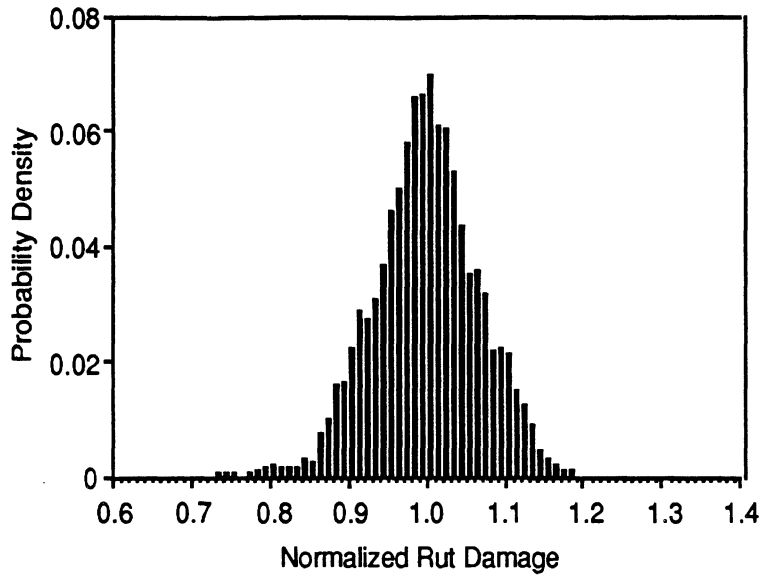
Figure C-15. Probability density functions of the normalized road damage profiles for rutting.
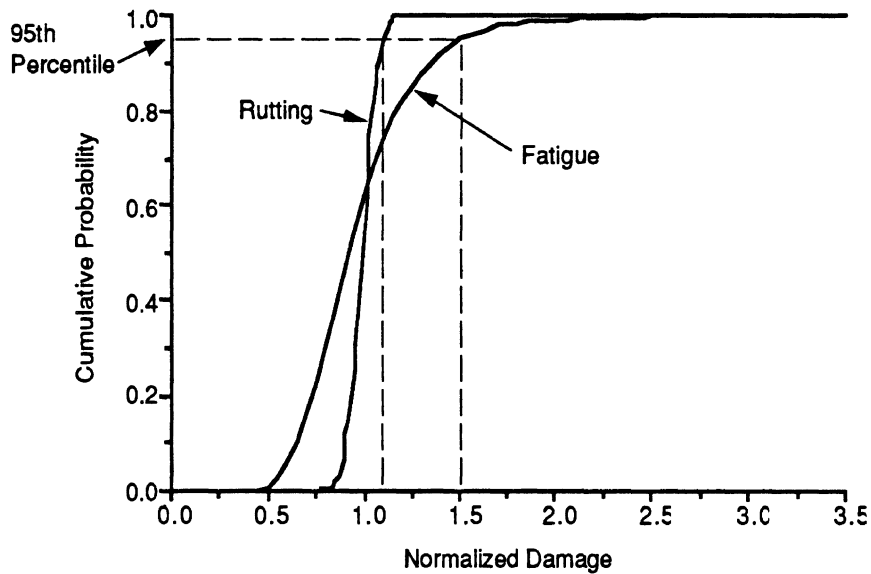
Figure C-16. Cumulative probability distributions, determined by integrating the probability density functions in Figures C-14 and C-15.

A useful statistic of damage due to dynamic wheel loads is the 95th percentile damage level (27,41). The basic premise is that 5% of the surface area of the road in the wheel paths incurs damage exceeding the 95th percentile level. Ultimate failure of the road surface is likely to be governed by the damage at these locations, particularly if the dynamic wheel

C—21

loads generated by the vehicle fleet are spatially repeatable. It is not necessary for the entire surface area of the road to fail before the road becomes unserviceable.

It can be seen from Figure C-16 that the 95th percentile normalized rut depth is approximately 1.12, and that the 95th percentile normalized fatigue damage is approximately 1.52. Therefore it can be concluded that 5% of the road surface area in the wheeltracks suffers rutting damage exceeding 1.12 times the rut depth due to the static loads, and 5% of the road surface suffers fatigue damage exceeding 1.52 times that due to the static loads.

Conclusions

1. From the above analysis it is apparent that dynamic wheel loads are very important when considering the fatigue of asphalt pavements. The damage levels are particularly sensitive to the value of k_2 in the fatigue damage relationship:

$$N = k_1 \, \varepsilon^{-k_2}.$$

2. For a single pass of a typical vehicle, traveling at 55 mph on a relatively smooth highway, the theoretical fatigue damage incurred at the worst 5% of points in the pavement is found to be approximately 1.5 times the damage due to the static axle loads.

3. If the vehicle fleet generates dynamic wheel loads that are "spatially repeatable," and the road is susceptible to fatigue cracking, then these high fatigue damage levels may be expected to result in premature failure at localized points on the road surface.

4. Permanent deformation of linear viscoelastic pavements depends more on the static axle loads and speed of the vehicle than on the dynamic wheel loads.

5. For a single pass of a typical vehicle, traveling at 55 mph on a relatively smooth highway, the theoretical rutting damage incurred at the worst 5% of points in the pavement is found to be approximately 1.1 times the damage due to the static axle loads.

FLEXIBLE PAVEMENT MATRIX

A family of flexible pavements was selected as a test bed for investigating how damage is related to truck characteristics. The objective in selecting the pavements was to achieve a representative sample from the spectrum of possible designs in order to minimize bias in the results.

Generally flexible pavements have four distinct parts; surface (asphalt concrete) course, base course, subbase course, and roadbed course or subgrade. There are various methods for the design of flexible pavements, but the one which is most widely accepted was developed by AASHTO (42). Table C-1 shows the matrix of pavement designs assembled for the study. The parameters in the table were selected to represent a range of designs that are compatible with current design practice, as described below.

AASHTO Design Procedure

Flexible pavement structural design involves the calculation of the different pavement layer thicknesses to provide a roadway that will achieve a given design life. The aim is to come up with the most economical design for a given life, magnitude and the volume of traffic, and material characteristics of the available subgrade, surfacing and paving courses. Though the most important and the critical factors are well recognized by pavement design engineers, various organizations have come up with different design procedures addressing their local problems and geographical conditions. Therefore, it is not uncommon for different designs to yield different pavement layer thicknesses for apparently identical variables.

Table C-1. Flexible Pavement Matrix.

Pavement Number	Traffic Volume	Surface Thickness (in)	Base Thickness (in)	Subbase Thickness (in)
1	Low	2.0	4.0	13.0
2	Low	3.0	6.0	13.0
3	Low	3.0	6.0	15.0
4	Low	3.0	6.0	16.5
5	Low	4.0	8.0	13.0
6	Medium	4.0	9.5	15.0
7	Medium	4.0	11.0	16.5
8	Medium	5.0	8.0	13.0
9	High	5.0	9.5	15.0
10	High	5.0	11.0	16.5
11	High	6.5	8.0	13.0
12	High	6.5	9.5	15.0
13	High	6.5	11.0	16.5

The two basic approaches to the calculation of layer thicknesses are based on either empirical procedures or mechanistic-empirical procedures. The empirical procedures depend upon observation or past experience. The basis of various empirical design methods is the relationship defining the interaction between performance, load and pavement thickness for a given climatic or geographic location. Generally the empirical methods are simple and easy to use. The AASHTO method is probably the most widely used of the empirical design methods.

The matrix of pavements given in Table C-1 consists of a range of pavement designs yielded by the AASHTO design procedure for a range of relevant design factors. These include: (1) reliability factor of 95%; (2) load applications of 1×10^6 for a low volume pavement, 5×10^6 for a medium volume pavement, and 40×10^6 for a high volume pavement; (3) a roadbed resilient modulus of 4500 psi; (4) moisture conditions in which the pavement structure is exposed to a moisture level approaching saturation 5 to 25% of the time; and (5) terminal serviceability at 2.5 PSI. Pavements 1 and 2 in the matrix are based on the minimum allowable thicknesses for surface and base courses in AASHTO design procedure. The flexible pavement matrix has been designed to cover structural numbers ranging from 2 to 6.5 in the different layers.

Table C-2 lists the elastic moduli and Poisson's ratios used for calculating stresses, and strains in all the pavements at surface temperatures of 77 and 120°F. The values shown were selected to match the material properties assumed in the AASHTO design procedure when the matrix was developed.

Creep behavior of the wear course was also included in the stress and strain calculations. Figure C-17 shows the relationship between strain and loading time that was used to characterize the creep behavior of the surface layer of all the pavements at 77°F. The effect of temperature on creep is incorporated by modifying the loading time based on temperature. The effective loading time is corrected by raising 10 to a power that is proportional to the difference in temperature from the reference temperature (77°F) at which the creep curve is given. The proportionality constant was set at 0.113 for all pavements. Other input parameters for VESYS such as the duration coefficients and variation coefficients were not used in primary response calculations. Therefore, no effort was made to rationalize the values used.

Table C-2. Flexible Pavement Layer Properties for Strain Calculations.

Layer	Elastic Modulus at 77°F (psi)	Poisson's Ratio at 77°F	Elastic Modulus at 120°F (psi)	Poisson's ratio at 120°F
Surface	1,000,000	0.33	470,000	0.33
Base	100,000	0.40	100,000	0.40
Subbase	25,000	0.40	25,000	0.40
Subgrade	2,500	0.40	2,500	0.40
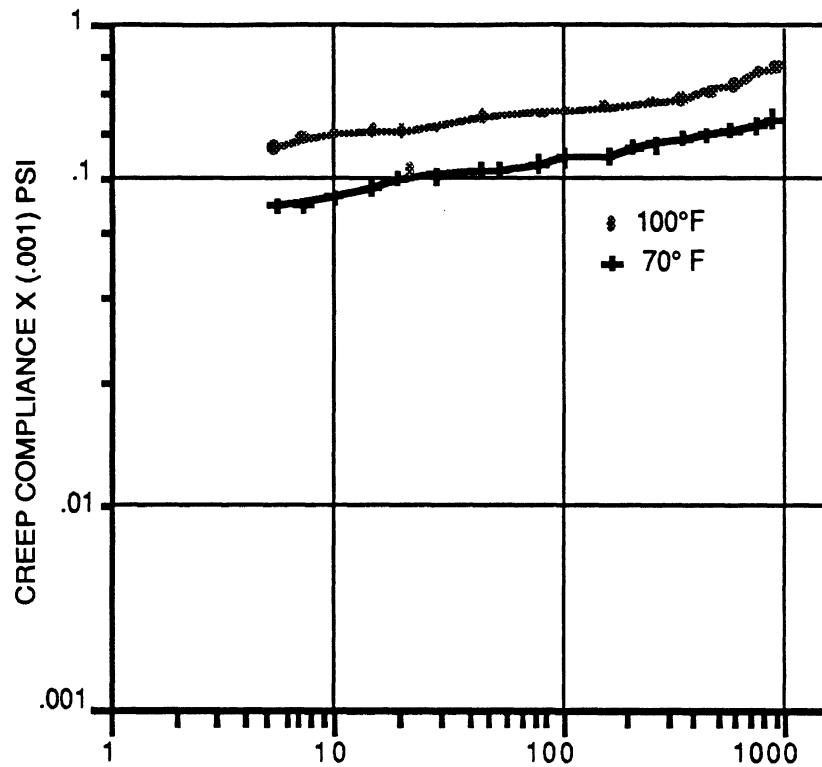
Figure C-17. Creep behavior for asphalt taken from (5).

Parameters Used for Rutting Analysis

Analysis of rutting behavior required development of a procedure to calculate the cumulative permanent deformation caused by the passing load. The analysis integrates the rate of vertical deformation throughout the period in which there is significant influence from the approaching or receding point of loading. Generally, this region does not extend beyond 100 inches from the point of loading. Figure C-12 shows an example an influence function used for rutting calculation.

At normal temperatures (77°F) the viscosities of the various pavement layers used for rutting analysis in all of the pavement designs considered were as follows:

Surface Layer	2.0×10^6
Base Layer	6.5×10^6
Subbase Layer	2.0×10^7
Subgrade	2.0×10^7

These values were based on the assumption that there is a relatively smooth temperature gradient throughout the pavement layers. For the purpose of simulating the effect of elevated temperatures (120°F) on the rutting, the pavement layers for the matrix of pavements defined in Table C-1 have been further subdivided as given in Table C-3. The viscosity values used for each pavement at a surface temperature of 120°F are given in the table. The surface layer in each pavement has been subdivided into two layers because at 120°F the temperature and viscosity change rapidly with depth near the surface.

Table C-3. Input Variable for Viscosity due to the Temperature Gradient in Different Layers of Flexible Pavements at a 120°F Surface Temperature.

Pavement Number	Viscosity (lb-s/in2)				
	Surface Layer (top half)	Surface Layer (bottom half)	Base	Subbase	Subgrade
1	13,000	23,000	1.2×10^5	1.4×10^6	5.0×10^6
2	14,000	52,000	1.4×10^5	1.4×10^6	5.0×10^6
3	14,000	52,000	1.4×10^5	1.4×10^6	5.0×10^6
4	14,000	52,000	1.4×10^5	1.4×10^6	5.0×10^6
5	19,000	60,000	5.0×10^5	1.4×10^6	5.0×10^6
6	19,000	60,000	5.0×10^5	1.4×10^6	5.0×10^6
7	19,000	60,000	5.0×10^5	1.4×10^6	5.0×10^6
8	23,000	140,000	5.0×10^5	1.4×10^6	5.0×10^6
9	23,000	140,000	5.0×10^5	1.4×10^6	5.0×10^6
10	23,000	140,000	5.0×10^5	1.4×10^6	5.0×10^6
11	27,000	140,000	7.0×10^5	1.4×10^6	5.0×10^6
12	27,000	140,000	7.0×10^5	1.4×10^6	5.0×10^6
13	27,000	140,000	7.0×10^5	1.4×10^6	5.0×10^6

REFERENCES

1. "BISAR: Bitumen Structures Analysis in Roads User's Manual." Koninklijke/Shell Laboratorium, Shell Research N.V., Amsterdam (1978).

2. Ahlborn, G., "ELSYM5, A Computer Program for the Analysis of Elastic Layered System with Normal Loads." The Institution of Transportation and Traffic Engineering, University of California at Berkeley (1972).

3. Van Cauwelaert, F.J., et al. "A Component Multi-layer Solution and Back Calculation Procedure for Personal Computers." *American Society of Testing and Materials STP 1026* (1988).

4. Raad, L. and J.L. Figueroa., "Load Response of Transportation Systems." *Journal of the Transportation Engineering Division,* American Society of Civil Engineers. Vol. 106, No. TE2 (1980) pp. 111-128.

5. Kenis, W.J., "Predictive Design Procedure, VESYS User Manual." *Federal Highway Administration, FHWA-RD-77-154* (1977).

6. Hardy, M.S.A. and Cebon, D., "On the Response of Continuous Pavements to Moving Dynamic Loads: Part 1 Theory and Experimental Validation." Submitted to ASCE Journal of Engineering Mechanics (1991).

7. Hardy, M.S.A. and Cebon, D., "On the Response of Continuous Pavements to Moving Dynamic Loads: Part 2 Influence of Vehicle Loading Parameters." Submitted to ASCE Journal of Engineering Mechanics (1991).

8. Hardy, M.S.A. and Cebon, D., "The Response of a Flexible Pavement to Moving Dynamic Loads." *Proc. Inst. Acoustics*. Vol. 10, Part 2 (1988) pp. 485-492.

9. Collop, A.C., "Effects of Traffic and the Environment on Road Damage." Cambridge University Engineering Department, Project Report (1991).

10. Papagiannakis, T., et al., "Heavy Vehicle Equivalence Factors from In-Situ Pavement Strains." RTAC Annual Conference, St John's, Newfoundland. *Proceedings* (1990).

11. Peattie, K.R., *Developments in Highway Pavement Engineering*. Chapter 1. "Flexible Pavement Design." P. S. Pell ed., Applied Science Publishers Ltd, London. (1978).

12. Thrower, E.N., "A Parametric Study of a Fatigue Prediction Model for Bituminous Road Pavements." *Transport and Road Research Laboratory, Laboratory Report LR892* (1979) 19 p.

13. Uzan, J. and Lytton, R.L., "Structural Design of Flexible Pavements: A Simple Predictive System." *Transportation Research Record*, No. 888 (1981) pp. 56-63.

14. Christison, J.T., et al., "In Situ Measurements of Strains and Deflections in a Full-Depth Asphaltic Concrete Pavement." *Proc. Assoc. Asphalt Paving Technology*, Vol. 47 (1978) pp. 398-430.

15. Dietmann, H., et al., *Fatigue Under Biaxial and Multiaxial Loading*. "Multiaxial Fatigue Behavior of Steels Under In-Phase and Out-of-Phase Loading, Including Different Wave Forms and Frequencies." K. F. Kussmaul, D. L. McDiarmid and D. F. Socie ed., Mechanical Engineering Publications Ltd, London (1991) pp.449-464.

16. Hoffmann, M., et al., *Fatigue Under Biaxial and Multiaxial Loading*. "Local Strain Approach in Non-Proportional Loading." K. F. Kussmaul, D. L. McDiarmid and D. F. Socie ed., Mechanical Engineering Publications Ltd, London (1991) pp. 357-376.

17. Jordan, E.H., et al., *Multiaxial Fatigue*. "Fatigue Under Severe Nonproportional Loading." K. J. Miller and M. W. Brown ed., ASTM Special Publication 853, Philadelphia. (1985) pp. 569-585.

18. Lefebvre, D., et al., *Fatigue Under Biaxial and Multiaxial Loading*. "Strain Parameters for Fatigue Life Prediction Under Out-of-Phase Biaxial Fatigue." K. F. Kussmaul, D. L. McDiarmid and D. F. Socie ed., Mechanical Engineering Publications Ltd, London (1991) pp. 433-448.

19. Brown, S.F., *Developments in Highway Pavement Engineering*. Chapter 2. "Material Characteristics for Analytical Pavement Design." P. S. Pell ed., Applied Science Publishers Ltd, London (1978).

20. Goddard, R.T.N., et al., "Fatigue Resistance of Dense Bituminous Macadam: The Effect of Mixture Variables and Temperature." *Transport and Road Research Laboratory, Supplimentary Report SR410* (1978) 26 p.

21. Maupin, G.W., "Test for Predicting Fatigue Life of Bituminous Concrete." *Transportation Research Record,* No. 659 (1977) pp. 32-37.

22. Francken, L. and Verstraeten, J., "Methods for Predicting Moduli and Fatigue Laws of Bituminous Road Mixtures Under Repeated Bending." *Transportation Research Record,* No. 515 (1974) pp. 114-123.

23. Francken, L., "Fatigue Performance of a Bituminous Road Mix Under Realistic Test Conditions." *Transportation Research Record,* No. 712 (1979) pp. 30-37.

24. Fuchs, H.O. and Stephens, R.I., *Metal Fatigue in Engineering*. John Wiley and Sons. New York (1980) Chapter 10.

25. Cole, D.J. and Cebon, D., "Simulation and Measurement of Dynamic Tyre Forces." Second International Symposium on Heavy Vehicle Weights and Dimensions, Kelowna, Canada. *Proceedings* (1989).

26. Christison, J.T., "Pavements Response to Heavy Vehicle Test Program: Part 2 - Load Equivalency Factors." *Vehicle Weights and Dimensions Study, Vol. 9. Canroad Transportation Research Corporation* (1986) 79 p.

27. Cebon, D., "Theoretical Road Damage Due to Dynamic Tyre Forces of Heavy Vehicles. Part 2: Simulated Damage Caused by a Tandem-Axle Vehicle." *Proc. I.Mech.E.,* Vol. 202, No. C2 (1988) pp. 109-117.

28. Majidzadeh, K. and Ilves, G.J., "Methods for Determining Primary Response Load Equivalency Factors." FHWA Load Equivalence Workshop, McLean VA. *Proceedings* (1988) 20 p.

29. American Society of Testing and Materials, *ASTM Annual Book of ASTM Standards.,* Vol. 03.01 Standard E 1049-85 (1986).

30. American Association of State Highway and Transportation Officials, *Report of the AASHTO Joint Task Force on Rutting.* AASHTO, Washington, D. C. (1986).

31. Thrower, E.N., et al., "Methods for Predicting Permanent Deformation - Flexible Pavements." *Transport and Road Research Laboratory, Contracts Report CR38* (1986) 36 p.

32. Thrower, E.N., "Permanent Deformation - A Linear Viscoelastic Model of a Road Pavement." *Transport and Road Research Laboratory, Supplimentary Report SR184UC* (1975) 16 p.

33. Haas, R.C.G. and Papagiannakis, A.T., "Understanding Pavement Rutting." Special Workshop on Rutting in Asphalt Pavements, Toronto, Roads and Transport Association of Canada. *Proceedings* (1986) 30 p.

34. Newland, D.E., *An Introduction to Random Vibrations and Spectral Analysis, 2nd Edition*. London, New York, Longman (1984).

35. Eisenmann, J. and Hilmer, A., "Influence of Wheel Load and Inflation Pressure on the Rutting Effect at Asphalt-Pavements - Experiments and Theoretical Investigations." Sixth International Conference on the Structural Design of Asphalt Pavements, Ann Arbor, *Proceedings* (1987) pp.392-403.

36. American Association of State Highway and Transportation Officials, *The AASHO Road Test. Report 5, Pavement Research*. Highway Research Board Report 61E (1962) 352 p.

37. Cebon, D., "Theoretical Road Damage Due to Dynamic Tyre Forces of Heavy Vehicles. Part 1: Dynamic Analysis of Vehicles and Road Surfaces." *Proc. I.Mech.E.*, Vol. 202, No. C2 (1988) pp. 103-108.

38. Dickerson, R.S. and Mace, D.G.W., "Dynamic Pavement Force Measurements with a Two-Axle Heavy Goods Vehicle." *Transport and Road Research Laboratory, Supplimentary Report SR688* (1981) 14 p.

39. Hahn, W.D., "Effects of Commercial Vehicle Design on Road Stress - Quantifying the Dynamic Wheel Loads for Stage 3: Single Axles, Stage 4: Twin Axles, Stage 5: Triple Axles, as a Function of the Springing and Shock Absorption System of the Vehicle." *Institut fur Kruftfahrwesen, Universitat Hannover, Report No. 453*. Translated by TRRL as WP/V&ED/87/40 (1987).

40. Sayers, M. and Gillespie, T.D., "The Effect of Suspension System Nonlinearities on Heavy Truck Vibration." Seventh IAVSD Conference on the Dynamics of Vehicles on Roads and on Tracks, Cambridge, U.K. *Proceedings* (1981) 13 p.

41. Sweatman, P.F., "A Study of Dynamic Wheel Forces in Axle Group Suspensions of Heavy Vehicles." *Australian Road Research Board Special Report 27* (1983) 65 p.

42. American Association of State Highway and Transportation Officials, *The AASHTO Guide for Design of Pavement Structures*. AASHTO, Washington, D. C. (1986).

VEHICLE DYNAMICS MODELING

This appendix describes the analytical methods used to determine the dynamic response of trucks and tractor-trailer combinations for purposes of determining the instantaneous wheel loads as they move along the road. The first section, Background, details the pitch-plane models that were employed in this study. Although the methods were largely analytical, some experimental measurements were made available by other cooperating organizations as a basis for validating the computer models. The section, Validation, presents that measured data, and shows comparisons between measurements and predictions from the truck models. This appendix concludes with a section, Truck Matrix, that presents the full matrix of vehicles that were simulated in the study, along with the rationale for their selection and a discussion of the sources of the parameter values selected to represent the trucks.

BACKGROUND

From the point of view of the pavement, a truck is a moving, time-varying set of contact stresses applied at the pavement surface. The stresses applied by the tires are determined by: (1) the static load carried by each tire; (2) the dynamic variation in load at each tire; (3) the nature of the pressure distribution (normal stress) arising from the total load (static and dynamic) which is applied to the surface under the tire; and (4) in-plane forces which are applied to the surface in the form of shear stresses.

The motions of the various components in a vehicle can be predicted mechanistically by solving differential equations that describe the dynamics and kinematics of its primary components. The equations are complicated and are therefore solved by a process that simulates the vehicle on a computer at discrete instants of time, separated by a very small "time step." There are many computer codes available for simulating motions of multi-body mechanical systems such as vehicles. However, in order to accurately predict pavement load, the model must deal properly with the peculiar nonlinear properties of the springs in heavy truck suspensions, the kinematics of the load-sharing tandem axles, and the sequential input of a single road profile into the various axles. In addition, the scope of the simulation activities required for this research places a premium on computational efficiency. The need for computational efficiency is further motivated by the data requirements associated with obtaining valid statistics for each simulated condition.

A variety of computer models of vehicles are available that are capable of predicting the variables of interest. However, most are unfeasible for this project due to computational considerations. General purpose analysis programs such as NASTRAN, ADAMS, DADS, and others have been used in the past to simulate vehicles (1-3). However, due to their generality, they are very inefficient. Selection of this type of program would require that the computations for the project be performed on a supercomputer. The next level of complexity is a full scale vehicle simulation, such as the FHWA program T3DRS developed by UMTRI, or similar programs such as the UMTRI Phase-4 or Yaw-Roll

Model (4). These computer codes are specifically written for vehicle dynamics applications and are much more efficient for that purpose than the general-purpose codes. They can compute performance in cornering, rolling, and braking, as well as pitch-plane response to pavement roughness. However, they are not set up to do so efficiently and are not optimal for use in this type of project.

Prediction of dynamic wheel loads is best made by a special-purpose computer code using a vehicle model with the pertinent degrees of freedom, but without degrees of freedom that are extraneous to the problem. Several research organizations have developed models falling in this category, including MIT, the University of Cambridge, and UMTRI. Further, almost every analytical study involving dynamic loading of pavement by moving vehicles has included a vehicle dynamics model developed for that study (5). In every case, the models are planar, with pitch being the only form of rotation allowed. (Pitch is the rotation seen by an observer from the side of the vehicle.) At UMTRI, a computer program called the UMTRI Pitch-Plane Model has been in use for several years prior to the project. It contains the pertinent aspects of vehicle behavior, and is designed to accept measured road profiles as input. The outputs are standardized files compatible with a library of pre- and post-processing software at UMTRI. This model was written under the sponsorship of several vehicle manufacturers to provide a design tool for studying effects of component design on ride vibrations and various forces in the system, including pavement loads.

A new software development tool became available during the research project. The software package, called AUTOSIM™, was developed at UMTRI to **automatically** generate computationally efficient simulation programs for mechanical systems composed of multiple rigid bodies (6,7). It formulates the equations of motion symbolically, and then writes a special-purpose program to solve them. Rather than modifying old simulation programs such as the original UMTRI Pitch-Plane Model to meet the requirements of the project, new programs were generated by AUTOSIM. The end result is no different than if the computer code was manually written. However, because the FORTRAN code is written by computer, efficient and error-free code can be prepared to represent each of the vehicle configurations of interest in a matter of a few hours.

DESCRIPTION OF PITCH-PLANE MODELS

All of the vehicle simulations for this project were run using a set of pitch-plane models. A different computer code exists for each vehicle configuration. These codes are written in the FORTRAN computer language, and are largely generated automatically using AUTOSIM. All of the codes draw on the same library of computer subroutines that represent elements in the vehicle.

Rigid-Body Kinematics and Dynamics

For purposes of predicting dynamic wheel loads the vehicle may be treated as several rigid bodies constituting lumped masses connected by compliant linkages. The vehicle body supported by suspension systems at each axle is the primary mass, and is appropriately designated as the "sprung mass." The sprung mass is considered rigid with mass properties concentrated at its center of gravity and a moment of inertia about the center

of gravity in the pitch plane. The additional masses significant to dynamic wheel load performance are those concentrated at each axle arising from the mass of the axle, brakes, steering knuckle, wheels, and portions of the suspension linkage. These are denoted as "unsprung masses."

The treatment of the various masses as rigid bodies ignores structural vibrations of the individual components. Unsprung masses generally have no structural vibration modes within the frequency range of interest (0 - 20 Hz). Trucks, tractors, and trailers usually have frame-bending vibration modes within this frequency range. While these may be significant to vibrations present on the body of the vehicle (the ride behavior), in general they have little influence on the loads experienced under the tires.

The full vehicle models used in this project consist of trucks (single-unit vehicles), tractor-semitrailers (articulated vehicles connected by a fifth wheel that allows pitch rotation), and full-trailers (single-unit vehicles which do not dynamically interact with the pitch-plane motions of the towing unit). Together, tractor and trailer sprung masses have three degrees of freedom (d.o.f.); bounce of the tractor, pitch of the tractor, and pitch of the trailer. In addition, each of the axles has a bounce d.o.f. Thus, a 5-axle tractor-semitrailer is modeled with a total of eight d.o.f. The layout of a tractor-semitrailer is shown in Figure D-1 as an example of the modeling. In the figure, the suspensions are all shown as being independent, even though other suspensions are often used.
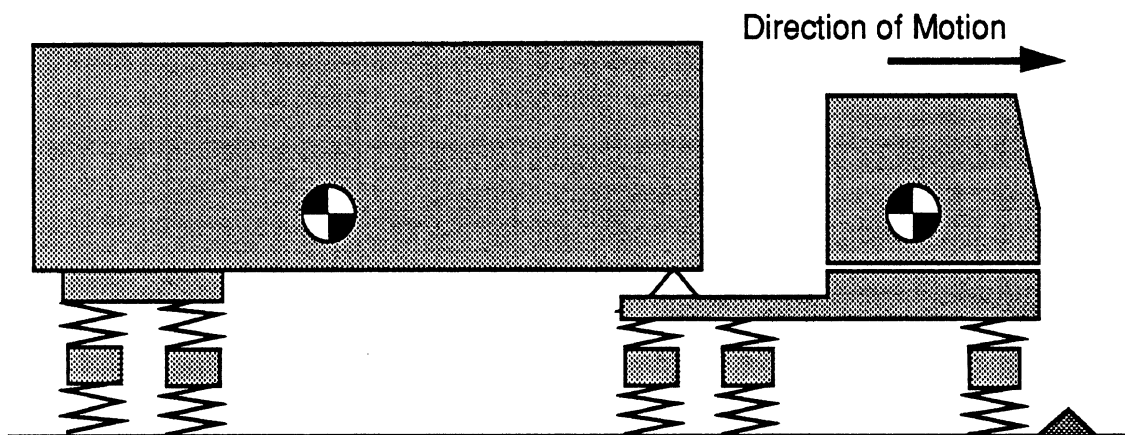
Figure D-1. Rigid body model of a tractor-semitrailer.

When other vehicle configurations are simulated, the number of degrees of freedom may be different. For example, a 2-axle truck or bus has a total of 4 d.o.f.; two for the body, and one for each axle. The actual form of the axle d.o.f. is dependent on the type of suspension, as discussed below.

The kinematics and dynamics of the tandem suspension configurations in use have been modeled as shown in Figure D-2. All springs are shown as a leaf-springs. However, the same mathematical model is used to describe leaf springs and air-springs differing only in the parametric values necessary to describe their characteristics. Degrees of freedom are indicated with the arrows. The four-leaf suspension has three degrees of freedom, to

Figure D-2. Tandem suspension schematics.

account for the free movement of the equalizer link. However, in the model, the inertial properties of the link are not significant. Including the inertial properties results in dynamical equations of motion that are "stiff" and require an order of magnitude more computation to predict vehicle motions. Instead, a quasi-static solution method is used to account for the load-equalization and the frictional behavior of the link. The motion and friction torque are computed and can be plotted.

UMTRI Spring Model

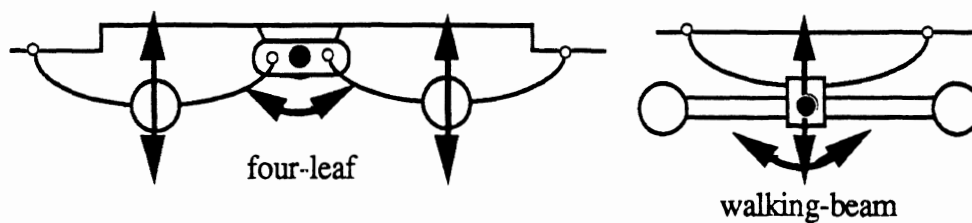A key system that must be modeled properly in order to accurately predict dynamic load performance of heavy trucks is the suspension spring, particularly leaf springs. Truck leaf springs, as well as other suspension components, exhibit a high magnitude of friction in their operation which produces complex force-displacement characteristics. Figure D-3 shows the force-displacement characteristics for a typical truck leaf spring measured experimentally in the Suspension Parameter Measurement Facility at UMTRI (8). This type of performance arises from the fact that friction between the leaves (inter-leaf friction) affects the force-displacement behavior. When the spring is being compressed (upper curve) friction adds to the force, while in the extension direction (lower curve) friction reduces the force. As a consequence the force-displacement behavior follows the complex intermediate curves for the small displacements typical of ride motions. Modeling this behavior is essential to duplicating the appropriate stiffness and damping properties in the suspension.
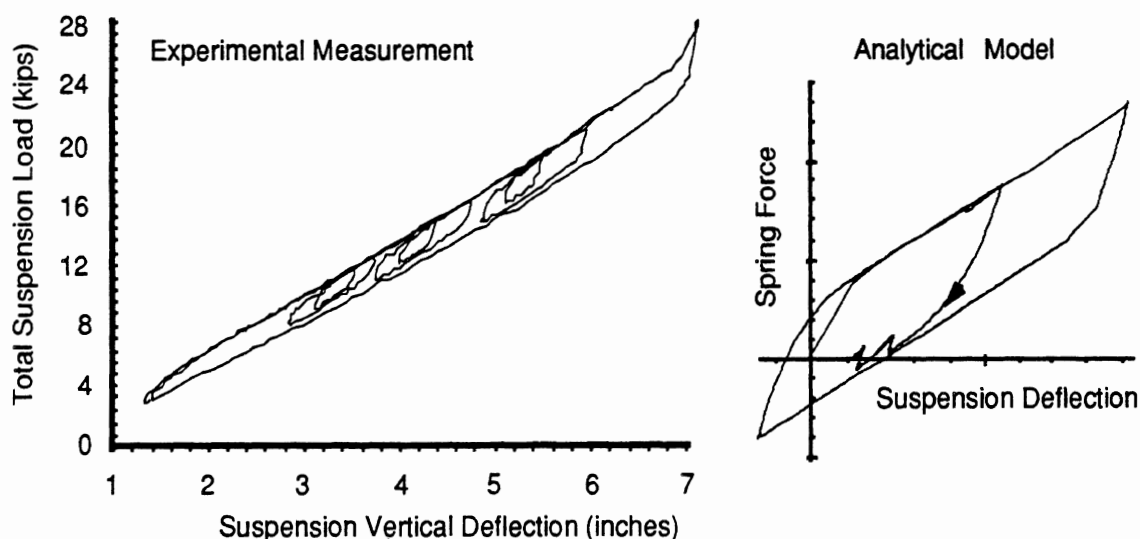

Figure D-3. Force-displacement properties of a leaf spring.

Figure D-3 also shows the behavior of the analytical model used to replicate leaf springs over the small displacements typical of ride motions. The model is based on representing the force properties of the system on a nominal stiffness plus a "coulomb" friction force dependent on previous motions and the direction of displacement. This model is derived from previous research at UMTRI and has been used in countless simulations of truck behavior and is documented elsewhere (9).

This type of behavior is inherent not only to leaf springs, but to many other components of a truck suspensions. Therefore, the model is useful for replicating friction effects from other components in truck suspensions even though other spring elements (such as air-springs) may be used. This model is used for all suspension systems, varying only in the kinematics or parameter values to distinguish the various suspension types.

Tire Model

The tire is a visco-elastic toroid that supports the unsprung mass on the road surface. Tires are modeled as springs and dampers connecting the axles to the ground. The tire springs and dampers are simple linear elements while in contact with the ground. Should the tire leave the ground, the tire force is set to zero (the ground cannot pull back on the tire). Tire damping is set automatically at 6 lb-sec/in, based on laboratory measurements described in the Validation section of this Appendix.

Profile Input

The road surface is described by a series of road elevation values spaced at fixed intervals along the road. The road surface is assumed to be straight (constant slope) between these points. The elevation in the tire contact patch is averaged over the length of contact to reflect the envelopment properties of the tires (10). The road profiles were synthesized on a custom basis to be representative of the spectral characteristics of the type of road surface under consideration. The synthesis process involves use of a random number generator along with algorithms that create random elevation profiles with the amplitude-wavelength characteristics typical of rigid or flexible road surfaces. In the case of rigid pavements, the profiles were modified by the addition of periodic components to replicate the effects of features characteristic of slab construction (faulting, slab-tilt, etc.). Details on the road profiles and their roughness characteristics are presented in Appendix E.

Output Variables

The pitch-plane model can list any of the variables computed in the simulation. The output required for application in the pavement analysis is quite brief; the instantaneous wheel loads and positions at each step of the simulation. These are written to a standard file format (ERD files) along with header data that identifies the vehicle, road surface, speed, engineering units, etc. The use of a standardized file format with identifier information eliminates errors in file management.

On occasion additional information was output from the simulations to aid diagnostics or for validation studies. These included such information as suspension forces and motions, and sprung mass motions (bounce and pitch).

VALIDATION

There were several types of experimental measurements used in this study. First, a test vehicle was provided and instrumented by PACCAR for use in on-road tests on a test track at the PACCAR proving grounds whose longitudinal profile had been measured. These measures were used to determine how well the pitch-plane model predicts loads when given the true measured road roughness profile. Second, the same vehicle was run over instrumented pavements in Illinois. These results were used to determine how well the ILLI-SLAB pavement analysis program predicts strains in the pavement due to known vehicle loads (see Appendix B). The third set of experimental data involved measurements of suspension behavior on other trucks taken in a laboratory using dynamic shaker facilities. These results were used to determine how the model predicts dynamic inter-axle load transfer behavior.

On-Road Response to Measured Profile

The test vehicle was a 3-axle Peterbilt tractor pulling a 2-axle trailer. The rear suspensions on the tractor and trailer were both four-spring suspensions.

Most of the parameters needed to describe the tractor were measured on UMTRI facilities. The spring rates and friction properties for the three axles were measured in the Suspension Parameter Measurement Facility at UMTRI (8). In the measurements, both axles are moved up and down together in the absence of roll and inter-axle load transfer. The center of gravity location and pitch moment of inertia was measured on the UMTRI pitch-plane inertia swing. All axle static loads were measured at the time of testing. For the trailer, the inertia properties were computed from drawings of the vehicle and the locations of the weights. Tire properties were estimated, based on published data for similar tires. Also estimated were the spring properties for the trailer.

The instrumented test vehicle was run over three sites at the PACCAR Test Center; (1) a quarter-mile section of the high-speed track, (2) a quarter-mile portion of a smooth section in the durability track (the smooth section by-passes the "hazards" used in durability testing), and (3) a "bump" test on a section of pavement several hundred feet in length.

The purpose of the bump tests was to obtain measurements of the vehicle responding to a known simple input. When the measured variables were processed and viewed, it was found that the response was dominated by the background roughness of the test site which had not been measured. The bump itself had a very small influence on the vehicle motions; hence, no further analysis of the data was attempted.

The sections on the high-speed track and the durability track were profiled with the FHWA PRORUT system in July, 1989. Therefore, the profiles were available as inputs to the pitch-plane model. In the course of the analysis the profile for the right-hand wheel path was found to be peculiar in ways that led to the conclusion that one of the accelerometers on the profilometer had an intermittent problem. As a result the profiles were sometimes accurate, but other times, included an error.

Using the profile from the left-hand wheel path as input to the pitch-plane model, reasonable agreement between the test vehicle and the model were observed. Power spectral density (PSD) functions were computed for the measured and simulated variables,

to: (1) reduce the entire quarter-mile of test data into a summary description that can be meaningfully plotted; and (2) reveal in the frequency domain where the model and test data agree and where they do not. Example results given in Figures D-4 and D-5, showing the PSD functions for the vertical force on the front axle and trailing tandem axle, at test speeds of 36 mph and 51 mph.

In the figures, one of the main differences between the measured and simulated forces for the trailing tandem axle is due to a nonuniformity of the wheel. The approximate 11.5-ft circumference corresponds to a frequency of 4.6 Hz at 36 mph, and 6.5 Hz at 51 mph. This effect is easily included in the simulation as a sinusoidal forcing function. (However, we see no reason to make this addition.)

The agreement between the model and the test data in Figures D-4 and D-5 show that the model does an excellent job of predicting the significant dynamics of the two axles of the tandem suspension, which carry the high loads. The PSD functions for the leading tandem axle, which are not shown, are virtually identical to those of trailing axle for a given test condition. The agreement on the front axle, while not as close, is still acceptable. The major significant modes of vehicle vibration are replicated with about the correct amplitudes and frequencies.

Note that the parameters used to describe the vehicle were determined independently of the test results. That is, none of the model parameters were adjusted to improve agreement.

As a result of this exercise, it is concluded that the pitch-plane model is suitable for predicting the dynamic load of heavy trucks, with confidence that the predicted behavior matches reasonably well the behavior of real trucks.

Laboratory Measures of Dynamic Inter-Axle Load Transfer

Separate tests were required to obtain experimenal data by which to characterize the dynamic behavior of tandem suspensions. Several of the major truck manufacturers have hydraulic road simulators that can apply vertical inputs independently at each wheel for investigating vibration behavior in the laboratory. During the setup of a vehicle combination they will often perform a "remote parameter characterization" (RPC) in which the transmissibility to various points on the vehicle is measured with road inputs at each wheel. RPC data for 4-spring and air-spring tandem suspensions was obtained from cooperating truck manufacturers as a reference for validating the models.

The most popular tandem suspension used on heavy trucks in the U.S. has four leaf springs. The leading and trailing axle leaf springs on each side of the vehicle lift against a balance (equalizer) beam in the center in an effort to obtain equal loads on both axles. A side view of the basic layout of a 4-spring suspension is shown in Figure D-6. The tandem suspension in the truck pitch-plane model emulates this system using leaf spring models on top of each axle with one end of each leaf spring loaded against an equalizer beam. The moment on the beam is balanced except for coulomb friction which inhibits its motion.

When one axle goes over a bump, the balance beam pivots in an effort to keep both axles at the same load. In the dynamic circumstances of road bumps encountered at high speed, the equalization is imperfect. The dynamic equalization behavior is characterized by the transmissibility of bumps at one axle causing vibrations at the other.
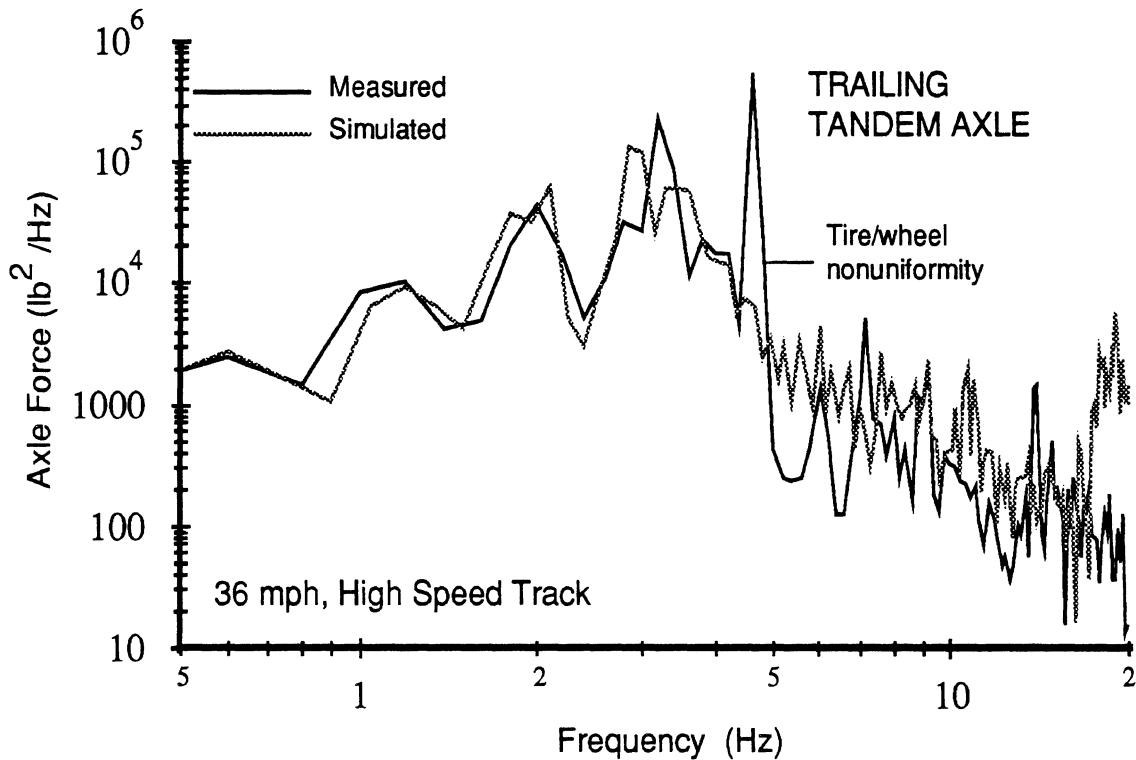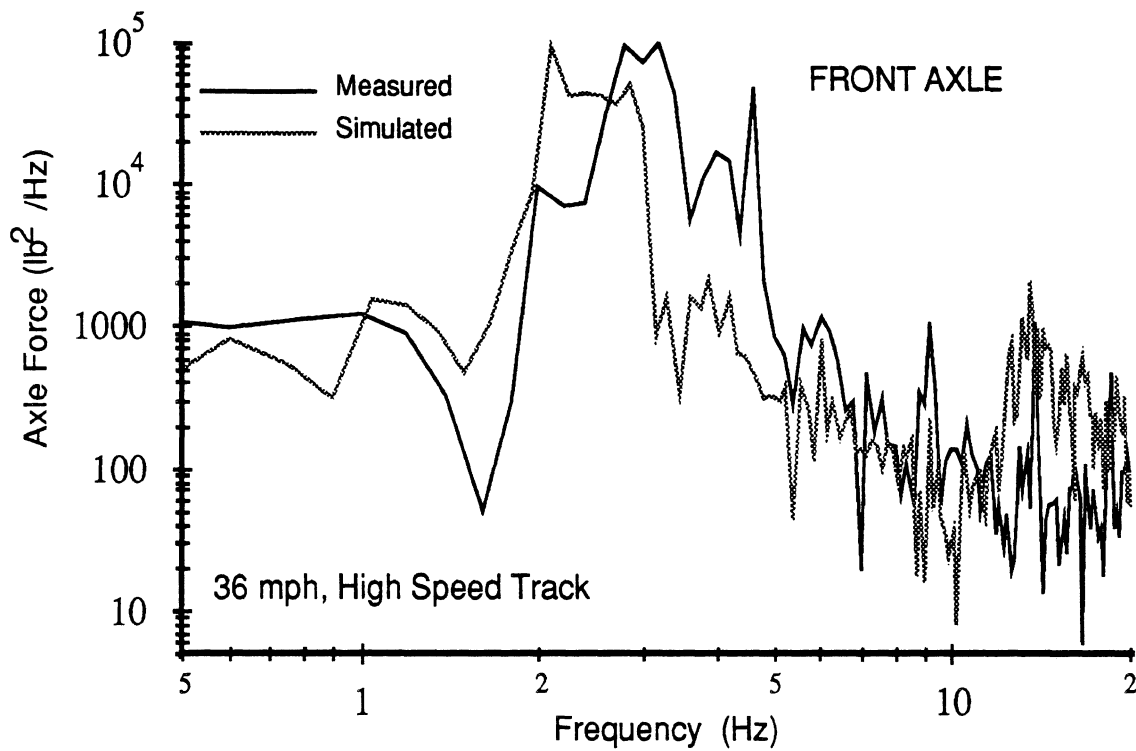
Figure D-4. Power spectral densities of axle force at 36 mph on the PACCAR test track.
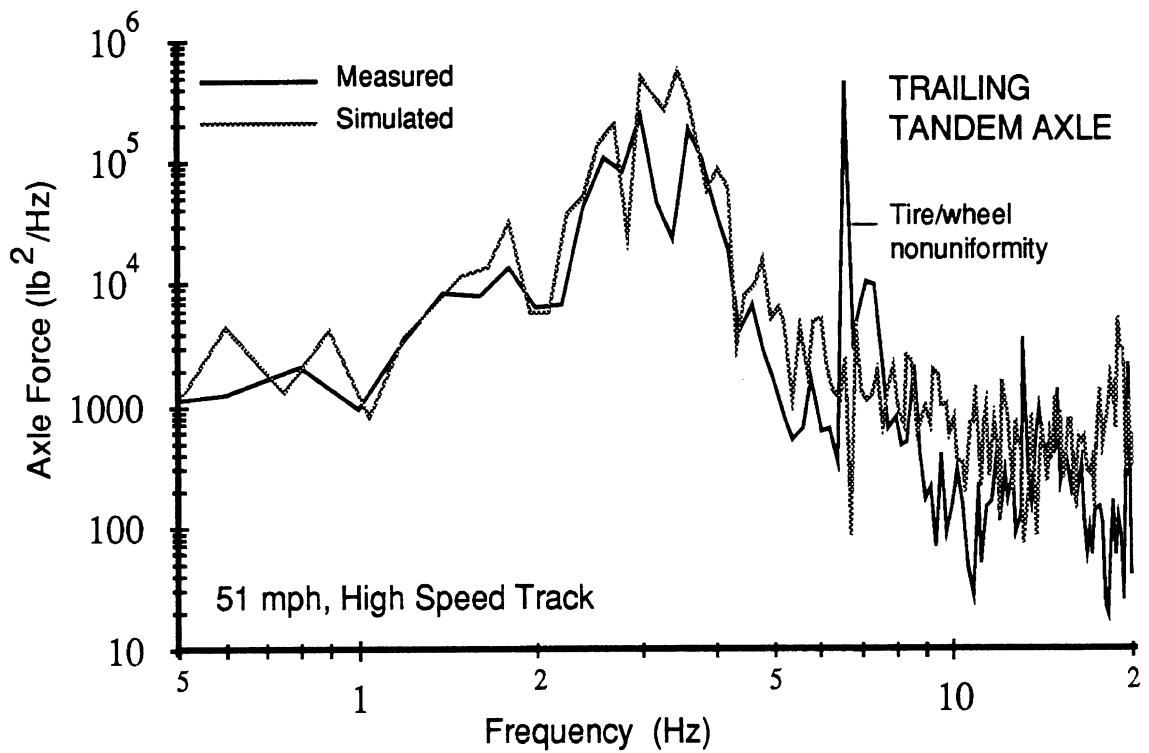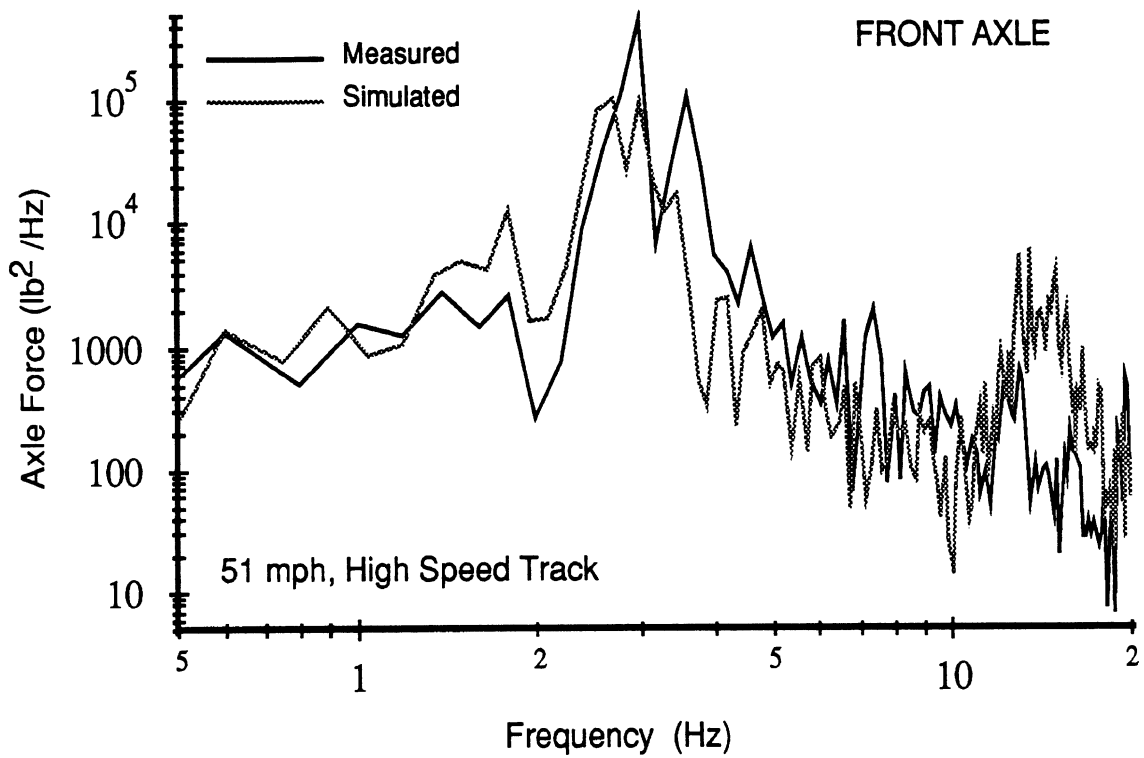
Figure D-5. Power spectral densities of axle force at 51 mph on the PACCAR test track.

In an effort to validate the 4-spring suspension computer model the truck simulation was given a random, narrow band excitation at the leading axle while the acceleration response on the trailing axle was calculated (a simulation analogous to the RPC experiments). Initial parameter values to describe the suspension were obtained from quasi-static truck suspension measurements on the Suspension Parameter Measurement Facility at UMTRI. The parameters were then varied in a parametric sensitivity study. Figure D-7 shows the comparison of dynamic behavior of the truck simulation model against experimental measurements obtained from the truck manufacturer.
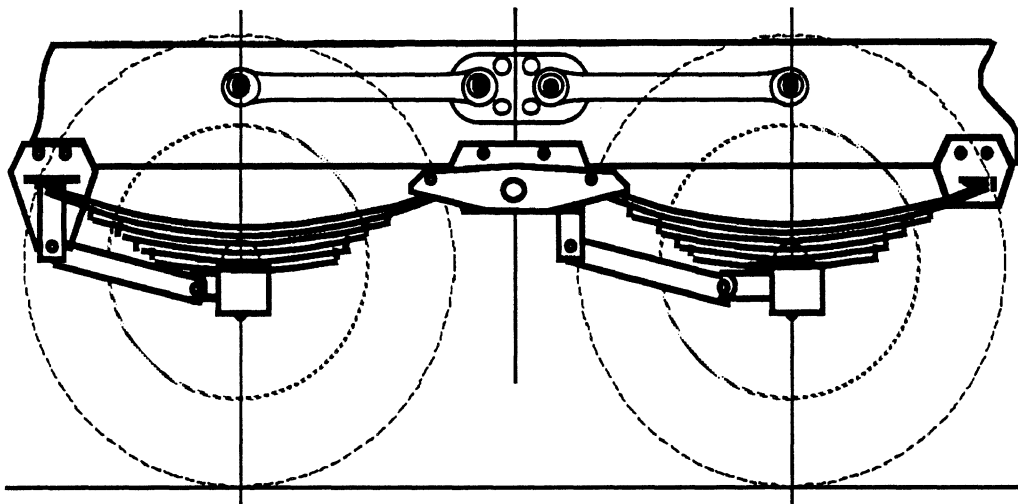
Figure D-6. Side view of a 4-spring suspension.
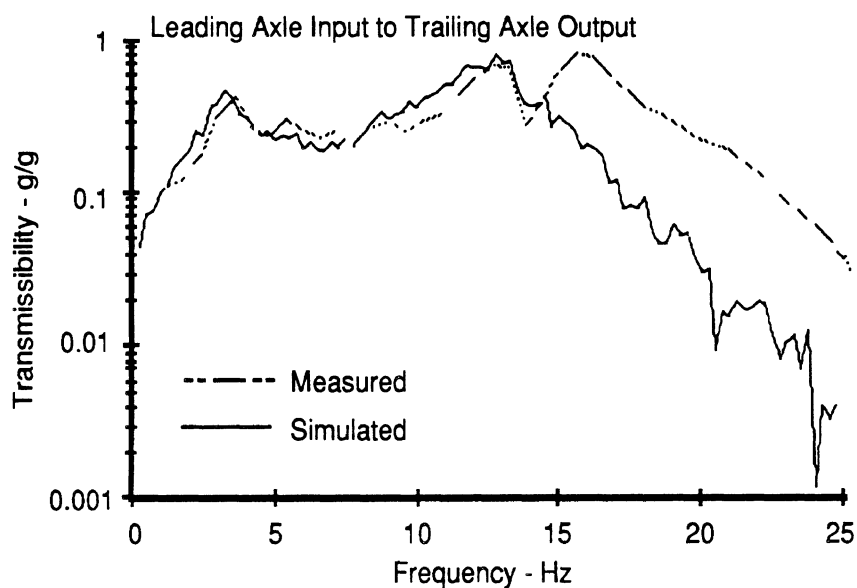
Figure D-7. Comparison between simulated and measured dynamic behavior of a 4-spring tandem suspension.

Very good agreement is obtained from 0 - 15 Hz frequency. This is a very important part of the range because it contains the rigid body bounce and pitch resonance frequencies and the axle hop resonance primarily responsible for dynamic wheel loads. Above 15 Hz the experimental data show somewhat higher response due to undetermined causes. It is hypothesized that the greater experimental response may reflect vehicle structural vibration modes not contained in the model. This is not viewed as a serious flaw in the model as vibrations on the axle at frequencies above the axle hop frequency do not propagate down to the tire contact patch.

The second most popular suspension used on tandem axles has air springs to carry the load. Figure D-8 provides an illustration of an air-spring suspension. Each axle is restrained by a trailing arm with the primary load support through the air spring. Shock absorbers are needed with this type of suspension because of the low friction in the system.

Air-spring suspensions are unique in that the load is supported by pressure in the air bags. Height sensing valves monitor the suspension deflection and adjust the pressure when the suspension operates for more than a few seconds off of its nominal ride height. Thus, the pressure is automatically adjusted whenever the load on the suspension is changed.

The stiffness in the air spring arises from compression of the air when the suspension deflects. Under normal suspension motions the compression is adiabatic and the spring stiffness is proportional to pressure and hence load. Since the stiffness changes proportionately with load, air suspensions have a constant natural frequency.

The common design in trucks feeds both air springs on one side of the vehicle from the same height control valve. Thus both leading and trailing axles have the same air spring force and achieve load equalization in this manner. Under dynamic conditions the air cannot flow quickly enough from one spring to the other to balance out load, so there is littledynamic load equalization. In the truck pitch-plane model air-spring tandem suspensions are modeled as two independent air suspensions with the same average load.

Dynamic characterization data for an air-spring tandem suspension was provided by one of the truck manufacturers. Figure D-9 compares the dynamic behavior of the air-spring tandem suspension calculated in the Pitch-Plane Model to experimental data. Good agreement was obtained again over the lower frequency range covering the body bounce and pitch motions and axle resonance. Because of the softer springs axle hop resonance occurs at a lower frequency on air suspensions (around 10 Hz.). As with the 4-spring suspension, the experimental measurements on the air-spring show a higher response above axle hop resonance due to undetermined causes.

Although not shown here the transmissibility through the lead axle was compared in the validation of the suspension models. Transmissibility is defined as acceleration response on the axle to acceleration excitation at the tire contact patch. Much better agreement was obtained over the entire frequency range. While it is important that the dynamics of individual axles are correct, the inter-axle behavior is the true indicator of whether the tandem dynamics are being replicated accurately. Proper replication of inter-axle load transfer is necessary to differentiate the pavement damaging potential of these suspensions.
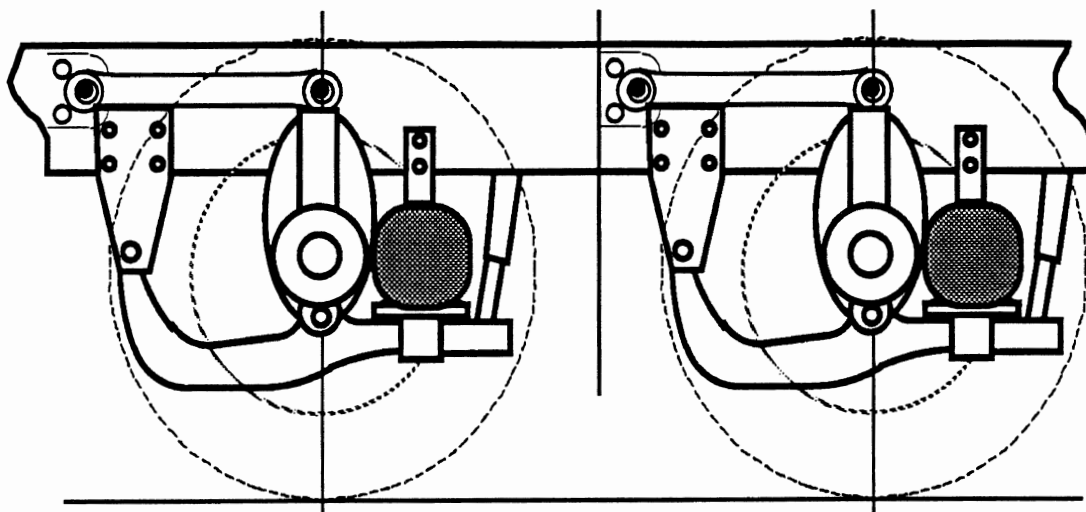
Figure D-8. Side view of an air suspension.
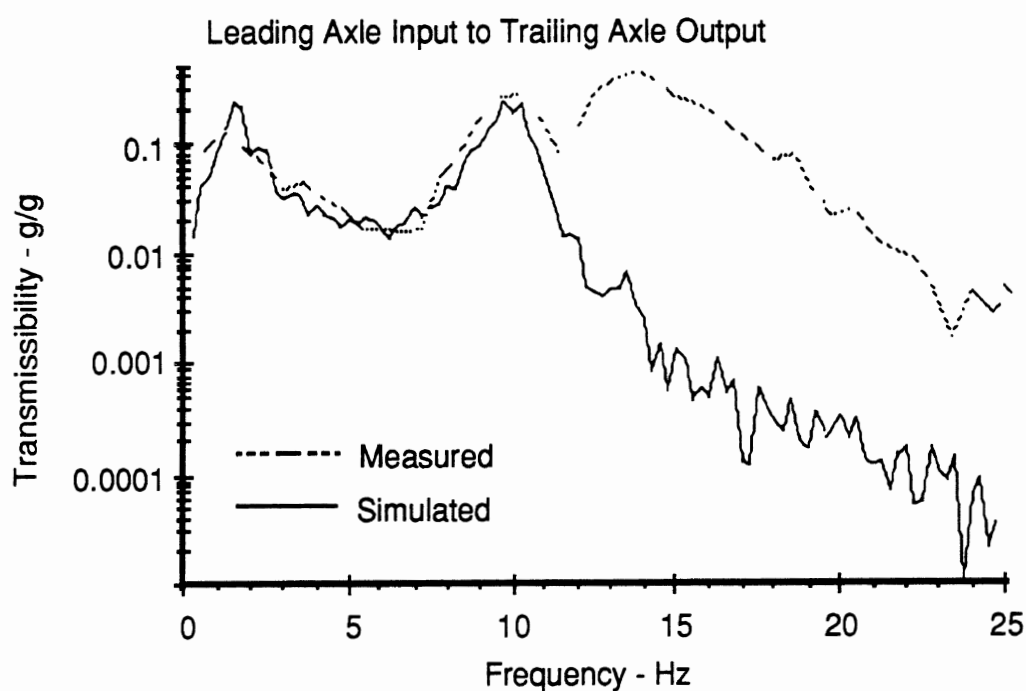

Leading Axle Input to Trailing Axle Output

Figure D-9. Comparison between simulated and measured dynamic behavior of an air-spring tandem suspension.

The walking beam suspension is used on a small fraction of heavy trucks today. It is most commonly found on vehicles used both on and off road (dirt and gravel haulers, etc.) because of its limber articulation in the off-road environment. The generic form of the walking beam suspension using leaf springs as the springing medium is shown in Figure D-10. Rubber in shear or compression is occasionally used in lieu of the leaf springs, but without significant change in the dynamic property most important to road loads; the tandem hop vibration mode.

It was not possible to obtain RPC data showing the dynamic behavior of the walking beam from any of the truck manufacturers. In lieu of this, earlier measurements of dynamic load behavior of a walking beam obtained by UMTRI was used for validation (*11*). In these experiments a wheel load transducer was placed on one axle and the measured loads were corrected for local accelerations to obtain the dynamic load in the tire contact patch while the vehicle was operated at different speeds on several roads. The measured dynamic loads were analyzed to determine their frequency content.

Figure D-11 compares the experimentally measured dynamic loads of a walking-beam tandem suspension to those simulated by the Pitch-Plane Model operating under similar road conditions. The dynamic loads arising from trucks with walking-beam suspensions are concentrated in two regions of frequency; from 1-5 Hz, which is the rigid body bounce and pitch motions, and from 8 - 12 Hz, which is axle hop. In the case of the walking-beam suspension, axle hop involves an out-of-phase bouncing of the leading and trailing axles which has been given the name "tandem hop." This mode can create significant dynamic loads because the walking-beam suspension has little damping for the out-of-phase motions of the two axles.

Good agreement of the amplitudes and frequency content of the simulations and measurements are obtained on both rough and smooth roads. The measured data on the smooth road (bottom left-hand graph) exhibits peaks at 7.5 and 15 Hz which are not matched by the simulation. These peaks are the first and second harmonics of tire/wheel nonuniformities which show up on smooth roads but are insignificant on rough roads. Although this could be duplicated easily in the simulation, they contribute little to the dynamic wheel loads and are therefore neglected.
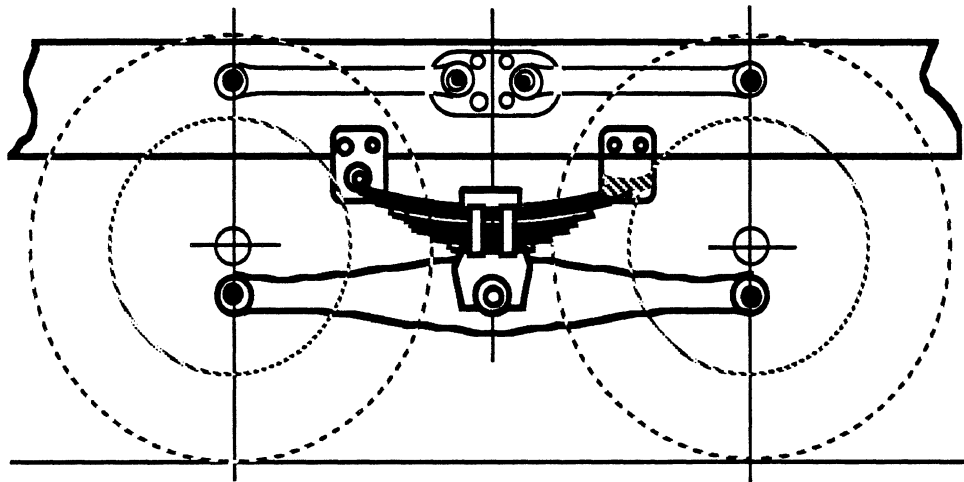
Figure D-10. Side view of a walking-beam suspension.
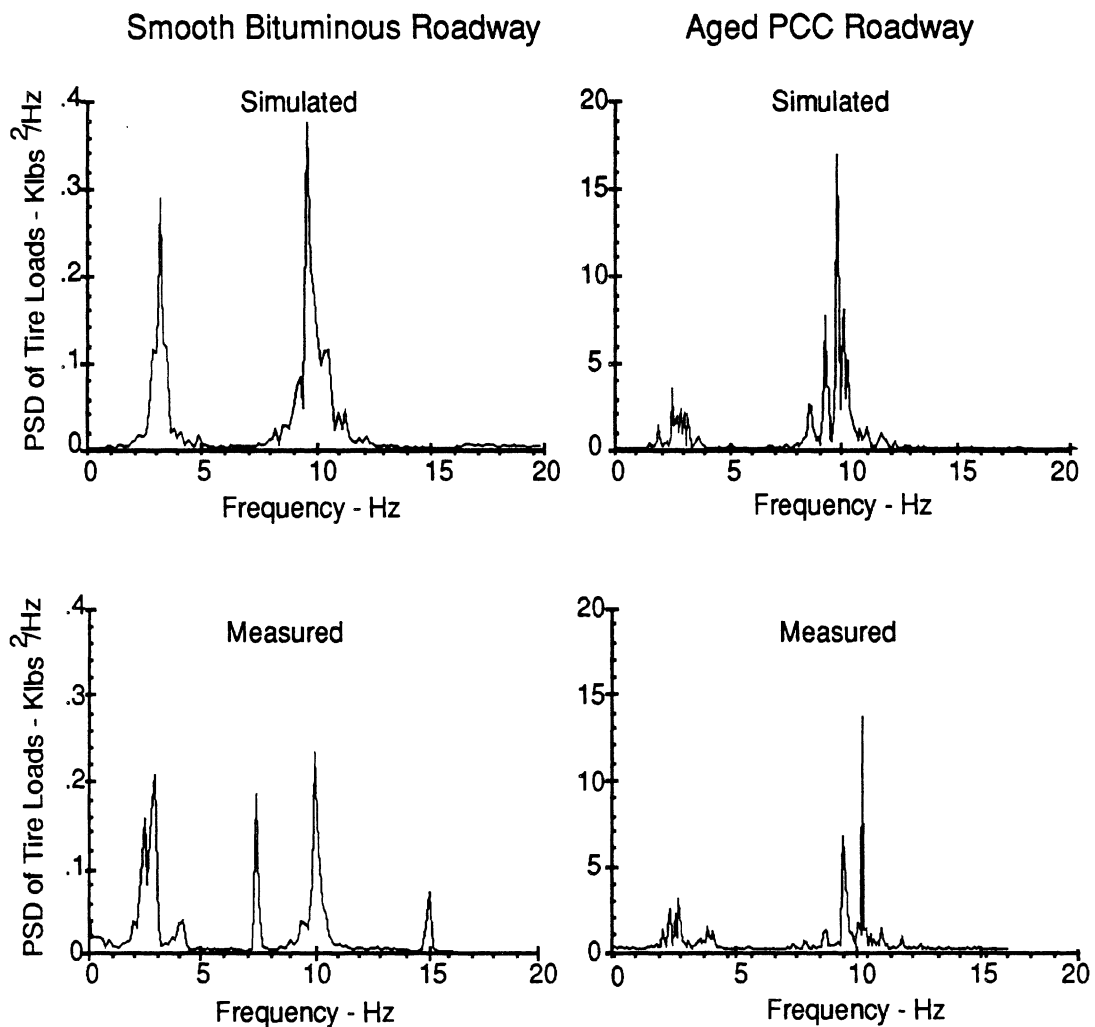
Figure D-11. Comparison between simulated and measured dynamic behavior of a walking-beam tandem suspension.

TRUCK MATRIX

Weights and Dimensions Matrix

For purposes of analyzing the trends in pavement damage as a function of truck characteristics, a baseline matrix of truck configurations was selected. Fifteen truck configurations, representing the primary size and weight variables, were identified. These form the basis for a larger matrix of 29 truck configurations when variations in suspensions and tires are taken into account. The truck characteristics of primary interest are:

Truck gross combination weight
Axles:
>>> Number
>>> Locations
>>> Loads
Tires:
>>> Type (conventional, wide-base single, low-aspect ratio)
>>> Pressure/contact area,
>>> Dual/single arrangements
Suspensions:
>>> Stiffness/damping
>>> Static and dynamic equalization

The purpose of the matrix is to provide a series of trucks which when used with the pavement models will establish trends in pavement damage associated with the above variables. The vehicles were selected to reflect the most common configurations with emphasis on the high loads that will be most damaging to the road. The trucks in common use reflect configurations that serve their mission within the constraints of road use laws. Current Federal limits on truck weight, length, and width are defined by the Surface Transportation Assistance Act of 1982 (*12*). These limits apply to all vehicles using the Interstate System and other qualifying Federal-aid highways. The weight limits are nominally defined as:

1. 20,000 lbs on a single axle.

2. 34,000 lbs on a tandem axle.

3. 80,000 lbs maximum gross weight.

4. Compliance with the bridge formula:

$$W = 500 \left[\frac{L\ N}{N - 1} + 12N + 36 \right]. \tag{D-1}$$

Where:

W = The maximum weight carried on two axles or more.

L = The spacing in feet between the outer axles of any two or more consecutive axles.

N = The number of axles being considered.
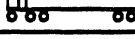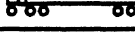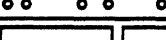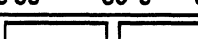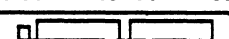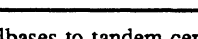
In addition, some states impose separate constraints on the maximum load that can be carried by truck tires, where those constraints limit the weight that can be carried in accordance with the width of the tire tread. Specifically the limits among the states range from 550 to 800 pounds of load per inch of tire tread width.

The matrix of trucks is shown in Table D-1, with additional characteristics listed in Table D-2. The progression in size generally follows the pattern from top to bottom in the table. Each truck is of the largest gross vehicle weight permitted for a given configuration and number of axles. The "Turner" truck at the bottom represents the likely progression in large tractor-trailers that may be seen in the future. The various tire and suspension options would not be used on all of the vehicles in the matrix, thus each vehicle configuration included the suspension types commonly used on it.

Straight Trucks

Approximately 70 percent of the registered trucks in the U.S. (excluding light trucks) are straight trucks. These vehicles accumulate about 30 percent of the truck mileage on the highways (*13*). Most frequently these are two or three axles, with four axles used in heavier applications such as concrete mixers.

Table D-1. Truck Matrix Sizes and Weights.

Truck Num.	Truck Configuration	Configuration Name	GVW (kips)	Axle Loads (kips)	Wheelbases* (feet)
1-2		2-Axle Straight Truck	32	12/20	15
3-4		3-Axle Straight Truck	46	12/34	18
5-8		3-Axle Refuse Hauler	64	20/44	17.5
9-12		4-Axle Concrete Mixer	68	18/38/12	20/12
13		3-Axle Tractor-Semitrailer	52	12/20/20	10/36
14-15		4-Axle Tractor-Semitrailer	66	12/20/34	12/36
16-20		5-Axle Tractor-Semitrailer	80	12/34/34	12/36
21		5-Axle Tractor-Semitrailer	80	14/33/33	10/36
22		5-Axle Tanker	80	12/34/34	12/36
23-24		6-Axle Tanker	85	12/34/39	12/38
25		5-Axle Doubles	80	10/18/17/18/17	10/22/22
26		5-Axle Doubles	80	10/20/15/20/15	10/22/22
27		7-Axle Doubles	120	12/34/34/20/20	12/38/22
28		9-Axle Doubles	140	12/32/32/32/32	12/38/38
29		Turner Doubles	114	10/26/26/26/26	12/22/22

* Wheelbases to tandem centers. Tandem spreads set at 52 inches.

Table D-2. Truck Matrix Tires and Suspensions.

Truck Num.	Tires	Steer Axle Suspension	Drive Axle Suspension	Semi-Trailer or Tag Axle Suspension	Hitch Load (kips)	Second Trailer Suspensions
1	S/D	Flat Leaf	Leaf Spring			
2	S/D	Taper Leaf	Leaf Spring			
3	S/D/D	Taper Leaf	4-Spring			
4	S/HD/HD	Taper Leaf	Walking Beam			
5	W/D/D	Flat Leaf	4-Spring			
6	W/HD/HD	Flat Leaf	Walking Beam			
7	W/W/W	Flat Leaf	4-Spring			
8	W/W/W	Flat Leaf	Walking Beam			
9	W/D/D/D	Flat Leaf	4-Spring	Air Spring		
10	W/HD/HD/D	Flat Leaf	Walking Beam	Air Spring		
11	W/W/W/W	Flat Leaf	4-Spring	Air Spring		
12	W/W/W/W	Flat Leaf	Walking Beam	Air Spring		
13	S/D/D	Taper Leaf	Flat Leaf	Flat Leaf	21.1	
14	S/D/D/D	Taper Leaf	Flat Leaf	4-Spring Taper	18.6	
15	S/D/D/D	Taper Leaf	Air Spring	4-Spring Taper	18.6	
16	S/D/D/D/D	Flat Leaf	4-Spring	4-Spring	29.4	
17	S/D/D/D/D	Taper Leaf	4-Spring	4-Spring Taper	29.4	
18	S/D/D/D/D	Flat Leaf	Air Spring	Air Spring	29.4	
19	S/HD/HD/D/D	Flat Leaf	Walking Beam	4-Spring	29.4	
20	S/D/D/L/L	Flat Leaf	4-Spring	4-Spring	29.4	
21	S/D/D/D/D	Flat Leaf	4-Spring	4-Spring	31.4	
22	S/D/D/D/D	Taper Leaf	4-Spring	4-Spring Taper	29.4	
23	S/D/D/D/D/D	Taper Leaf	4-Spring	6-Spring Taper	29.4	.
24	S/D/D/W/W/W	Taper Leaf	4-Spring	6-Spring Taper	29.4	
25	S/D/D/D/D	Taper Leaf	Flat Leaf	Flat Leaf	16.6	Flat Leaf
26	S/D/D/D/D	Taper Leaf	Flat Leaf	Flat Leaf	19.1	Flat Leaf
27	S/D/D/D/D/D	Taper Leaf	4-Spring	4-Spring	29.4	Flat Leaf
28	S/D/D/D/D/D/D/D	Taper Leaf	4-Spring	4-Spring Taper	27.4	4-Spring Taper
29	S/D/D/D/D/D/D/D	Taper Leaf	4-Spring	4-Spring Taper	19.4	4-Spring Taper

Two-axle straight trucks are used in a broad range of applications such as local delivery vans, utility vehicles, beverage trucks, flatbed (stake) trucks and small dump trucks. While their weights vary significantly with the application, the most common heavy vehicles are limited to a 12,000 lb front axle rating and a 20,000 lb rear axle rating. The 20-

kip rear axle weight limit arises from road use laws. The 12-kip front axle rating is common because the tire size that can handle 20 kips on the rear in a dual wheel arrangement will accommodate 12 kips on the front axle in a single tire arrangement. Thus, the same tires can be used on both front and rear axles. There is little variation in suspension systems among the two axle trucks. Virtually all have leaf springs on the front axles as well as rear. In recent years taper-leaf suspensions have been introduced in lieu of flat-leaf suspensions on the front axle in order to obtain better ride performance. Two-axle trucks are included in the matrix, differing by the type of leaf spring used on the front axle.

Three-axle straight trucks serve many of the same roles as 2-axle trucks when higher load capacity is required. The primary difference is the use of a load-sharing tandem axle at the rear. The common axle ratings used with 3 axles are a 12,000-lb front axle with a 34,000-lb rear. Although heavier front axles are occasionally used, the 12/34 combination is popular because the same tires are used on the front and rear. The most common tandem suspension is the 4-spring in which each axle has two leaf springs, and the springs on the leading and trailing tandem axles are connected by a balance beam known as an "equalizer." For off-road applications, such as construction work, a walking-beam tandem is often used because of its superior articulation and durability. Two variations of the 3-axle straight truck are included in the matrix; one with a 4-spring tandem suspension and one with a walking beam.

A special class of the 3-axle straight truck is used in refuse hauling. Refuse haulers are distinguished from other 3-axle straight trucks by the high loads they carry. Based on discussions with the National Refuse Haulers Association axle weights of 20,000 lb for the front and 44,000 lb on the rear tandem were selected. Wide-base single tires are required on the front axle to handle this load. Dual tires are usually used on the rear axle, but a variation with wide-base singles is also included. Tandem rear suspensions are usually of the 4-spring variety, but the off-road operations of a refuse hauler makes the walking-beam a candidate as well. Both walking-beam and 4-spring tandem suspensions are included in the refuse hauler category.

Four-axle straight trucks are not common except for special applications such as concrete mixers or heavy bulk haulers such as the coal trucks used in the Appalachian states of Pennsylvania and Kentucky. The fourth axle is normally a pusher or tag axle that would be placed forward or rear of the tandem axle. The extra axle utilizes an air suspension. Typical axle loads in a concrete mixer application are 18,000-lb front axle, a 38,000-lb tandem axle and 12,000-lb tag axle. That configuration is used in the matrix. Variants on the base vehicle in the matrix are: use of wide-base single tires on all axles, and the 4-spring and walking-beam tandem suspensions.

Tractor-Semitrailers

Tractor-semitrailers represent about 30 percent of the registered heavy vehicles in the U.S. and are responsible for approximately 70 percent of the heavy-truck highway mileage (*13*). The variations among tractor-semitrailers of most significance here are the number of axles and the axle loads. Although cab style (conventional versus cab-over-engine) is an obvious distinction between different kinds of tractors, this variable is not directly of interest in the study, except as it affects axle loads and tractor wheelbase.

Historically, most tractors have used a 12,000-lb front axle (allowing the front axle to use the same tire sizes as on other axles). Recent changes in road use laws allow the front axle to be set back some distance from the front bumper, in which case the axle load increases to about 14,000 lb. All tractor-semitrailer front axle loads are set at 12,000 lb, except for one at 14,000 lb representing the setback front axle configuration.

The tractor-semitrailer configurations progress from three to five axles. Rear single axles are set at 20,000 lb and tandems at 34,000 lb, all with dual tires. Three tractor rear suspensions are included in the tractor-semitrailer matrix. Most often they are leaf spring (denoted as 4-spring in the case of a tandem) on both tractors and semitrailers. The second most popular is the air spring. The walking-beam would be used only on the tractor rear suspension in the case of 5-axle combinations in construction applications. Variations in the type of leaf spring (i.e. flat versus taper) are included in the matrix, along with low-aspect ratio tires.

Tankers

Three bulk haul tankers are included in the matrix. The 5-axle tanker is commonly seen throughout the nation, and has little variation in tires and suspensions. Advanced designs for greater safety and productivity feature tridem trailer suspensions with dual tires or wide-base single tires. Both combinations are included in the matrix.

Doubles

There are various combinations of doubles (tractor, semitrailer, full-trailer configurations) varying from 55 to 100+ feet in length. The most common combinations are included in the matrix. In the case of the short doubles two possibilities are examined; one being the most favorable (uniform) load distribution among the rear axles, and the other being the most unfavorable (two axles loaded to maximum). The doubles with tandem suspensions are not limited to 80,000 lb gross weight but are chosen to represent likely operating limits.

Suspension Properties

The suspension properties significant to dynamic load performance are the vertical force-displacement characteristics. Those used in the project simulations are shown in Table D-3. The upper envelope stiffness, lower envelope stiffness and beta parameter characterize the spring and friction properties in the suspension. The linear damping coefficient represents damping forces arising from shock absorbers, when present. The unsprung weight arises from the axle, brakes, and wheels. In the case of tandem suspension the unsprung weight shown is the sum of both axles, and is distributed approximately 50/50 between axles.

The general model for the 4-spring tandem suspension includes a dynamic load leveling feature between axles. The parameter values for modeling this performance are listed in Table D-4. The air-spring suspension is modeled similarly with properties that provide no dynamic load equalization. The walking-beam tandem suspension is a separate model. Interaction between the axles is incorporated directly in the model.

Table D-3. Suspension Vertical Properties.

Suspension Location	Suspension Type	Upper Envelope Stiffness (lb/in)	Lower Envelope Stiffness (lb/in)	Beta Parameter	Linear Damping Coef. (lb-s/in)	Unsprung Weight (lb)
Steer Axle	Flat Leaf (12k)	1650.0	1350.0	0.080	16.0	1400.0
Steer Axle	Taper Leaf	1075.0	925.0	0.160	16.0	1400.0
Steer Axle	Flat Leaf (18k)	2400.0	2100.0	0.080	16.0	1400.0
Single Drive Axle	Leaf Spring	3300.0	2700.0	0.080	36.0	2400.0
Tandem Drive Axle	4-Spring Flat	3300.0	2700.0	0.080	36.0	4700.0
Tandem Drive Axle	4-Spring Taper	2200.0	1800.0	0.160	36.0	4700.0
Tandem Drive Axle	Air Spring	1000.0	900.0	0.150	50.0	4700.0
Tandem Drive Axle	Walking Beam	18000.0	15000.0	0.050	0.0	4900.0
Drop Axle	Air Spring	1000.0	900.0	0.150	50.0	1400.0
Single Semitrailer Axle	Leaf Spring	3300.0	2700.0	0.080	36.0	1500.0
Tandem Semitrailer Axle	4-Spring Flat	3300.0	2700.0	0.080	36.0	3000.0
Tandem Semitrailer Axle	4-Spring Taper	2200.0	1800.0	0.160	36.0	3000.0
Tandem Semitrailer Axle	Air Spring	1000.0	900.0	0.150	50.0	3000.0
Single Trailer Axle	Leaf Spring	3300.0	2700.0	0.080	16.0	1500.0
Tandem Trailer Axle	4-Spring Taper	2200.0	1800.0	0.080	36.0	3000.0

Table D-4. Suspension Load Transfer Properties.

Tandem Suspension Type	Load Leveler Link Length (in)	Load Leveler Coulomb Friction (in-lb)	Load Leveler Beta Parameter
4-Spring, Flat Leaf	12.0	10000.0	0.020
4-Spring, Taper Leaf	12.0	10000.0	0.020
4-Spring, Air Springs	N.A.	Infinite	N.A.

The original plan for simulation included a torsion-bar tandem suspension because of its study by Sweatman (14) and UMTRI (11). The torsion-bar suspension, which was made only by Kenworth Truck Co., never became very popular. Under these circumstances, it did not seem fruitful to include it in the matrix of truck variables, so it was dropped from the study.

D—20

Tire Properties

The mechanical properties of truck tires vary with size, ply type, and inflation pressure. Wherever the effect of these variables on road wear was specifically examined, close attention was paid to the distinguishing tire properties. However, for studies that did not include the effect of these variables, a generic set of tire properties was used to distinguish between conventional single, dual, and wide-base single tires. A set of properties was selected to represent the behavior exhibited by each of these three tire configurations over the range of sizes appropriate to the loads imposed on them.

Inserting tire contact conditions into a pavement structural model involves consideration of the tire contact pressure and geometry, and lateral placement of the contact patch. The pavement structural models used in this research are the ILLI-SLAB (15) finite element model for rigid pavement and the VESYS (16) multi-layer elastic model for flexible pavement.

The tire contact pressures were treated as uniform throughout the contact patch. Measurements have shown that tire contact pressure is actually not uniform (17). Rigid pavement fatigue, which is computed under the first pavement layer in this study, is not affected by contact pressure distribution, so a uniform pressure is sufficient. Flexible pavement fatigue and surface rutting, however, are expected to vary with tire contact pressure distribution, but the VESYS flexible pavement model only allows a uniform pressure as input.

Four reference tires were selected for primary attention in the analysis; 11R22.5, 15R22.5, and 18R22.5, and a low-profile tire. The first three tires represent the nominal sizes necessary to carry front axle loads of 12,000, 16,000 and 20,000 lb respectively in a single tire configuration. The 11R22.5 is also suited to service in dual tire applications on 20,000 lb single axles and 34,000 lb tandems. The low-profile tire is limited to service in dual-tire applications on axles to 17,000 lb capacity. The 15R22.5 and 18R22.5 tires are wide-base singles that are used for extra-heavy front axles, as well as replacements for duals on rear axles.

The contact geometry used for the basic tire configurations were obtained from data supplied by the Rubber Manufacturers Association and confirmed by various sources in the literature (18,19). The rigid pavement structural model ILLI-SLAB accepts tire contact patches that are rectangular in shape. Although a truck tire contact footprint is not rectangular (19,20), a reasonable approximation can be obtained for modeling stresses under a concrete slab. Table D-5 shows the footprint length and width for each tire configuration. The footprint length and width refer to their longitudinal and lateral dimensions, respectively.

From a pavement damage standpoint, tread width is a very important tire property. Maximum tread widths are set by the Tire & Rim Association at 80% of section width for rib tires and 90% of section width for traction tires; however, the tread widths on typical production tires may vary. Tread widths were noted from the literature and were also measured on a random sample of tires in each size range. These are reflected in the nominal tread width range for each reference tire. The footprint lengths were adjusted to approximate the contact area under each tire configuration for the range of loads imposed

on them in the truck matrix. The VESYS flexible pavement model accepts tire contact footprints that are circular in shape. The tire contact radii were selected to correspond to the contact areas used for rigid pavement modeling.

Table D-5. Tires Selected for Analysis.

Name	Tire Size (and Equivalent)	Axle Load Capacity (kips)		Nominal Tread Width Range[1] (in)	Assumed Contact Dimensions (in)	
		Single	Dual		Width	Length
Conventional	11R22.5 10.00-20 11R24.5 295/75R22.5	12	20	7 - 9	8	9 (single) 8 (dual)
Low-profile	215/75R17.5 245/75R19.5	NA	17	6.5 - 8	7	7
Wide-base single	15R22.5 385/65R22.5	16	NA	10 - 12	11	11
Wide-base single	18R22.5 445/65R22.5	20	NA	13 - 15	14	12

1. Observed range from a random sample of tires

The first row of cells in Table D-5 represents the minimum tire sizes used on axles rated to 12,000 lb with single tires and 20,000 lb with dual tires. Any of four tire designations may be used to identify this size; 11R22.5 for the tubeless radial tire, 10.00-20 for the tube-type bias-ply tire, 11R24.5 for the tubeless radial, and 295/75R22.5 for the P-metric series. This tire will be referred to in the analysis as the "conventional" tire, and the findings will apply to tires of any of the size designations shown. Recent changes in road use laws have allowed front axles to be set back from the front bumper. This design pushes front axle loads upward, typically to about 14,000 lb. At the 14,000 lb loading slightly larger tires (11R24.5 or 12R22.5) are needed. A truck with a 14,000 lb front axle load is included in the truck matrix. Tire contact dimensions for this configuration are assumed to be the same as for the 11R22.5.

The second row in Table D-5 lists low-profile tires. Truck fleets that need high cubic capacity in trucks and trailers are attracted to low profile tires. The smallest of these, the 215/75R17.5, has sufficient load capacity to allow its use on 34,000 lb tandem axles, but at tire pressures of 120-125 psi. Used in place of a 295R22.5 the overall tire diameter can be reduced from 40 inches to 30.7 inches. These tires have a tread width on the order of 7 inches wide. The contact patch length varies with tire size. A 7-inch length has been assumed for calculations in this analysis.

The last two rows of Table D-5 are the wide-base single tires selected for study. The vertical stiffness and damping coefficient for each group of tires is given in Table D-6.

Table D-6. Tire Vertical Properties.

Table D-2 Abbreviation	Tire Type	Vertical Stiffness (lb/in)	Tire Damping Rate (lb-s/in)	Dual Tire Spacing (in)
S	Conventional Single	4700.0	6.0	
W	Wide Based Single	7000.0	6.0	
D	Conventional Dual	4700.0	6.0	13.0
HD	Heavy Duty Dual[1]	6000.0	6.0	13.0

1. Used on walking beam suspensions.

REFERENCES

1. Nikravesh, P.E. and Haug E.J., "Generalized Coordinate Partitioning for Analysis of Mechanical Systems with Nonholonomic Constraints." *American Society of Automotive Engineers Journal of Mechanisms, Transmissions, and Automation in Design,* Vol. 105 (1983) pp. 379-384.

2. Orlandea, N., et al., "A Sparsity-Oriented Approach to the Dynamic Analysis and Design of Mechanical Systems, Parts I and II." *Journal of Engineering for Industry,* Vol. 99 (1977) pp. 773-784.

3. Trom, J.D., et al., "Modeling a Mid-Size Passenger Car Using a Multi-Body Dynamics Program." *American Society of Automotive Engineers Journal of Mechanisms, Transmissions, and Automation in Design,* Vol. 109 (1987) pp. 518-523.

4. Gillespie, T.D. and C.C. MacAdam, "Constant Velocity Yaw/Roll Program: User's Manual." *University of Michigan Transportation Research Institute, UMTRI-82-39* (1982) 119 p.

5. Cebon, D., "An Investigation of the Dynamic Interaction Between Wheeled Vehicles and Road Surfaces." PhD dissertation, University of Cambridge (1985) 251 p.

6. Sayers, M.W., "Symbolic Computer Language for Multibody Systems." *Journal of Guidance, Control, and Dynamics,* Vol. 14, No. 6 (1991) pp. 1153-1163.

7. Sayers, M.W., "Symbolic Vector/Dyadic Multibody Formalism for Tree-Topology Systems." *Journal of Guidance, Control, and Dynamics,* Vol. 14, No. 6 (1991) pp. 1240-1250.

8. Winkler, C.B. and Hagan, M., "A Test Facility for the Measurement of Heavy Vehicle Suspension Parameters." *Society of Automotive Engineers Paper No. 800906* (1980) 29 p.

9. Fancher, P.S., et al., "Measurement and Representation of the Mechanical Properties of Truck Leaf Springs." *Society of Automotive Engineers Paper No. 800905* (1980) 16 p.

10. Gillespie, T.D., et al., "Calibration of Response-Type Road Roughness Measuring Systems." *National Cooperative Highway Research Program Report 228, University of Michigan Transportation Research Institute, UMTRI-80-30* (1980) 81 p.

11. Ervin, R.D., et al., "Influence of Truck Size and Weight Variables on the Stability and Control Properties of Heavy Trucks. Volume II." *University of Michigan Transportation Research Institute, UMTRI-83-10/2, Federal Highway Administration, FHWA-RD-83-030* (1983) 179 p.

12. Ninety Seventh Congress, "Surface Transportation Act of 1982." Washington, D. C. *Public Law 97-424* (1983) 103 p.

13. Blower, D. and Pettis, L.C., "National Truck Trip Information Survey." *University of Michigan Transportation Research Institute, UMTRI 88-11* (1988) 88 p.

14. Sweatman, P.F., "A Study of Dynamic Wheel Forces in Axle Group Suspensions of Heavy Vehicles." *Australian Road Research Board Special Report 27* (1983) 65 p.

15. Tabatabaie, A.M. and Barenberg, E.J., "Finite-Element Analysis of Jointed or Cracked Concrete Pavements." *Transportation Research Record,* No. 671 (1978) pp. 11-19.

16. Kenis, W.J., et al., "Verification and Application of the VESYS Structural Subsystem." Fifth International Conference on the Structural Design of Asphalt Pavements. *Proceedings.* Vol. 1 (1982) pp. 333-345.

17. Clark, S. K. ed., *Mechanics of Pneumatic Tires.* U. S. Department of Transportation National Highway Traffic Administration, U. S. Government Printing Office, Washington, D. C. (1971) 854 p.

18. Ford, T.L. and Zekoski, J., "Impact of Truck Tire Selection on Contact Pressures." Paving and Transportation Conference, Symposium on Pavement Rutting, University of New Mexico, *Proceedings* (1988).

19. Sharp, K.G., et al., "A Comparative Study of the Effects of Wide Single and Dual Tyres on Rebound Pavement Deflection." *Austrailian Road Research Board, Internal Report AIR 1137-1* (1986) 102 p.

20. Marshek, K.M., et al., "Experimental Determination of Pressure Distribution of Truck Tire-Pavement Contact." *Transportation Research Record,* No. 1070 (1986) pp. 9-13.

APPENDIX E
ROAD ROUGHNESS MODELING

Pavement roughness encompasses all variations in a pavement from a true planar reference surface that cause vibrations in traversing vehicles. These variations include distinct localized pavement failures, such as potholes or slab misalignment, and random deviations that reflect the practical limit of precision to which a pavement can be constructed and maintained. Roughness is the major cause of dynamic load variations in heavy trucks, and roughness inputs are therefore needed for the vehicle models used in this study. When traveling in a straight line, the input to each wheel of the vehicle is described by a longitudinal profile of the pavement. Thus, the ground input is normally treated as one or more longitudinal profiles.

An "average pavement" model was used in this research to ensure that predictions of vehicle response are representative over a range of actual conditions. A standardized input is obtained with a mathematical model of the statistical properties of the road input, as characterized by a power spectral density (PSD) function. For rigid pavements, a periodic faulting discontinuity is added.

BROAD-BAND ROUGHNESS MODEL

Figure E-1 shows two plots of measured longitudinal profile. In both cases, the profiles have been "filtered" to remove subtle, large-amplitude deviations that have no effect on vehicle response (that is, hills and valleys). In both plots of the figure, variations in elevation are random in appearance. That is, there is no single wavelength that characterizes the roughness.

Viewing a pavement from the ground, one can easily discern that a road profile is not truly random, at least in the time span of a few hours. Repeated measures of a clearly marked line on the pavement produce the same profile measurement when suitable equipment and methods are employed (1). However, from the point of view of a traversing vehicle, the fact that the profile is a fixed characteristic of the road is irrelevant. Because the vehicle is "seeing" the road as a continuously varying vertical input, the road elevations under the front wheels appear as variables that change randomly with time. Thus, in many vehicle dynamics studies, road inputs are treated as random variables.

Although a road profile appears random to a vehicle, the relationship between profile inputs under the different axles is deterministic. Each axle input is part of the same profile, separated by the wheelbase of the vehicle.

Because road profiles do not show any simple characteristic shape, they are generally described statistically. A stochastic profile model is defined by specifying not the profile itself, but its statistics. When used as inputs for vehicle models, the statistical

E—1
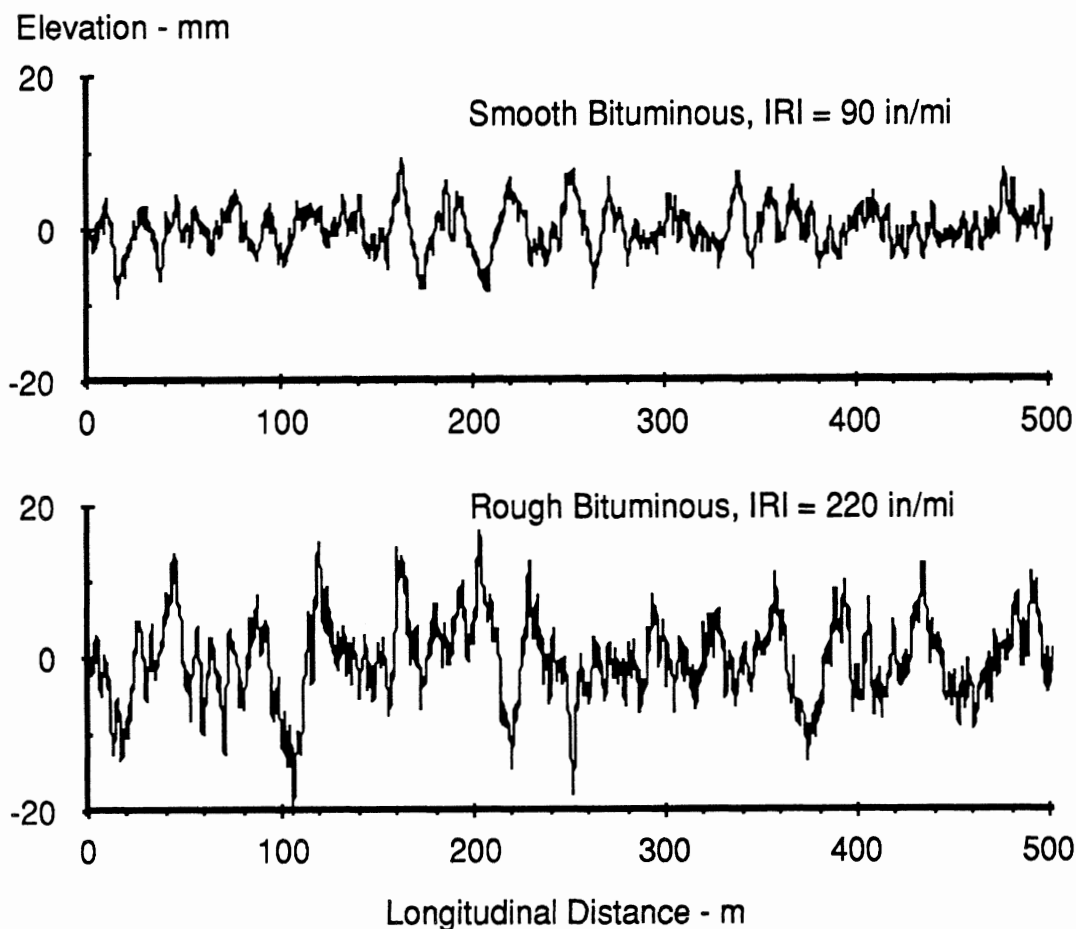
Figure E-1. Example profiles for a smooth and rough road.

representation is designed to fit into methodologies developed for characterizing random vibrations of dynamic systems. Random variables that are not associated with a narrow band of wavelengths are called "broad-band" variables, and are commonly described statistically with the Power Spectral Density (PSD) function.

Power Spectral Density (PSD) Models

Early measures of longitudinal profiles of airport runways and other traveled surfaces were processed to obtain plots of PSD functions, and the PSD was proposed as a convenient means for characterizing ground inputs to vehicles (2,3). For example, PSD functions for the two profiles of Figure E-1 are shown in Figure E-2. The PSD function shows how the variance of a variable such as elevation is distributed over frequency (4). In most applications of the PSD analysis, the variables of interest are functions of time and the frequency shown on the x-axis is temporal, with units of Hz (cycle/sec) or rad/sec.
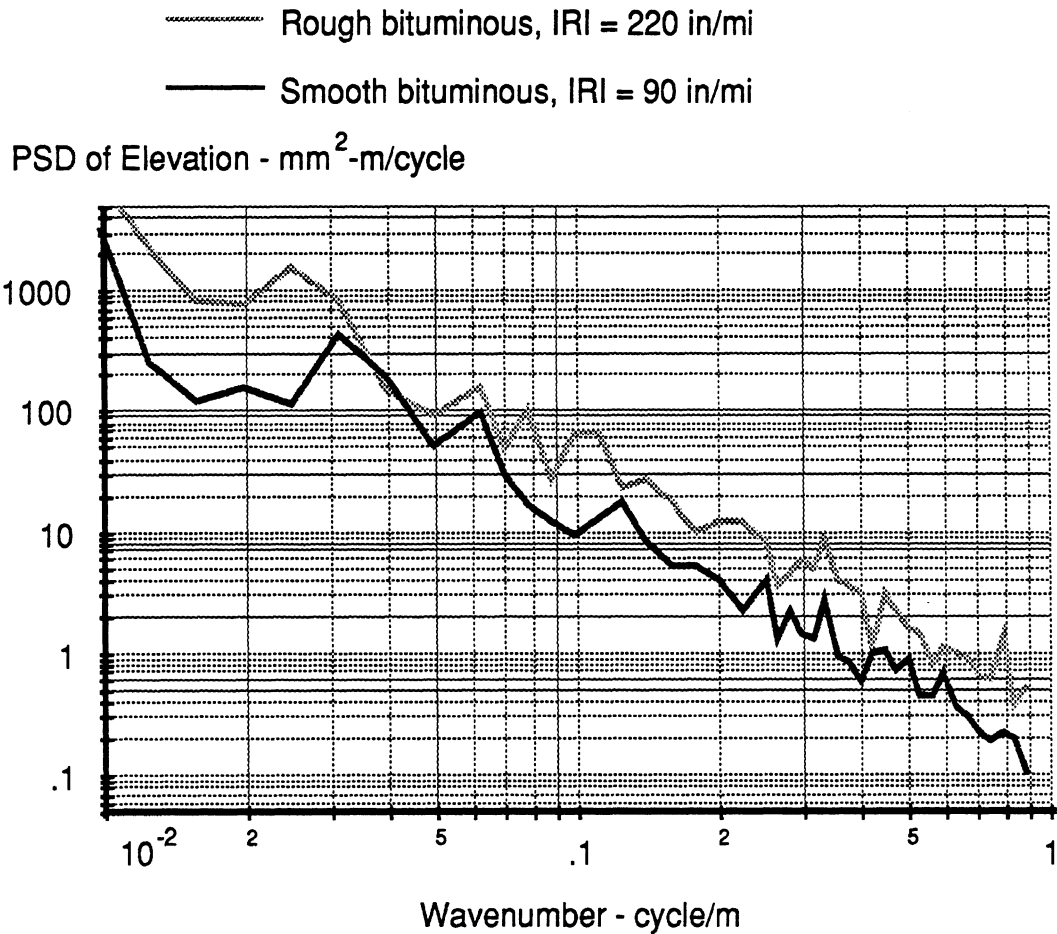
Figure E-2. Power spectral density (PSD) functions for two road profiles.

For variables that are functions of spatial distance, the equivalent to frequency is called wavenumber (1/wavelength). Spatial wavenumber can be related to temporal frequency by the speed of a traversing vehicle by the relationship:

$$v = f / V \qquad \text{(E-1)}$$

where v is wavenumber (cycle/length), f is frequency (cycle/sec), and V is vehicle speed (length/sec).

Figure E-2 shows that the PSD functions for the two example profiles are very similar in appearance, differing approximately by a constant scale factor. It also shows that the roughness is distributed continuously over the full range of wavenumbers shown, confirming that roughness is a "broad-band" characteristic. In fact, whenever PSD functions have been computed for measured road profiles, the same type of shape has been found. Some investigators who have published such data have also recommended stochastic models for use when measured data are not available. One of the first proposed stochastic models (2) is an equation of the form:

$$G_z(v) = \frac{A}{(2\pi v)^2}$$ (E-2)

where $G_z(v)$ is the PSD function of elevation (z), v is wavenumber, and A is a roughness coefficient obtained by fitting the PSD of a measured road to Eq. E-2. This model has been widely used in the field of vehicle dynamics when a simple and generic road roughness input is needed to study the behavior of a vehicle model. Alternate PSD models have been proposed to provide closer agreement with measured data than the white-noise slope model. One of these is a straight line on log-log paper, with the form:

$$G_z(v) = A \, v^\alpha.$$ (E-3)

When a PSD cannot be reasonably characterized by a single straight line, a piece-wise fit has been used, with different values of A and α selected to cover two or more wavenumber ranges (5). This model was proposed for analyses in the frequency domain and is not particularly well suited for the nonlinear, time-domain vehicle model employed in this study. It is not impossible to apply such a model. Inverse FFT methods have been used in other studies (6). However, the approach is computationally intensive.

A useful characteristic of frequency-domain analyses is that the operations of integration and differentiation are represented by dividing or multiplying by circular frequency. In the case of road profile PSDs, the elevation PSD is converted to a slope PSD by multiplying by the factor $(2\pi v)^2$. Thus, when Eq. E-2 is converted to a PSD of profile slope, the result is simply

$$G_{z'}(v) = A.$$ (E-4)

That is, the PSD of profile slope is the constant A.

Figure E-3 shows slope PSD functions for the same two roads used for the previous figures. Note that the scale is expanded to show details of the PSD functions in much greater detail than was possible in Figure E-2. Thus, if one is interested in inspecting details of a road PSD, it is possible to draw the plot in much more detail using a slope PSD than an elevation PSD. For this reason, PSD functions are often converted to units of slope-squared per unit of spatial frequency. A similar convention has been used in other publications involving numerous measured road profile PSDs (1,7,8).

PSD functions of profile slope, published by several researchers for road profiles measured in North America, England, and Brazil, show that the model of Eqs. E-2 and E-4 are not fully representative for all kinds of pavements (1,5,7,8). A model used in an earlier NCHRP study (9) was later extended to match PSD functions obtained with a wide range of modern profile measuring equipment, for all kinds of pavements, for profiles measured in Michigan, Texas, Brazil, and England (7,10-12). The model is defined in terms of independent "white-noise sources." Models defined in this way are compatible with virtually every application in which a stochastic road model might be needed: (1) a profile can be generated analytically for any desired length with a random-number generating

─────── Rough Bituminous, IRI = 220 in/mi

───────── Smooth Bituminous, IRI = 90 in/mi
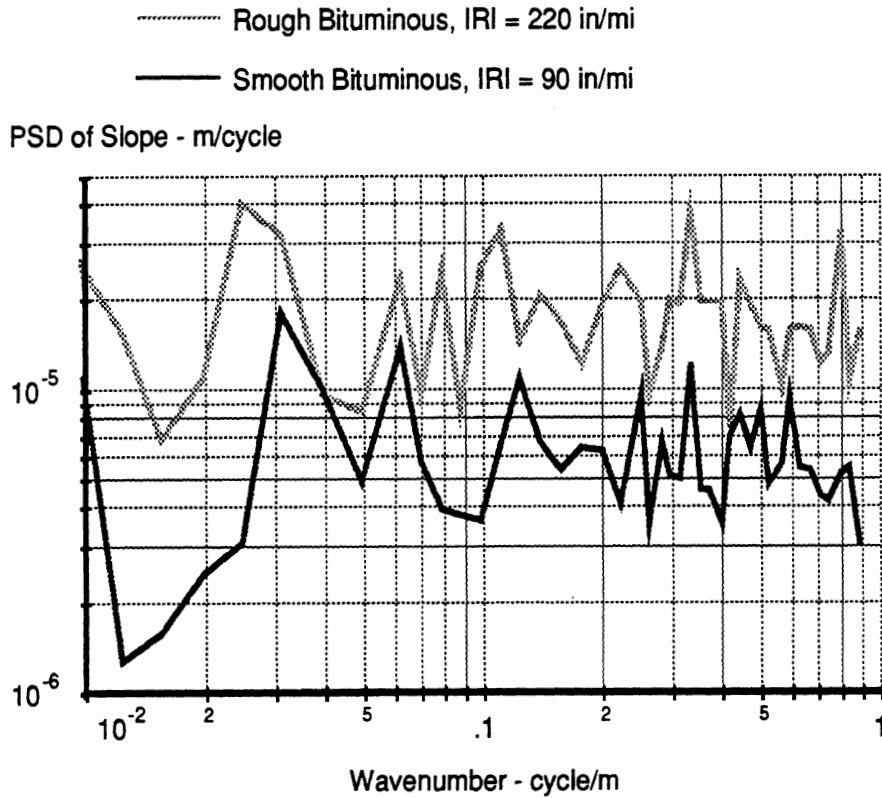
Figure E-3. Slope PSD functions for two roads.

algorithm; (2) a profile can be generated in real-time for laboratory testing with electrical white-noise sources; and (3) the profile can be represented in state-space analyses as a set of white-noise sources and integrators. Thus, the same model can be used for frequency-domain calculation involving the PSD equation, time-domain simulations such as the pitch-plane models described in Appendix D, real-time, hardware-in-the-loop test facilities, and design and analysis methods used in state-space control theory.

The equation for the PSD model is:

$$G_z(v) = \frac{G_a}{(2\pi v)^4} + \frac{G_s}{(2\pi v)^2} + G_e. \qquad \text{(E-5)}$$

The first component, with the amplitude G_a, is a white-noise acceleration that is integrated twice. The second, with amplitude G_s, is a white-noise slope that is integrated once. The third, with amplitude G_e, is a white-noise elevation. The model can also be written to define the PSD of profile slope by looking at the derivative of Eq. E-5

$$G_{z'}(v) = \frac{G_a}{(2\pi v)^2} + G_s + G_e (2\pi v)^2. \qquad \text{(E-6)}$$

Figure E-4 shows comparisons between the slope version of the model and PSD functions for two measured profiles.

Slope PSD functions — m/cycle
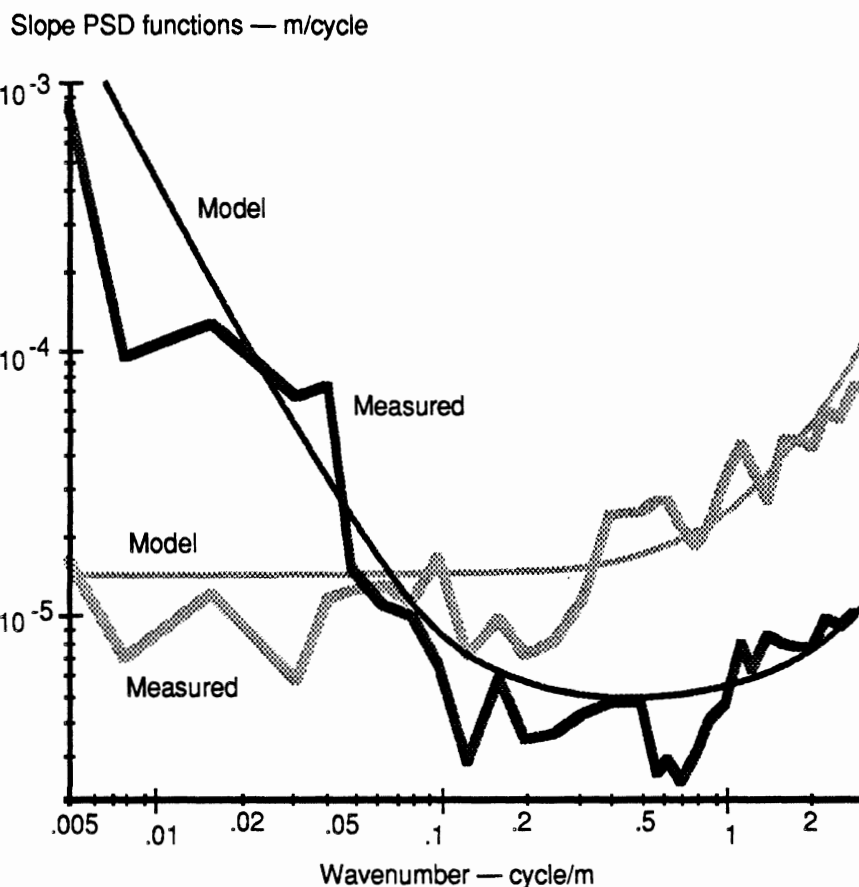
Figure E-4. Fitted PSD model for two roads.

Range of Application for the PSD Model

There is a characteristic shown in some published data that is not included in this model, namely, a roll-off at high and low wavenumbers. All profiling instruments have limited bandwidth, and more often than not, the bandwidth is not specified. Extensive data collected with a variety of instruments showed that the roll-off was due to the instrumentation in every case (1). That is, there were no sites where the road PSDs roll-off as if subject to a high-pass or low-pass filter for wavenumbers between 0.001 and 1 cycle/ft (wavelengths between 1 and 1000 ft), which is the range of wavenumbers "seen" by the profile measuring instruments.

None of the PSD models cited above are valid for wavenumbers approaching zero, because this implies a profile with a mean-square elevation approaching infinity. Although this may seem surprising at first, this obviously incorrect limit-behavior does not confine the practical use of the models. (The mean-square elevation approaches infinity only for roads of infinite length.) When a vehicle analysis involves a long time duration, a high-pass filter can be used to attenuate the roughness amplitudes for very long wavelengths that are outside the bandwidth of a vehicle. In this research, a one-pole high-pass filter with a cut-

off set for a wavenumber of 0.002 cycle/ft (500-ft wavelength) was used to prevent the elevation levels from drifting to infinity, while retaining all of the roughness characteristics that are known to influence a vehicle.

At the upper frequency limit, the mean-square elevation reaches a limiting value if the elevation PSD decreases with wavenumber with a negative exponent of one or greater ($\alpha < -1$ for a model of the form of Eq. E-3). This condition is not satisfied if Eq. E-5 is used and G_e is non-zero, as it is for most rigid pavements. When G_e is non-zero, the mean-square value of elevation increases in proportion to the upper wavenumber bound. Given that the mean-square elevation levels of real roads should not grow without limit as the sample interval decreases (thereby increasing the upper wavenumber), the PSD functions of real roads must roll off at high wavenumbers. The exact nature of the roll-off is not well understood, because most profile measurements that have been made in the United States are not accurate for very high wavenumbers. To prevent aliasing problems, low-pass filters are used to attenuate the measurements for wavenumber with a cut-off at about one-fourth of the sample frequency, which is typically about 0.25 ft. Thus, the profile data forming the basis of the model are valid only to wavenumbers of 1 cycle/ft (1-ft wavelength).

At 15 mi/h, Eq. E-1 indicates that a 1-ft wavelength corresponds to a frequency of 22 Hz, which is at the upper limit of the frequency range of interest for this study. The vehicle models described in Appendix D attenuate inputs at higher frequencies to the point that they have a negligible effect on pavement loads. At higher speeds, the 1-ft wavelength corresponds to higher frequencies well beyond the range of interest. Thus, the road PSD model covers the range of wavenumbers needed for this study.

Experimental measurements of tire enveloping properties have shown that truck tires "filter" short wavelengths from the road by "enveloping" small bumps, as illustrated in Figure E-5 (13). In an earlier NCHRP project, it was found that for vehicle dynamics studies, the tire enveloping behavior is well-represented by a "moving average" filter (9). The tire enveloping effect was included in the current study by applying a 1-ft moving average to all profiles used as vehicle inputs. This filter completely eliminates any roughness due to 1-ft wavelengths, and significantly attenuates roughness inputs for wavenumbers above 0.5 cycle/ft (wavelengths shorter than 2 ft).

To summarize, roughness inputs for this study should be valid for wavelengths longer than 1 or 2 ft, up to a few hundred ft. The broad-band profile model defined by the PSD statistical function of Eq. E-5 matches available measurements for wavelengths from 1 to 1000 ft/cycle, and is therefore well-suited for this study.
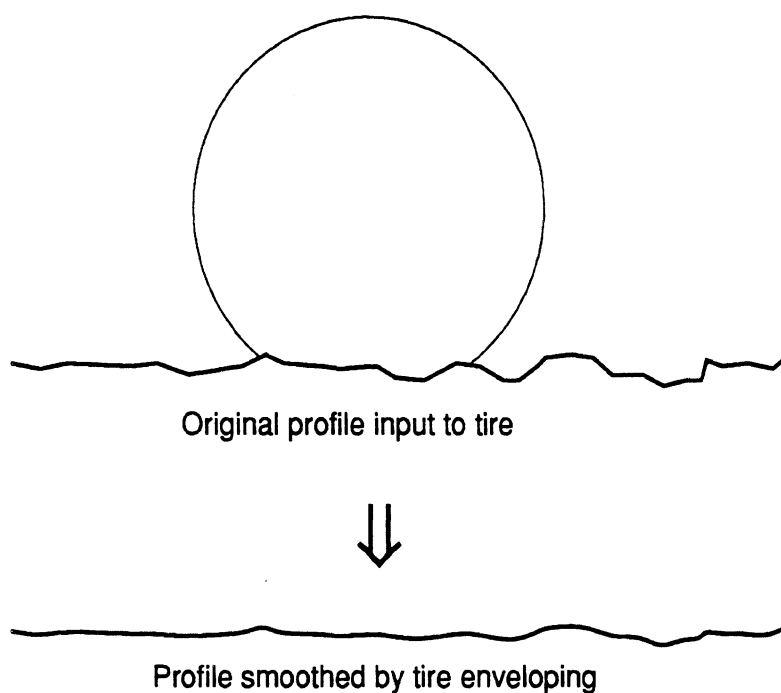
Original profile input to tire

⇓

Profile smoothed by tire enveloping

Figure E-5. Tire enveloping.

Model Parameter Values

A number of profiles measured for paved roads were processed to determine the three coefficients needed for the above model using a step-wise curve-fitting method (10,11). The ranges of values for these coefficients are summarized in Table E-1 for four classes of surface type. The range of values shown for the slope coefficient G_s mainly reflects the roughness range covered by the roads in each category. The other two coefficients describe additional roughness increasing for very short and very long wavelengths. Amplitudes of very long wavelengths, indicated by non-zero values of G_a, might be associated with the quality of grading performed in building the road. High amplitudes of very short wavelengths, typified by non-zero values of G_e, are commonly caused by surface defects that are extremely localized such as faults, tar strips, potholes, etc.

Table E-1. Roughness Parameters for the White-Noise PSD Model.

Surface Type	G_s m/cycle× 10^{-6}	G_a 1/(m·cycle)× 10^{-6}	G_e m^3/cycle× 10^{-6}
Asphalt (Ann Arbor)	1 — 300	0 — 7	0 — 8
Asphalt (Brazil)	4 — 100	.4 — 4	0 — .5
PCC (Ann Arbor)	4 — 90	0 — 1	0 — .4
Surface Treatment (Brazil)	8 — 50	0 — 4	.2 — 1.2

The data used to prepare Table E-1 are shown graphically in Figures E-6 and E-7, to indicate the distribution of the roughness parameters. Figure E-6 shows that there is little correlation between the G_s and G_a coefficients. The maximum acceleration coefficients are found on roads with moderate slope values. This is to say that the roads with very low G_s values are not likely to have the highest G_a values. Figure E-7 shows that roads with low G_s values nearly always have low G_e values. That is, smooth roads with low G_s values are unlikely to have much of the localized surface failures that cause significant G_e values. Roads with high G_s values might or might not have high G_e values, meaning that the roughness may come from localized failures or from other causes.

Asphalt pavements generally show the highest G_a coefficients, and PCC pavements show the lowest. This indicates that, on the average, asphalt roads have proportionately more of their roughness at very long wavelengths and less at short wavelengths. However, the figures also show that individual PCC roads can have the same coefficients as individual asphalt roads. Surface type alone is not sufficient to determine the relative distribution of roughness as characterized by the three coefficients of the model. Overall, the figures indicate that there is no hard and fast rule relating surface type to specific PSD signatures. Instead, they show the limits of PSD signatures that are encountered, based on the model. Any combination of coefficients shown in the figures represents a road that has been measured.
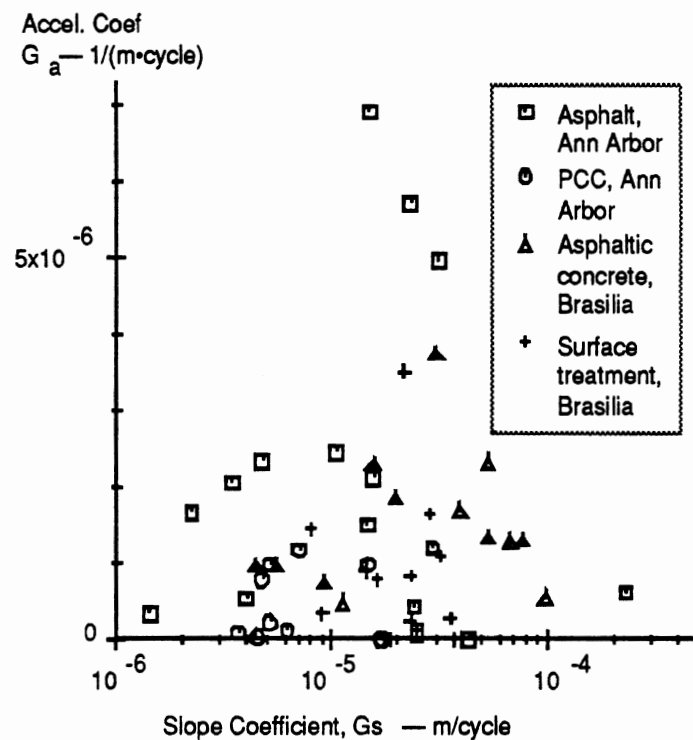

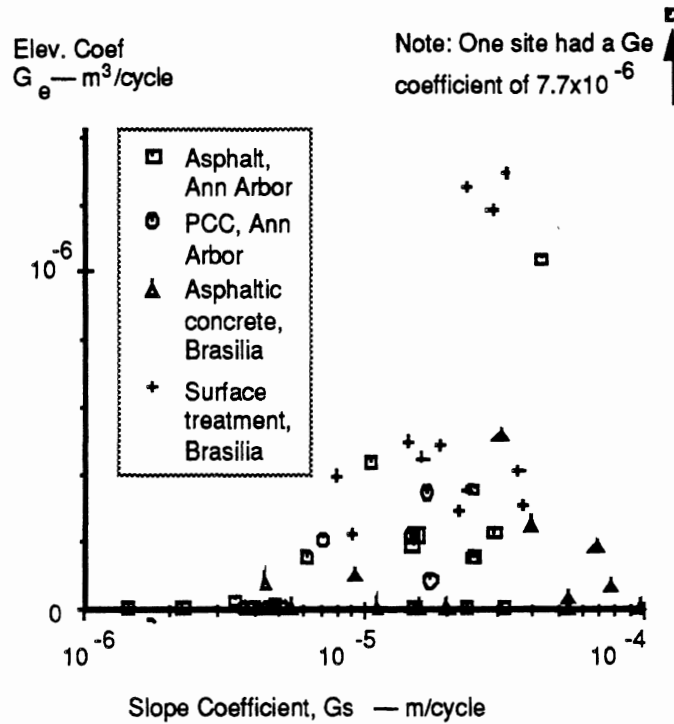**Figure E-6. Correlation between Gs and Ga coefficients.**

Figure E-7. Correlation between Gs and Ge coefficients.

FAULTING MODEL

Faulting and other joint failures have not been given the same attention as random roughness in the vehicle dynamics literature. For this research, the simple faulting model shown in Figure E-8 was used to generate faulting roughness. The faulting model permits profile deviations only at constant intervals (the slab length). The statistical autocorrelation function of the slope is very high for the short length of a joint, and zero for all distances greater than the length of a joint. Mathematically, the autocorrelation function of the profile slope is approximated well by a Dirac delta function. The slope PSD associated with such a function is constant, as in Eq. E-4. Thus, the elevation PSD matches the simple model of Eq. E-2. In both cases, the roughness coefficient A is proportional to the variance of the faulting.

Since the peak tensile stress level under a tire depends on its position on a slab (i.e. its proximity to a joint or crack), road profile inputs for faulted or tilted pavements must be synchronized with the influence functions at the time of damage calculation. This is done to insure that when a profile with faulting or tilting is used to generate truck tire loads, those loads are applied to the pavement in the correct location with respect to slab joints. This is accomplished by inserting profiles into the pavement models that always begin at a slab end. Similarly, the rigid pavement damage model always begins damage computation at the slab end. A keyword system was used in the simulation software to ensure that influence functions entered into the pavement model correspond to the same slab length as that of the road profile for a particular set of truck loads.
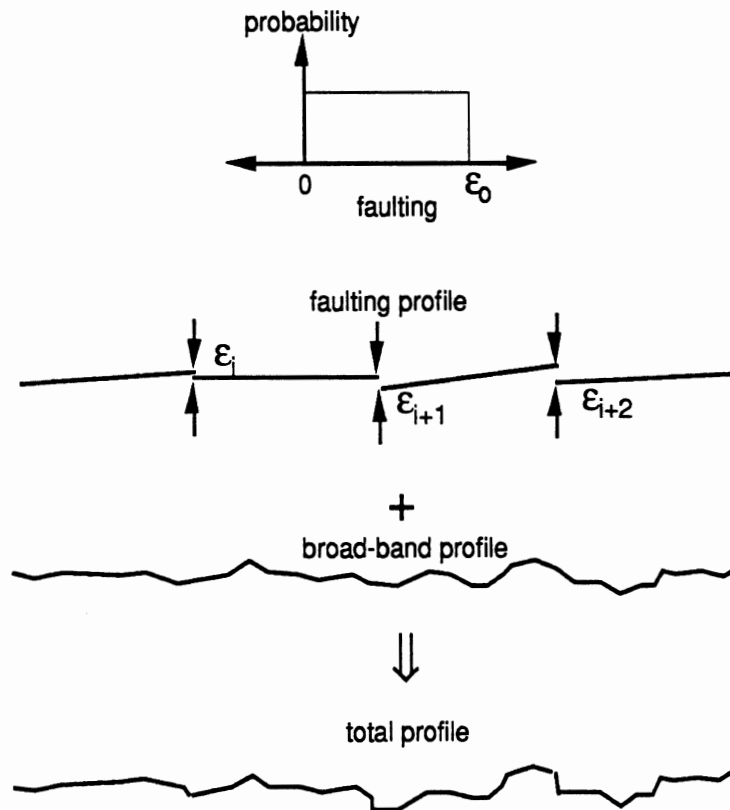
Figure E-8. Model to add faulting to profiles.

ROUGHNESS INDICES

Road roughness is usually thought of as a quantitative summary index of road surface variations. In this study, it is actually not the roughness index that is of interest, because the mechanistic vehicle models require profiles as input. However, the profiles generated for use as inputs are described in terms of a roughness index, to indicate to the reader the type of inputs used.

The serviceability of a pavement was defined for the AASHO Road Test with indices reflecting Present Serviceability Rating (PSR) and Present Serviceability Index (PSI). PSR was obtained from a panel of experts, and PSI is an estimate of PSR obtained from measurements and an empirically-derived regression equation. The PSI equation shows that the primary factor in the determination of PSI is longitudinal roughness of the pavement, as measured with equipment that was used in the AASHO Road Test. Unfortunately, the roughness-measuring methods used in the AASHO Road Test are not reproducible. For example, different states measuring roughness converted to units of PSI can obtain PSI estimates differing by 1 on a scale of 5 (*14*).

The modern measure of road roughness is the International Roughness Index (IRI). The IRI is defined as a characteristic of the longitudinal profile of a traveled wheel path. It is a measure of a ratio of the accumulated suspension motion of a vehicle to the distance

traveled by the vehicle, with units of slope such as in/mi or mm/m (m/km) (15). The IRI is a standardized roughness measurement related to those obtained by response-type road roughness measurement systems (RTRRM systems), and is derived from a mathematical reference developed in a previous NCHRP project (9). Although IRI is not the only measure of roughness in use, it has been demonstrated to be reproducible and transportable when measured according to guidelines published by The World Bank (15), FHWA (14), and ASTM (16). The IRI guidelines define various levels of measurement quality, ranging from highly accurate measures of profile (Class 1) to estimates of IRI obtained from RTRRM systems (Class 3) and subjective ratings (Class 4).

Although roughness measuring technology has improved to the point that roughness can be determined with great accuracy, there is not a standard conversion from roughness to PSI. However, it is clear that PSI is inversely related to roughness; as roughness increases, PSI decreases, as shown in Figure E-9. For example, Cumbaa (17) has used the World Bank data and some data from Louisiana rigid and flexible pavements to estimate the relationship between IRI and PSI.
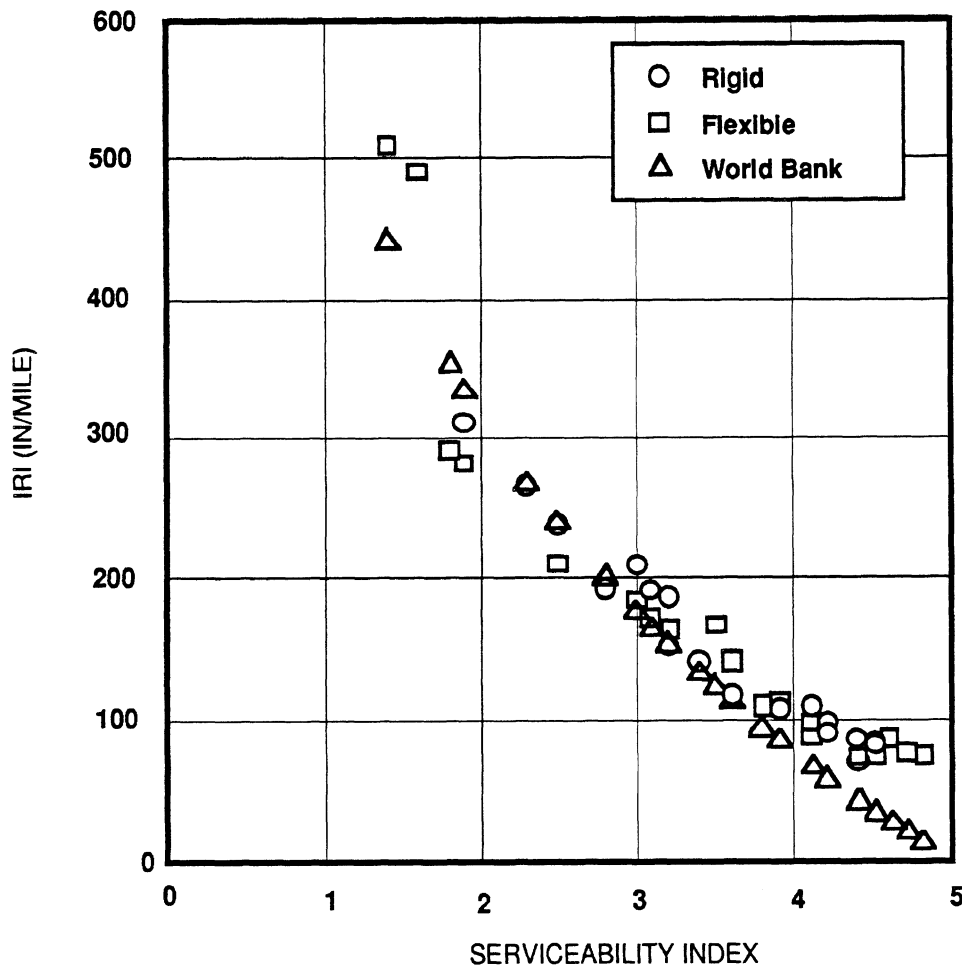

Figure E-9. Relationship between IRI and PSI (17).

PROFILES

A random signal can be generated digitally using a random number algorithm. In using such an algorithm, several parameters must be specified; a type of distribution, a mean value, and a standard deviation. For this research, a Gaussian distribution was used, with a mean value of zero, and the standard deviation defined as

$$\sigma = \sqrt{\frac{G}{2\Delta}} \tag{E-7}$$

where G is a white-noise amplitude for one of the three terms in Eq. E-5 (G_s, G_e, and G_a), and Δ is the interval between samples, expressed in the inverse units used for wavenumber. For example, if wavenumber is cycle/ft, then Δ should be specified in ft.

A simulated road profile that matches the PSD model of Eq. E-5 is generated by: (1) creating an independent sequence of random numbers for each of the three white-noise sources, scaled according to Eq. E-7 to match a model PSD amplitude; (2) integrating each sequence as needed to obtain the desired distribution over wavenumber; and (3) summing the outputs of the filters. Thus, the sequence corresponding to the G_a term is integrated twice, the sequence corresponding to the G_s term is integrated once, and the sequence corresponding to the G_e term is not integrated.

Table E-2 summarizes the values for the three PSD coefficients used in this project. IRI values calculated for each profile are also shown.

Table E-2. PSD Coefficients in the Roughness Model.

Surface Type	IRI in/mi	G_s m/cycle$\times 10^{-6}$	G_a 1/(m•cycle)$\times 10^{-6}$	G_e m³/cycle$\times 10^{-6}$
Smooth Flexible	75	6	0.00	0.000
Flexible	150	12	0.17	0.000
Rough Flexible	225	20	0.20	0.003
Smooth Rigid	80	1	0.00	0.000
Rigid	161	20	0.25	0.100
Rough Rigid	241	35	0.30	0.100

Although the synthesis of artificial road profiles was done digitally for this research, the same process can be performed electronically, for use in laboratory simulators. Instead of numerical methods, electronic components are used to perform the same functions. Independent white-noise generators are fed into analog filters, whose outputs are summed to obtain a voltage signal with the desired statistical properties of the profile. That voltage can be used as excitation to laboratory shakers or an analog computer simulation.

When faulting is a factor, a random faulting is added to the profile at intervals corresponding to the slab length, as was described earlier. Based on data reported recently by FHWA (*18*), a maximum faulting value of 0.25 in was assumed. Thus, the random change in profile at each joint was characterized by a uniform probability distribution going from 0 to + 0.25 in.

REFERENCES

1. Sayers, M.W. and Gillespie, T.D., "The Ann Arbor Road Profilometer Meeting." *Federal Highway Administration, FHWA/RD-86/100* (1986) 237 p.

2. Houbolt, J.C., "Runway Roughness Studies in the Aeronautical Field." *Transactions of the American Society of Civil Engineers,* Vol. 127, Part IV (1962) pp. 427-448.

3. Van Deusen, B.D. and McCarron, G.E., "A New Technique for Classifying Random Surface Roughness." *Society of Automotive Engineers Paper No. 670032* (1967) 11 p.

4. Bendat, J.S. and Piersol, A.G., *Engineering Applications of Correlation and Spectral Analysis.* John Wiley and Sons. New York (1980).

5. Dodds, C.J. and Robson, J.D., "The Description of Road Surface Roughness." *Journal of Sound and Vibration,* Vol. 31, No. 2 (1973) pp. 175-183.

6. Cebon, D. and Newland, D.E., "The Artificial Generation of Road Surface Topography by the Inverse FFT Method." Eighth IAVSD Symposium on the Dynamics of Vehicles on Roads and on Railway Tracks, Cambridge, Mass. *Proceedings.* Ed. B. V. e. Lisse., Swets & Zeitlinger (1984).

7. La Barre, R.P., et al., "The Measurement and Analysis of Road Surface Roughness." *Motor Industry Research Association Report No. 1970/5* (1969) 31 p.

8. Sayers, M.W., et al., "The International Road Roughness Experiment: Establishing Correlation and a Calibration Standard for Measurements." *World Bank Technical Paper No. 45,* The World Bank, Washington, D. C.(1986) 453 p.

9. Gillespie, T.D., et al., "Calibration of Response-Type Road Roughness Measuring Systems." *National Cooperative Highway Research Program Report 228, University of Michigan Transportation Research Institute, UMTRI-80-30* (1980) 81 p.

10. Sayers, M.W., "Characteristic Power Spectral Density Functions for Vertical and Roll Components of Road Roughness." Symposium on Simulation and Control of Ground Vehicles and Transportation Systems, Anaheim, Calif. *Proceedings.* American Society of Mechanical Engineers (1986) pp. 113-126.

11. Sayers, M.W., "Dynamic Terrain Inputs to Predict Structural Integrity of Ground Vehicles." *Wright-Patterson Air Force Base, University of Michigan Transportation Research Institute, UMTRI-88-16* (1988) 114 p.

12. Smith, C.C., et al., "The Prediction of Passenger Riding Comfort from Acceleration Data." *Council for Advanced Transportation Studies Research Report 16*, University of Texas at Austin (1976) 107 p.

13. Lippman, S.A., et al., "Enveloping Characteristics of Truck Tires—A Laboratory Evaluation." *Society of Automotive Engineers Paper No. 650184* (1966) 6 p.

14. Gillespie, T.D. and Sayers, M.W., "Methodology for Road Roughness Profiling and Rut Depth Measurement." *Federal Highway Administration, FHWA/RD-87/042* (1987) 50 p.

15. Sayers, M.W., et al., "Guidelines for Conducting and Calibrating Road Roughness Measurements." *World Bank Technical Paper No. 46*, The World Bank, Washington, D. C. (1986) 87 p.

16. American Society of Testing and Materials, "Standard Test Method for Measuring Road Roughness by Static Level Method." *ASTM Annual Book of Standards*, Vol 4.03, Standard E 1364-91 (1991).

17. Cumbaa, S.L., "Correlation of Profile-Based and Response-Type Roughness Devices for Louisiana's Highway Performance Monitoring System." *Transportation Research Record*, No. 1260 (1990) pp. 99-105.

18. Smith, K. D., et. al., "Performance of Jointed Concrete Pavements. Volume IV." *Federal Highway Administration, FHWA-RD-89-141* (1990) 389 p.

APPENDIX F
METHODOLOGY

This appendix describes the analytical methods used to calculate pavement life consumption due to truck loading by combining pavement response models, vehicle dynamics models, and pavement damage models. To quantify the effects of wheel loads on pavement deterioration, it is necessary to examine the accumulated damage due to all axles of a passing vehicle at specific points in the road and then assess the damage over all the points.

The calculation procedure used in this study was to divide the road surface along each wheel path into a large number of equally spaced intervals. The theoretical damage incurred in each interval due to the dynamic tire forces of a vehicle was calculated according to the fatigue and rutting criteria described below. The intervals were sufficiently short to resolve peak damage at the highest frequency of interest in the truck wheel loads (20 Hz). The total number of intervals in the simulation was sufficient to ensure reasonable statistical accuracy in the results.

A schematic diagram of the calculation methodology is shown in Figure 2 in the main section of the report. The process involves three main stages: (1) calculation of dynamic tire forces in a pitch–plane vehicle simulation; (2) combination of the tire forces with influence functions to yield the strain time history (primary response) at each response point in the pavement; (3) processing of the primary responses with pavement damage models, to yield the fatigue or rut depth at each response point. The pitch-plane vehicle simulation is described in Appendix D, and the pavement models from which the influence functions are obtained are described in Appendices B and C.

Analyses and interpretation of the resulting damage profiles depend on assumptions concerning the phenomenon of 'spatial repeatability' described in the literature review in Appendix A. Several authors have postulated that most vehicles in the highway "fleet" are likely to apply their peak forces near to the same locations on the road surface (1-8). On this basis it is reasonable to assume that loss of serviceability will be governed by a small proportion of locations at which large damage is incurred; so called "hot spots." The theoretical damage at these points can be determined by appropriate statistical analysis of the damage distribution.

The alternative hypothesis is that all points along the road incur a statistically similar distribution of wheel loads and that road failure is governed by the points that are inherently weaker, due to construction defects: so called 'weak spots' (9,10). The real situation must lie somewhere between these two extreme viewpoints; with high damage occurring both at "weak spots" and at "hot spots." Which of these mechanisms dominates the degradation of a particular road surface will depend on many variables, including the uniformity of the initial road construction, the types and thicknesses of materials used, the initial surface roughness, the uniformity of the vehicle fleet using the road, and various environmental factors.

The objective of this study is to compare the road–damaging potential of various vehicles and vehicle features. It is appropriate, therefore, to assume that the road is of

uniform strength, and to assess the theoretical damage done by each vehicle on that road, assuming that all other factors "remain equal."

INFLUENCE FUNCTIONS

Because the load from a truck tire moves along a wheel path, the response at a point of interest must be determined for a load applied anywhere along that path. The relationship between the position of a load on the wheel path and the response at a point is called an "influence function," defined as:

$$I_{kj} = \frac{R_j}{L_k}.$$ (F-1)

Where:

I_{kj} = The influence of a tire load at point k on the response at point j.

R_j = The response (stress, strain, or deflection) at point j.

L_k = The load applied at point k.

The pavement models used in this study are linear. Thus, the influence functions are also linear and can be expressed as response per unit load for a given set of tire contact conditions. Further, the response at a point to the multiple wheels of a truck can be determined by superposition of the responses to individual wheels.

Rigid Pavement Fatigue

The finite element pavement analysis program ILLI-SLAB was used to generate rigid pavement influence functions. The software was modified for this project to compute pavement response many times at incremental tire positions along the wheel path. This allowed any primary response at a point of interest to be expressed as a function of tire position along the wheel path. For the study of fatigue, longitudinal stress under the pavement slab is the primary response of interest. Thus, for the matrix of pavements given in Appendix B, longitudinal stress at the bottom surface of the slab is used to define the influence function.

Figure F-1 shows a rigid pavement stress influence function at a location that is far from any joints or cracks. In the figure, the function is plotted as stress at the point of interest per pound of tire load versus the position in the wheel path relative to the point. As the tire approaches the point of interest, the pavement material goes gradually into compression. When the tire passes directly over the point of interest, it goes sharply into tension and back to compression as the tire moves away. Gradually, the tire moves sufficiently far away from the point of interest that the influence function approaches zero. It should be noted that several influence functions are required to characterize the behavior of a rigid pavement. This is because the influence functions differ with proximity to slab ends. The shape and peak level of the influence function have been found to vary with pavement layer thicknesses, with tire contact conditions, and in the presence of joints or cracks. How the influence function changes with tire and pavement variables will be discussed with the findings of how each variable affects pavement damage.
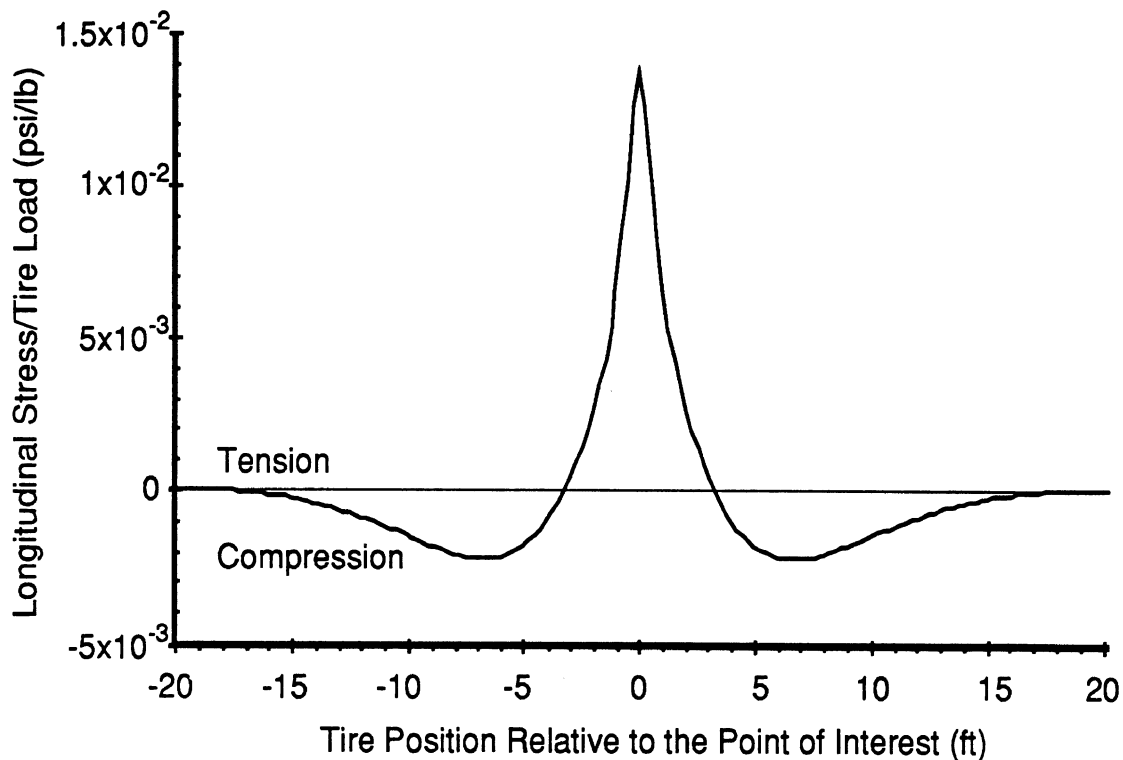
Figure F-1. Rigid pavement stress influence function.

Flexible Pavement Fatigue

The multi-layer elastic pavement analysis program VESYS was used to generate the primary responses for calculating influence functions for flexible pavement fatigue. Each influence function was obtained with a single run of the VESYS program. This could be done because VESYS is based on a model in which the pavement is assumed to cover an infinite half-space with radial symmetry. That is, the model allows no position-dependent changes in the pavement structure such as cracks or joints. Thus, the response at a point to a tire at various distances could be determined simply by applying a single tire load to the pavement and calculating the response at all distances of interest. For fatigue analysis, the primary response of interest is the longitudinal strain under the surface layer, because it has been observed that the maximum strain occurs at the bottom of the surface layer and it is almost always longitudinal strain (see Appendix C).

Figure F-2 shows a flexible pavement strain influence function. In the figure, the function is plotted as longitudinal strain at the point of interest per pound of tire load versus the position in the wheel path relative to the point. As the tire approaches the point of interest, the pavement material goes gradually into compression. When the tire passes directly over the point of interest, it goes sharply into tension and back to compression as the tire moves away. Gradually, the tire moves sufficiently far away from the point of interest that the influence function approaches zero. The shape and peak level of the influence function have been found to vary with pavement layer thicknesses, pavement layer properties, and tire contact conditions. How the influence function changes with tire and pavement variables will be discussed with the findings of how each variable affects pavement damage.
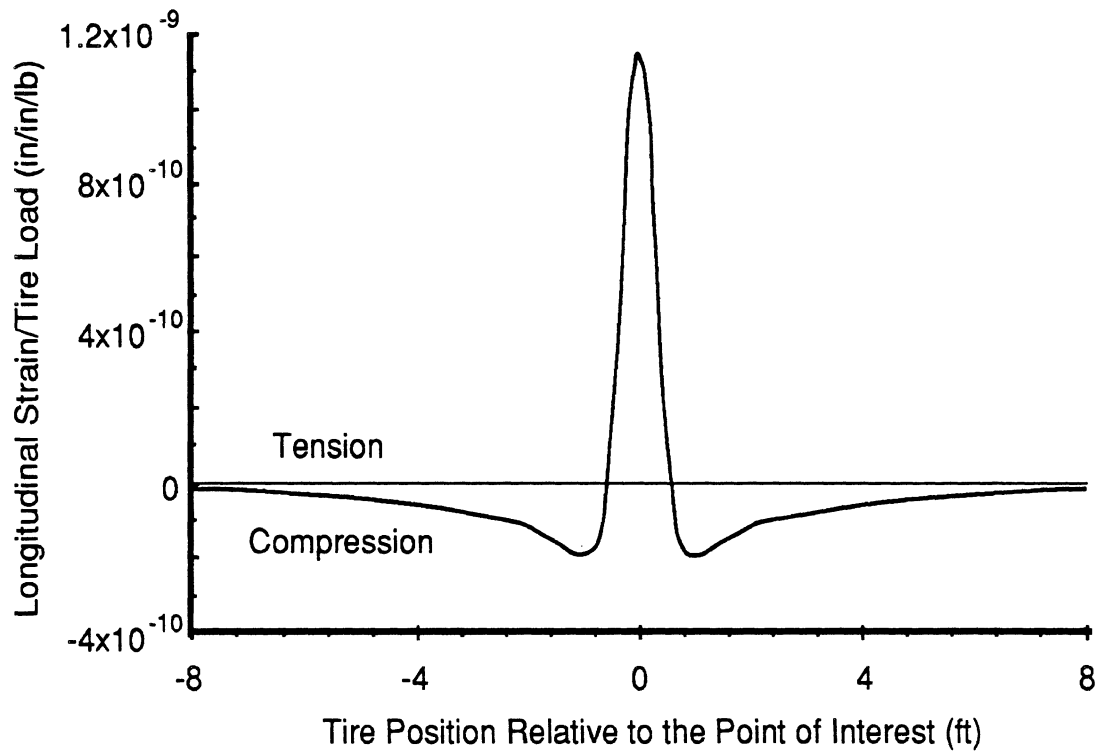
Figure F-2. Flexible pavement strain influence function.

Flexible Pavement Rutting

The program VESYS was also used to generate influence functions for flexible pavement rutting. For rutting analysis, the primary response of interest is the rate of permanent vertical displacement at the pavement surface. As was the case for the strain (fatigue) influence function, the rutting influence function was obtained with a single run of the VESYS program. Rut depth is subsequently calculated from these influence functions using an integration technique (see Appendix C). Therefore, care must be taken to generate influence functions with sufficient detail to accurately estimate the area under them.

Figure F-3 shows an influence function used for calculating incremental change in rut depth caused by a single vehicle pass. In the figure, the function is plotted as the rate of permanent vertical displacement at the point of interest per pound of tire load versus the position in the wheel path relative to the point. As the tire approaches the point of interest, the rate of displacement increases. The rate of displacement is at its peak level when the tire is directly over the point of interest. Gradually, the tire moves sufficiently far away from the point of interest that the influence function approaches zero. The shape and peak level of the influence function both vary with pavement layer thicknesses, pavement layer properties, and tire contact conditions. How the influence function changes with tire and pavement variables will be discussed with the findings of how each variable affects pavement damage.
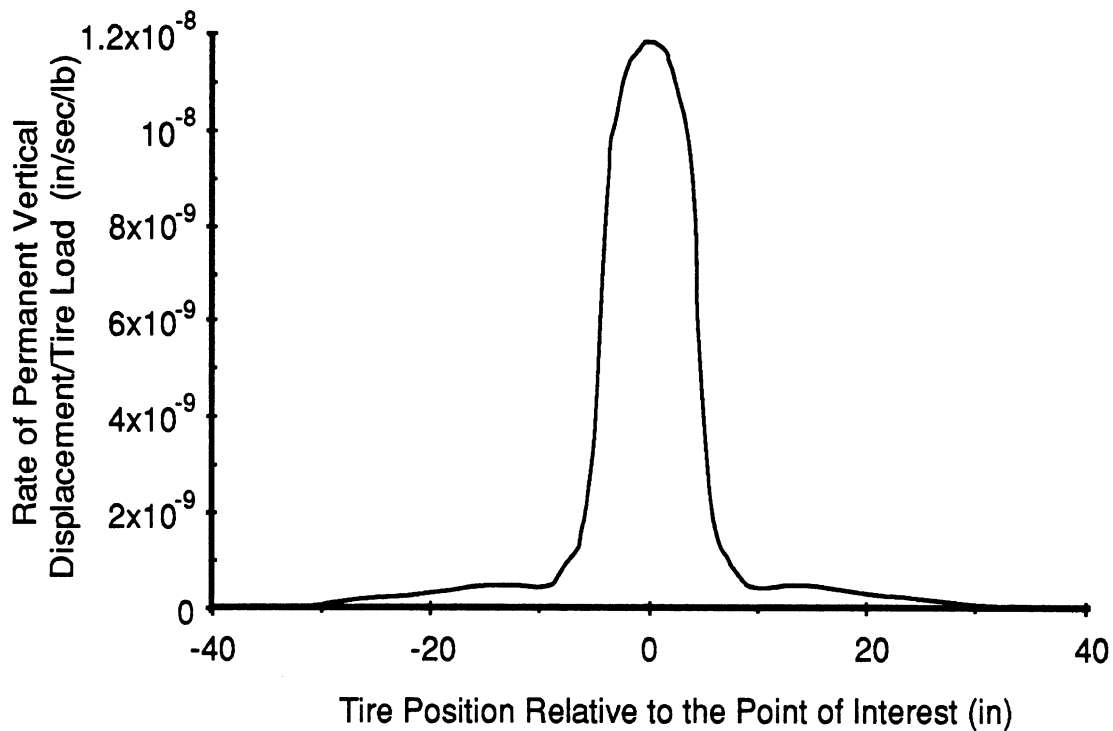
F—4

Figure F-3. Flexible pavement influence function for the calculation of rut depth.

STATIC LOAD FACTORS[1]

Much of the pavement damaging potential of various truck designs is inherent in the basic layout of the vehicle. Although dynamics of the vehicle are considered afterward, the study of truck equivalence under non-dynamic conditions simplifies the explanation of many of the relevant mechanisms for damaging pavements. Thus, the trucks can be simulated in this manner to yield an understanding of how basic truck design variables such as static axle loads, axle spacing, and tire contact conditions contribute to road damage. Once this simplified analysis is carried out and the results understood, the dynamic component of truck loading can be studied.

Within the highway community, the road damage due to a heavy truck has been quantified on a relative basis by comparison to the damage caused by a single axle loaded to 18,000 pounds (18 kips). Damage quantified in terms of Equivalent Single Axle Loads (ESALs) is referred to as "equivalence." The practice of considering relative damage circumvents the problem of trying to predict damage on an absolute basis in the presence of many uncertain variables. Because the 18-kip reference is itself a "static" load, it is a reasonable basis for establishing equivalence of trucks under static load conditions.

---

[1] In this discussion, the term "static" is from the point of view of the vehicle, and indicates that axle loads are held to their static values as if the truck is running on a perfectly smooth road. However, from the point of view of the pavement, the "static" loads are indeed moving and thus changing with time.

Equivalence factors can be assigned to variations in axle load, axle spacing, and tire type considered separately. Using these factors to assess the equivalence of a complete truck layout is also possible if the range of the influence function is limited to the sorts of distances seen in tandem axle spreads. Figures F-2 and F-3 show that both of the influence functions of interest for flexible pavements are rather localized, such that it is reasonable to combine effects of individual axles to make approximate statements about the damage inflicted by an entire vehicle. In contrast, Figure F-1 shows that influence functions for rigid pavements cover much greater distances, up to 20 ft. Because there are many potential interactions between axle groups, a detailed analysis is required for rigid pavements even when considering static vehicle loads. However, a simpler analysis is sufficient for flexible pavements, as described below.

Flexible Pavement Fatigue

The relative level of fatigue caused by a truck with axle loads held to their static values can be calculated by summing the fatigue caused by each axle group. An axle group is defined as any set of axles in which the distance to adjacent axles is less than 8 ft. To do this, equivalence factors are developed for axle load, tire type, and the spacing of axles within a group. The equivalence factors for axle loads are calculated simply by dividing the axle load by a standard axle load such as 18 kips and raising the ratio to the power of the fatigue law applied to the pavement. Equivalence factors are assigned to various tire types as the ratio of the strain cycle size per pound of load induced in the pavement by that axle to the strain cycle size per pound of load induced in the pavement by standard tire type, such as conventional dual tires, raised to the power of the pavement fatigue law. These ratios are obtained via the influence functions. Equivalence factors for the spacing of axles within an axle group must be obtained from a table or graph. They are calculated by constructing a time history of pavement strain induced by the axle group, extracting the strain cycle sizes from the history, and inserting the strains into a fatigue law. The result is then divided by the damage caused by the number of axles in the group acting individually. The process of generating time histories to calculate damage is the same method used to evaluate flexible pavement fatigue due to dynamic truck loading and is described in the following section. These axle load, tire type, and axle spacing equivalence factors are used to compute the relative fatigue life consumed by a passing truck in ESALs according to the following relation:

$$\frac{F}{F_s} = \sum_{i=1}^{n} (s_i) \sum_{h=1}^{m_i} (t_h l_h)^p. \qquad \text{(F-2)}$$

Where:

F = Fatigue life consumed by a single pass of a "static" truck.

F_s = Fatigue life used by a single pass of a reference axle such as an 18-kip axle fitted with conventional dual tires.

n = The number of truck axle groups.

s_i = The equivalence factor for axle group i (equal to 1 for independent axles).

m_i = The number of axles in axle group i.

t_h = The ratio of the strain cycle size under the tire type on axle h of group i to the strain cycle size under a standard tire type such as conventional duals at the same load.

l_h = The ratio of the static load on axle h of group i to a standard axle load.

p = The power of the pavement fatigue law.

The absolute level of fatigue life consumed by a truck at its static loads is calculated using the following relation:

$$F = \sum_{i=1}^{n}(s_i)\sum_{h=1}^{m_i}K(T_hL_h)^p. \qquad \text{(F-3)}$$

Where:

T_h = The strain cycle size per pound of tire load for the tire type on axle h of group i.

L_h = The static load on axle h of group i.

K = The proportionality constant of the pavement fatigue law.

Flexible Pavement Rutting

Because the range of influence of a truck tire on flexible pavement is small (see Figure F-3), loads from nearby axles are nearly independent with respect to their effect of rutting. This independence, combined with the linearity of the rutting damage model (see Appendix C), implies that the rut depth caused by a truck's static loads is simply the sum of the increase in rut depth due to each axle considered individually. Thus, equivalence factors for various axle loads can be calculated simply by dividing the axle load by a standard load such as 18 kips.

The rut depth caused by a passing axle also depends on the tire type. Equivalence factors are assigned to various tire types as the ratio of the rut depth per pound of load on that axle to the rut depth per pound of load on a standard tire type such as conventional dual tires. These axle load and tire type equivalence factors are used to compute the relative rut depth in ESALs caused by a passing truck according to the following relation:

$$\frac{D}{D_s} = \sum_{i=1}^{n}t_i\, l_i. \qquad \text{(F-4)}$$

Where:

D = Rut depth caused by a truck at its static axle loads.

D_s = Rut depth caused by a standard axle.

n = The number of truck axles.

t_i = The ratio of the rut depth under the tire type on axle i to the rut depth under a standard tire type at the same load.

l_i = The ratio of the static load on axle i to a standard axle load.

The absolute level of rut depth caused by a truck at its static axle loads is calculated using the following relation:

$$D = \sum_{i=1}^{n} T_i L_i. \tag{F-5}$$

Where:

T_i = The rut depth per pound of tire load for the tire type on axle i.

L_i = The static load on axle i.

COMBINING THE MODELS TO PREDICT DAMAGE

Fatigue

The general approach for estimating rigid and flexible pavement fatigue damage for a given pavement design, vehicle speed, and roughness condition is to: (1) compute an influence function or functions for the pavement design with the appropriate pavement model; (2) compute the vehicle response to road roughness at a given speed; (3) combine the pavement and vehicle responses to obtain histories of primary pavement response variables (stress, strain, or deflection) at closely spaced points over a length of pavement; and (4) extract the levels of stress or strain cycling for insertion into a fatigue law. The procedure for calculating histories of pavement response is summarized below, and is explained in more detail in Reference (*11*).

The influence functions, computed as described earlier in this appendix, are stored in output files by the pavement response models. Time histories of the vehicle axle loads are computed with the pitch-plane models and road roughness models described in Appendices D and E, respectively. The time histories of the axle loads are written into computer files by the pitch plane models. Another computer program, developed for this research, combines the vehicle response with the pavement influence function to obtain the time history of the response variable of interest (stress, strain, or deflection) at one point on the pavement. The "combine" program selects a starting point for the truck where the leading tire is sufficiently distant from the point of interest that the influence function is nearly zero. The truck is then moved along in a series of discrete time steps, and for each step the response is computed at the point of interest from the combined influence of all the truck axles. The time steps must be small enough to reflect rapid variations in dynamic wheel loads. For this work, time steps corresponding to 3 inches of truck movement along the pavement were used. This process of computing the response of the pavement to dynamic loads of all the axles of a truck is outlined by the following equation:

$$R_{jt} = \sum_{i=1}^{n} I_{ij} L_{it}. \tag{F-6}$$

Where:

R_{jt} = The primary response (stress, strain, etc.) at point j at time step t.

L_{it} = Truck wheel load applied by axle i at the location of axle i at time step t.

I_{ij} = Influence function for point j due to a load at the location of axle i.

n = The number of truck axles.

The dynamic variations in vehicle axle load are due to the response of the vehicle to road roughness. Given that roughness has the appearance to the vehicle of a random input, a sufficient length of pavement must be simulated to accumulate time histories for which reasonable statistics can be extracted. In most cases, at least 1200 ft of pavement were simulated. Combined with the point-spacing of 3 inches, about 5000 points were studied for each combination of pavement design, vehicle type, speed, and roughness level.

Rigid Pavement Fatigue

The fatigue law described in Appendix B predicts damage as a function of the peak tensile stress at the bottom of the pavement layer. Thus, Eq. F-6 is applied to obtain time histories of pavement stress:

$$\sigma_{jt} = \sum_{i=1}^{n} I_{ij} L_{it} \qquad \text{(F-7)}$$

where σ_{jt} is the stress at point "j" at time step "t". Figure F-4 shows a time history of pavement stress, calculated via Eq. F-7, for a 5-axle tractor-semitrailer passing at 55 mph. Each tensile spike corresponds to an axle traversing the pavement location of interest.

Once the time history of pavement stress is generated, the peak tensile stresses are extracted and inserted into the Vesic fatigue law described in Appendix B. Peak tensile stresses were chosen as the equivalent cycle sizes for insertion into the Vesic fatigue law because the law is based on peak tensile stresses. The effects of all of the peak stresses are added using Miner's rule, which states that the fraction of fatigue life consumed by several stress cycles is the sum of the fraction of fatigue life used by each.

Figure F-5 shows a map of the damage caused by a 5-axle tractor-semitrailer over 120 ft. In the figure, the damage is normalized by the damage caused by the same truck with its axle loads held to their static values. Once this damage map is generated, the probability distribution of the damage values is generated and statistical summary numbers are compiled using the distribution. The statistical summary numbers include the mean, standard deviation, and percentile levels. These summary numbers can be generated for normalized or absolute damage values. Once generated, they are used to evaluate the relative effects of vehicle speed, pavement roughness, suspension design, and other variables that affect truck dynamic wheel loads.
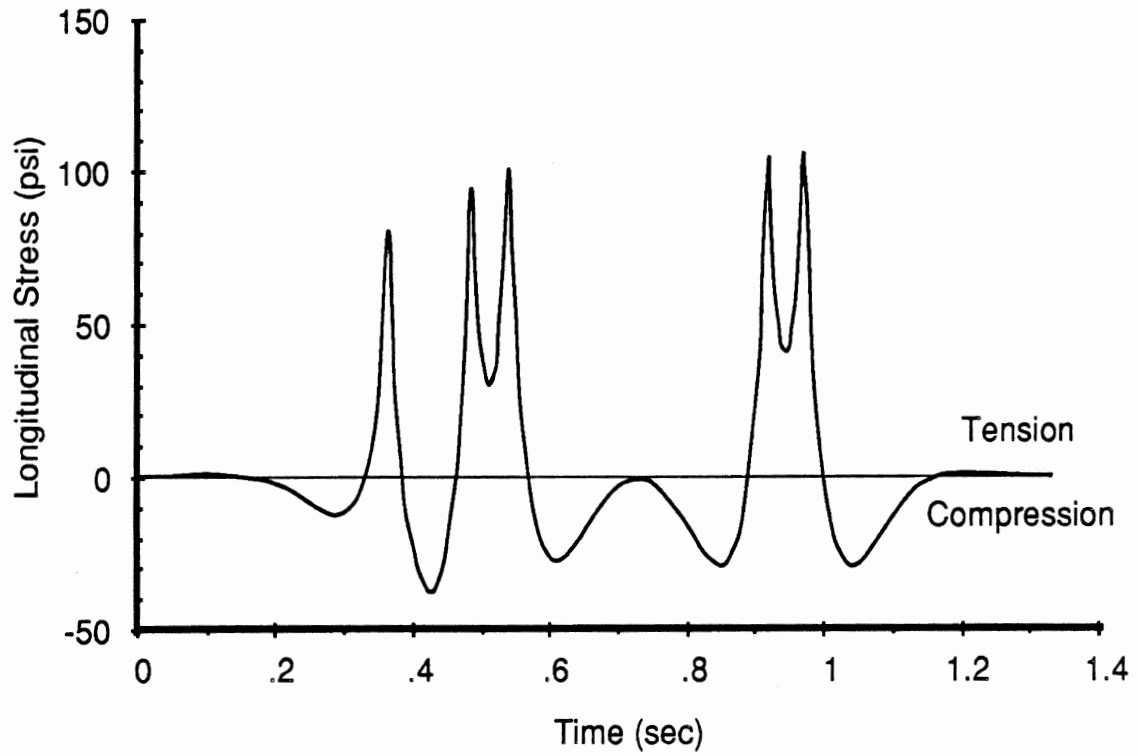
Figure F-4. Calculated time history of rigid pavement stress caused by a passing 5-axle tractor-semitrailer.
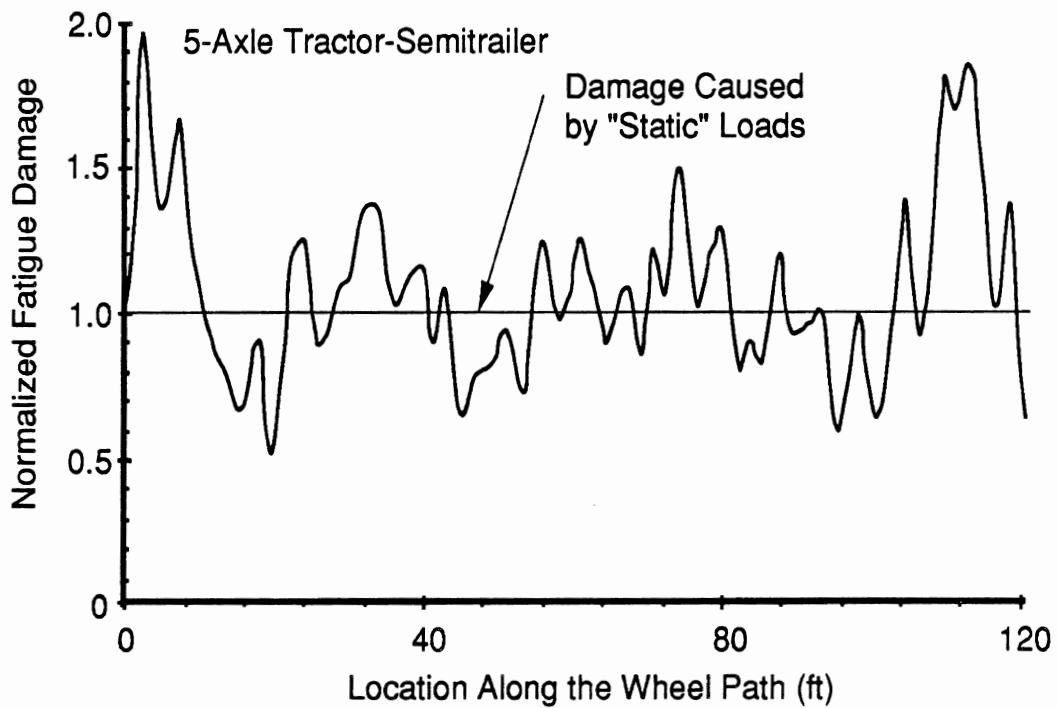

Figure F-5. Normalized rigid pavement fatigue along a wheel path due to dynamic loading.

Flexible Pavement Fatigue

The fatigue law described in Appendix C predicts damage as a function of the amplitude of a strain cycle. Thus, Eq. F-6 is applied to obtain time histories of pavement strain:

$$\varepsilon_{jt} = \sum_{i=1}^{n} I_{ij} L_{it} \qquad (F\text{-}8)$$

where ε_{jt} is the strain at point "j" at time step "t". Figure F-6 shows a time history of pavement strain, calculated via Eq. F-8, for a 5-axle tractor-semitrailer passing at 55 mph. Each tensile spike corresponds to an axle traversing the point of interest.

Because the time history of strain involves several amplitudes of peak tension and compression, a method is needed to reduce the complex response to an equivalent strain cycle size for use in the damage equation. Two methods were considered for this purpose; simple peak counting and the "rainflow" method of cycle counting. Each method is described below, and a rationale for selecting the rainflow method as the primary means of cycle counting is given.

The *peak-counting* method uses peak tensile strains under each truck axle as the size of the equivalent strain-cycle. This method was employed by Christison in the Canadian Vehicle Weights and Dimensions Study (*12*) and by Cebon in a previous study of fatigue damage due to dynamic tire forces (*13*). It is often used when evaluating fatigue due to measured strains (*14-16*). The simple peak counting method does not account for compressive strains between tensile peaks, nor does it consider cases in which the strain level does not recover to zero between axles.
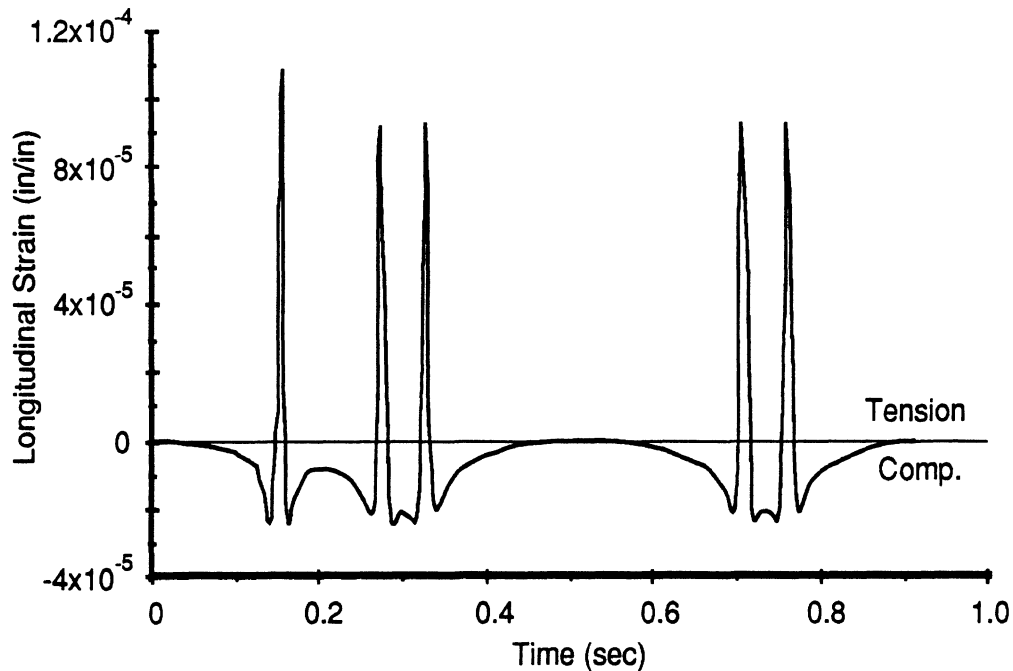

Figure F-6. Calculated time history of flexible pavement strain caused by a passing 5-axle tractor-semitrailer.

The basis of the *rainflow* cycle counting method is that the overall difference between the highest peak and the lowest valley in a strain time history is more important than intermediate small fluctuations (*17*). The method corresponds to counting complete hysteresis loops in the stress–strain curve for the material. The overall range of strain (lowest valley to highest peak) is first found and removed from the time history. The next highest range is then found and removed, and this process is continued until all strain reversals have been considered. This method is commonly employed for analysis of metal fatigue due to complex response time histories and is described in detail in (*16-18*).

Once obtained, the strain cycles from the rainflow analysis of the strain time histories are inserted into the fatigue law described in Appendix C. It is one in which fatigue life consumed is equal to the strain cycle size raised to a power and scaled by a constant. The effects of all strain cycles are added using Miner's rule, which states that the fraction of fatigue life consumed by several strain cycles is the sum of the fraction of fatigue life used by each.

Figure F-7 shows a map of the damage caused by a 5-axle tractor-semitrailer over 120 ft. In the figure, the damage is normalized by the damage caused by the same truck with its axle loads held to their static values. Once this damage map is generated, the probability distribution of the damage values is compiled and statistical summary numbers are calculated using the distribution. The statistical summary numbers include the mean, standard deviation, and percentile levels. These statistical summary numbers can be generated for normalized or absolute damage values. The statistics are then used to evaluate the relative effects of vehicle speed, pavement roughness, suspension design, and other variables that effect truck dynamic wheel loads.
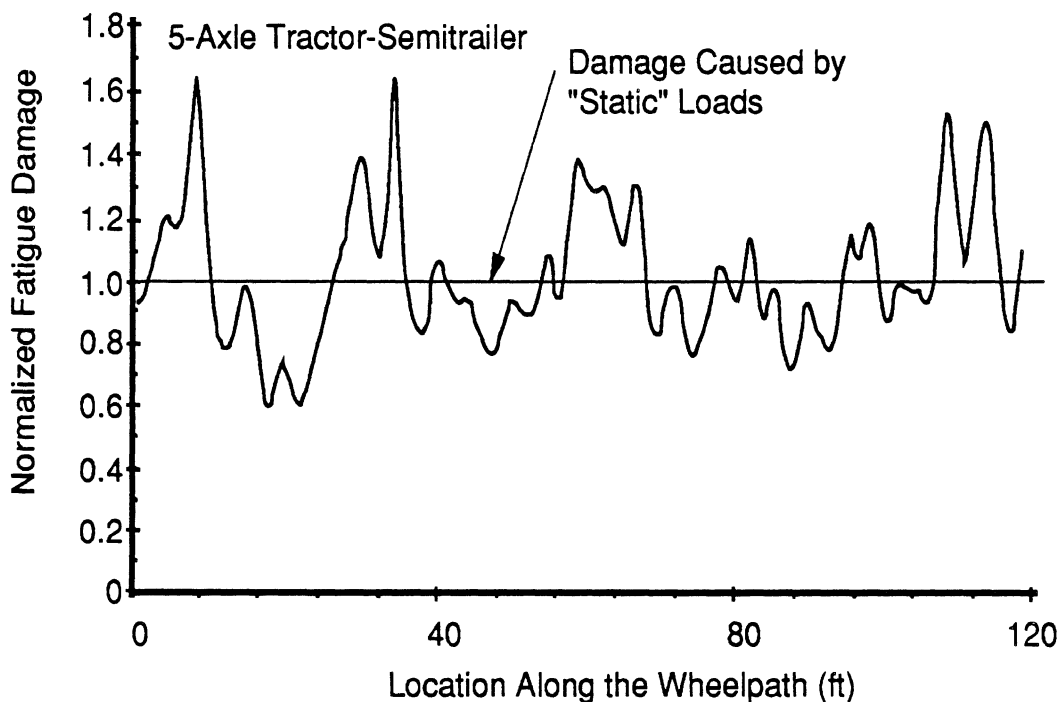

Figure F-7. Normalized flexible pavement fatigue along a wheel path due to dynamic loading.

Flexible Pavement Rutting

Flexible pavement rut depth due to dynamic truck loading is computed using an aggregate force technique (*19*), modified to account for variations in tire type between axles. Rut depth is assumed to be equal to the sum of the instantaneous tire loads that pass over a point on the road, scaled by the "rut depth per pound of load" for the tire type at each axle. The "rut depth per pound of tire load" is computed for each tire type by integrating the influence functions with respect to distance. Then, the rut depth due to a passing axle is approximated by scaling the instantaneous tire load by the vehicle speed and the rut depth per pound of tire load for the proper tire type. The rut depth due to an entire truck is simply the sum of the rut depth induced by each axle.

In the aggregate force method, rut depth is computed by the following relation:

$$D(x) = \sum_{i=1}^{n} d_i \, L_i(x). \qquad\qquad \text{(F-9)}$$

Where:

x = Location on the pavement wheel path.

D(x) = Rut depth at pavement location x.

n = The number of truck axles.

d_i = The rut depth per unit static load of the tire type on axle i.

$L_i(x)$ = The instantaneous tire load at axle i that strikes pavement location x.

This relation is used to calculate rut depth at several locations along the wheel path. The points are generally 3 inches apart. Rut depth at incremental spacing over a distance of at least 1200 ft must be calculated to capture the full range of dynamic truck load behavior. A map of the rut depth caused by a 5-axle tractor-semitrailer over a distance of 120 ft is shown in Figure F-8. In the figure, the rut depth is normalized by the rut depth caused by the same truck with its axle loads held to their static values. Once this damage map is generated, the probability distribution of the damage values is generated and statistical summary numbers are compiled using the distribution. The statistical summary numbers include the mean, standard deviation, and percentile levels. These statistical summary numbers can be generated for normalized or absolute damage values. The statistics are then used to evaluate the relative effects of vehicle speed, pavement roughness, suspension design, and other variables that effect truck dynamic wheel loads.
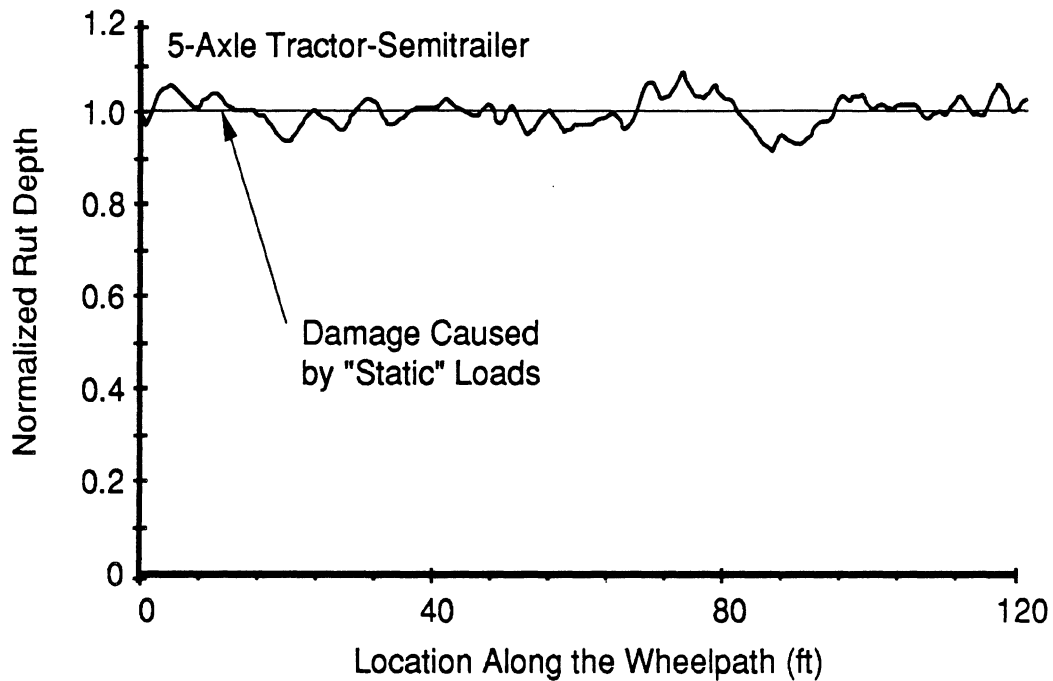
Figure F-8. Normalized rut depth along a wheel path due to dynamic loading.

REFERENCES

1. Addis, R.R., et al., "Dynamic Loading of Road Pavements by Heavy Goods Vehicles." Congress on Engineering Design, Seminar 4A-03, Institution of Mechanical Engineers, Birmingham. *Proceedings* (1986) 26 p.

2. Cole, D.J., "Measurement and Analysis of Dynamic Tyre Forces Generated by Lorries." PhD dissertation, Cambridge University, Engineering Department (1990).

3. Ervin, R.D., et al., "Influence of Truck Size and Weight Variables on the Stability and Control Properties of Heavy Trucks. Volume II." *University of Michigan Transportation Research Institute, UMTRI-83-10/2, Federal Highway Administration FHWA-RD-83-030* (1983) 179 p.

4. Gorge, W., "Evaluation of Research Reports Concerning the Influence of Commercial Vehicle Development and Design on the Road Fatigue." English translation by the International Transport Union, Geneva (1984).

5. Hahn, W.D., "Effects of Commercial Vehicle Design on Road Stress - Quantifying the Dynamic Wheel Loads for Stage 3: Single Axles, Stage 4: Twin Axles, Stage 5: Triple Axles, as a Function of the Springing and Shock Absorption System of the Vehicle." *Institut fur Kruftfahrwesen, Universitat Hannover, Report No. 453.* Translated by TRRL as WP/V&ED/87/40 (1987).

6. Hahn, W.D., "Effects of Commercial Vehicle Design on Road Stress - Vehicle Research Results." Institut fur Kruftfahrwesen, Universitat Hannover. Translated by TRRL as WP/V&ED/87/38 (1985).

7. Papagiannakis, A.T., et al., "Impact of Roughness-Induced Dynamic Load on Flexible Pavement Performance." First International Symposium on Surface Characteristics, Penn. State University. *Proceedings*. American Society of Testing and Materials (1988).

8. Woodrooffe, J.H.F., et al., "Suspension Dynamics - Experimental Findings and Regulatory Implications." *Society of Automotive Engineers Paper No. 881847* (1988) pp. 69-77.

9. Monismith, C.L., et al., "Modern Pavement Design Technology Including Dynamic Load Conditions." *Society of Automotive Engineers, Paper No. 881845* (1988) pp. 33-52.

10. O'Connell, S., et al., "Analyses of Moving Dynamic Loads on Highway Pavements, Part I: Vehicle Response." International Symposium on Heavy Vehicle Weights and Dimensions, Kelowna, British Columbia. *Proceedings* (1986) pp. 363-380.

11. Nasim, M.A., et al., "The Behavior of a Rigid Pavement Under Moving Dynamic Loads." *Transportation Research Record,* No. 1307 (1991) pp. 129-135.

12. Christison, J.T., "Pavements Response to Heavy Vehicle Test Program: Part 2 - Load Equivalency Factors." *Vehicle Weights and Dimensions Study, Vol. 9. Canroad Transportation Research Corporation* (1986) 79 p.

13. Cebon, D., "Theoretical Road Damage Due to Dynamic Tyre Forces of Heavy Vehicles. Part 2: Simulated Damage Caused by a Tandem-Axle Vehicle." *Proc. I.Mech.E.,* Vol. 202, No. C2 (1988) pp. 109-117.

14. Christison, J.T., et al., "In Situ Measurements of Strains and Deflections in a Full-Depth Asphaltic Concrete Pavement." *Proc. Assoc. Asphalt Paving Technology,* Vol. 47 (1978) pp. 398-430.

15. Majidzadeh, K. and Ilves, G.J., "Methods for Determining Primary Response Load Equivalency Factors." FHWA Load Equivalence Workshop, McLean VA. *Proceedings* (1988) 20 p.

16. Papagiannakis, T., et al., "Heavy Vehicle Equivalence Factors from In–Situ Pavement Strains." RTAC Annual Conference, St. John's, Newfoundland. *Proceedings* (1990).

17. Fuchs, H.O. and Stephens, R.I., *Metal Fatigue in Engineering.* John Wiley and Sons. New York. (1980) Chapter 10.

18. American Society of Testing and Materials, *ASTM Annual Book of ASTM Standards.,* Vol. 03.01 Standard E 1049–85 (1986).

19. Cebon, D., "Assessment of the Dynamic Wheel Forces Generated by Heavy Road Vehicles." ARRB/FORS Symposium on Heavy Vehicle Suspension Characteristics, Canberra, Australia. *Truck Designers Sprung?* (1987) pp. 143-162.